pH Dependence of Redox Potential in c-Type Cytochromes

Fiona A. Leitch

Thesis submitted for the degree of
Doctor of Philosophy
University of Edinburgh
1984

The work described in this thesis is my own, unless otherwise indicated. Some of the data are published in Pettigrew, G.W., Leitch, F.A. & Moore, G.R. (1983) Biochem. Biophys. Acta 725, 409-416 and Moore, G.R., Harris, D.E., Leitch, F.A. & Pettigrew, G.W. (1984) Biochem. Biophys. Acta 764, 331-342, which are bound in Appendix II, and Leitch, F.A., Moore, G.R. & Pettigrew, G.W. (1984) Biochemistry (in press).

Edinburgh, May 1984

ACKNOWLEDGEMENTS

I am greatly indebted to Graham Pettigrew for his support, encouragement and generosity with ideas over the last three (and a half) years. His enthusiasm for, and belief in the importance of basic research have been a constant stimulus. My thanks must also go to the rest of the staff and research students at the Dick Vet., in particular Bill Ramsay, Celia Goodhew and John Leaver, for making it such a happy working environment.

I am also particularly grateful to Geoff Moore for teaching me some NMR, and to Geoff and Professor Bob Williams for giving me the opportunity to spend some time in Oxford. Science was good fun in CG1. Thanks to Glyn Williams for the horse cytochrome c spectra on pages 45 and 48.

Finally, I should acknowledge that Richard Ambler kindly provided me with unpublished cytochrome c_{551} sequence data, which has been central to this thesis.

ABBREVIATIONS

E_O	Standard oxidation-reduction (redox) potential measured at pH0, with oxidant and reductant species present at unit activity.
E_m	Midpoint redox potential (quoted at a defined pH); this obtains when [oxidised species] / [reduced species] = 1.
E_h	Ambient redox potential.
$\tilde{E}$	Redox potential obtained by extrapolating E_m along a line of constant slope to pH0.
$pK_{O/O1/O2}$	pKs in the oxidised form of a redox protein.
pK_R	pK in the reduced form of a redox protein.
NMR	Nuclear magnetic resonance.
ppm	Parts per million.
pH^*/pK^*	pH/pK measured in D_2O.
EFA	Ethoxyformic anhydride (diethylpyrocarbonate).
DNS Cl	Dansyl chloride.

SUMMARY

The midpoint redox potential (E_m) of mitochondrial cytochrome c is independent of pH below pH9 (Rodkey & Ball, 1950). For several bacterial homologues of cytochrome c, however, E_m is markedly influenced by pH between pH5 and 9; in the case of Pseudomonas aeruginosa cytochrome c_{551}, the pH dependence has been interpreted as being due to the redox state dependent ionisation of a haem propionic acid substituent, which has a pK of 6.3 in the oxidised form of of the cytochrome and 7.2 in the reduced form (Moore et al., 1980). The redox state imposed separation of the propionic acid pK values was suggested to occur through the electrostatic influence of the haem, which carries a net charge of +1 in the ferricytochrome but 0 net charge in the ferrocytochrome.

In an extension of the studies initiated with P. aeruginosa cytochrome c_{551}, the bulk of the work described in this thesis deals with the effect of pH on E_m for a closely related cytochrome, Pseudomonas stutzeri 221 cytochrome c_{551}. The P. stutzeri cytochrome shows a similar pattern of pH dependence of E_m in that two pKs (pK_O and pK_R) influence E_m below pH9; however, pK_O and pK_R occur nearly one pH unit higher (pK_O = 7.6, pK_R = 8.3) than in P. aeruginosa cytochrome c_{551}. Using high resolution ^1H NMR it was possible to show that haem propionic acid-7 ionises at pK = 7.6 in P. stutzeri ferricytochrome c_{551} and also that a histidine residue, His47, is deprotonated with pK = 7.6 in the ferricytochrome and pK = 8.3 in the ferrocytochrome. The pK of propionic acid-7 in the ferrocytochrome could not be measured by NMR and so it was not possible to demonstrate directly that its pK is redox state dependent. However, by chemically modifying His47 with ethoxyformic anhydride, which prevents the histidine from ionising between pH5 and 9, it was shown that the redox potential of P. stutzeri cytochrome was still pH dependent, implying

that the redox state dependent ionisation of propionic acid-7 must indeed contribute to the fall in E_m at alkaline pH. Since propionic acid-7 and His47 appear to ionise with exactly the same values of pK_O and pK_R in the unmodified cytochrome, and since the propionic acid pKs are lowered by nearly 2 pH units upon modification of His47 with ethoxyformic anhydride, it was deduced that the two groups must interact with each other in a manner that raises the pKs of both species and allows their conjoint ionisation. A hydrogen bonding scheme is proposed in which propionic acid-7 and His47 both exist in a partially charged state at low pH.

It was predicted that propionic acid-7 will ionise with redox state dependent pKs in all other cytochromes c_{551}, and that the nature of the amino acid at sequence position 47 will be important in determining the values of pK_O and pK_R. In this respect it was shown that P. stutzeri 224 and P. mendocina cytochromes c_{551}, which both contain histidine at sequence position 47, have similar E_m versus pH curves and pK_O/pK_R values to the P. stutzeri 221 cytochrome. NMR data for P. mendocina cytochrome c_{551} confirmed that propionic acid-7, and His47, ionise in this cytochrome also. However, P. denitrificans and Azotobacter vinelandii cytochromes c_{551} show only very slight pH dependence of redox potential below pH9 (i.e. pK_O and pK_R very close together), a pattern which was not predictable in either case simply from consideration of the identity of the amino acid occurring at position 47 in the sequence.

The E_m versus pH curve was also obtained for Chlorobium thiosulphatophilum cytochrome c_{555}, a cytochrome which is distantly related in sequence to the cytochromes c_{551}. The general shape of the curve is similar to that observed for the cytochromes c_{551}, with pK_O = 6.3 and pK_R = 7.1. NMR data showed that a histidine residue is deprotonated with these pKs; this histidine may be sequentially analogous to His47 of P. stutzeri and P.

mendocina cytochromes c_{551}. The NMR data also suggested that a propionic acid substituent ionises. Thus the redox potential of cytochrome c_{555} appears to be affected by the same mechanism as in P. stutzeri and P. mendocina cytochromes c_{551}, despite their diverse origins.

These results are compared and contrasted with data obtained by Pettigrew et al. (1975, 1978) for another major group of bacterial cytochromes, the cytochromes c_2 from photosynthetic bacteria. The cytochromes c_2 differ from the cytochromes c_{551} in that E_m can be affected either by the redox state dependent ionisation of a haem propionic acid substituent or of a histidine residue in the polypeptide backbone. In this respect it was shown for Rps. viridis cytochrome c_2 that ethoxyformylation of His39 abolishes the pH dependence of E_m normally observed for this cytochrome. This work also led to the successful prediction that two mitochondrial cytochromes which contain His39 should have pH dependent redox potentials.

CONTENTS

CHAPTER I: INTRODUCTION

Section 1 - Structure and Function of c-Type Cytochromes with Special Reference to the Cytochromes c-551

A. The c-type cytochromes

Cytochrome c is a small, highly stable , coloured protein which is the only buffer soluble protein component of the mitochondrial respiratory chain - these physical properties undoubtedly explain why it is the most thoroughly characterised of electron transport proteins (for a review, see Dickerson & Timkovich, 1975).

Although cytochrome c is for most people synonymous with mitochondrial electron transfer, the mitochondrial proteins belong to a much larger family of c-type cytochromes, members of which are ubiquitous in the bacterial kingdom. This family of proteins includes the cytochromes c_2 of photosynthetic bacteria, Paracoccus cytochrome c_{550}, Pseudomonas cytochromes c_{551}, Chlorobium cytochromes c_{555} and also the soluble cytochromes f from algae. Their wide distribution and relatively small size encouraged R.P. Ambler and E. Margoliash, amongst others, to sequence a great number of the c-type cytochromes with the ultimate aim of constructing phylogenetic trees. Some 70 mitochondrial and over 50 bacterial c-type cytochromes have so far been sequenced. From these data, Ambler has proposed a classification scheme in which four main groups of cytochromes are distinguished. Class I in this scheme contains most of the cytochromes which have been sequenced and includes the mitochondrial cytochromes c and the bacterial cytochromes to be discussed in this thesis. The main characteristics of the group are as follows: (i) the cytochromes are low-spin and have relatively high oxidation-reduction potentials (150-400mV) (ii) each has a single haem c group covalently attached near the N-terminus of its polypeptide chain (iii)a histidine about 1/4 along the

sequence and a methionine about 3/4 along the sequence provide the 5th and 6th ligands to the haem iron.

The Class II cytochromes, on the other hand, have the single haem binding site located towards the C-terminal end of their polypeptide chain and the class includes the high-spin cytochromes c′ from photosynthetic bacteria as well as the low-spin cytochrome c_{556} from Agrobacterium. Class III comprises cytochromes with more than one haem and the Class IV cytochromes have another prosthetic group in addition to haem c (e.g. flavin). There are relatively few structural data available yet for these latter two classes. The four classes bear little structural similarity to each other beyond the presence of one or more covalently bound haem c groups and so the phylogenetic studies have been confined to cytochromes from the same class.

The sequence data for the Class I cytochromes indicate that they may all be descended from a common evolutionary ancestor, despite their diverse origins. Although the structure of mitochondrial cytochrome c appears to have changed little in the time since the emergence of the first eukaryotes, there is considerable structural diversification amongst the prokaryotic members of the class (which is consistent with the view that the eukaryotes emerged relatively recently). The sequence evidence for the common evolutionary origin of the Class I cytochromes is borne out by the analogous nature of their physiological functions- these cytochromes generally act as electron carriers between a membrane bound reductase complex containing cytochrome b or c_1 and the terminal electron acceptor protein of their respective electron transport chains; in photosynthetic bacteria, for instance, cytochrome c_2 donates electrons to photooxidised P700 of Photosystem I.

The Class I cytochromes range in size from 82 to 134 amino acids which allows for a further subdivision of the class on the basis of polypeptide chain length:

Pseudomonas cytochromes c_{551} (82aa) and Chlorobium cytochromes c_{555} (86aa) belong to the short group, the medium length group comprises the mitochondrial cytochromes c and some cytochromes c_2 (103-107aa) and Paracoccus denitrificans cytochrome c_{550} (134aa) is an example of a long cytochrome. The variability in polypeptide chain length complicated early attempts at sequence alignment. However, when crystal structures for some of the cytochromes became available, it was evident that the tertiary structure of Class I cytochromes is strongly conserved. X-ray work on representatives of the three size classes show a similar polypeptide chain fold and side group packing around the haem, with the size differences being accommodated in extended loops of chain at the surface of the molecules. This structural homology is not particularly evident from sequence comparisons. When the crystal structure of Pseudomonas aeruginosa cytochrome c_{551} was solved, it was clear that all previous attempts to align its sequence with that of horse cytochrome c had been incorrect.

B. The Electron Transport Chain of Anaerobically Grown Pseudomonas

A number of species of Pseudomonas are facultative anaerobes, which use nitrate as a terminal electron acceptor in the absence of oxygen (a process known as nitrate respiration or dissimilatory nitrate reduction). In the first step of nitrate reduction, nitrate is reduced to nitrite by a dissimilatory nitrate reductase. Extensive studies on the enzyme from E. coli (Forget, 1974; MacGregor et al., 1974; Clegg, 1976) and, more recently, the P. aeruginosa enzyme (Carlson et al., 1982) show them to be large membrane-bound Mo, Fe-S proteins. In the case of E. coli, the reductase appears to accept electrons at the level of a b-type cytochrome and then reduces nitrate at the cytoplasmic surface of the membrane. In E. coli and P. aeruginosa, the nitrite

generated by reductase action is also used as a terminal electron acceptor, being converted to gaseous products (N_2O, NO, N_2) by the process of denitrification. A soluble protein with nitrite reductase activity has been purified from P. aeruginosa (Gudat et al., 1973; Kuronen et al., 1975); the enzyme, called cytochrome cd_1, is a 120000 mol. wt. homodimer containing one haem c and one haem d_1 per monomer. Cytochrome cd_1 can be released from cells of P. aeruginosa by spheroplast formation, implying that its location is periplasmic and the fact that the enzyme can accept electrons from P. aeruginosa azurin and cytochrome c_{551}, both periplasmic proteins, would support this conclusion (Wood, 1978; Horio et al., 1961; Barber et al., 1976). Cytochrome cd_1 has also been observed in P. stutzeri and the enzyme has been purified from P. perfectomarinus (possibly a marine form of P. stutzeri). In the latter case, its properties are very similar to those of the P. aeruginosa cytochrome cd_1 (Kodama & Mori, 1969; Liu et al., 1983).

Facultative anaerobes might be expected to possess different electron transfer proteins when grown under aerobic and anaerobic conditions. Unfortunately, very few systematic comparisons of the cytochrome components of aerobically and anaerobically grown pseudomonads have been reported, and it is not clear which of the many cytochromes produced by nitrate grown cells are particular to the denitrification process. The c-type cytochrome content of whole cells is considerably greater for pseudomonads grown under denitrifying conditions and these cytochromes are generally assumed to be involved with respiration to nitrite. The cytochrome profile of many species is still incomplete because extraction procedures like acetone powdering, used routinely in the purification of cytochome c_{551}, destroy less stable proteins like cytochrome cd_1. However, there appear to be at least three soluble c-type cytochromes present in most denitrifying pseudomonads: (i) cytochrome

c_{551} is a class I c-type cytochrome of 10000 mol.wt. which is located in the periplasmic space. It is by far the most abundant cytochrome in all denitrifying species and it has been extensively characterised but, despite that, its physiological function has not yet been defined. It reacts rapidly with cytochrome cd_1 (Horio et al., 1961) but this is also true of the blue copper protein azurin (see below). That the cytochrome is involved in denitrification is supported by its distribution within the genus, since only very actively denitrifying species contain a cytochrome c_{551}, and by the fact that its level is depressed in these species when grown aerobically (ii) cytochrome c_4 is characterised by the presence of two haems per molecule of about 20000 daltons. It has been purified from P. stutzeri , P. aeruginosa and A. vinelandii (Kodama & Shidara, 1969; Leitch, Grieve & Pettigrew, unpublished data; Ambler & Murray, 1973; Campbell et al., 1973) and in the case of the latter two proteins, the amino acid sequence has been determined (Ambler, 1980; R.P. Ambler, unpublished data). A low resolution X-ray structure for the P. aeruginosa cytochrome c_4 shows that the molecule comprises two globular domains, each containing one haem (Sawyer et al., 1981). The sequence and X-ray work together indicate that this cytochrome may have arisen by a gene duplication event at the cytochrome c_{551} gene. Cytochrome c_4 appears to be membrane associated although it is not an integral protein - it is most efficiently released from cells by treatment with butanol but it is completely soluble in aqueous media. Its role in electron transport is enigmatic although being dihaem in nature it is attractive to think of it as the reductant of another dihaem protein viz. cytochrome cd_1 (iii) cytochrome c_5 is a monohaem cytochrome of mol. wt. 12000 daltons, usually occurring as a dimer. It has the characteristic spectral features of a class I, low spin c-type cytochrome and it has a haem binding site located towards its N-terminus

(although it has a second Cys-X-Y-Cys sequence near its C-terminus). However, Ambler & Taylor (1973) observed a N-terminal "raggedness" when sequencing the P. mendocina cytochrome and suggested that cytochrome c_5 might be part of a larger cytochrome such as cytochrome c_{551} peroxidase - as yet there is no evidence available to support this suggestion. In addition to these cytochromes, a soluble cytochrome c_{551} peroxidase has been purified from P. aeruginosa; the protein, which is isolated as a dimer, contains two covalently bound haem c groups per monomer of 40000 daltons (Ellfolk & Soininen, 1970). A spectrally similar protein has been observed in P. stutzeri (Kodama & Mori, 1969). Finally, a 16000 dalton Cu protein, azurin, is present in many denitrifying pseudomonads. Azurin has a similar redox potential to cytochrome c_{551} and intermolecular electron exchange between the two proteins proceeds at an extremely high rate (Pecht & Rosen, 1973; Brunori et al., 1974). Like cytochrome c_{551} it is an efficient electron donor to both cytochrome cd_1 and cytochrome c_{551} peroxidase and it has been suggested that cytochrome c_{551} might fulfill the role of azurin in conditions of limiting copper (P.M. Wood, unpublished data).

The distribution of the various c-type cytochromes, azurin and cytochrome cd_1 amongst denitrifying species of Pseudomonas and the strict aerobes P. putida and Azotobacter vinelandii is shown in Table I. A tentative scheme for the arrangement of these electron transfer components in Pseudomonas is presented in Figure 1. The solid lines represent electron transfer routes which have been experimentally established and the broken lines represent possible (and likely) routes of electron flow. The membrane bound c-type cytochrome, which Wood & Willey (1980) have proposed is analogous to mitochondrial cytochrome c_1 seems likely to be the direct reductant of cytochrome c_4, cytochrome c_{551} or azurin. The soluble proteins interact with one of (at least) three terminal

Table I: Distribution of Soluble Redox Proteins in Pseudomonas and A. vinelandii

Organism	Mode of Growth	c_{551}	c_4	c_5	azurin	cd_1
P. aeruginosa	denitrifying	+	+	+	+	+
P. mendocina	"	+	+	+	nd	nd
P. denitrificans (NCIB 9496)	"	+	nd	+	+	nd
P. stutzeri 224	"	+	+	+	-	+
P. perfectomarinus	"	+	+	+	+	+
P. fluorescens (Biotype C)	"	+	nd	nd	+	nd
P. fluorescens (Biotypes A,E,G)	aerobic	-	nd	+	+	nd
P. putida	"	-	nd	nd	+	nd
A. vinelandii	aerobic, N-assimilation	+	+	+	-	nd

Figure 1: The Electron Transport Chain of Denitrifying Pseudomonas

A tentative scheme for the arrangement of electron transfer components in denitrifying pseudomonads. Solid lines indicate established pathways of electron transfer and dashed lines indicate likely routes. Dashed circles represent poorly characterised redox proteins.

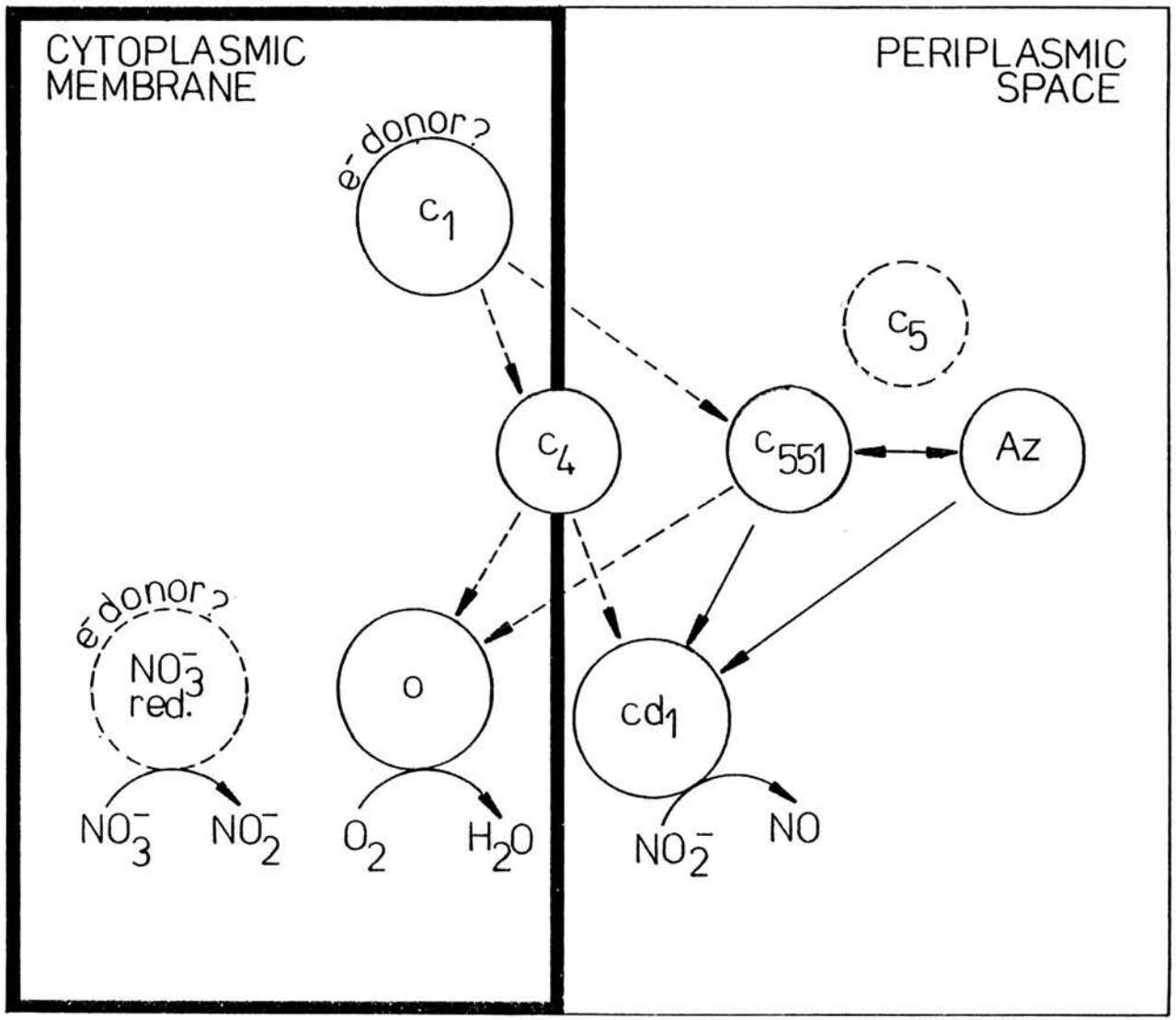
CYTOPLASMIC MEMBRANE
PERIPLASMIC SPACE
é donor ?
c1
c5
c4
c551
Az
é donor ?
NO3 red.
o
cd1
NO3
NO2
O2
H2O
NO2
NO

enzyme complexes *viz.* nitrite reductase, cytochrome cd_1 or cytochrome o. Cytochrome o is a membrane bound oxidase which has been identified in cells of *P. aeruginosa* (Matsushita et al., 1982). The immediate reductant of cytochrome o may be cytochrome c_4, by analogy with the proposed situation for *A. vinelandii* (see below). The role of cytochrome c_5 in this scheme is particularly uncertain since nothing is known about its interaction with any of the other proteins, and since some doubt remains as to whether it actually occurs *in vivo*. Nitrate reductase probably accepts electrons at the level of a b-type cytochrome, by analogy with the nitrate reductases of *Pa. denitrificans* and *E. coli* (Haddock & Jones, 1977).

The Respiratory Electron Transport Chain of Azotobacter vinelandii

Azotobacter vinelandii is a nitrogen fixing obligate aerobe. Its respiratory chain branches into two pathways at cytochrome b with one limb terminating in cytochrome d and the other in cytochrome o. The more active cytochrome b - d pathway is thought to be important in protecting nitrogenase from high levels of oxygen (nitrogenase is oxygen labile) while the cytochrome b - o segment is implicated in energy conservation at low oxygen tension (see Haddock & Jones, 1977). This latter segment resembles the *Pseudomonas* electron transfer chain discussed above in that it contains a cytochrome c_4, cytochrome c_5 and (possibly) cytochrome c_{551}. Cytochrome c_4 is found to co-purify with the membrane bound cytochrome o and their close physical association suggests that cytochrome c_4 may be the immediate electron donor to the oxidase (Yang & Jurtshuk, 1978).

C. Sequence Comparison of Pseudomonas Cytochromes c-551

Members of the genus *Pseudomonas* are common

Table II: Cytochrome c-551 Sequences

```
                10        20        30        40        50        60        70        80
                |         |         |         |         |         |         |         |
(A)  EDPEVLFKNKGCVACHAIDTKMVGPAYKDVAAKFAGQAGAEAELAQRIKNGSQGVWGPIPMPPNAVSDDEAQTLAKWVLSQK
(B)  EDGAALFKSKPCAACHTIDSKMVGPALKEVAAKNAGVKDADKTLAGHIKNGTQGVWGPIPMPPNQVTDAEALTLAQWVLSLK
(C)  QDGEALFKSKPCAACHSIDAKLVGPAFKEVAAKYAGQDGAADLLAGHIKNGSQGVWGPIPMPPNPVTEEEAKILAEWILSQK
(D)  QDGEALFKSKPCAACHSVDTKMVGPALKEVAAKNAGVEGAADTLALHIKNgsqgvwGPIPMPPNPvteeeakilAEWVLSLK
(E)  ASGEELFKSKPCGACHSVQAKLVGPALKDVAAKNAGVDGAADVLAGHIKNGSTGVWGAMPMPPNPVTEEEAKTLAEWVLTLK
(E)  STGEELFKAKACVACHSVDKKLVGPAFHDVAAKYGAQGDGVAHITNSIKTGSKGNWGPIPMPPNAVSPEEAKTLAEWIVTLK
(F)    dealfkskpciachsvdaklvgpslkveaakhaggvzazzllaghiknqssgvwgpipmppnavseeeaqtlaewvltlk
(G)  ETGEELYKTKGCTVCHAIDSKLVGPSFKEVTAKYAGQAGIADTLAAKIKAGGSGNWGQIPMPPNPVSEAEAKTLAEWVLTHK
```

(A) P. aeruginosa NCIB 10332 (B) P. fluorescens biotype C-18 (C) P. stutzeri 221 (D) P. stutzeri 224 ("stanieri") (E) P. mendocina CH-110 (F) P. denitrificans NCIB 9496 (F) P. denitrificans NCIB 10465 (G) Azotobacter vinelandii NCIB 8789

Note: Residues in the lower case have not yet been definitvely located in sequence.

inhabitants of soil, fresh water and marine environments. They are chemoorganotrophs, able to grow in mineral media with a single organic compound as sole source of carbon and energy. The majority of species are obligate aerobes but four of the thirty well-characterised species described by Bergey (1974) are capable of anaerobic respiration with nitrate (viz. P. aeruginosa, P. stutzeri, P. mendocina and P. fluorescens). To these four can be added P. perfectomarinus and P. denitrificans, which are incompletely characterised pseudomonads. Cytochrome c_{551} is produced in large amounts by denitrifying pseudomonads and so it has been a convenient tool for studying their evolutionary relationship. Homologous proteins from different species differ in amino acid sequence and the amount of difference appears to be related to the evolutionary distance between the species. The Pseudomonas cytochrome c_{551} sequences which have been determined by R.P. Ambler are shown in Table 2 and the cytochrome c_{551} from Azotobacter vinelandii is included for comparison (Ambler & Wynn, 1973; Ambler, 1976; R.P. Ambler, unpublished data). Two points should be made. (i) The GC content of the DNA from various strains of P. stutzeri ranges from 60.7 to 66.3 moles% and it was primarily because this range appeared too wide to characterise a single species that Mandel (1966) proposed a division of P.stutzeri into two species - P. stutzeri strains with a high GC content (ca.65 mole%) were to retain the name P. stutzeri while those strains with a low GC content (ca. 62 moles%) were to become a separate species called P. stanieri. However, Palleroni et al. (1970), on examining a larger cross-section of strains, could find no justification for such a specific separation on the basis of phenotypic differences, and the current edition of Bergey does not distinguish two species. On sequencing the cytochrome c_{551} from several strains, Ambler found that the cytochrome sequence from "P. stanieri" strains were distinct from the sequences of

cytochromes from P. stutzeri strains. Hence, Table II shows two sequences for P. stutzeri cytochrome c_{551}. (ii) Doudoroff et al. (1974) have questioned the taxonomic validity of P. denitrificans. From a careful study of a number of organisms previously designated P. denitrificans, they concluded that several different species had been studied under the same name and that at least one organism did not belong to the genus Pseudomonas. P. denitrificans NCIB 10465 and P. denitrificans NCIB 9496 were shown to be separate, as yet unclassified, Pseudomonas species but neither has been renamed.

The cytochrome sequences are compared in the form of a dendrogram in Figure 2, where the dendrogram was constructed by adding increasingly divergent sequences to the P. stutzeri group. As a convenient scale of reference, mammalian cytochromes c differ from amphibian cytochromes c by about 18% and from insect cytochromes c by about 33%. Clearly, the extent of variation between the cytochromes c_{551} even of very closely related species (P. aeruginosa and P. fluorescens are distinguished only with great difficulty by classical bacteriological methods) is great compared with the mitochondrial cytochromes c. Interestingly, A. vinelandii cytochrome c_{551} is more closely related to the P. stutzeri cytochromes than is P. denitrificans NCIB 9496 cytochrome c_{551}- this observation would support Ambler's view that horizontal gene transfer may have contributed to bacterial evolution since A. vinelandii is completely unrelated to Pseudomonas as judged by classical criteria.

D. The Structure of Psueudomonas aeruginosa Cytochrome c-551

The molecular structure of cytochrome c_{551} from P. aeruginosa has been determined at 1.6Å resolution (Matsuura et al., 1982) and is thus the most refined

Figure 2: Dendrogram of Cytochrome c-551 Sequences

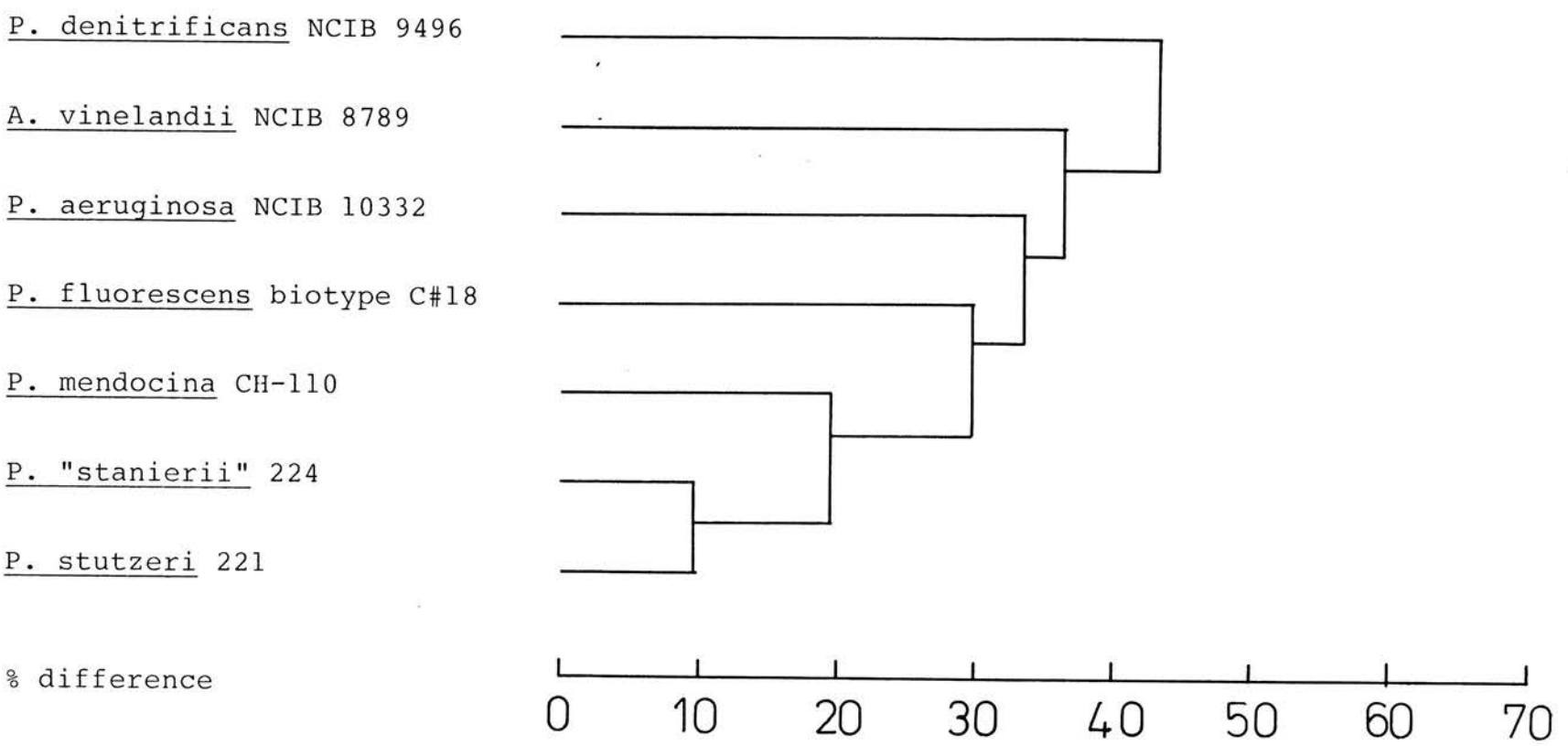

structure available for a cytochrome to date. Matsuura et al. examined both the ferri- and ferrocytochrome at this resolution and found that their structures were virtually superimposable, precluding the possibility of a conformational change occurring in electron transfer, and in agreement with the work on tuna cytochrome c (Takano et al., 1981)

Cytochrome c_{551} is a compact, globular protein in which the haem group is enfolded by polypeptide chain to the extent that only one edge is exposed to solvent. It is shown in Figure 3. The protein secondary structure contains no β-sheet but a considerable amount of α-helix; the amino terminal, 20's, 40's and carboxy terminal α-helices are readily seen in the ribbon diagram, Figure 4a. The haem actually sits in a crevice in the protein (although this is not easy to see in conventional "front face" views of the molecule, like Figures 3 and 4a) and is held by covalent thioether linkages to Cys12 and Cys15, by coordinate bonds from His16 and Met61 to the iron and by hydrogen bonding between the propionic acid side chains of the haem and a number of amino acids in the polypeptide backbone. The haem crevice is lined with hydrophobic and aromatic residues and, since these may well be important in determining the level of haem redox potential (Kassner 1972, 1973), it is not surprising that many of them are conserved amongst the Class I cytochromes - Phe7, Pro25, Leu44 and Leu74, for example, occur at sequentially analogous positions in tuna cytochrome c and are haem contact residues in this protein also.

The structure of haem c (iron-protoporphyrin IX) is shown in Figure 5. The individual pyrrole rings of the porphyrin are tilted from the mean of the haem plane in P. aeruginosa cytochrome c_{551} so that the porphyrin assumes a saddle shape. Redox state changes do not affect the haem geometry (c.f. haemoglobin) nor the location of the haem relative to the polypeptide. As mentioned above, the polypeptide chain of cytochrome c_{551} does not

Figure 3: Three-Dimensional Structure of P. aeruginosa Cytochrome c-551

Taken from Dickerson (1980).

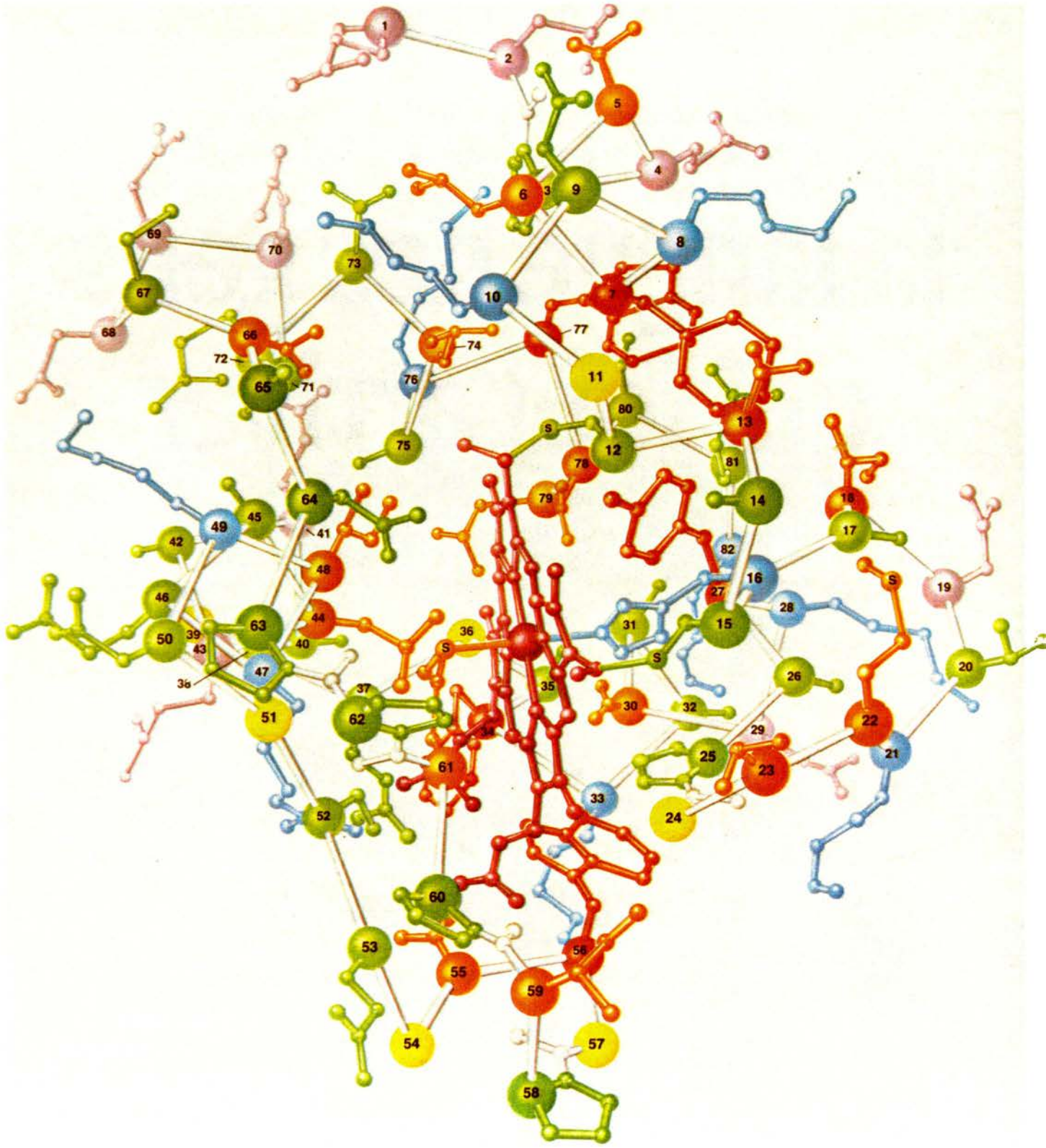

HYDROPHOBIC, AROMATIC RINGS

HYDROPHOBIC, NOT AROMATIC

AMBIVALENT

AMBIVALENT

HYDROPHILIC, ACIDIC

HYDROPHILIC, BASIC

HEME

Figure 4: Main Chain Folding in Class I c-Type Cytochromes

(a) P. aeruginosa cytochrome c_{551}; regions of α -helix are dotted. (b) Tuna cytochrome c; shaded area (I) indicates loop of polypeptide which is absent in cytochrome c_{551}.

a.

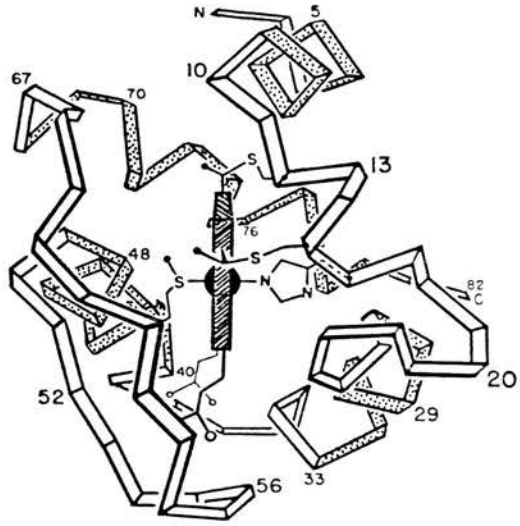
N
5
10
67
70
S
13
76
48
S
S
N
N
82
C
40
52
20
29
33
56

b.

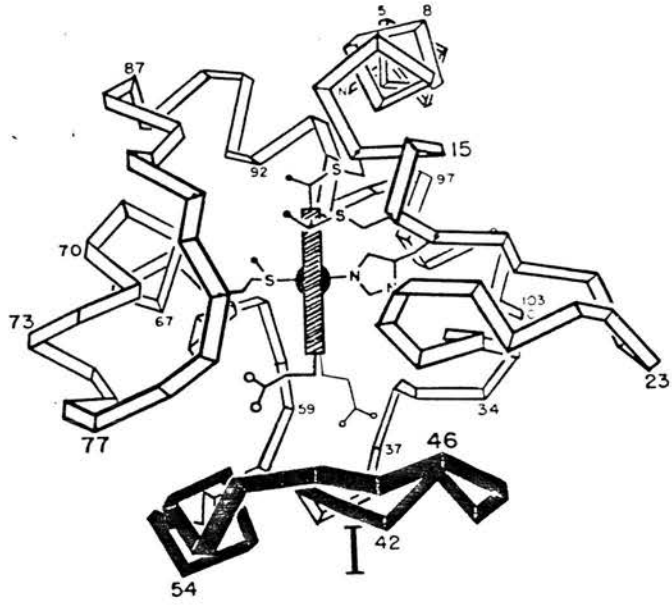
5
8
87
15
92
S
97
S
70
S
N
73
67
103
C
23
59
34
77
37
46
42
I
54

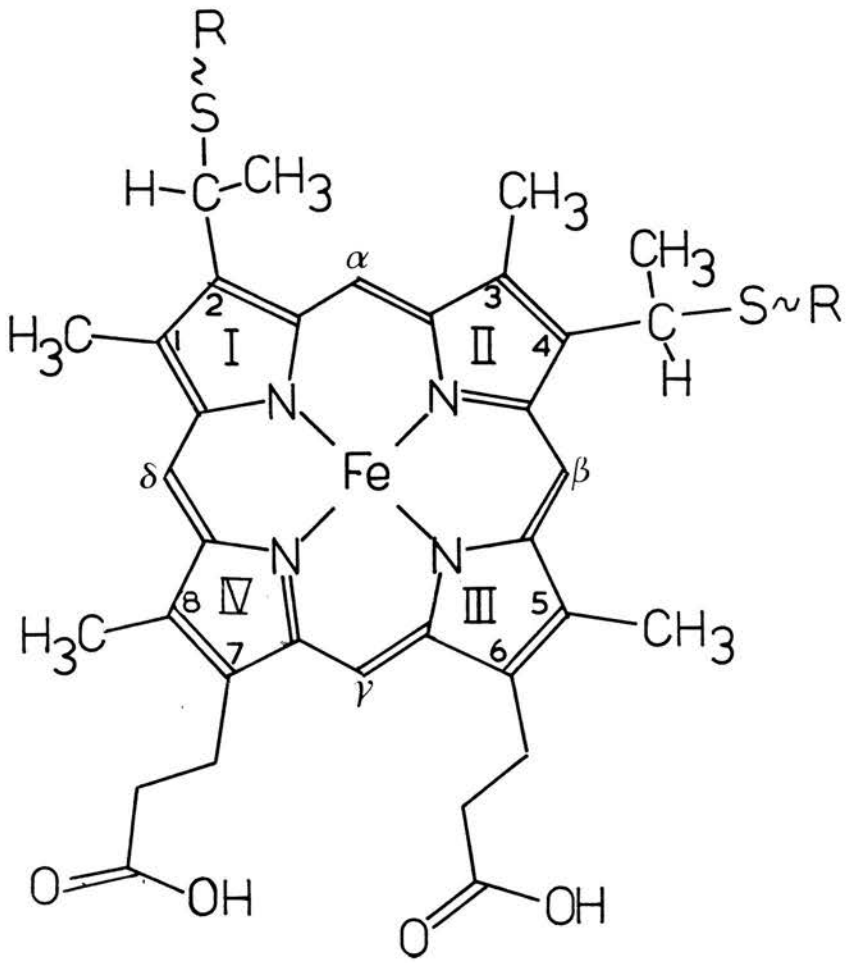

Figure 5: Haem c

The pyrrole rings are numbered I-IV and their substituents are numbered clockwise 1-8. The meso protons are designated α, β, γ and δ.

completely envelope the haem and it is pyrrole rings II and III which are left relatively exposed to solvent. In fact, propionic acid-6 on pyrrole ring III can be regarded as being freely accessible to solvent. This is somewhat different from the situation with tuna cytochrome c where only pyrrole ring II is solvent exposed; the origin of this difference lies with a loop of polypeptide in the tuna cytochrome which has been deleted in Pseudomonas cytochrome c_{551}, as shown in Figure 4. Loop I closes off the bottom of the haem crevice in tuna cytochrome c and its absence in cytochrome c_{551} is only partially compensated for by a downward swing of the 50's loop (70's loop in tuna).

Propionic acids -6 and -7 are both hydrogen bonded to amino acids in the polypeptide, restricting their orientation with respect to the haem plane. Propionic acid-7 (the inner propionic acid) forms hydrogen bonds with Arg47 and Trp56, and propionic acid-6 (the outer propionic acid) is hydrogen bonded to Val55 and a water molecule. The precise interactions can be summarised as:

6O1...Val55NH = 2.9Å
6O2...H_2O = 2.6Å
7O1...Trp56N = 2.8Å
7O2...Arg47N = 2.6Å

Trp56 is conserved in all Pseudomonas cytochromes c_{551} and a similar hydrogen bond occurs between Trp59 and the inner propionic acid of mitochondrial cytochromes c, although Trp59 is not sequentially homologous to Trp56. Arg47 appears to be less important as a hydrogen bonding residue, in that it is replaced by His, Lys or Ser in the other Pseudomonas cytochromes. However, this thesis will contend that the nature of amino acid 47 is important in modulating the pH dependence of redox potential observed for the cytochromes c_{551} through its interaction with propionic acid-7.

P. aeruginosa cytochrome c_{551} contains eight lysines, one arginine, five aspartates and five

glutamates, and so has a net charge of approximately -1 at neutral pH. Almassy & Dickerson (1977) have pointed out that these charges are asymmetrically distributed over the surface of the molecule with 6/9 positive charges occurring in roughly one hemisphere and 8/10 negative charges occurring in the other. However the positive charges do not form a cluster on the front face of the cytochrome c_{551} molecule as they do in the mitochondrial cytochromes. This might explain the observation the the cytochromes c_{551} are poorly reactive with mitochondrial cytochrome oxidase, since cytochrome c is proposed to interact with its oxidase via complementary charge interactions involving the front face lysines.

Section II - The Effect of pH on the Redox Potentials of Some c-Type Cytochromes

A. Derivation of some redox equations

Mitochondrial cytochromes c and their bacterial homologues are soluble proteins, essentially, although they appear to be loosely associated with the cytoplasmic/periplasmic side of the inner mitochondrial/bacterial membrane. On account of their solubility, these cytochromes are relatively easy to purify and much redox potential data on them has accrued; in many cases little else is known about the redox potential properties of the electron transport chains in which they occur. Generally speaking, the cytochromes are stable over a wide range of pH values, consistent with the (chemiosmotic) notion of fluctuating pH at biological membranes. It is often assumed that the redox potential measured ca. pH7 is the typical potential at all pH values, but when considering proteins this is an unreasonable assumption since pH can have such a profound influence on structure. Careful studies, particularly with the cytochromes c_2 from Rhodospirillaceae, have shown that redox potential of cytochromes can be very significantly affected by pH, even within the pH range normally considered to be physiological (~pH6-8). Clark (1960) has discussed the types of E_m versus pH curves obtained for simple inorganic redox systems and has shown that such curves can be analysed in terms of the ionisations perturbing redox potential. His methods of analysis have been successfully applied to curves obtained for more complex redox systems (i.e. biological macromolecules) and, in particular, have been used by Pettigrew et al. to discuss E_m curves obtained for c-type cytochromes. The variety and complexity of these curves justifies some discussion here of how they are analysed.

In the following examples, the redox reaction of a protein involves one or more protons.

(i) One ionisation in the oxidised form. Consider a redox protein containing an ionisable group which ionises at pK_O in the ferric protein; in the ferrous protein, this group does not ionise. Below pK_O, then, the following redox equation holds:

$$oxH + e^- \rightleftharpoons redH.$$

Above pK_O, however, the redox reaction of the protein involves a proton:

$$ox^- + H^+ + e^- \rightleftharpoons redH$$

At low pH, the appropriate form of the Nernst equation is:

$$E_h = E_o + \frac{RT}{nF} \ln \frac{[oxH]}{[redH]} \qquad *$$

This equation applies when the only oxidised and reduced species present are oxH and redH (i.e. when $pH << pK_O$). A general form of the Nernst equation which applies at all pH values is derived below.

Total [oxidised species] = $[oxH] + [ox^-]$

Since $K_O = \frac{[ox^-][H^+]}{[oxH]} \iff [ox^-] = \frac{K_O[oxH]}{[H^+]}$,

then $[oxH] = \frac{\text{total [oxidised species]}}{1 + K_O/H^+}$

Total [reduced species] = [redH]

Therefore, by substituting in *,

$$E_h = \tilde{E} + \frac{RT}{nF} \ln \frac{\text{total [ox.]}/(1 + K_O/H^+)}{\text{total [red.]}}$$

$$\iff E_h = \tilde{E} + \frac{RT}{nF} \ln \frac{\text{total [ox.]}}{\text{total [red.]}} + \frac{RT}{nF} \ln \frac{1}{1 + K_O/[H^+]}$$

When total [oxidised species] = total [reduced species],

$$E_m = \tilde{E} + \frac{RT}{nF} \ln \frac{1}{1 + K_O/[H^+]}$$

$$\iff E_m = \tilde{E} + \frac{RT}{nF} \ln \frac{[H+]}{[H^+] + K_O} \qquad \boxed{\text{Equation 1}}$$

Figure 6: Theoretical Redox Potential versus pH Curves

Equations 1, 2 and 3 in the text describe E_m versus pH curves of the general shape shown in (a), (b) and (c), respectively: (a) one ionisation in the ferricytochrome [Equation 1]; (b) one ionisation in the ferricytochrome and one in the ferrocytochrome [Equation 2]; (c) two ionisations in the ferricytochrome and one in the ferrocytochrome [Equation 3].

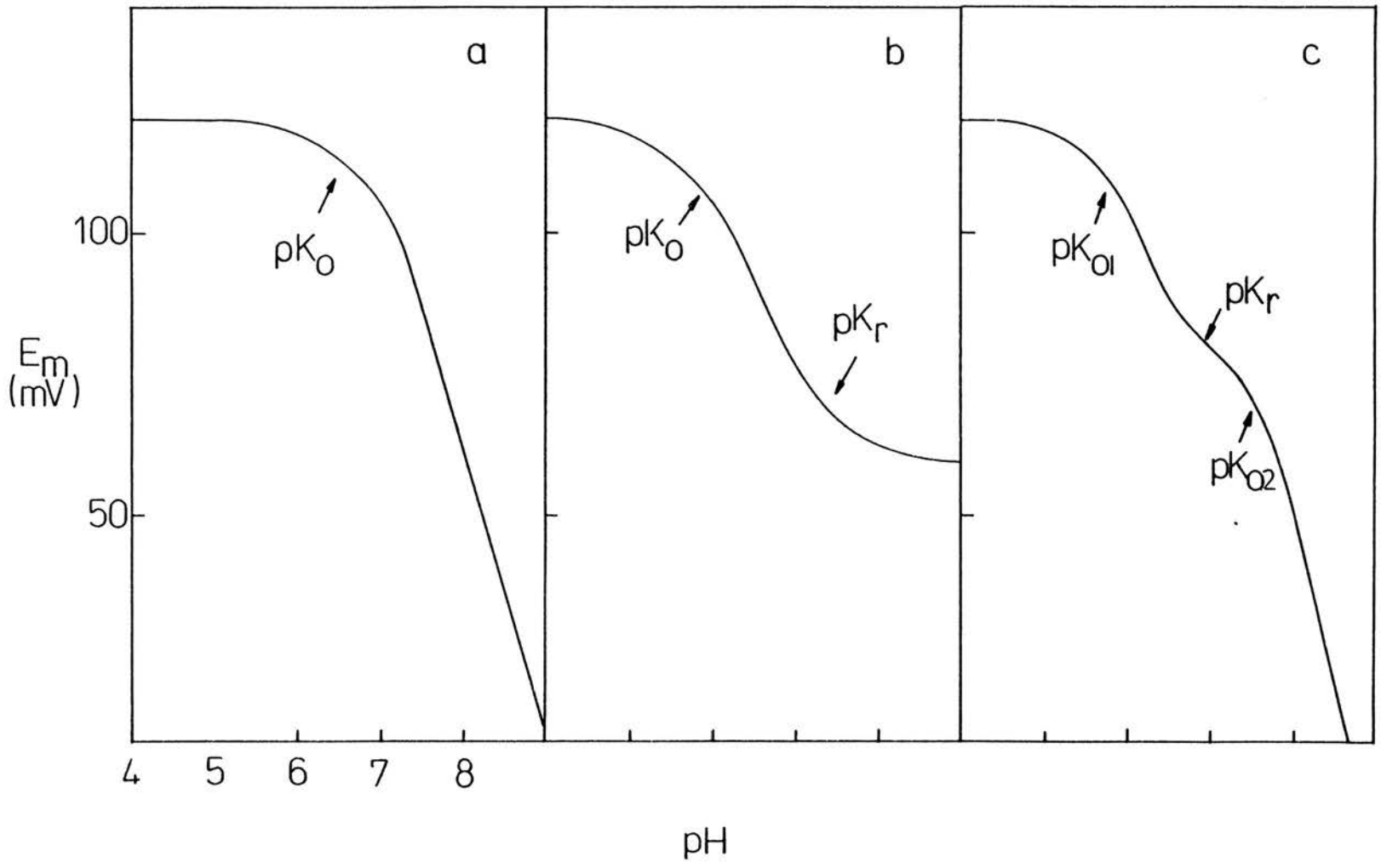
a
b
c
100
50
E_m (mV)
pK_o
pK_o
pK_r
pK_{o1}
pK_r
pK_{o2}
4
5
6
7
8
pH

This equation describes a curve of the general shape shown in Figure 6a. Above pK_O the slope of the curve approaches -60mV/pH unit (when n=1). The symbol $\tilde{E}$ in Equation 1 is obtained by extrapolating the E_m value observed in the region of zero slope below pK_O to pH0; $\tilde{E}$ is not strictly equivalent to E_O since the latter is measured under standard conditions (i.e. oxidant and reductant species present at unit activity etc.). Additionally, $\tilde{E}$ is a theoretical value obtained by extrapolation and may bear no resemblance to E_O if other pKs intervened.

(ii) One ionisation in the oxidised form and one ionisation in the reduced form. In some proteins it may be that an ionisable group ionises with a different pK in each of the two redox states; this may come about if the redox forms of the protein are conformationally distinct or if the redox centre carries a different net charge in its oxidised and reduced states. For example, ferrocytochrome c carries 0 net charge but ferricytochrome c carries a net charge of +1; from electrostatic considerations, therefore, an ionisable species might be expected to ionise preferentially in the ferricytochrome (i.e. $pK_O<pK_R$). Let us then consider the situation where some species ionises with pK_O in the oxidised protein but with a higher pK, pK_R, in the reduced protein. At pH values below pK_O, the following redox equation applies:

$$oxH + e^- \rightleftharpoons redH$$

When $pK_O>pH<pK_R$, a proton is involved in the redox reaction of the protein:

$$ox^- + H^+ + e^- \rightleftharpoons redH$$

At pH values above pK_R, the redox reaction becomes:

$$ox^- + e^- \rightleftharpoons red^-$$

The form of the Nernst equation which is appropriate at low pH values (when the redox potential is not affected by pK_O and pK_R) is:

$$E_h = E_O + \frac{RT}{nF} \ln \frac{[oxH]}{[redH]}$$

In a similar way to the case shown above for one ionisation, a Nernst equation which is applicable at all pH values can be derived by expressing [oxH] in terms of total [oxidised species] and [ox^-] and [redH] in terms of total [reduced species] and [red^-]. Thus,

$$[oxH] = \frac{\text{total [oxidised species]}}{1 + K_O/[H^+]}$$

and $$[redH] = \frac{\text{total [reduced species]}}{1 + K_R/[H^+]}$$

Therefore,

$$E_h = \tilde{E} + \frac{RT}{nF} \ln \frac{\text{total [ox.]}}{\text{total [red.]}} + \frac{RT}{nF} \ln \frac{1 + K_R/[H^+]}{1 + K_O/[H^+]}$$

And when total [ox.] = total [red.]

$$E_m = \tilde{E} + \frac{RT}{nF} \ln \frac{[H^+] + K_R}{[H^+] + K_O} \qquad \boxed{\text{Equation 2}}$$

This equation describes a curve of the general shape shown in Figure 6b. The degree of separation of pK_O and pK_R affects the steepness of the curve between pK_O and pK_R (i.e. the fall in potential) - when the two pKs are separated by more than 1 pH unit, the slope of the curve approaches -60mV/pH unit.

(iii) Two ionisations in the oxidised form and one in the reduced form. Clearly, more than one ionisable species may ionise with redox state dependent pK values and in this example a Nernst equation is derived to describe the situation where three ionisations occur in the order pK_{O1}, pK_R, pK_{O2}. At low pH,

$$oxH_2 + e^- \rightleftharpoons redH_2$$

and the appropriate Nernst equation is

$$E_h = E_O + \frac{RT}{nF} \ln \frac{[oxH_2]}{[redH_2]}$$

The following ionisations occur:

$$oxH_2 \rightleftharpoons oxH^- + H^+ \qquad K_{O1} = \frac{[oxH^-][H^+]}{[oxH_2]}$$

$$redH_2 \rightleftharpoons redH^- + H^+ \qquad K_R = \frac{[redH^-][H^+]}{[redH_2]}$$

$$oxH^- \rightleftharpoons ox^= + H^+ \qquad K_{O2} = \frac{[ox^=][H^+]}{[oxH^-]}$$

Total oxidised species = $[oxH_2] + [oxH^-] + [ox^=]$
Total reduced species = $[redH_2] + [redH^-]$
As in the previous examples, $[oxH^-]$ and $[ox^=]$ can be expressed in terms of $[oxH_2]$ and $[redH^-]$ in terms of $[redH_2]$. Thus,

$$E_h = \tilde{E} + \frac{RT}{nF} \ln \frac{\text{total [ox.]}}{\text{total [red.]}} + \frac{RT}{nF} \ln \frac{1 + K_R/[H^+]}{1 + K_{O1}/[H^+] + K_{O1}K_{O2}/[H^+]^2}$$

When total [oxidised species] = total [reduced species],

$$E_m = \tilde{E} + \frac{RT}{nF} \ln \frac{[H^+]^2 + K_R[H^+]}{[H^+]^2 + K_{O1}[H^+] + K_{O1}K_{O2}} \qquad \boxed{\text{Equation 3}}$$

The shape of the theoretical curve generated by Equation 3 is shown in Figure 6c; it can be regarded as a combination of the curves described by equations 1 and 2. The precise shape of the curve is defined by the degree of separation of pK_{O1}, pK_R and pK_{O2}.

Equations can be derived in this way to cover any number of ionisations occuring in the sequence pK_{O1}, pK_{R1},.... pK_{On}, pK_{Rn}, and similar equations can be derived for redox systems in which pK_R occurs before pK_O (see Harbury, 1957). In plots of E_m versus pH, pKs occuring in the oxidised form involve a change in the slope of the curve to more negative values; pK_R values can be correlated with a change in slope to more positive values. A theoretical curve can thus be constructed for any set of E_m versus pH data by observing the number and type of inflection points, since these will indicate the appropriate equation; a best-fitting curve is then obtained by choosing suitable values for the pKs.

B. Mitochondrial cytochromes c

Only one or two representatives of the mitochondrial cytochrome c family have been thoroughly studied by redox potentiometry, but they form a very homogeneous class as regards physicochemical properties.

The redox potential of horse cytochrome c has been measured over a range of pH values by Rodkey & Ball (1959) and by Margalit & Schejter (1973), who found that the E_m versus pH curve could be described by Equation 1 above i.e. a single pK occurs in the ferricytochrome. In Figure 7 (F.A. Leitch, unpublished data), the theoretical curve was obtained by setting $pK_O = 8.9$ in Equation 1.

It has now been shown by a number of kinetic experiments that pK_{ox} is an apparent pK which results from rapid deprotonation of a group with pK = 11 and a much slower coupled conformational change (Brandt et al., 1966; Davis et al., 1974; Kihara et al., 1976) This "alkaline isomerisation" is completely reversible. The conformational change is associated with loss of the near-infrared absorption band at 695nm in the ferricytochrome spectrum and the disappearance of the Met80 methyl resonance from the ferricytochrome NMR spectrum (Wilson & Greenwood, 1971; Gupta & Koenig, 1971); Met80 is the 6th ligand to the haem iron and the 695nm band is associated with the Met80-iron bond,so the evidence suggests that the conformational change leads to breakage of the Met80-iron bond. Since the iron remains low-spin above pK_O, then Met80 must be replaced by another strong field ligand. Two lines of evidence suggest that Met80 is replaced by a lysine (i) EPR spectra indicated a ϵ-amino nitrogen: haem iron bond in the alkaline state of ferricytochrome c (Brautigan et al., 1977) (ii) the pK of the triggering ionisation is compatible with that of a lysine side chain. Met80 is immediately adjacent to a lysine residue (Lys79) and only a limited conformational rearrangement would be required

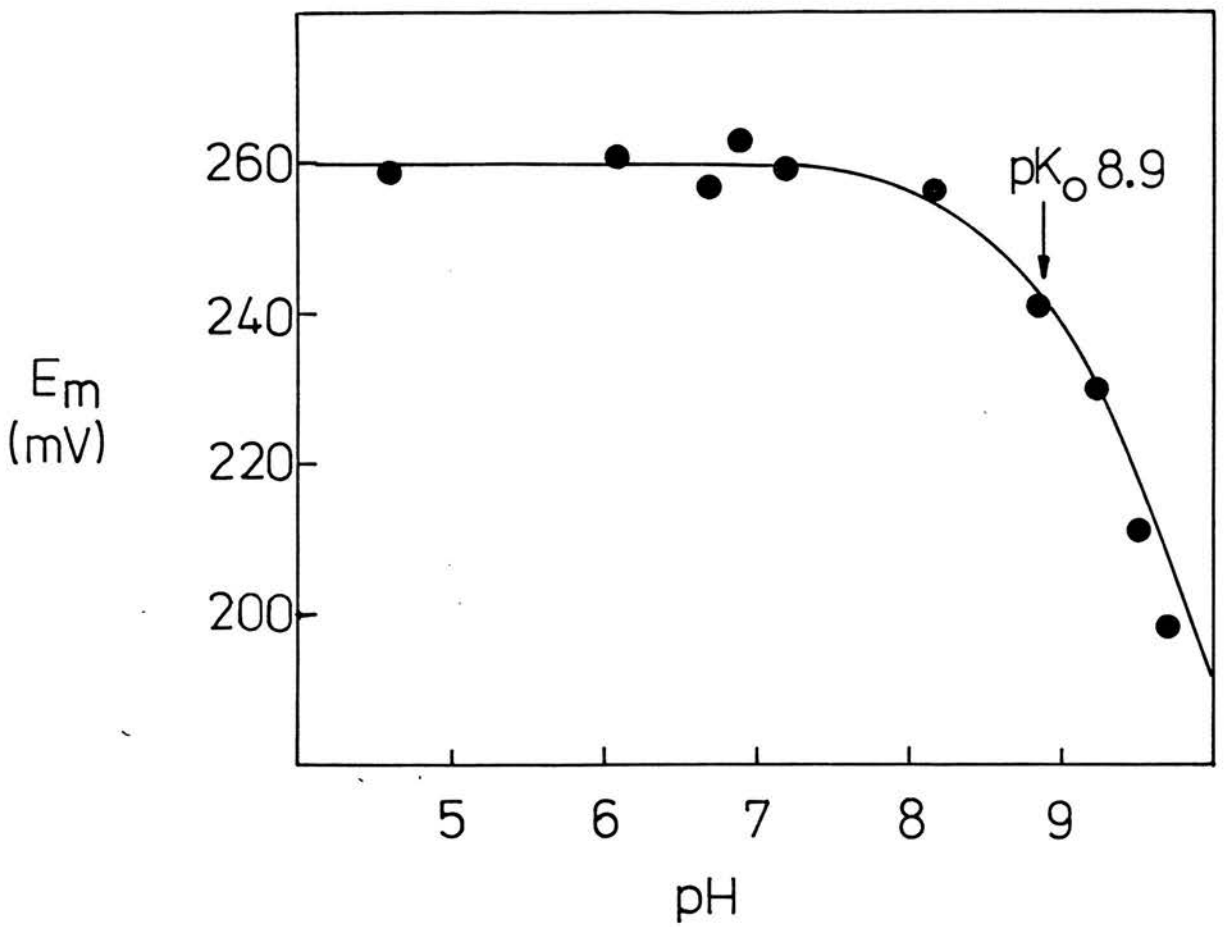

Figure 7: $\underline{E_m}$ versus pH for Horse Cytochrome c

The solid line is the theoretical curve obtained with Equation 1 using $pK_o = 8.9$.

to effect its substitution, so Lys79 has been the preferred candidate for the new ligand. Another nearby lysine, Lys72, has also been proposed. However, Pettigrew et al. (1976) found that fully amidinated cytochrome c (i.e. no free lysines) loses its 695nm band with a pK of 9.2, indicating that lysine is not involved in the alkaline isomerisation. Additionally, Bosshard (1981) showed that both Lys72 and Lys79 were acetylated at identical rates at pH7 and pH11 - reactivity with acetylating reagents should be drastically reduced if the ϵ-amino group of either lysine forms a coordination bond with the haem iron. Thus, the identity of the 6th ligand at alkaline pH remains controversial.

In ferrocytochrome c, the alkaline isomerisation is not observed below pH12 and above pH12 the ferrocytochrome adopts a partially denatured conformation (Theorell & Åkeson, 1941).

Pettigrew et al. (1975) have studied cytochrome c_{557} from Crithidia oncopelti and cytochrome c_{558} from the alga, Euglena gracilis. These cytochromes are unusual amongst the mitochondrial cytochromes c (and, indeed, amongst c-type cytochromes generally) in that the haem is covalently bound via only one thioether linkage. Their redox potentials measured at pH7 are only slightly lower (ca. 10-20mV) than the potential of horse cytochrome c and the E_m versus pH curves are also described by a single pK occurring in the ferrictyochrome; for cytochrome c_{557}, pK_O = 8.6 and for cytochrome c_{558}, pK_O = 9.8. The alkaline isomerisation of cytochrome c_{557}, but not cytochrome c_{558}, appears to follow the same kinetic path as for horse cytochrome c; for the latter protein, a model involving two ionisations followed by a conformational change has been proposed.

C. Cytochromes c-2

The cytochromes c_2 are found in purple non-sulphur bacteria (Rhodospirillaceae) where their function appears

to be as immediate electron donor to the photochemical reaction centre or as reductant to the terminal oxidase of the respiratory chain, depending on the mode of growth of the organism. Within Class I (see page), the cytochromes c_2 are the group most closely related to the mitochondrial cytochromes c. Within the group, the cytochromes c_2 show greater than 30% identity in amino acid sequence but the polypeptide chain length varies from 100-124 amino acids and redox potentials (measured at pH5) span the range 290-400mV (Pettigrew et al., 1978). Pettigrew and co-workers (Pettigrew et al., 1975; Pettigrew et al., 1978) have measured the midpoint redox potentials of some 13 different cytochromes c_2 between pH4 and 10 and find that the E_m versus pH profile for all the cytochromes belongs to one of two categories. In the first category, the curve can be described by a single pK on the oxidised cytochrome, as is the case for horse cytochrome c (i.e. Equation 1 in above section). Examples of cytochromes showing this behaviour are Rps. capsulata, Rps. acidophila and R. photometricum cytochromes c_2 - their E_m versus pH profiles are shown in Figure 8. In the second category, the curve shows three pKs, one in the reduced form and two in the oxidised form of the cytochrome, in the sequence pK_{O1}, pK_R, pK_{O2} - this category is exemplified by Rm. vannielii and Rps. sphaeroides cytochromes c_2 (Figure 9). The appropriate equation to describe Type 2 curves is Equation 3 discussed above.

The pK_O in Type 1 curves and pK_{O2} in Type 2 has been correlated with the loss of the 695nm absorbance band, indicating that the 6th ligand Met: iron bond ruptures. Prince & Bashford (1979) carried out a kinetic analysis of Rps. sphaeroides cytochrome c_2 and showed that pK_{O2} can be attributed to the combination of a pK above 11 and a relatively slow conformational change. Thus, at alkaline pH values, the cytochromes c_2 behave much like their mitochondrial counterparts. It is interesting to

Figure 8: E_m versus pH for Some Cytochromes c-2 Showing Type 1 Curves

The solid lines are theoretical curves obtained using Equation 1 and the pK_o values indicated. The experimental data are taken from Pettigrew et al. (1978) and are for ○ R. photometricum, ● Rps. capsulata and ◊ Rps. acidophila cytochromes c_2.

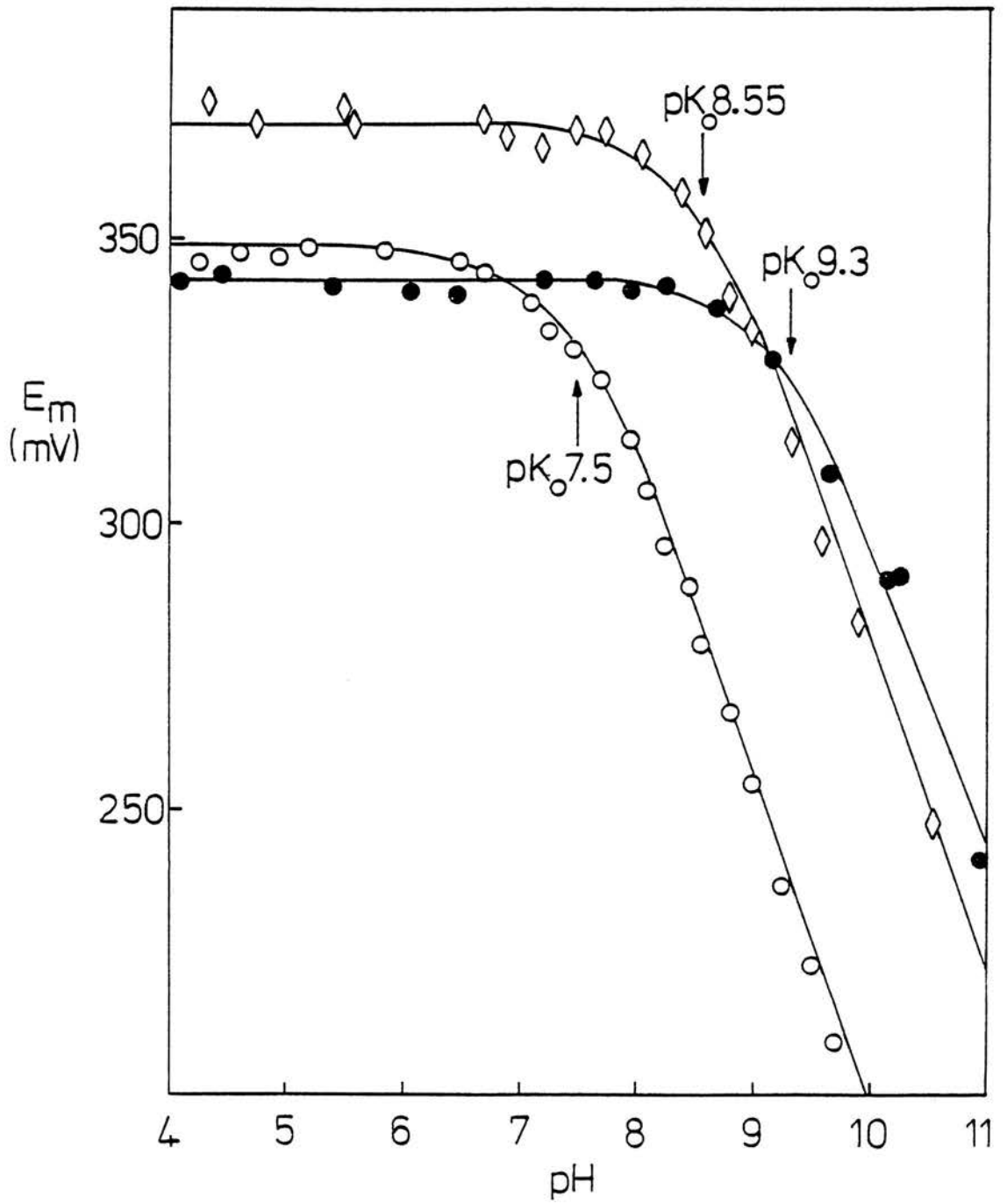
pK 8.55
pK 9.3
pK 7.5
350
300
250
E_m
(mV)
4
5
6
7
8
9
10
11
pH

Figure 9: E_m versus pH for Some Cytochromes c-2 Showing Type 2 Curves

The solid lines are theoretical curves obtained with Equation 3 using the pK values indicated. The experimental data are taken from Pettigrew et al. (1975, 1978) and are for O*Rm. vannielii* and ●*Rps. sphaeroides* cytochromes c_2.

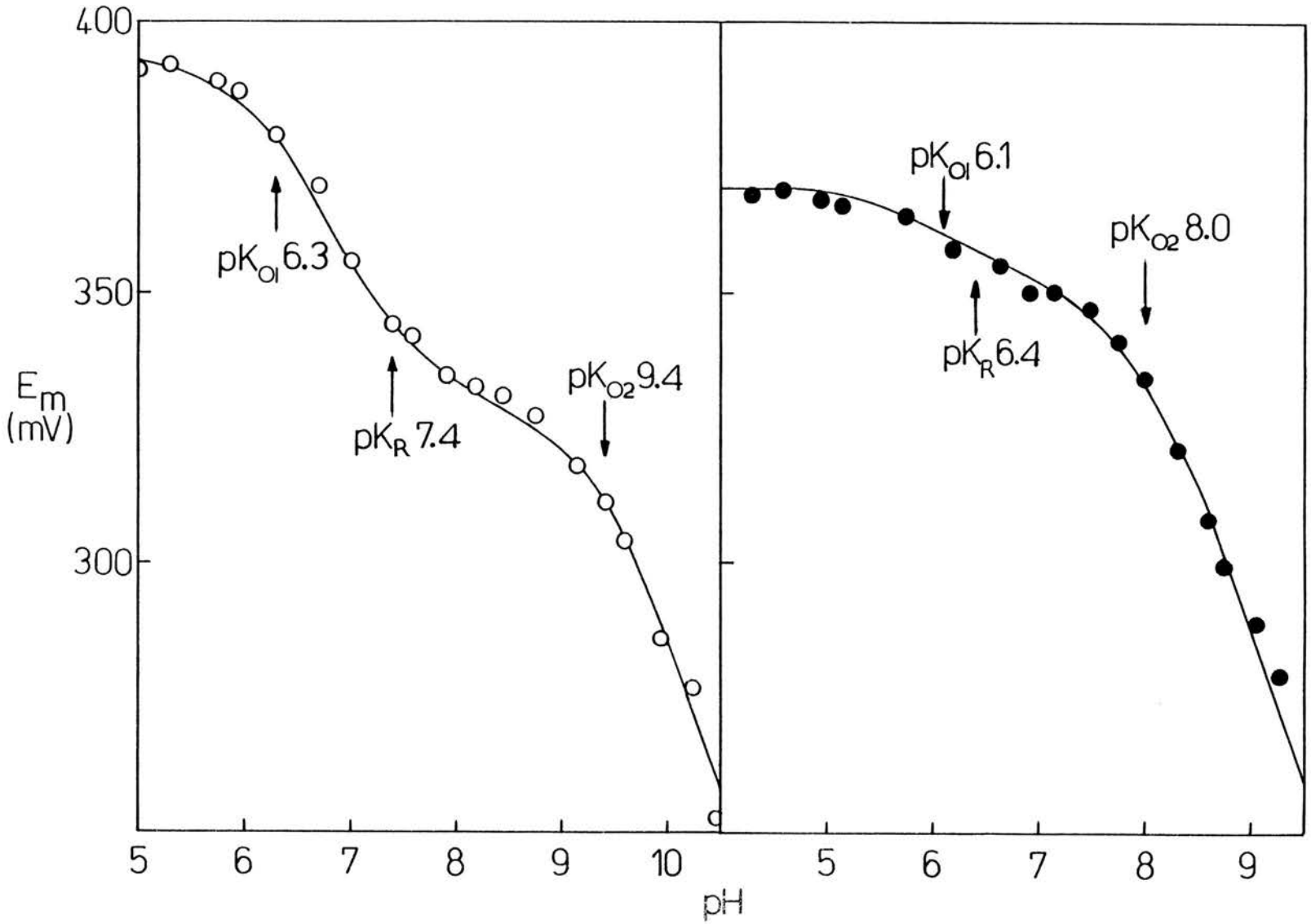
400
350
300
E_m (mV)
pK_{O1} 6.3
pK_R 7.4
pK_{O2} 9.4
pK_{O1} 6.1
pK_R 6.4
pK_{O2} 8.0
5
6
7
8
9
10
pH

note, then, that not all cytochromes c_2 contain a lysine residue adjacent to the 6th ligand methionine, so pK_O (or pK_{O2}) cannot generally be explained by substitution of methionine by this lysine. Since $pK_{O/O2}$ occurs above pH9 in some cytochromes c_2 but occurs as low as pH7.35 in R. molischianum iso-1-cytochrome c_2, then the environment of the 6th ligand methionine must vary considerably within the cytochrome c_2 group (consistent with the large span of $E_{m,5}$ values).

With regard to pK_{O1} and pK_R of Type 2 curves, it has been assumed that a single species ionises with redox state dependent pK values; the separation of its pK values in the two oxidation states of a cytochrome is attributed to the electrostatic influence of the haem, which has 0 net charge in the ferrocytochrome but a net charge of +1 in the ferricytochrome (since two of the pyrrole nitrogens of protoporphyrin IX carry negative charges). The degree of separation between pK_{O1} and pK_R (and pK_{O2}) defines the shape of the E_m versus pH curve - the closer these values are together then the smoother the resulting curve. As can be seen from Figure 9, the cytochromes show varying degrees of separation for pK_{O1} and pK_R, ranging from 0.3 pH units (Rps. sphaeroides cytochrome c_2) to 1.1 pH units (Rm. vannielii cytochrome c_2). Generally, pK_{O1} and pK_R do not influence the absorption spectrum of these cytochromes, but some recently obtained data (Moore et al., 1983 - see Appendix II) show that these pKs are observed in pH titrations of NMR spectra - these data will be considered subsequently in Discussion. Wood et al. (1977) studied the kinetics of oxidation and reduction of R. rubrum cytochrome c_2 with a number of inorganic redox reagents and observed the same pK_{O1} and pK_R values deduced by Pettigrew et al. (1978) from their redox measurements on the cytochrome; they proposed that pK_{O1} and pK_R reflected the ionisation of haem propionic acid-6. Pettigrew et al. also felt that a propionic acid substituent might be the ionising group in

all the cytochromes but suggested that it is propionic acid-7 rather than propionic acid-6. Their reason for preferring the former lies with the fact that this propionic acid is adjacent to an arginine residue (Arg38) in nearly all the cytochromes studied, with the exception of R. rubrum and Rm. vannielii cytochromes c_2, which have Asn38 and Gln38, respectively. These two cytochromes also show the largest separation of pK_{Ol} and pK_R values. It was speculated that Arg38 can stabilise the negative charge produced when propionic acid-7 ionises and that, in its absence (R. rubrum and Rm. vannielii cytochromes), the pK values of the propionic acid in the oxidised and reduced cytochromes may be separated by the influence of the haem group. Presumably, propionic acid-7 also ionises in those cytochromes with Type 1 E_m versus pH curves, but at the same pK value in both oxidation states. However, no explanation was offered for why some cytochromes c_2 (e.g. Rps. viridis cytochrome c_2) have Type 2 curves even though they contain Arg38. This point will be dealt with further in Discussion.

Prince and co-workers (Prince & Dutton, 1977; Prince & Bashford, 1979) questioned the in vivo significance of the various pK values observed for the purified cytochromes c_2. They claim that the redox potentials of Rps. sphaeroides and Rps. capsulata cytochromes c_2 bound to their chromatophore membranes are independent of pH between pH5 and 11. However, two points should be made regarding methodolgy: (i) Prince & Dutton (1977) carried out flash-activated redox titrations of the cytochrome c_2 in chromatophores, in which antimycin A was used to prevent re-reduction of cytochrome c_2 (following oxidation by the photooxidised reaction centre). Since two saturating flashes of light are required to completely oxidise the cytochrome c_2 (in the presence of antimycin A), and since Dutton et al. (1975) had found 2 cytochrome c_2 molecules in association with each reaction centre, Prince & Dutton analysed their redox titration

curves according to the appropriate statistical model. However, Bowyer et al. (1979) subsequently showed that the antimycin block is leaky, allowing re-reduction of some cytochrome before the second flash, and that byadding UHDBT (a quinone analogue) all the cytochrome c_2 is reduced after the first flash. In addition, these authors found only one cytochrome c_2 per reaction centre. The conclusions reached by Prince & Dutton are invalidated by these latter findings (ii) Prince & Bashford (1979) measured the midpoint potential of Rps. sphaeroides cytochrome c_2 bound to chromatophore membranes by a different method to that used above, and concluded that the redox potential is independent of pH in the range pH7-12. Moore & Pettigrew (1984) have pointed out that this analysis of Rps. sphaeroides cytochrome c_2 in situ assumes that only one c-type cytochrome species is present in chromatophores (i.e. cytochrome c_2) and that this assumption is unjustified in the light of Wood's demonstration (Wood, 1980 a,b) that a cytochrome resembling mitochondrial cytochrome c_1 occurs in Rps. sphaeroides membranes; in chromatophores the cytochrome is present in an approximately 1:1 ratio with cytochrome c_2.

D. Pseudomonas aeruginosa cytochrome c-551

Denitrifying species of Pseudomonas are rich in c-type cytochromes, of which cytochrome c_{551} is the most abundant. Hence, P. aeruginosa cytochrome c_{551} has been a popular choice for structural and functional studies on haemoproteins. This cytochrome is much more distantly related to the mitochondrial cytochromes c than any of the cytochromes c_2 and so its redox potential behaviour is interesting from a comparative point of view.

Moore et al. (1980) measured the redox potential of P. aeruginosa cytochrome c_{551} between pH4 and 10 and obtained the E_m versus pH profile shown in Figure 10. The theoretical curve was drawn using Equation 2 above and pK_O = 6.2 and pK_R = 7.3. The 695nm absorption band was

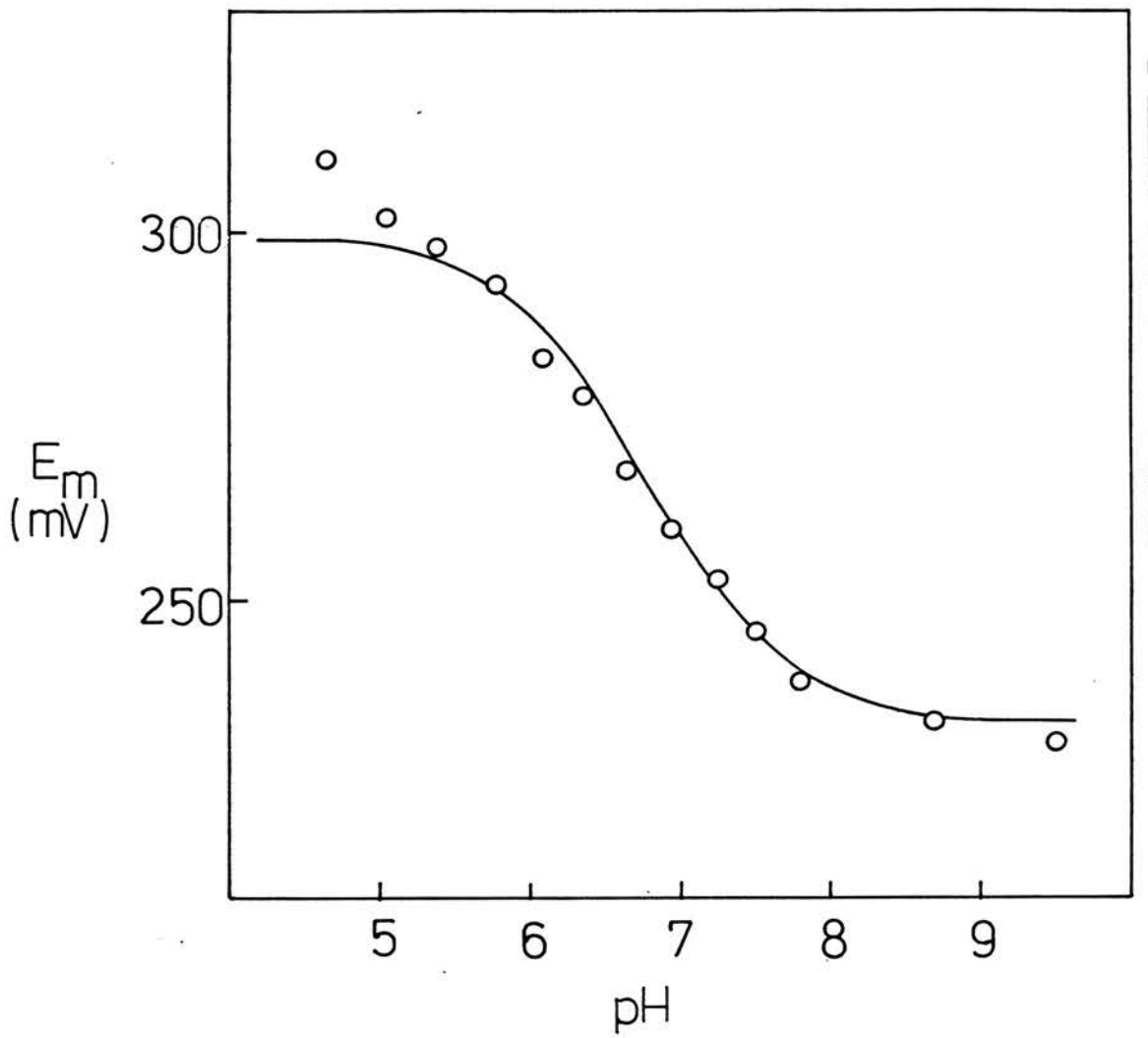

Figure 10: E_m versus pH for P. aeruginosa Cytochrome c-551

The data are taken from Moore et al. (1980). The theoretical curve was drawn using Equation 2 with pK_O = 6.2 and pK_R = 7.3.

unaffected below pH10.1 but these authors did not comment on whether its eventual disappearance above this pH is due to an alkaline isomerisation or simply to denaturation. However, the ESR work of Chao et al. (1979) indicated that although the 695nm band is lost with a pK of 10.6, the cytochrome remains low spin below pH11. Some other ligand must then replace Met61 between pH10 and pH11.

The values of pK_O and pK_R derived from the redox potential profile were confirmed experimentally in two ways: (a)the α-peak maximum of ferrocytochrome c_{551} shifts from 551 to 553nm with increasing pH and the shape of the peak becomes markedly asymmetrical; these spectroscopic changes were fitted to a pK of 7.2 (b) the ^1H NMR spectrum of the ferricytochrome showed that the chemical shifts of a number of haem substituent resonances were affected by a pK of approximately 6 (Chao et al. [1979] independently obtained a similar pK value); in the ferrocytochrome, resonances of the 6th ligand methionine shifted slightly with a pK of 7.2. Moore et al. reasoned that the size of the pH dependent chemical shifts experienced by the haem substituent resonances means that the ionisable group is close to the haem, and suggested that pK_O and pK_R may be due to the ionisation of the haem 5th ligand, His16, or to one of the propionic acid substituents. They further argued that ionisation of His18 would result in large structural changes since protonated imidazole cannot function as a ligand; as only minor structural changes are observed, then this possibility can be eliminated. No suggestion was made as to which of the two propionic acids ionises. From their NMR work on ferricytochrome c_{551}, Chao et al. proposed that it is propionic acid-7 which ionises; they pointed out that propionic acid-6 is exposed to solvent in this cytochrome whereas propionic acid-7 is not - since the pK of 6 is fairly high for a solvent exposed carboxylic acid, then it must be propionic acid-7 which ionises.

There is less information on the nature of the group which ionises in the ferrocytochrome, mainly because most of the haem substituent resonances are not resolved in the NMR spectrum of the ferrocytochrome; it is assumed to be propionic acid-7 also.

Section 3 - NMR Aspects

N.B. The numbered superscripts in this section refer to the notes in Appendix I.

1. The ^{1}H NMR spectrum of c-type cytochromes

NMR spectroscopy is one of the most flexible techniques available for protein structural studies: it can be used to determine many different molecular parameters through measurement of resonance chemical shifts, intensities, linewidths and multiplicities, and by measuring perturbations in all these parameters which result from changes in molecular environment. The most severe limitation in applying NMR to biological problems is that useful spectra can only be obtained from relatively low molecular weight proteins (<30000 daltons); resonance linewidths in spectra of larger proteins are very broad, obscuring multiplet structure, and so assignment of resonances is virtually impossible. In this respect, though, the Class I c-type cytochromes are well suited to NMR studies as they occur towards the low end of the protein molecular weight range.

However, even with small proteins resonance assignment is never a particularly straightforward process; the bulk of resonances occur within a very limited region of the spectrum, giving rise to considerable overlap. Figure 11 indicates the approximate chemical shift positions for the various types of proton resonances in a typical Class I cytochrome ^{1}H NMR spectrum (horse ferricytochrome c). The aliphatic region between 5 and 0 ppm contains several hundred overlapping resonances, and even at an operating frequency of 300 MHz much of the structural information inherent in this part of the spectrum is masked[1]. Generally speaking, aliphatic assignments <u>are</u> possible using high field instruments and multiple pulse methods but it is an enormously time consuming (and thus largely impracticable) process.

Figure 11: ^{1}H NMR Spectrum of Horse Ferricytochrome c

(Narrow Sweep)

The spectrum was obtained at pH* 6.7, 27°C. The regions of the spectrum containing NH resonances, aromatic resonances and aliphatic resonances are indicated. The HOD resonance was minimised by solvent suppression.

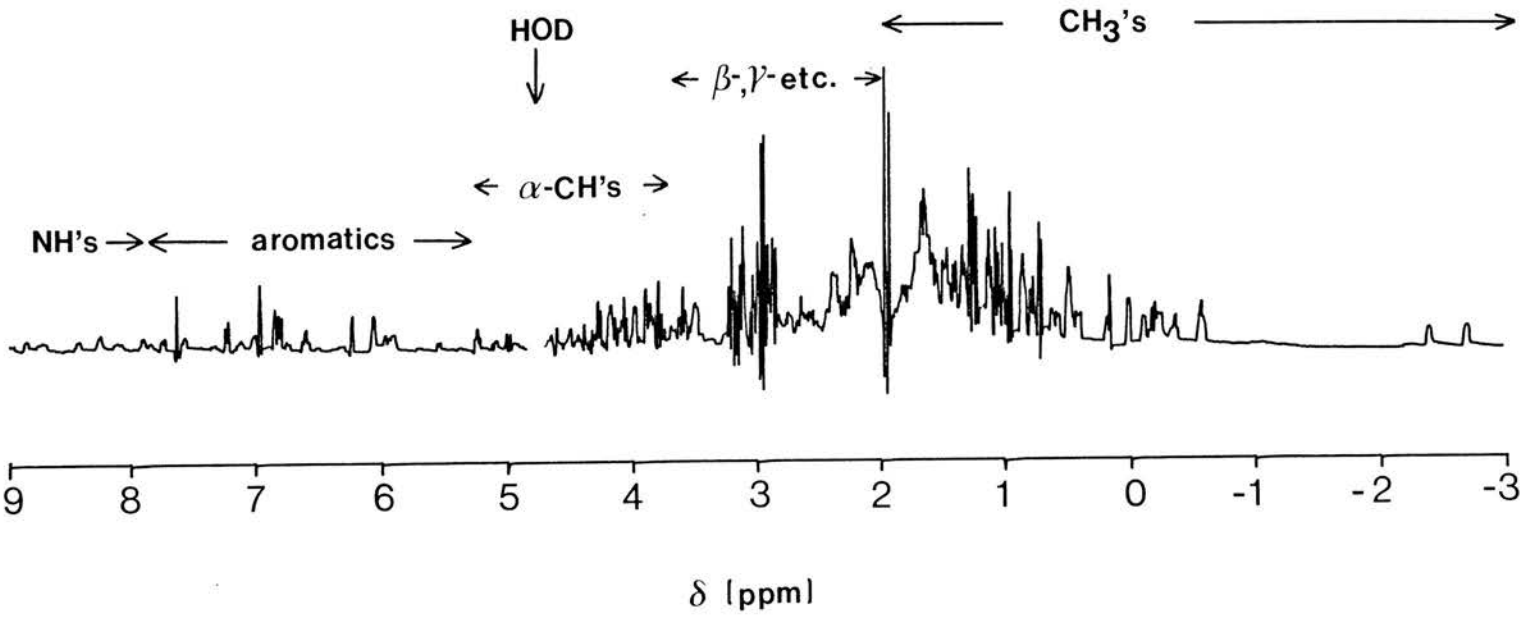

The aromatic region from 10 to 5 ppm is much more accessible. Aromatic resonances are resolved from aliphatics because protons directly attached to aromatic rings experience deshielding ring current effects[2]. Aromatic amino acids are relatively rare in most proteins (horse cytochrome c contains 12 out of 100) and only ca. 20-30 resonances might occur in this region. Individual resonances and their multiplet structures are observable so complete assignment of the aromatic resonances is quite feasible. Although fairly limited in number, consideration of these resonances should be sufficient to give a general picture of how a protein responds to changes in its molecular environment.

In ^{1}H NMR spectra of c-type cytochromes there are a number of resonances other than those of the aromatic amino acids which are resolved from the aliphatic region. These are resonances from substituent groups on haem c and from the 5th (His) and 6th (Met) iron ligands. The conjugated π-bond system of the porphyrin ring gives rise to shielding and deshielding ring current effects much like the rings of aromatic amino acids. The haem substituent resonances tend to be downfield shifted from the aliphatic resonances by these diamagnetic effects while the axial ligand resonances are upfield shifted. In horse ferrocytochrome c, for example, the four haem meso proton resonances occur ca. 9-10 ppm, the His 18 resonances ca. 0 ppm and the methyl resonance of Met 80 at -3.3 ppm (Keller & Wüthrich, 1978a; Moore & Williams, 1980e).

There is one other property of c-type cytochromes which gives rise to unusally large chemical shifts for certain resonances in the ferricytochrome: low spin ferric iron is paramagnetic (s=1/2). The magnetic environment of a group in direct contact with a paramagnetic centre is profoundly influenced by the spin of the unpaired electron: as indicated in Figure 12, ferricytochrome spectra contain resonances between 5 and

Figure 12: ^{1}H NMR Spectrum of Horse Ferricytochrome c (Wide Sweep)

The spectrum was obtained at pH* 6.7, 27°C. Me8, Me3 and M80 are, respectively, the haem methyl 8, haem methyl 3 and Met80 methyl resonances.

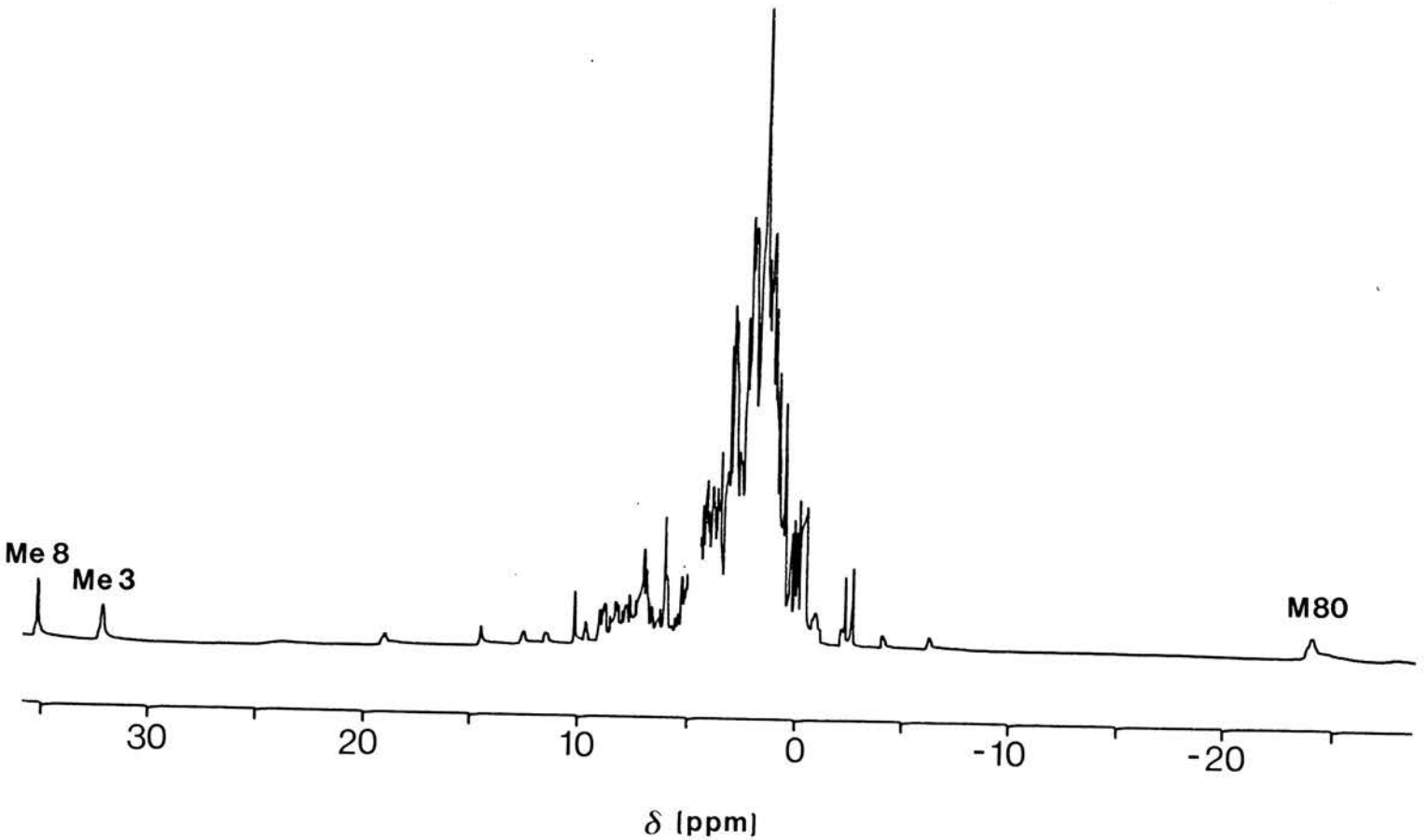
Me 8
Me 3
M80
30
20
10
0
-10
-20
δ (ppm)

40 ppm and between -5 and -20 ppm. The magnitude of their shifts means that these resonances must arise from protons of haem substituent or iron ligand groups so their assignment in the ferricytochrome is quite straightforward. Low spin ferrous iron is diamagnetic, which accounts for the different distribution of axial ligand and haem substituent resonances in the two oxidation states.

2. Some more about haem substituent and axial ligand resonances

Since haem substituent and axial ligand resonances have a central role in this thesis, it is appropriate here to say a few words about them. From Figure 5 it can be seen that there are four methyl substituents at positions 1, 3, 5 and 8 on the haem ring, four meso protons designated α, β, γ, and δ, two thioether groups at positions 2 and 4, and two propionic acid substituents, 6 and 7. Because single protons and methyl groups are asymmetrically distributed around the haem ring, nuclear Overhauser enhancement (NOE) experiments[9] can be used to assign many of the resonances (Keller & Wüthrich, 1978a); nuclear Overhauser effects between neighbouring substituents are facilitated by the rigidity of the haem ring. Chemical shifts for the substituent resonances in horse cytochrome c are given in Table III.

In ferrocytochrome c, the shifts of these resonances are influenced mainly by the haem aromatic ring current but in the ferric state, hyperfine coupling of the protons with the unpaired electron is dominant over the ring current effect. As discussed below, distribution of the unpaired electron spin density over the haem ring is asymmetric and some resonances (e.g. methyl 8) experience much larger hyperfine shifts[10] than others (e.g. methyl 5). The direction in which resonances are shifted by hyperfine coupling is also variable (Wüthrich, 1970); the methyl and propionic acid resonances are shifted downfield from their diamagnetic positions but the

Table III: Chemical Shifts of Some Haem Substituent and Iron Ligand Resonances in Horse Cytochrome c

	Chemical Shift (ppm)	
Resonance	Ferrocytochrome	Ferricytochrome
haem methyl 1	3.52[a]	7.4[a]
3	3.87	31.2
5	3.61	10.5
8	2.19	33.9
haem meso α	9.32[a]	
β	9.59	
γ	9.62	
δ	9.04	
propionate-6		19[b]
		12
propionate-7		14.5[b]
		8.5
thioether-2 -CH	5.25[a]	
$-CH_3$	1.5	-2.1[a]
thioether-4 -CH	6.34[a]	
$-CH_3$	2.6	3.1[a]
Met 80 ϵ-CH_3	-3.28[c]	-21.0[c]
γ-CH^3	-3.73	-24.9
γ^2-CH	-1.87	-22.2
β-CH	-2.58	
β-CH	-0.19	
His 18 C-2	0.5[d]	
C-4	0.13	

a. Keller & Wüthrich, 1978(a); b. G. Williams & G. Moore, unpublished data; c. Moore & Williams, 1980(b); d. Moore & Williams, 1980(a).

thioether-2 and at least some of the meso resonances are shifted upfield. Also, some of the axial methionine resonances are shifted far upfield by contact coupling. The histidine resonances have not been assigned in horse ferricytochrome c; the His18 α-CH resonance occurs at 8.96 ppm (pH*5.5) in tuna ferricytochrome c (G. Williams & G. Moore, unpublished data) and studies with yeast cytochromes indicate that the His18 C-4 resonance appears downfield, ca. 25 ppm (Senn et al., 1983).

3. Assignment of amino acid resonances

In a protein NMR spectrum a resonance is first assigned to a type of amino acid (first-stage assignment) and then to a specific residue in the protein sequence (second-stage assignment).

To accomplish first-stage assignment, it is essential to resolve the individual resonances. Three factors contribute to the difficulty in resolving the peaks in a protein spectrum: (i) the number of resonances (ii) the limited spread of chemical shift values (iii) the linewidths of resonances. Levine et al. (1979) have discussed the different methods for resolution enhancement and suffice to say here that improved spectral resolution can be achieved at higher spectrometer operating frequencies (number of Hz/ppm increases), by heating samples (decreases resonance linewidth) or by isotopic substitution (decreases number of resonances). Additionally, mathematical manipulations can be performed on the free induction decay to give a better resolved spectrum.

When satisfactory resolution has been attained, groups of coupled resonances are then identified and assigned to a particular type of amino acid on the basis of intensity and characteristic coupling patterns. Table VIII (page 119) shows the coupling patterns observed for each of the aromatic amino acids. Thus, a doublet appearing in the aromatic spectrum might arise from Phe, Trp or Tyr and so it must be ascertained to which other

aromatic multiplets it is coupled. This can be accomplished by the double resonance method of spin-decoupling, which is outlined in Appendix (note 3); briefly, irradiation at the doublet will remove the multiplet splitting of other resonances to which it is coupled.

The successful first-stage assignment of a protein will, for example, enable one to discriminate from all other peaks in the spectrum each of the resonance families that correspond to each of the phenylalanine side chains in the protein. However, this information in itself is of no immediate value in the search for structural information; it is only when each group of resonances can be assigned to its specific residue in the protein sequence that conformational data can be obtained. How then are second stage assignments made? Some possibilities are: (i) chemical modification - modification of a specific amino acid residue and observation of the corresponding change in the NMR spectrum provides a good method of assignment, although it must be remembered that in a folded molecule the modification of one residue may perturb the resonances from other residues. (ii) comparison of homologous proteins - this has proved a very successful method for the second stage assignment of cytochrome c resonances (Moore & Williams, 1980f). Some 70 eukaryotic cytochromes c have been sequenced and they differ from each other by 1 to 45 residues per hundred. (iii) secondary shifts - the secondary shifts[8] in the spectrum of a non-random coil protein are caused by a number of effects, including hydrogen bonding, the shielding attributable to carbonyl groups and the degree of ionisation of an ionisable group. In diamagnetic proteins, the perturbation of most interest is the ring current shift produced by aromatic groups. The resonances of nuclei close to an aromatic ring are shifted from their random coil positions in a way that depends on their orientation with respect to the

ring[2]. In cytochromes, the ring current shifts induced by the aromatic haem are particularly useful in resonance assignment. In paramagnetic proteins, such as ferricytochrome c , large secondary shifts are observed for resonances close to the paramagnetic centre, facilitating second stage assignments. (iv) extrinsic probes - any ion or small molecule that binds to a specific site on a protein is an extrinsic probe; if it is known where a probe binds on the protein then second stage assignments can be made from consideration of the perturbing effects of the probe on the protein spectrum. Paramagnetic ions form an important group of probes. Binding of these molecules will shift and/or broaden resonances at their binding site to an extent that depends on the geometry and symmetry of the particular paramagnetic complex. Iron hexacyanides, for example, have been used as extrinsic probes in studies with cytochrome c (Boswell et al., 1982; Eley et al., 1982). The H^+ ion can also be considered as an extrinsic probe; measurement of the pK value for an ionisable group is useful in assessing whether the group is buried in the centre of the protein or occurs near the surface.

4. ^{1}H NMR studies on the c-type cytochromes

NMR studies on the c-type cytochromes have aimed at elucidating structural features which might be important for the electron transfer function, as the mechanism of electron transfer is still unknown. Two groups have dominated the field - Moore, Williams and co-workers have concentrated on the role of the polypeptide chain, while Wüthrich and co-workers have considered the haem and its axial ligands. Horse and tuna mitochondrial cytochromes c (and, more recently, P. aeruginosa cytochrome c551) have been the focus of the NMR studies, since crystal structures are available for these. NMR is the only technique which can, in principle, yield the same sort of detailed structural information as X-ray crystallography, but for proteins in solution, and so much of the NMR work

on cytochrome c has sought to distinguish whether its solution structure is different from the static, crystal structure. Redfield & Gupta (1971) and Keller & Wüthrich (1978) assigned many of the haem substituent and axial ligand resonances in both oxidation states of horse cytochrome c and Moore & Williams (1980 a,b) assigned most of the aromatic and a number of aliphatic resonances. Moore & Williams (1980e) concluded that "... the positions in space of Ala 15, His 18, Tyr 46, Tyr 48, Trp 59, Met 80 and Phe 82 as given by the X-ray structure provide a uniquely acceptable description for the solution structure; we do not believe that it is possible to fold the protein in any other way and to explain these [NMR] data." The same data have also been able to reveal something of the dynamic behaviour of cytochrome c - it appears that the molecule is rigidly constructed at the centre (presumably because of the constraints imposed by side chain packing around the haem group) but that it is more flexible at the surface. One region of the molecule, in the vicinity of Ile 57 (see ribbon diagram on page 19), was shown to be particularly mobile (Moore & Williams, 1980 c). The NMR work largely confirms the conclusion from X-ray crystallography that there is little conformational difference between ferri- and ferrocytochrome c, despite much physicochemical data indicating the contrary. However, a small conformational change was detected by NMR in the region of Ile 57 (Moore & Williams, 1980d). This observation is particularly interesting in view of the fact that horse ferri- and ferrocytochrome are antigenically distinct and that there is a major antigenic site near residue 57 (Margoliash et al., 1970; Nisonoff et al., 1970). (The most recent X-ray data for tuna cytochrome c shows that the positions of a number of amino acids are affected in a minor way by redox state changes; these include residues of the 50's region [Takano & Dickerson, 1981]).

One noticeable feature of the unpaired electron in

horse ferricytochrome c is the asymmetrical distribution of its spin density over the haem ring. A large proportion of the spin densitiy (ca. 2% of the unpaired electron) is localised on porphyrin ring carbon atoms 3 and 8, whereas much smaller spin densities (<0.5% of the electron) reside on ring carbons 1 and 5. The concentration of spin density on carbons 3 and 8 has a marked effect on the ferricytochrome spectrum in that relatively large hyperfine chemical shifts are observed for the methyl substituents attached to these carbon atoms compared to the shifts observed for methyls 1 and 5 (δ = 33.9 ppm [M8], 31.2 ppm [M3], 10.5 ppm [M5] and 7.4 ppm [M1]). Keller & Wüthrich (1978a) originally commented that this might be an invariant feature of all c-type cytochromes and an essential factor in their biological function. When they assigned the haem substituent resonances in P. aeruginosa cytochrome c_{551}, however, the chemical shifts of the four methyls indicated that in this cytochrome the spin density is concentrated on haem ring carbon atoms 1 and 5 (Keller & Wüthrich, 1978b). In view of the striking conservation of tertiary structure within the Class I group of cytochromes, this major difference in haem electronic structure between horse ferricytochrome c and P. aeruginosa ferricytochrome c_{551} seemed a little surprising. Senn et al. (1980) suggested that rather subtle differences in polypeptide conformation near the haem might be responsible. Since assignment of the haem resonances themselves is straightforward and since resonances of groups in close spatial proximity to the haem can be identified by nuclear Overhauser enhancement experiments[3], Senn et al were able to show that the axially liganded methionine has a different chirality in the two species. In cytochrome c Met 80 has R chirality, while Met 61 of c_{551} has S chirality, as shown in Figure 13. A possible explanation for the influence of the axial methionine on the unpaired electron distribution in ferric haem stems

Figure 13: Chirality of Methionine Liganding to the Haem Iron in Class I c-Type Cytochromes

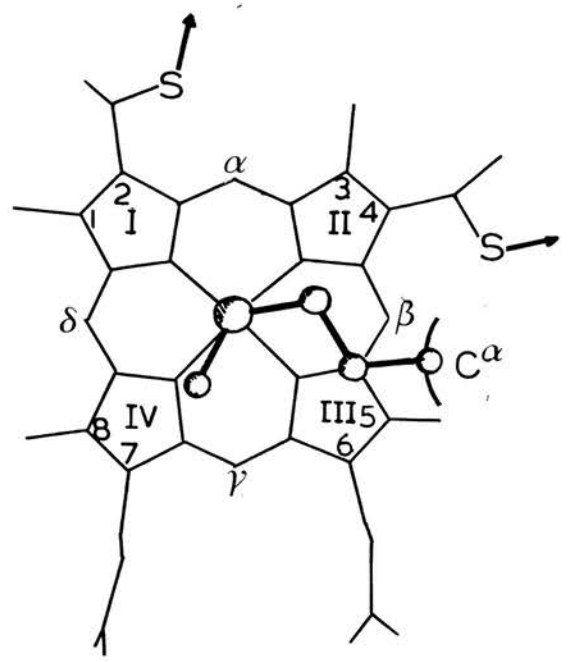

S chirality

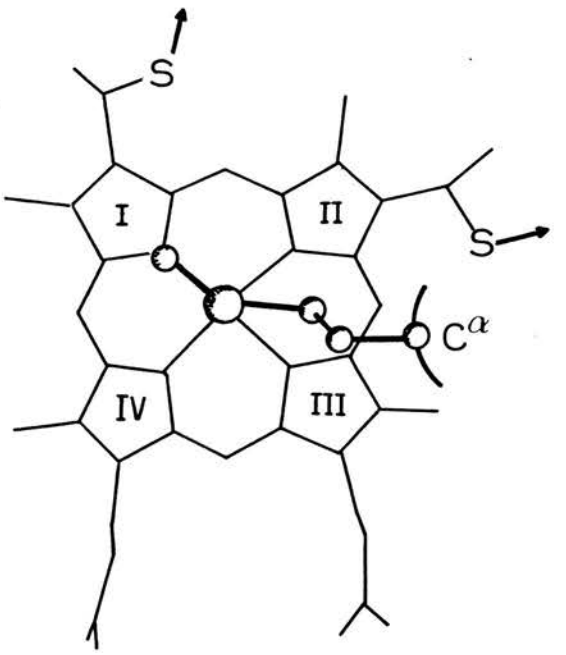

R chirality

from the observation that a lone pair orbital of the sulphur atom is directed towards the nitrogen atom of pyrrole ring IV in the R chiral case and towards pyrrole ring I in the case of S chirality; different relative energies are therefore to be expected for the molecular orbitals involving the d_{xz} and d_{yz} atomic orbitals of the iron. Senn & Wüthrich have now shown that R chirality is a property of a number of mitochondrial cytochromes and at least one bacterial cytochrome (R. rubrum cytochrome c_2) and that S chirality is not limited to Pseudomonas cytochromes, but the physiological significance of the two chiralities is not apparent (Senn et al, 1983; Senn & Wüthrich, 1983 a,b).

5. The effect of pH on the NMR spectrum of P. aeruginosa cytochrome c-551

Moore et al. (1980) studied P. aeruginosa cytochrome c_{551} by ^1H NMR in order to elucidate the nature of an ionisable group which was proposed to ionise at pK = 6.2 in ferricytochrome c_{551} and at pK = 7.3 in the ferrocytochrome. In an earlier publication Moore et al. (1977) had assigned a number of the aromatic resonances in both oxidation states of the cytochrome; Keller et al.(1976) and Keller & Wüthrich (1978b) had assigned some of the haem substituent and axial ligand resonances.

NMR spectra of the ferricytochrome were obtained over the pH range 3.5 - 10.5. The region of the spectrum from 10 to 40 ppm is shown at various pH values in Figure 14a. Four resonances displayed marked pH dependent chemical shifts viz. two of the methyl resonances (M2 and M3) and the two 1-proton resonances, P1 and P2. Chemical shift (δ) versus pH is plotted for these resonances in Figure 14b; the solid line is a theoretical curve constructed using the Henderson-Hasselbach equation and $pK^* = 6$.

The assignment of resonances P1 and P2 was uncertain. A NOE experiment showed an intensity change in P2 upon irradiation of P1 suggesting that they are the

Figure 14: pH Titration of P. aeruginosa Ferricytochrome c-551 ^{1}H NMR Spectrum

(a) Downfield shifted haem substituent resonances at various pH values. (b) δ versus pH for the haem substituent resonances. Solid lines are theoretical curves calculated from the Henderson-Hasselbach equation using pK~6. These data are taken from Moore et al. (1980).

a

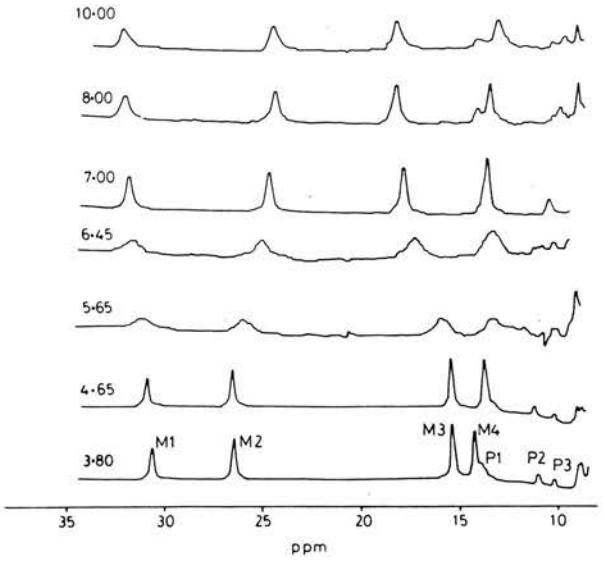
10·00
8·00
7·00
6·45
5·65
4·65
3·80
M1
M2
M3
M4
P1
P2
P3
35
30
25
20
15
10
ppm

b

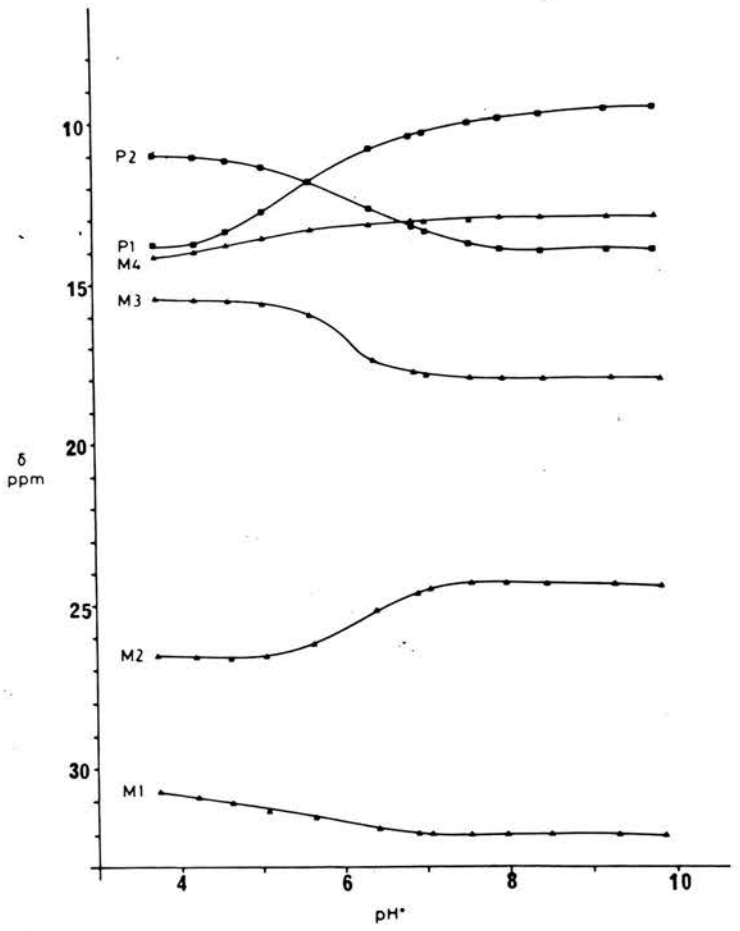
10
15
20
25
30
δ
ppm
P2
P1
M4
M3
M2
M1
4
6
8
10
pH*

geminal protons of a methylene group. The likliest possibilities seemed to be that P1 and P2 are the β-CH_2 protons of propionic acid-6/-7 or the β-CH_2 protons of the histidine ligand to the iron. Moore et al. favoured the former possibility, on the grounds that ionisation of the histidine ligand should occur at pK<3 and that protonation/deprotonation of this histidine should result in large structural changes in the cytochrome (of which there was no indication).

Additionally, the Met61 methyl resonance at -17.0 ppm (pH4.2) in the ferricytochrome spectrum shifted to -16.0 ppm (pH10.5) such as to be consistent with a $pK^* = 6$.

Of the haem substituent/axial ligand resonances resolved in the ferrocytochrome, Met61 resonances and the meso resonance showed small pH dependent chemical shifts (ca. 0.1 ppm). These were consistent with a $pK^* = 7.2$.

In the aromatic regions of the ferri- and ferrocytochrome spectra, pH changes produced very little effect. The resonances of Tyr27 shifted overall by about 0.2 ppm in the ferricytochrome pH titration and with a $pK^* = 6$. In the ferrocytochrome titration Phe34 resonances were slightly affected by a pK^* of 7.2.

Hence, these data confirmed the prediction made by Moore et al. on the basis of their redox experiments (see page 41) that there is a group ionising with $pK_O = 6.2$ and $pK_R = 7.3$. The spectra also showed that the ionisation of this group has very little effect on the tertiary structure of the protein, despite its pronounced effect on redox potential.

CHAPTER II: MATERIALS & METHODS

MATERIALS

Carboxymethylcelluloses (CM 23 and CM 52) were purchased from Whatman Ltd., Kent and Sephadexes (G-25 Coarse, Fine and Superfine, and G-75 standard and Superfine) were obtained from Pharmacia (Great Britain) Ltd., Middlesex. Ethoxyformic anhydride, acetonitrile and dansyl chloride were supplied by the Sigma Chemical Co. Ltd., Dorset and ^2H_2O by Merck, Sharp & Dohme (Canada) Ltd. These and all other reagents were of AnalaR grade.

Pseudomonas denitrificans NCIB 9496 cytochrome c_{551} and Pseudomonas mendocina CH 110 cytochrome c_{551} were generous gifts from Dr. Richard Ambler. Dr. Terry Meyer kindly donated some P. stutzeri 221 cytochrome c_{551} and some Chlorobium thiosulphatophilum cytochrome c_{555} for initial experiments. Azotobacter vinelandii NCIB 8789 cytochrome c_{551} was purified from cells grown at the Vet. School by Janet Grieve. Cytochrome c_{555} was purified from Chlorobium thiosulphatophilum Tassajara cells grown by Dr. Graham Pettigrew.

METHODS

A. Organisms and Acetone Powder Preparation

Growth of organisms: Pseudomonas stutzeri 221 (Stanier et al., 1966; A.T.C.C. 17588), Pseudomonas stutzeri 224 (Mandel, 1966; A.T.C.C. 17591) and Pseudomonas aeruginosa 10332 (Ambler, 1974; A.T.C.C. 10145) were obtained as peptone-dried stubs from Dr. R.P. Ambler, University of Edinburgh. The stubs were resuspended in 2-3 drops of nitrate medium and incubated at 37°C until signs of growth were apparent (usually within 24 hr). The stub cultures were then stepped up to 12 litres via 10, 250 and 1000ml cultures. The 12 litre batches were grown anaerobically in unstirred bottles for 12-24 hr on the nitrate medium described by Lenhoff & Kaplan (1956).

Cells were collected by centrifugation (Alfa-Laval LAB102B-05 centrifuge). Optimal cell yields were ca. 300g wet weight/100 litre culture medium, but poorer yields were frequently obtained with the P. stutzeri strains as a result of erratic slime production (which inhibited growth).

Since several batch growths of each bacterium were necessary, the organisms were maintained on nutrient agar plates; these comprised 1% peptone, 1% NaCl, 0.5% yeast extract and 1.5% agar. The inoculated plates were sealed with Parafilm.

Acetone powdering: Acetone powders were usually prepared immediately after harvesting cells. The procedure was as follows: the cell paste obtained by centrifugation was mixed with a little water and thoroughly stirred to produce a thick homogeneous sludge. The sludge (<200ml) was then poured very slowly into ca. 2 litres of rapidly stirring cold acetone; the acetone was precooled by storing at -40°C for 2-3 hr. The resulting suspension was left stirring for 5 min., whereupon the acetone was removed by suction through a Buchner funnel. The acetone treated cells were partially dried under suction for ca. 1 hr, then the material removed to a fume cupboard to dry completely overnight. It was subsequently ground into a fine powder and stored at 4°C until required further.

B Protein Purification Methods

Polyacrylamide gel electrophoresis: SDS-polyacrylamide gels were prepared, run and stained according to the method of Laemmli (1970). Non-denaturing polyacrylamide gels (usually 10% [w/v]) were polymerised in 0.1M sodium acetate-acetic acid pH4.0 and run in the same buffer.

DNS method of N-terminal identification: 10-20 nmoles of protein was precipitated with ethanol in a 1x100 mm Pyrex test tube. The precipitate was centrifuged down and the ethanol blown off with nitrogen. 10μl of 1% $NaHCO_3$ was added and dried down to remove ammonia. 20μl of H_2O then

20μl of DNS Cl (2.5 mg/ml in acetone) were added and the tube covered and incubated at 37°C until colourless. The solution was dried down, 50μl of 6M HCl added and the tube sealed in air and incubated overnight at 100°C. The HCl was then desiccated and the residue dissolved in 0.2 ml of 90% ethanol and spotted on either side of a 7.5 x 7.5 cm polyamide sheet. On one side of the sheet a standard mixture of dansylated amino acids was spotted on top of the protein hydrolysate. This mixture contained DNS-Thr, Arg, Asp, Gly, Ile, Phe, Val, Pro, Tyr, Lys, Ala.

The plates were run by ascending chromatography in three different solvents - Solvent 1, 3% formic acid; Solvent 2, toluene: acetic acid (9:1); Solvent 3, butyl acetate: methanol: acetic acid (20:1:1). Solvents 2 and 3 were run at right angles to Solvent 1. Dansylated amino acids were detected by their fluorescence under U.V. light. Co-chromatography with the standard amino acid mixture allows unambiguous identification of dansylated amino acids which have similar chromatographic mobilities e.g. DNS-Leu/Ile, DNS-Glu/Asp and DNS-Thr/Ser.

Amino acid analyses: 0.15 ml of 12M HCl was added to 0.15 ml of a protein solution containing 5-10 nmoles of protein in <2mM buffer. Thioglycollic acid was added to 0.03% (v/v) and the analysis tube was then sealed under vacuum. After incubation at 100°C for 20 hr, the tube was broken open and the hydrolysate desiccated and redissolved and sodium citrate pH2.2 (the loading buffer). Samples were analysed by the method of Spackman (1963) on a Locarte analyser.

Pyridine haemochrome: If a cytochrome is dissolved in pyridine the axial iron ligands are replaced by pyridine molecules, giving a "pyridine haemochrome". The pyridine haemochrome absorbance spectrum is diagnostic of the type of haem present e.g. all c-type cytochromes have a pyridine haemochrome α-peak at 550 nm with ϵ = 29 $mM^{-1}cm^{-1}$. The amount of haem present in a protein sample

can thus be measured by converting it to pyridine haemochrome.

0.1ml of 4M NaOH was added to an accurately measured quantity of cytochrome dissolved in 2.4 ml of H_2O; 0.5 ml of 12M pyridine was quickly added, followed by a few grains of dithionite, and the spectrum recorded. The sample was read against a pyridine-NaOH-H_2O blank.

For measurement of $\epsilon_{cytochrome}$, exactly the same quantity of cytochrome was dissolved in water and A measured at α(max). In a pure monohaem cytochrome sample [haem] = [cytochrome] and so

$$\epsilon_{cytochrome} = \frac{29.A_{cytochrome}}{A_{pyridine\ haemochrome}} \quad mM^{-1}cm^{-1}$$

C. Absorbance Band Titrations

695nm band: The pH of an unbuffered solution of ferricytochrome was adjusted with 0.1M NaOH/HCl and the spectrum in the region of the 695nm band was recorded after each addition. Titrations were performed in the presence of a small excess of ferricyanide. The cytochrome concentration was ca. 10^{-4}M (ϵ_{695} ~ $mM^{-1}cm^{-1}$).

α-band: *P. stutzeri* 221 cytochrome c_{551} (10μM) was partially reduced with 4mM sodium ascorbate pH7 and then completely reduced by titrating in small amounts of sodium dithionite solution until no further increase in α-band absorbance occurred. The pH was adjusted with 0.1M NaOH/HCl and the spectrum (490-590nm) recorded at each pH. A few grains of solid dithionite were added at the end of the experiment to check that no re-oxidation had occurred.

These experiments were performed on either a Pye Unicam SP1800 or a Cary 219 spectrophotometer.

D. Redox Potentiometry

Method of mixtures: The midpoint oxidation-reduction potential (E_m) at a particular pH was measured by the method of mixtures (Davenport & Hill, 1952; Velick &

Strittmatter, 1965; Pettigrew et al., 1975). Figure 15 shows a typical experiment. A solution of cytochrome in buffer was completely oxidised by addition of a known amount of ferricyanide and the spectrum (1) recorded at the α-peak. A known amount of ferrocyanide was then added to the solution and the extent of cytochrome reduction noted by recording a second spectrum (2). The pH of the solution was measured and then solid sodium dithionite added to completely reduce the cytochrome. A fully reduced spectrum (3) was then recorded. The following equations apply:

$$E_{h(cn)} = E_{m(cn)} + \frac{RT}{nF} \ln \frac{[cn]_{ox}}{[cn]_{red}}$$

and $$E_{h(cyt)} = E_{m(cyt)} + \frac{RT}{nF} \ln \frac{[cyt]_{ox}}{[cyt]_{red}}$$

At equilibrium, $E_{h(cn)} = E_{h(cyt)}$

so, $$E_{m(cyt)} = E_{m(cn)} + \frac{RT}{nF} \ln \frac{[cyt]_{ox}.[cn]_{red}}{[cyt]_{red}.[cn]_{ox}}$$

Here, "cn" refers to the ferro-ferricyanide couple. The values of $[cyt]_{ox}$ and $[cyt]_{red}$ can be measured from the spectra; $[cn]_{ox}$ and $[cn]_{red}$ are added to the cytochrome solution as known quantities but have to be corrected for the amount of ferricyanide formed by partial reduction of the cytochrome ($= \mathbf{a}/(\mathbf{a}+\mathbf{b}).[cyt]_{total}$).

The potential of the ferro-ferricyanide couple is dependent on pH below pH 4.5 and also on ionic strength (Hanania et al., 1967). Generally , total ionic strength was kept within the range 0.007-0.009 mol/l, for which $E_{m(cn)}$ is ca. 380mV (above pH4.5). For pH values below 4.5, this figure was corrected using the data from Figure 3 of Hanania et al. (1967).

Method of mixtures with azurin: The blue copper protein azurin has a simple visible absorption spectrum with an absorbance maximum at 625 nm in the oxidised form (ϵ = 3.5 $mM^{-1}cm^{-1}$ [Silvestrini et al., 1981]). The reduced protein has no absorption maxima in the visible region.

Figure 15: Measurement of Redox Potential by the Method of Mixtures

The spectra are: 'as is' - spectrum before any additions have been made; (1) ferricyanide oxidised; (2) ferrocyanide reduced; (3) dithionite reduced. a = Fraction of total cytochrome which is reduced by addition of ferrocyanide. b = Fraction of total cytochrome which remains oxidised after the addition of ferrocyanide.

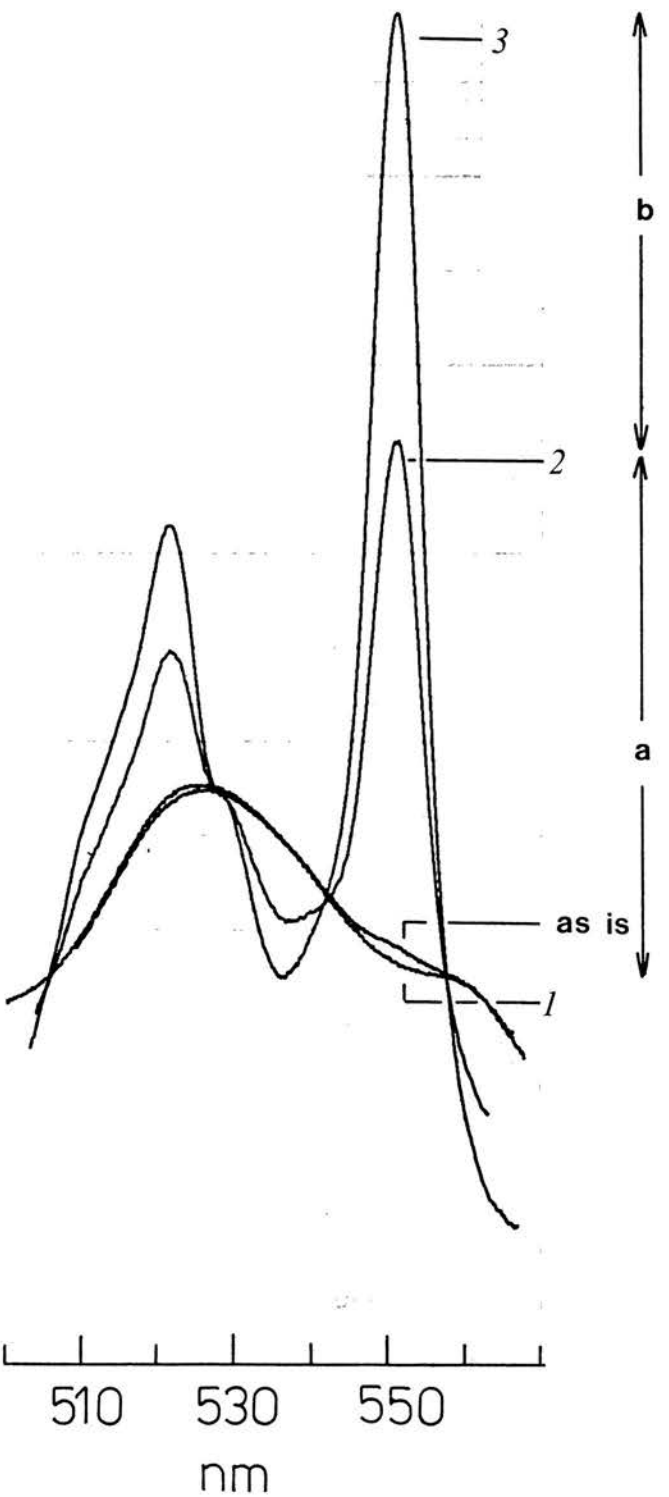
3
2
as is
1
b
a
510
530
550
nm

Azurin is able to rapidly exchange electrons with Pseudomonas cytochrome c_{551} and this feature, together with its convenient spectral properties, allows it to be used in a method of mixtures type of experiment in which ΔE_m(cytochrome - azurin) can be measured.

Azurin was purified from acetone powders of P. aeruginosa by essentially the same method used in purifying cytochrome c_{551} (see Chapter III). Azurin was resolved from cytochrome c_{551} by ion-exchange chromatography on CM-52 and was pure (as judged by SDS polyacrylamide gel electrophoresis) after a subsequent gel filtration step on Sephadex G-75 Superfine.

P. stutzeri 221 cytochrome c_{551} was reduced with dithionite and the excess reductant removed by passage through Sephadex G-25 Superfine. The ferrocytochrome was mixed with P. aeruginosa azurin in a ratio of approximately 1:1 and the spectrum recorded immediately. The spectrum was scanned again after 1 min to check that a stable redox equilibrium had been established. The mixture was then oxidised with ferricyanide and fully reduced with dithionite, the spectrum being recorded after each of the additions. The mixtures were contained in 2-3mM buffers, so that ΔE_m(cytochrome-azurin) values could be compared with those obtained at low ionic strength in mixtures with ferro-ferricyanide. The following expression was used to calculate $E_{m(cyt)}$:

$$E_{m(cyt)} = E_{m(az)} + \frac{RT}{nF} \ln \frac{[cyt]_{ox} \cdot [az]_{red}}{[cyt]_{red} \cdot [az]_{ox}}$$

and $$\Delta E_{m(cyt-az)} = \frac{RT}{nF} \ln \frac{[cyt]_{ox} \cdot [az]_{red}}{[cyt]_{red} \cdot [az]_{ox}}$$

Anaerobic titrations with Fe^{2+}/Fe^{3+}EDTA: Titrations were performed in an anaerobic cuvette equipped with a combination Pt-Ag/AgCl redox electrode (Russell pH, Auchtermuchty, U.K.). The electrode and three disposable syringe needles (Yale Microlance 19G2/50-11) were inserted into a rubber bung which could be fitted tightly into the neck of the cuvette; two of the needles served

as argon inlet and outlet, while the third was used to make additions of oxidant and reductant to the solution in the cuvette. The cuvette contents were stirred by a Teflon coated cell stirrer (Bel-Art) driven by a stirring magnet fitted to the sample compartment of a Pye Unicam SP1800 spectrophotometer. Anaerobiosis was maintained by bubbling the cuvette contents with argon for 15 min before, and throughout, titrations.

In a typical titration, the cuvette contained 0.05M sodium acetate, sodium phosphate, Tris-HCl or glycine-NaOH buffer, 0.5mM ferric ammonium sulphate, 5mM EDTA and 5-10μM cytochrome. After anaerobiosis had been established the cytochrome was reduced by injection of small volumes (μl) of an anaerobic solution of ferrous ammonium sulphate; the state of reduction was recorded spectrophotometrically after each addition and the ambient potential noted. Before adding solid sodium dithionite to achieve complete reduction, the redox electrode was removed and the pH measured.

E_m was obtained from a plot of $\log([cy]t_{ox}/[cyt]_{red})$ against ambient potential (E_h). The standard potential of the Ag/AgCl electrode was taken as 198mV (Bates, 1954), but this value was periodically checked against the Fe^{2+}/Fe^{3+}EDTA couple ($E_{m,5}$=112mV [Kolthoff & Auerbach, 1952]).

E. Chemical Modification of Histidine

Assessment of EFA concentration: Ethoxyformic anhydride (EFA) as obtained from Sigma was diluted in acetonitrile and the concentration of active reagent determined by the absorbance change produced in a 10mM solution of neutralised imidazole; 5μl of "100mM" EFA is expected to give an absorbance change of 0.55 at 230nm (ϵ_{230}= $3mM^{-1}cm^{-1}$).

Modification of cytochromes with EFA: To a solution of horse cytochrome c, P. aeruginosa or P. stutzeri 221 cytochrome c_{551} in 50mM sodium phosphate pH7, a single addition of EFA was made to give an excess of 15-20 mol

EFA per mol cytochrome. The extent of reaction was followed by difference spectroscopy ca. 238nm and the modification allowed to proceed at 20°C until there was no further absorbance change at 238nm. With horse cytochrome c and P. stutzeri 221 cytochrome c_{551} modification was essentially complete after ca. 60 min, although a very slow upward drift in absorbance appeared to occur for several hours afterwards. The amount of N-ethoxyformylhistidine formed was calculated using $\Delta\epsilon_{240}$ = $3.2mM^{-1}cm^{-1}$ (Ovadi et al., 1967). The modified cytochrome solution was subsequently applied to a Sephadex G25 column equilibrated in 2mM sodium phosphate pH7 to remove unreacted EFA. Redox potential measurements with ferro-ferricyanide were then made as desribed above.

Modification for NMR: For NMR experiments, the cytochrome was modified as described above. The EFA-modified cytochrome was concentrated by adsorption to DE52 at pH7.0 followed by elution with 0.5M NaCl; it was then desalted on Sephadex G25 into 10mm NaCl, 0.5mM sodium phosphate (pH7) in ^2H_2O.

F. NMR Spectroscopy

Concentrated cytochrome samples (>1mM) were prepared for NMR spectroscopy by passage through Sephadex G25 packed into a Pasteur pipette and equilibrated in 10mM NaCl, 0.5mM sodium phosphate (pH7) in ^2H_2O. Final cytochrome concentrations were in the range 0.5-3mM.

The pH values of solutions in NMR experiments were monitored with a glass electrode (Radiometer) which was inserted directly into the NMR tubes. The pH was adjusted by addition of small aliquots of NaO^2H or ^2HCl in ^2H_2O. The pH values quoted are direct meter readings and since they are not corrected for any isotope effect (see Appendix) they are denoted pH^*.

NMR spectra were obtained using a Brucker 300MHz spectrometer operating in the Fourier transform mode. Free induction decays were collected in a Nicolet 1085 computer, in which mathematical manipulations were

carried out. Resolution enhancement was obtained with convolution difference spectroscopy (Campbell et al., 1973). The residual water peak was minimised by selective saturation at the water frequency. Chemical shifts are quoted in parts per million (ppm) downfield from the methyl resonance of 2,2-dimethyl-2-silapentane 5-sulphonate. 1,4-Dioxan was used as an internal reference.

CHAPTER III: PURIFICATION OF CYTOCHROMES

A. P. stutzeri 221 Cytochrome c-551

(i) Purification scheme

The purification scheme for this cytochrome, and for P. stutzeri 224 cytochrome c_{551} discussed below, is essentially the same as the method used by Ambler (1972); it is summarised in Figure 16. Ambler's version differs in the final stages of the purification in that the cytochromes are chromatographed on DEAE-cellulose after elution from CM-52, and are subsequently precipitated with $(NH_4)_2SO_4$; Sephadex G-75 gel filtration then follows the $(NH_4)_2SO_4$ treatment. In the scheme shown in Figure 16, where the Sephadex G-75 gel filtration step immediately follows chromatography on CM-52, P. stutzeri 221 cytochrome c_{551} is highly pure without the additional DEAE-cellulose and $(NH_4)_2SO_4$ steps. This is probably because (i) the Superfine grade of Sephadex G-75 affords a very good separation of proteins in the molecular weight range 10000-30000 and (ii) there are very few contaminants with molecular weights as low as cytochrome c_{551} (as judged from SDS-polyacrylamide gels on samples from earlier stages of the purification).

Two cytochromes are eluted from CM-52 by chromatography with 50mM ammonium acetate pH4.4. However, they are spectroscopically indistinguishable, both showing a typical cytochrome c_{551} absorption spectrum, and their molecular weights are identical as judged from SDS-polyacrylamide gels. They are called Form I and Form II cytochrome c_{551} and the difference between the two forms is discussed below. A small amount of red material remains bound at the top of the CM-52 column after the pH4.4 chromatography and it can be eluted with 0.1M ammonium acetate pH6.5. The eluate has a low α/β ratio compared to cytochrome c_{551} and a red shifted α-band, suggesting that it contains c_4 (α/β =1.2, α_{max}=552nm) and cytochrome c_5 (α/β= 1.4, α_{max}=555nm), two cytochromes

Figure 16: Preparation of Cytochrome c-551 from Pseudomonas stutzeri (221)

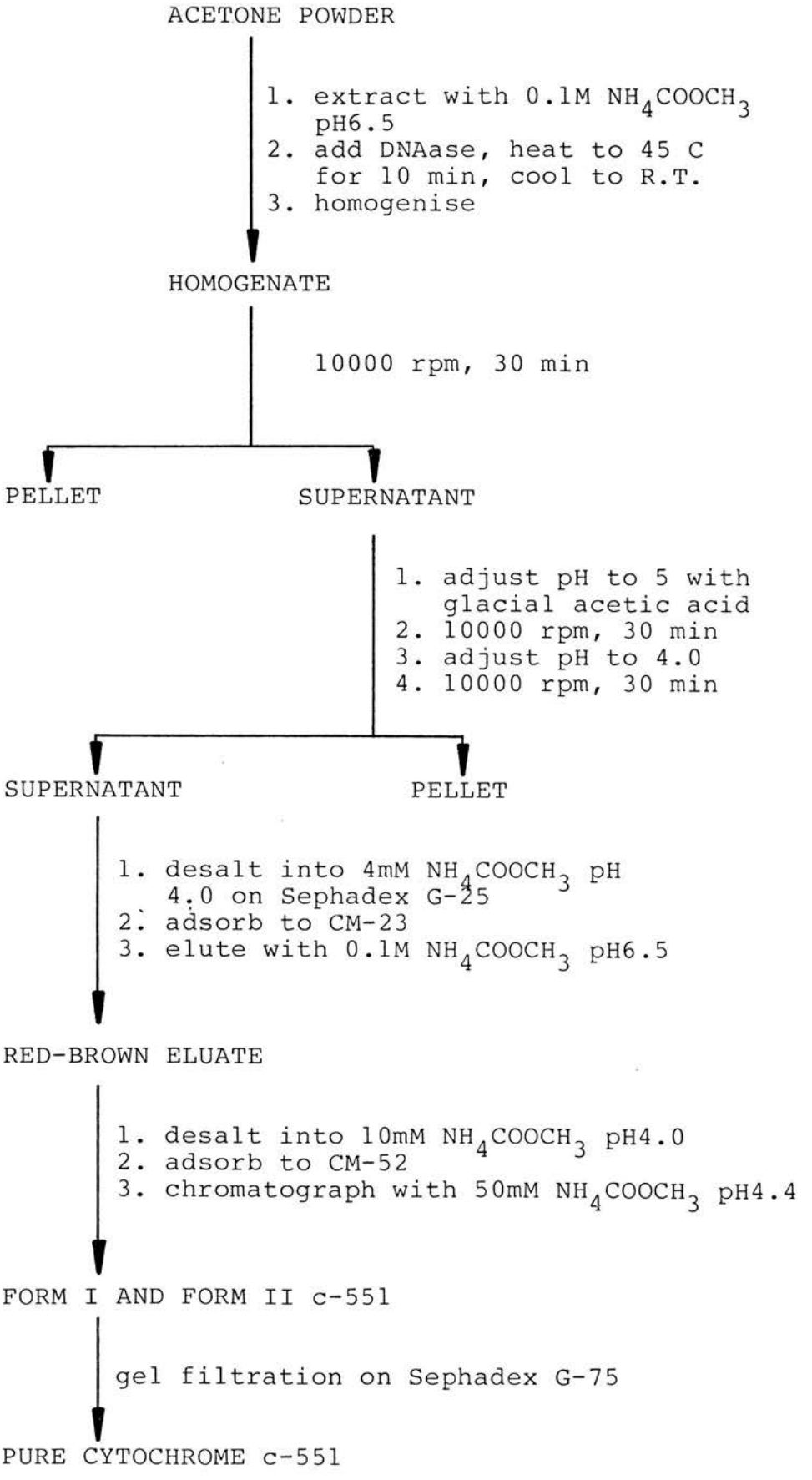
ACETONE POWDER
1. extract with 0.1M NH_4COOCH_3 pH6.5
2. add DNAase, heat to 45 C for 10 min, cool to R.T.
3. homogenise
HOMOGENATE
10000 rpm, 30 min
PELLET
SUPERNATANT
1. adjust pH to 5 with glacial acetic acid
2. 10000 rpm, 30 min
3. adjust pH to 4.0
4. 10000 rpm, 30 min
SUPERNATANT
PELLET
1. desalt into 4mM NH_4COOCH_3 pH 4.0 on Sephadex G-25
2. adsorb to CM-23
3. elute with 0.1M NH_4COOCH_3 pH6.5
RED-BROWN ELUATE
1. desalt into 10mM NH_4COOCH_3 pH4.0
2. adsorb to CM-52
3. chromatograph with 50mM NH_4COOCH_3 pH4.4
FORM I AND FORM II c-551
gel filtration on Sephadex G-75
PURE CYTOCHROME c-551

which occur at low levels in other Pseudomonas species (see Chapter I).

(ii) Purity of cytochrome c-551

The purity of both chromatographic forms of cytochrome c_{551} was established spectrally, by amino acid analysis and by SDS-polyacrylamide gel electrophoresis.

(a) Spectrum: The spectrum of Form I cytochrome c_{551} is shown in Figure 17. The α/β ratio of 1.95 is rather higher than that of P. aeruginosa cytochrome c_{551} which, like the mitochondrial cytochromes c, has a characteristic α/β ratio of 1.8. The extinction coefficient for the α-band, calculated from the pyridine haemochrome, is $31 mM^{-1}cm^{-1}$. The ratio $A_{551(red)}/A_{280(ox)}$ is used as a criterion of purity and Ambler (1973) found that this ratio is approximately 1.2 for pure cytochrome c_{551}.

(b) Amino acid analysis: A typical analysis for Form I cytochrome c_{551}, purified as described above is shown in Table IV, where the data are compared with the known amino acid content of the protein. Since this cytochrome contains no arginine, the amount of arginine determined in analyses is a useful measure of the level of contamination by other proteins.

(c) SDS-polyacrylamide gel electrophoresis: Purified cytochrome c_{551} is shown in Figure 18, lanes 2 and 3. Generally speaking, these small bacterial cytochromes stain rather poorly with Coomassie Blue, compared to their larger eukaryotic counterparts, which may not be due to their smaller size per se but to a combination of their size and the fact that their isoelectric points are considerably more acidic (Coomassie Blue is negatively charged).

(iii) Form I and Form II cytochrome c-551

These two forms of cytochrome c_{551} elute separately from the ion-exchange resin CM-52, so indicating a difference in net charge. The two forms can also be resolved on non-denaturing gels run in sodium

Figure 17: U.V.-Visible Absorption Spectrum of
P. stutzeri (221) Cytochrome c-551 (Form II)
Spectrum obtained in 0.1M sodium phosphate, pH7.0.

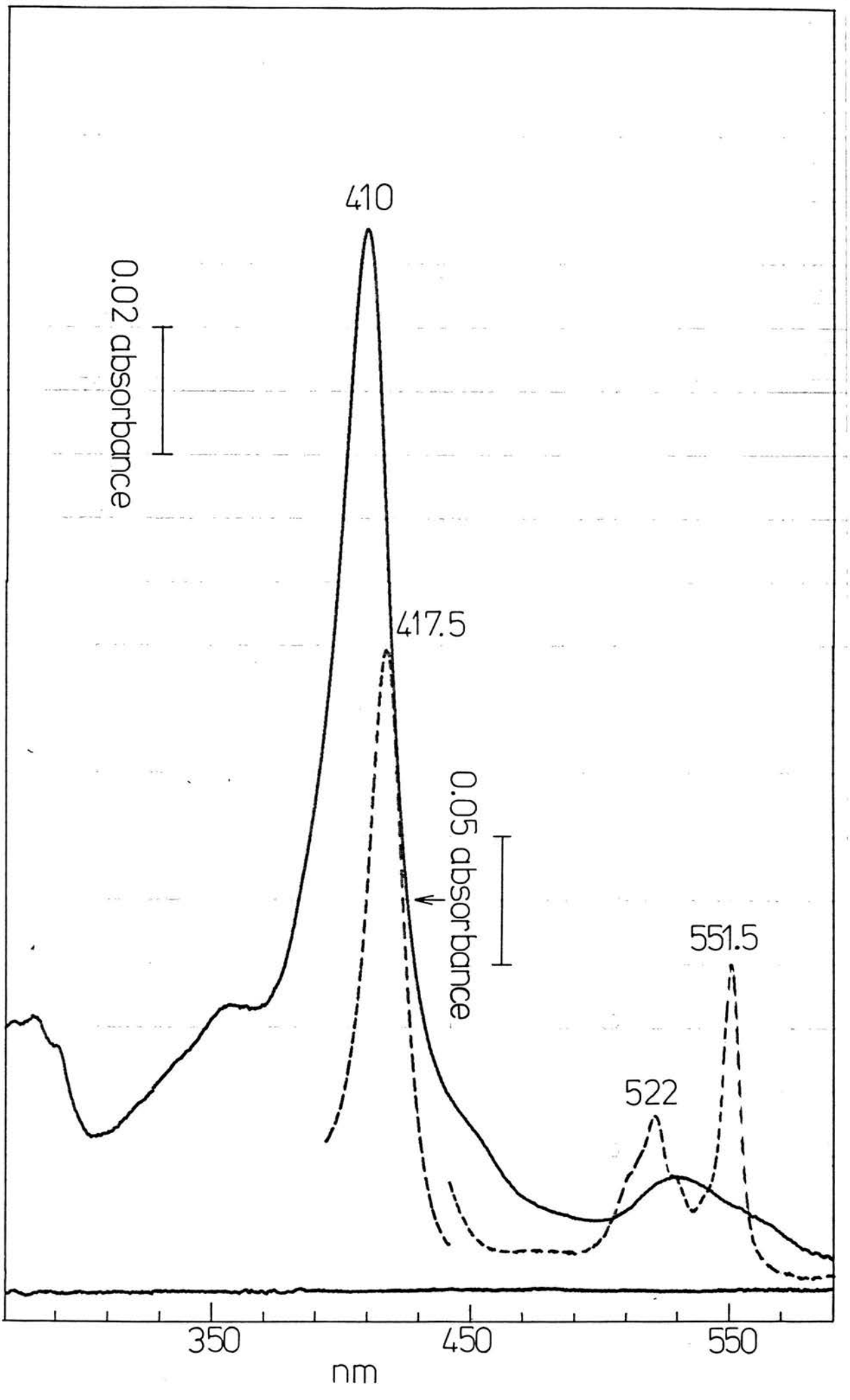
410
0.02 absorbance
417.5
0.05 absorbance
551.5
522
350
450
550
nm

Table IV: Amino Acid Analysis of P. stutzeri (221) Form I Cytochrome c-551

Amino acid	Nanomoles	Number of residues (analysis)	Number of residues (sequence)
Asx	33.6	6.45	6
Thr	5.6	1.1	1
Ser	19.6	3.8	4
Glx	52	10.1	10
Pro	-	-	7
Gly	41	7.9	8
Ala	71	13.8	13
Val	21	4.1	4
Met	4.7	0.9	1
Ile	22.2	4.3	5
Leu	31	6.0	6
Tyr	5	1	1
Phe	10.5	2	2
His	10.7	2	2
Lys	37	7.1	8
Arg	0.6	0.1	0

Figure 18: SDS-PAGE Electrophoresis of Cytochromes c-551

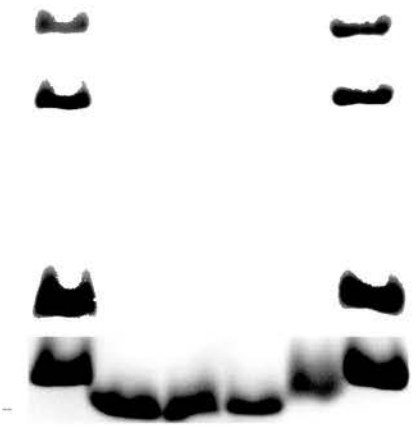

Channel	
1 and 6	P.aeruginosa c-551 (10000, 2 nmol), horse cytochrome c (12000, 1 nmol), yeast cytochrome c peroxidase (34000, 0.5 nmol) and ovalbumin (43000, 0.5 nmol)
2	P.stutzeri 221 (Form I, 1.6 nmol)
3	P.stutzeri 221 (Form II, 1.4 nmol)
4	P.stutzeri 224 (1.4 nmol)
5	A.vinelandii (1.3 nmol)

acetate-acetic acid pH4. However, their U.V.-visible spectra are identical, they behave identically on SDS-polyacrylamide gels (compare lanes and of Figure 18) and no sequence differences can be detected by amino acid analysis. Ambler (1973) suggested that the N-terminal amino acid glutamate might be converted to pyrrolidonecarboxylic acid in a proportion of the cytochrome molecules. This is a cyclisation reaction which is acid or base catalysed:

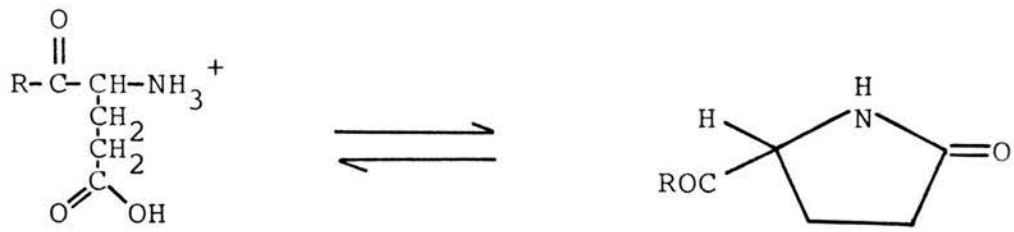

With its N-terminus blocked in this way, the molecule will carry one less positive charge at pH4.4. Thus, Form I, which adheres less tightly than Form II to CM-52 at pH4.4, is proposed to have a blocked N-terminus and Form II a free N-terminal glutamate. This proposal was checked by dansylating the two forms - the blocked form is not expected to react with dansyl chloride. Indeed, only Form I yielded a dansylated derivative (which co-chromatographed with DNS-Glu). It seems a little surprising that a single charge difference is sufficient to allow two distinct species to be resolved by ion exchange chromatography or on non-denaturing polyacrylamide gels, but ferricytochrome and ferrocytochrome c_{551} also have distinct chromatographic properties and these differ by only one charge.

In all preparations of P. stutzeri 221 cytochrome c_{551}, Form I and Form II were purified in approximately equimolar amounts. Whether the blocking reaction occurs in vivo or whether it is an artifact of purification has not been investigated but the relative amount of the two forms does not appear to change throughout purification and they do not interconvert during storage.

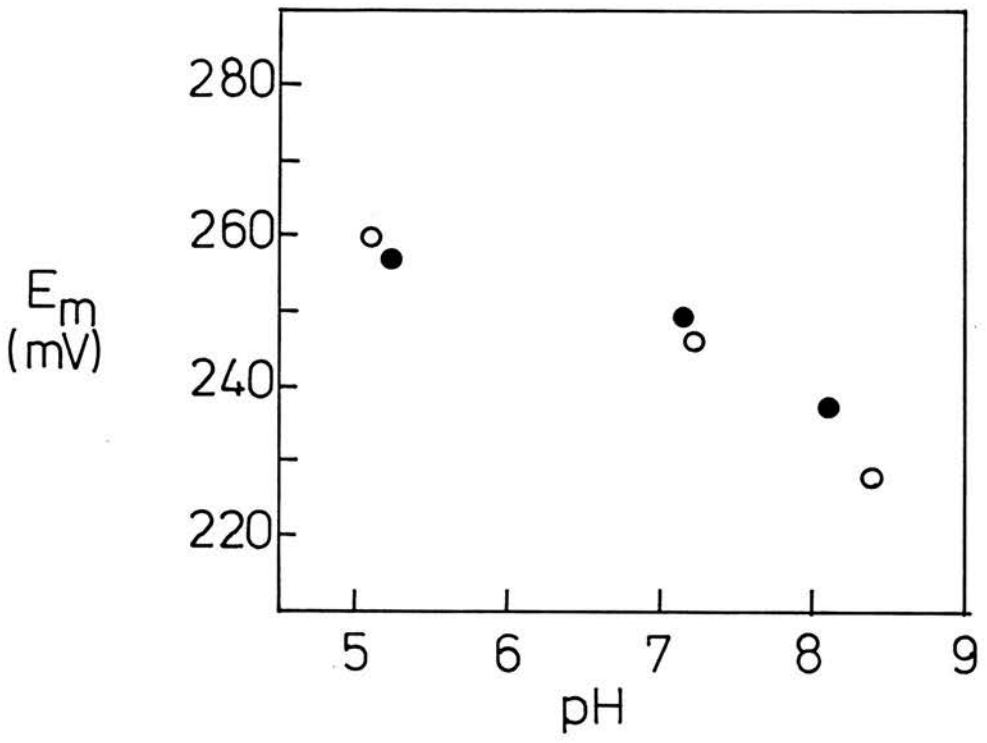

Figure 19: E_m versus pH for the Two Forms of P. stutzeri (221) Cytochrome c-551

● Form I (blocked N-terminus); ○ Form II.

Since this work is concerned with redox potential, then it was pertinent to check that there is no difference in redox potential between Forms I and II. Figure 19 shows this to be the case (the redox potential is markedly pH dependent above pH7.2 [see Chapter IV] and so a small difference in pH during measurement would account for the difference in potential between the two high pH points). The two forms were therefore used interchangeably in all redox experiments.

B. P. stutzeri 224 Cytochrome c-551

Since this cytochrome differs from the cytochrome c_{551} from P. stutzeri 221 by only 11 amino acids, none of these being charged residues, its purification procedure was expected to be essentially the same as described above. However, P. stutzeri 224 grown under the same conditions as P. stutzeri 221 produces considerably more cytochrome c_4 and another cytochrome which appears to be cytochrome c_5 (although it was not carefully characterised) and these chromatograph rather differently from their P. stutzeri 221 homologues. The cytochrome c_5 co-elutes with the Form I cytochrome c_{551} from CM-52 using 50mM ammonium acetate pH4.35. Form II elutes more slowly and is spectrally pure after the CM-52 chromatography step. Cytochrome c_4 chromatographs extremely slowly at pH4.35 and has to be eluted at higher pH (it is further purified by chromatography on DE-52).

The mixture of Form I cytochrome c_{551} and cytochrome c_5 was adsorbed to DE-52 equilibrated in 5mM Tris pH7.3 (R.T.); the two cytochromes could be eluted separately using a salt gradient of 10mM Tris, 0-100mM NaCl pH7.3, with cytochrome c_{551} eluting at the lower salt concentration.

The spectrum of purified Form I cytochrome c_{551} is shown in Figure 20. The absorbance maxima are nearly identical to those noted for the P. stutzeri 221 cytochrome but the ratios α/β (=2.05) and $A_{551(red)}/A_{280(ox)}$ (=1.7) are noticeably higher. The

Figure 20: U.V.-Visible Absorption Spectrum of
P. stutzeri (224) cytochrome c-551

Spectrum obtained in 0.1M sodium phosphate, pH7.0.

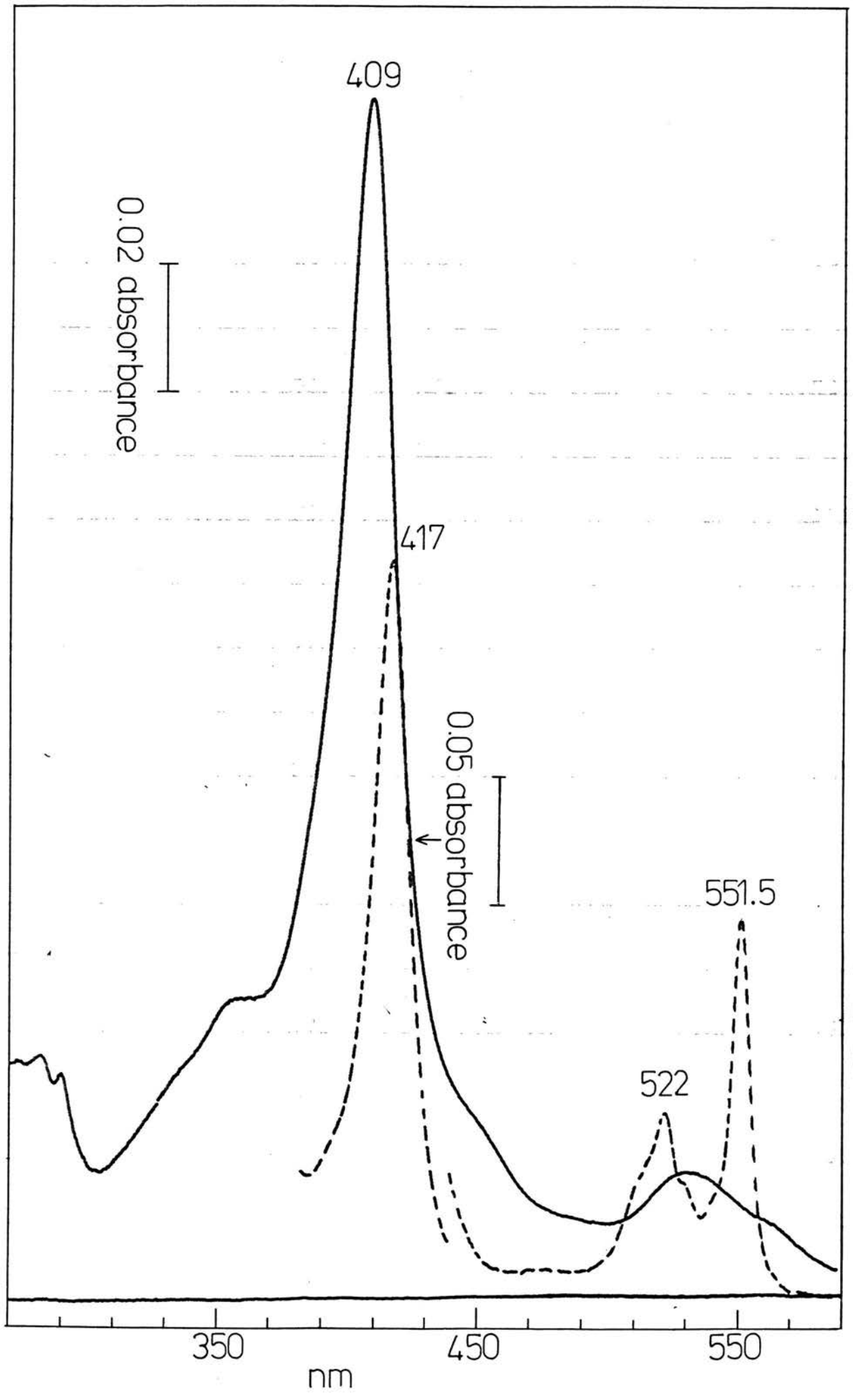
409
0.02 absorbance
417
0.05 absorbance
551.5
522
350
450
550
nm

higher value for the latter ratio is explained by the absence of tyrosine in this cytochrome (since tyrosine contributes to the absorbance at 280). The extinction coefficient calculated for the α-band is $33 mM^{-1}cm^{-1}$. The amino acid analysis shown in Table V and SDS-polyacrylamide gel electrophoresis (Figure 18, lane +) confirm the cytochrome is pure.

C. A. vinelandii Cytochrome c-551

A. vinelandii cytochrome c_{551} was prepared from a French press extract of cells by a modification of the method described by Swank & Burris (1969) and Campbell et al. (1973). The soluble extract, which contains cytochrome c_{551}, cytochrome c_4 and cytochrome c_5, was adsorbed onto DE-23 equilibrated in 2mM Tris pH7.3 (R.T.). Cytochrome c_{551} was then eluted with very little contamination from the other two cytochromes by washing the column with 20mM Tris, 20mM NaCl pH7.3 (R.T.). After concentration, the crude cytochrome c_{551} was further purified by gel filtration on Sephadex G-75 Superfine. At this stage the cytochrome was already quite pure, on the basis that the absorbance ratio $A_{551(red)}/A_{280(ox)}$ was 1.2 - Campbell et al. quote a value of 1.2-1.4 for pure cytochrome c_{551}. However, this ratio was improved to 1.35 by addition of another purification step in which the cytochrome was adsorbed to CM-52 at pH4.2 and chromatographed with 50mM ammonium acetate pH4.7.

The absorption spectrum of this cytochrome is shown in Figure 21 and an amino acid analysis is given in Table VI. The cytochrome is virtually indistinguishable spectrally from the Pseudomonas cytochromes.

D. C. thiosulphatophilum Cytochrome c-555

C. thiosulphatophilum cytochrome c_{555} was purified by a slightly modified version of the method developed by Meyer et al. (1968). The soluble extract obtained from French pressed cells was centrifuged at 100000g for 100 min. The supernatant obtained from this centrifugation

Table V: Amino Acid Analysis of P. stutzeri (224) Form I Cytochrome c-551

Amino acid	Nanomoles	Number of residues (analysis)	Number of residues (sequence)
Asx	43.1	6.7	6
Thr	23.2	3.6	3
Ser	25.4	4	4
Glx	55.5	8.7	9
Pro	-	-	7
Gly	43.1	6.7	7
Ala	75.6	11.8	12
Val	36.1	5.6	7
Met	11.5	1.8	2
Ile	14.9	2.3	3
Leu	39.2	6.1	7
Tyr	0	0	0
Phe	6.5	1	1
His	14.3	2.2	2
Lys	47.4	7.4	8
Arg	0.4	0.06	0

Table VI: Amino Acid Analysis of A. vinelandii Cytochrome c-551

Amino acid	Nanomoles	Number of residues (analysis)	Number of residues (sequence)
Asx	12.8	4.0	4
Thr	22.7	7.1	7
Ser	13.6	4.2	4
Glx	28.1	8.8	9
Pro	17.1	5.3	5
Gly	25.0	7.8	9
Ala	32.2	10.1	11
Val	14.1	4.4	5
Met	2.8	0.9	1
Ile	9.8	3.1	4
Leu	13.7	4.3	5
Tyr	5.1	1.6	2
Phe	3.0	0.95	1
His	8.1	2.5	2
Lys	29.2	9.1	9
Arg	~0	~0	0

Figure 21: U.V.-Visible Absorption Spectrum of A. vinelandii Cytochrome c-551

Spectrum obtained in 0.1M sodium phosphate, pH7.0.

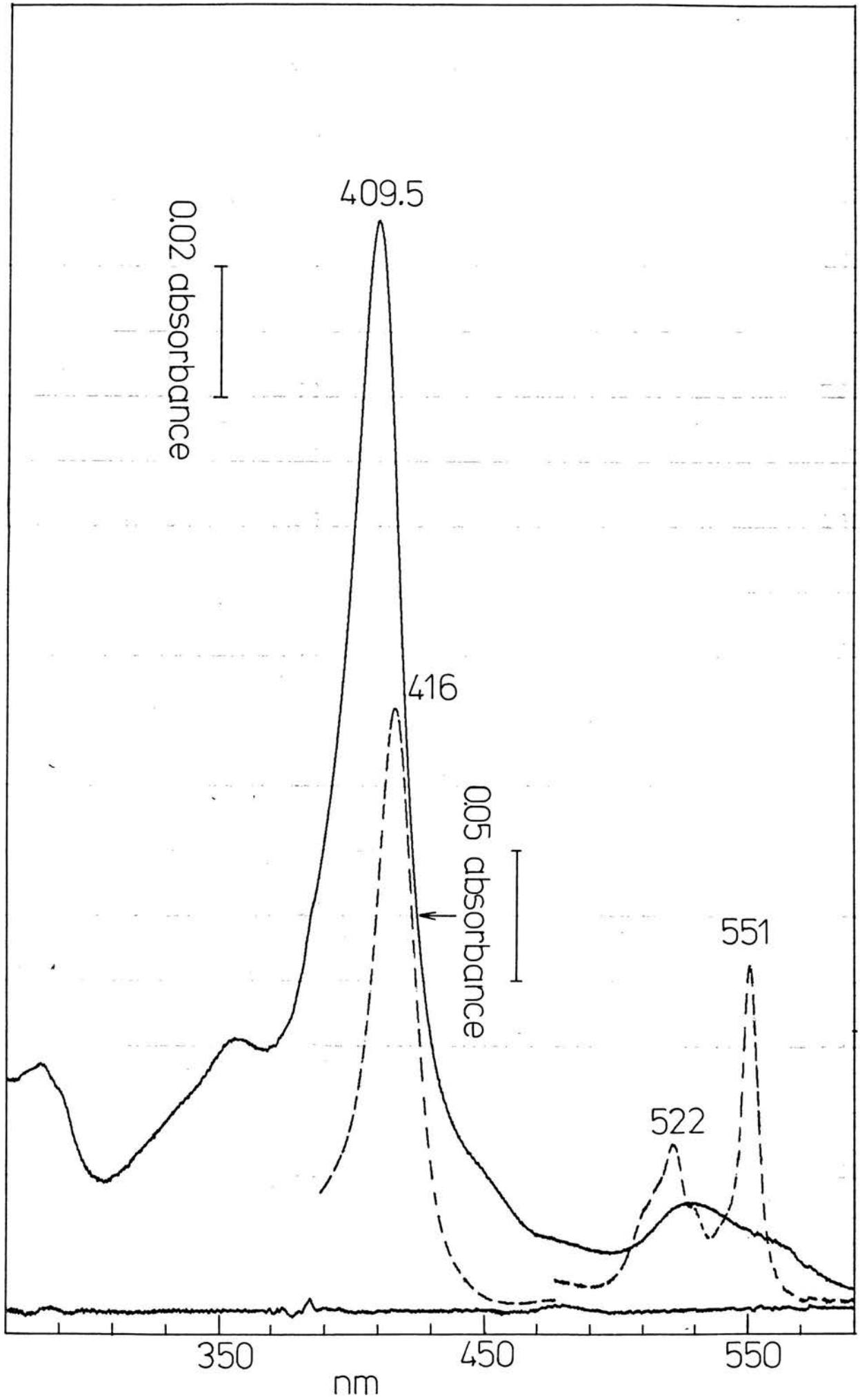
409.5
0.02 absorbance
416
0.05 absorbance
551
522
350
450
550
nm

Figure 22: U.V.-Visible Absorption Spectrum of
C. thiosulphatophilum Cytochrome c-555

Spectrum obtained in 0.1M sodium phosphate, pH7.0.

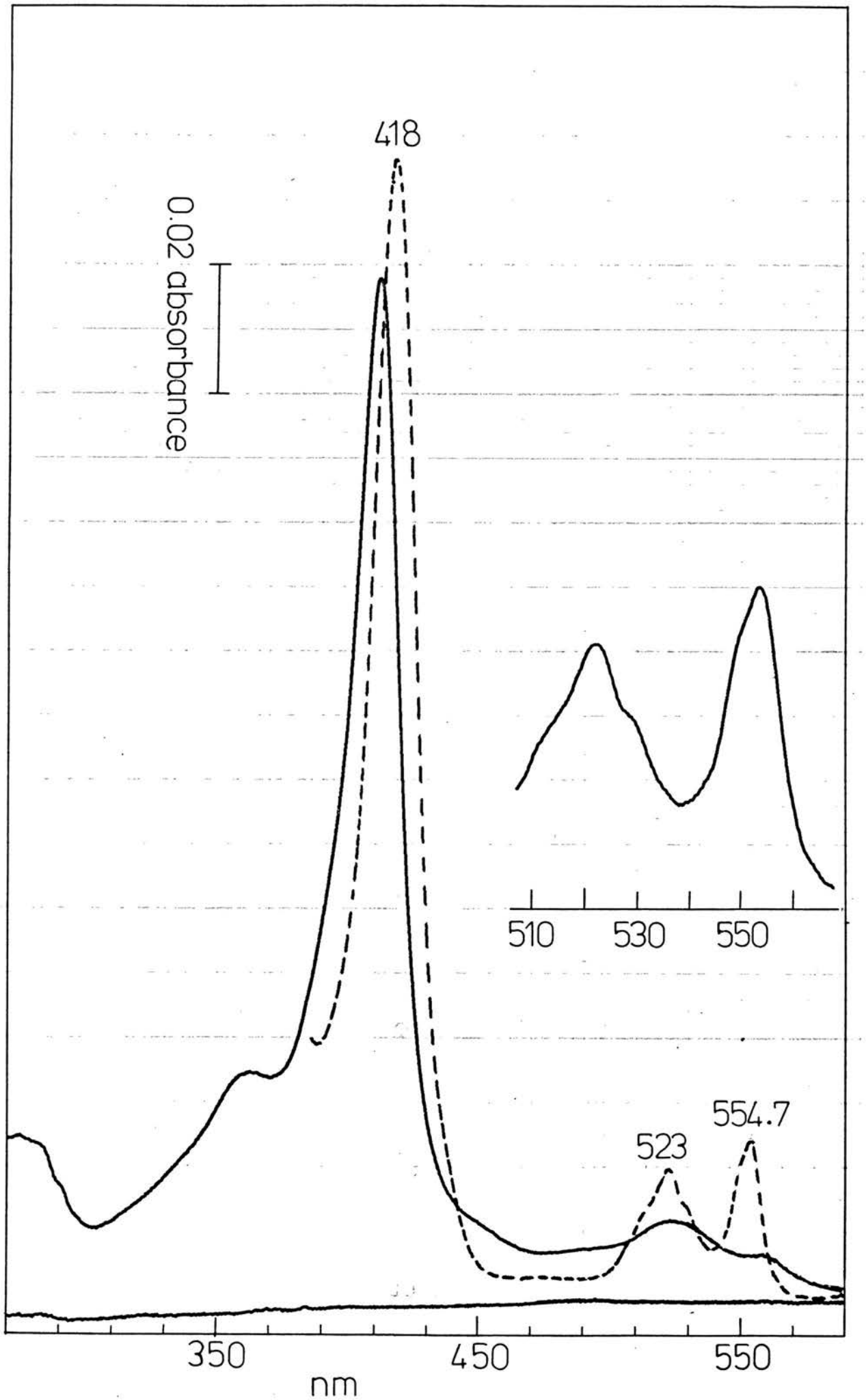
418
0.02 absorbance
510
530
550
554.7
523
350
450
550
nm

was then passed through a column of DE-23 equilibrated in 0.1M potassium phosphate pH7.5 in order to remove ferredoxin and nucleic acids. The eluate was desalted into 20mM Tris pH7.8 (4°C) and passed through a column of DE-52 equilibrated in the same buffer. Under these conditions cytochrome c_{555}, which has a basic isoelectric point, does not adsorb to the column but two other cytochromes which have acidic isoelectric points do (see Meyer et al., 1968). The unadsorbed eluate was then adjusted to pH7.0 and applied to CM-52 equilibrated in 20mM Tris pH7.8 (4°C). A sharp red band formed at the top of the column and all other material was removed by washing with the 20mM Tris buffer. The adsorbed cytochrome c_{555} was subsequently eluted in a few ml with 0.5M NaCl, 5 mM sodium phosphate pH7.0. As a final purification step, the cytochrome was subjected to gel filtration on Sephadex G-75 Superfine.

An amino acid analysis is given in Table VII and the spectrum is shown in Figure 22. this cytochrome shows three distinctive spectral features: (i) its α-band maximum occurs at an unusually long wavelength for a Class I c-type cytochrome (ii) its α-band is markedly asymmetric and (iii) it has a very low α/β ratio. With regard to this last property, Meyer (1970) obtained an α/β ratio of 1.2 and $A_{555(red)}/A_{280(ox)}$ of 0.88 for his preparation of cytochrome c_{555} - identical values were obtained here.

Table VII: Amino Acid Analysis of C. thiosulphatophilum Cytochrome c-555

Amino acid	Nanomoles	Number of residues (analysis)	Number of residues (sequence)
Asx	52.8	8.5	8
Thr	27.4	3.8	4
Ser	16.9	2.7	3
Glx	14.2	2.3	2
Pro	35.3	5.7	4
Gly	67.0	10.8	12
Ala	95.9	15.5	16
Val	32.6	5.3	6
Met	39.0	6.3	8
Ile	8.7	1.4	2
Leu	6.4	1.0	1
Tyr	19.6	3.2	4
Phe	~0	~0	0
His	14.3	2.3	2
Lys	68.8	11.1	11
Arg	~0	~0	0

CHAPTER IV: REDOX POTENTIAL MEASUREMENTS

This chapter deals with the effect of pH on the redox potentials of four closely related Pseudomonas cytochromes, viz. P. stutzeri 221, P. stutzeri 224, P. mendocina and P. denitrificans cytochromes c_{551}. Two other cytochromes are included for comparison: (i) A. vinelandii cytochrome c_{551}, which is extremely similar in terms of sequence and physicochemical properties to the Pseudomonas cytochromes c_{551} (ii) C. thiosulphatophilum cytochrome c_{555}, which is only distantly related in sequence to the other five cytochromes (<25% homology), although it clearly belongs to the Class I group of c-type cytochromes.

Moore et al. (1980) showed for P. aeruginosa cytochrome c_{551} that haem propionic acid-7 is likely to be the ionising group which gives rise to the observed pH dependence of redox potential. Given that this species ionises with redox state dependent pKs in the other cytochromes c_{551} it was hoped that any differences in pKs could be explained in terms of amino acid substitutions between the cytochromes. On this basis, it should be possible to obtain some idea of how the surrounding polypeptide can affect the pH range over which the redox potential of a cytochrome is pH dependent. The E_m versus pH curve of the Chlorobium cytochrome is expected to show similarities with the Pseudomonas cytochromes on the basis that it is about the same size as the cytochromes c_{551} and shows the same polypeptide deletion relative to the mitochondrial cytochromes and the cytochromes c_2 (Korzun & Salemme, 1978). Cytochrome c_{555} was also of interest because it is so divergent in sequence terms from the other Class I cytochromes; since we were seeking to establish a general mechanism for the pH dependence of redox potential amongst the bacterial cytochromes, it was

useful to include this rather different cytochrome in the study.

A. P. stutzeri 221 Cytochrome c-551

(i) The redox potential measured against the ferri-ferrocyanide couple

The midpoint redox potential of P. stutzeri 221 cytochrome c_{551} was measured by the method of mixtures with ferri-ferrocyanide over the pH range 4.5-10; E_m is plotted against pH in Figure 23. The theoretical curve was drawn using equation 2 (page 28) which assumes one ionisation occurring in the oxidised cytochrome and one in the reduced i.e.

$$E_m = \tilde{E} + \frac{RT}{nF} \ln \frac{[H^+] + K_R}{[H^+] + K_O}$$

$\tilde{E}$, the midpoint potential at pH values below pK_O, was assigned a value of 243mV and the ionisation constants K_O and K_R were set at 2.51×10^{-8} M (pK_O=7.6) and 5.0×10^{-9} M (pK_R=8.3), respectively.

The theoretical curve gives a very good fit to the experimental data between pH5 and 9. Below pH5 it is possible that another ionisation affects the redox potential - a similar ionisation appears to influence the redox potential of P. aeruginosa cytochrome c_{551} below pH5 (see Figure 10). Above pH9 the data are rather scattered, which is largely due to the fact that the redox potential measurements are less reliable at these high pH values; this is because the amount of partially reduced cytochrome generated upon addition of the ferrocyanide becomes progressively smaller as the cytochrome redox potential falls - the ratio $[cyt]_{ox}/[cyt]_{red}$ used in the calculation of E_m is more sensitive to error when $[cyt]_{red}$ (or $[cyt]_{ox}$) is very small. The "695nm band" pK which affects eukaryotic cytochromes and the cytochromes c_2 at alkaline pH does not appear to occur in this cytochrome below pH10 - it has a very pronounced effect on E_m and should be evident

P.stutzeri 221 cyt.c-551

pKo1 - 7.6
pKr - 8.3

POINT	X	Y
1	4.65	251
2	4.8	251
3	5.35	242
4	5.7	244.5
5	6.3	241.5
6	6.3	242
7	6.7	238
8	7.1	238
9	7.13	237.5
10	7.3	236.5
11	7.4	231
12	7.93	226
13	8.15	214
14	8.3	212
15	8.1	215
16	8.6	207.5
17	8.8	210.5
18	8.9	202
19	8.9	207.5
20	9.3	208.5
21	9.55	201
22	9.8	197.5
23	10	196.5

Figure 23: E_m versus pH for P. stutzeri (221) Cytochrome c-551

The theoretical curve was obtained using Equation 2 with $\tilde{E}$ = 243mV, pK_O = 7.6 and pK_R = 8.3.

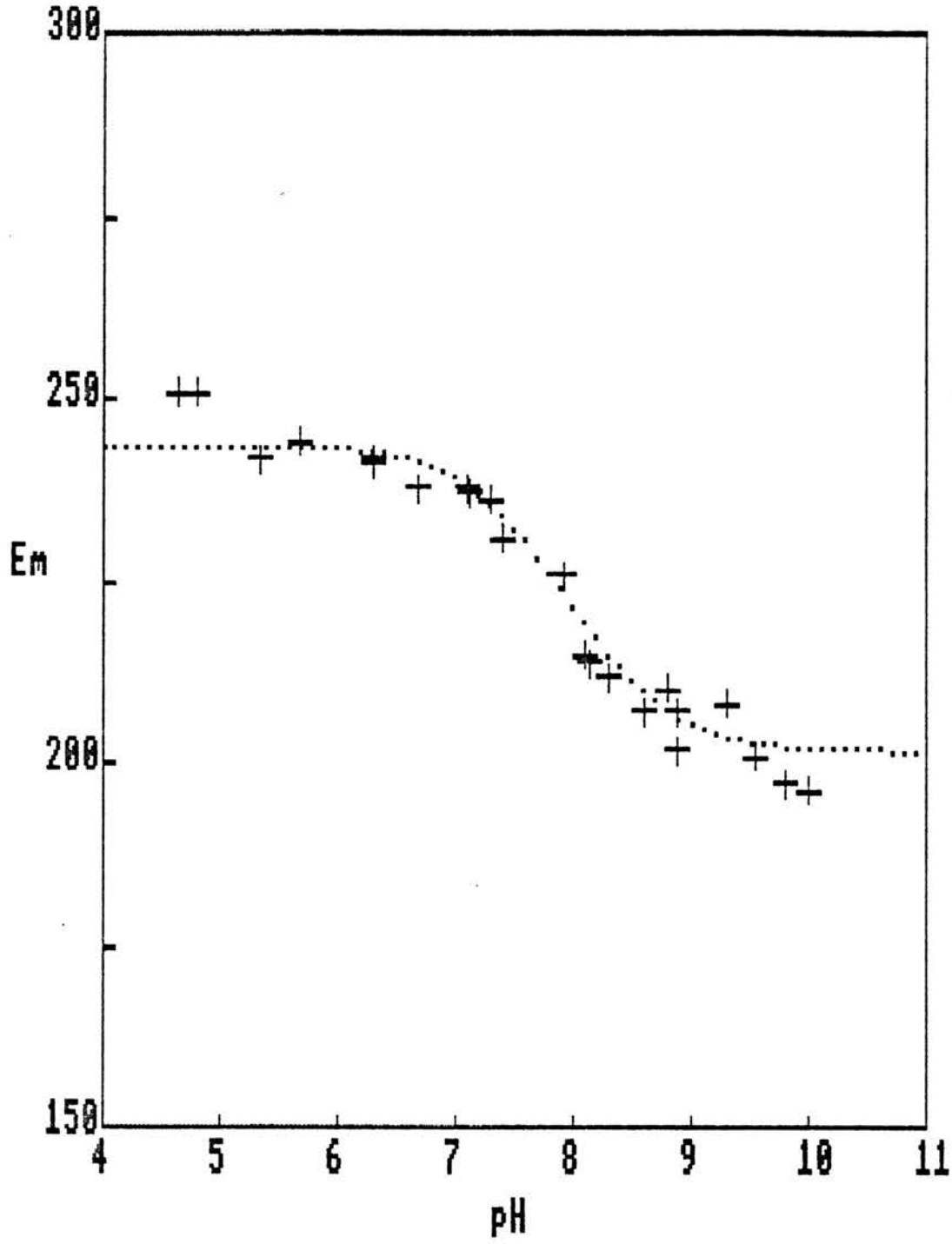
300
250
200
150
Em
4
5
6
7
8
9
10
11
pH

despite the scatter. Also, two pieces of experimental evidence indicate that the Met61:iron bond remains intact until beyond pH10: (i) the 695nm absorption band was unaffected during a pH titration over the pH range 6.4-10.9 (ii) the Met61 methyl resonance remains in its characteristic upfield position in the ^1H NMR spectrum while the ferricytochrome is titrated over the pH range 5.0-9.8 (see Chapter V).

(ii) The redox potential measured against azurin

The ferri-ferrocyanide couple has been extensively used in the determination of redox potentials of c-type cytochromes. It has now been shown, however, that ferricyanide binds to horse cytochrome c (Butler et al., 1981; Miller & Cusanovich, 1975; Stellwagen & Cass, 1975; Eley et al., 1982), and if it binds differentially to the two redox states of the cytochrome then a perturbation of redox potential would be observed according to the equation:

$$E_m = E_{m(NL)} + \frac{RT}{nF} \ln \frac{1 + K_R[L]}{1 + K_O[L]}$$

where $E_{m(NL)}$ is the midpoint potential in the absence of ligand and K_O and K_R are association constants for the ligand binding (Dutton, 1974). The possibility then exists that the apparent pH dependence of redox potential observed for P. stutzeri 221 cytochrome c_{551} (and the other cytochromes discussed subsequently) is due simply to differential ferricyanide binding to the protonated and unprotonated forms of the cytochrome. This being so, then the pH dependence should disappear if the redox potential is measured by another method.

As an alternative, the cytochrome c_{551} redox potential can be measured in a method of mixtures type of experiment with another redox protein, rather than with the ferri-ferrocyanide couple. The protein of choice in this case was P. aeruginosa azurin. The absorbance maximum of oxidised azurin occurs at 625nm (the reduced protein does not absorb in the visible region) and so the

Figure 24: Measurement of Cytochrome c-551 Redox Potential by Method of Mixtures with Azurin

(1) Redox equilibrium obtained by adding P. stutzeri (221) ferrocytochrome c_{551} to P. aeruginosa azurin; (2) ferricyanide oxidised; (3) dithionite reduced.

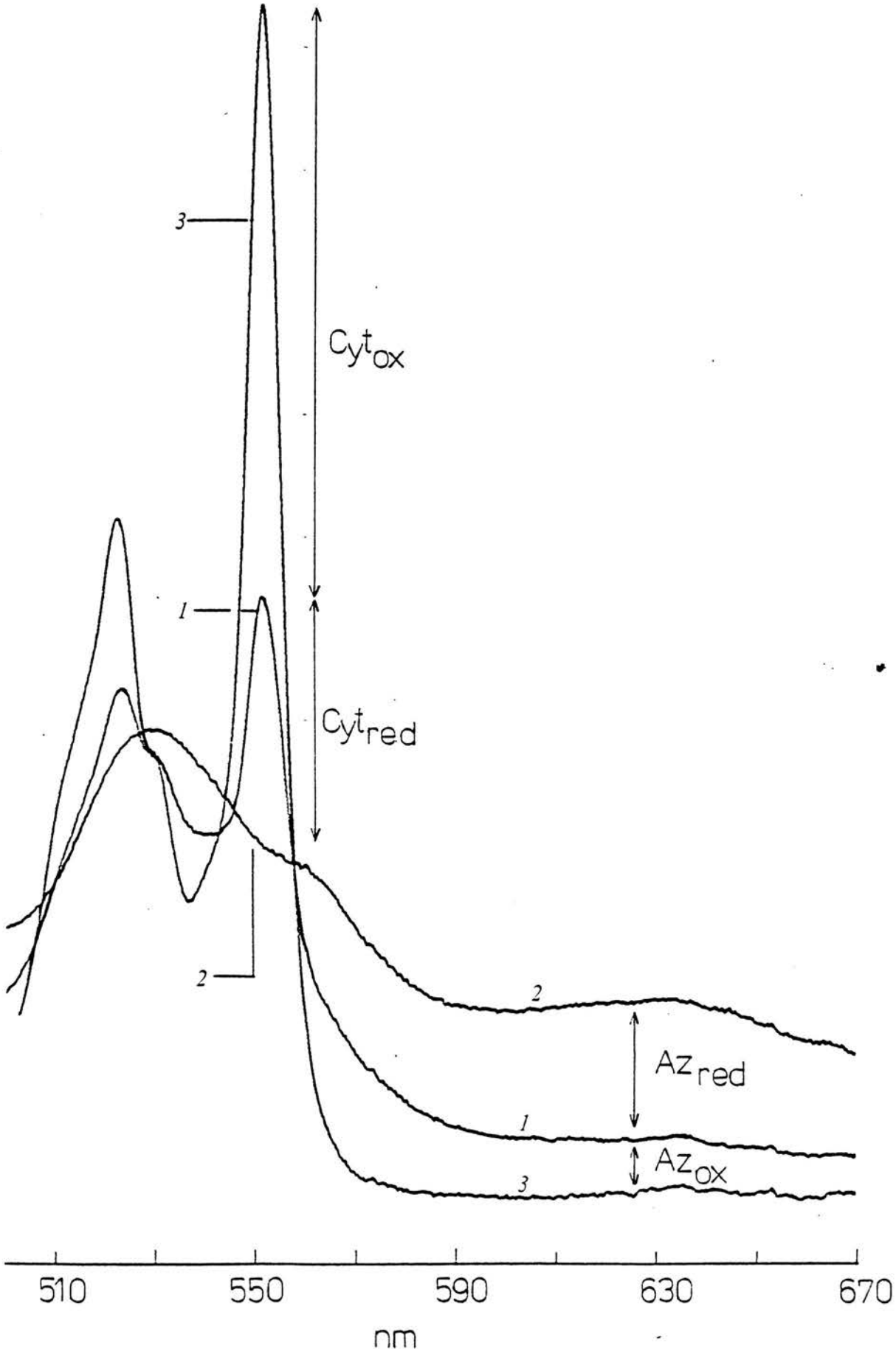
3
1
2
Cyt ox
Cyt red
Az red
Az ox
510
550
590
630
670
nm

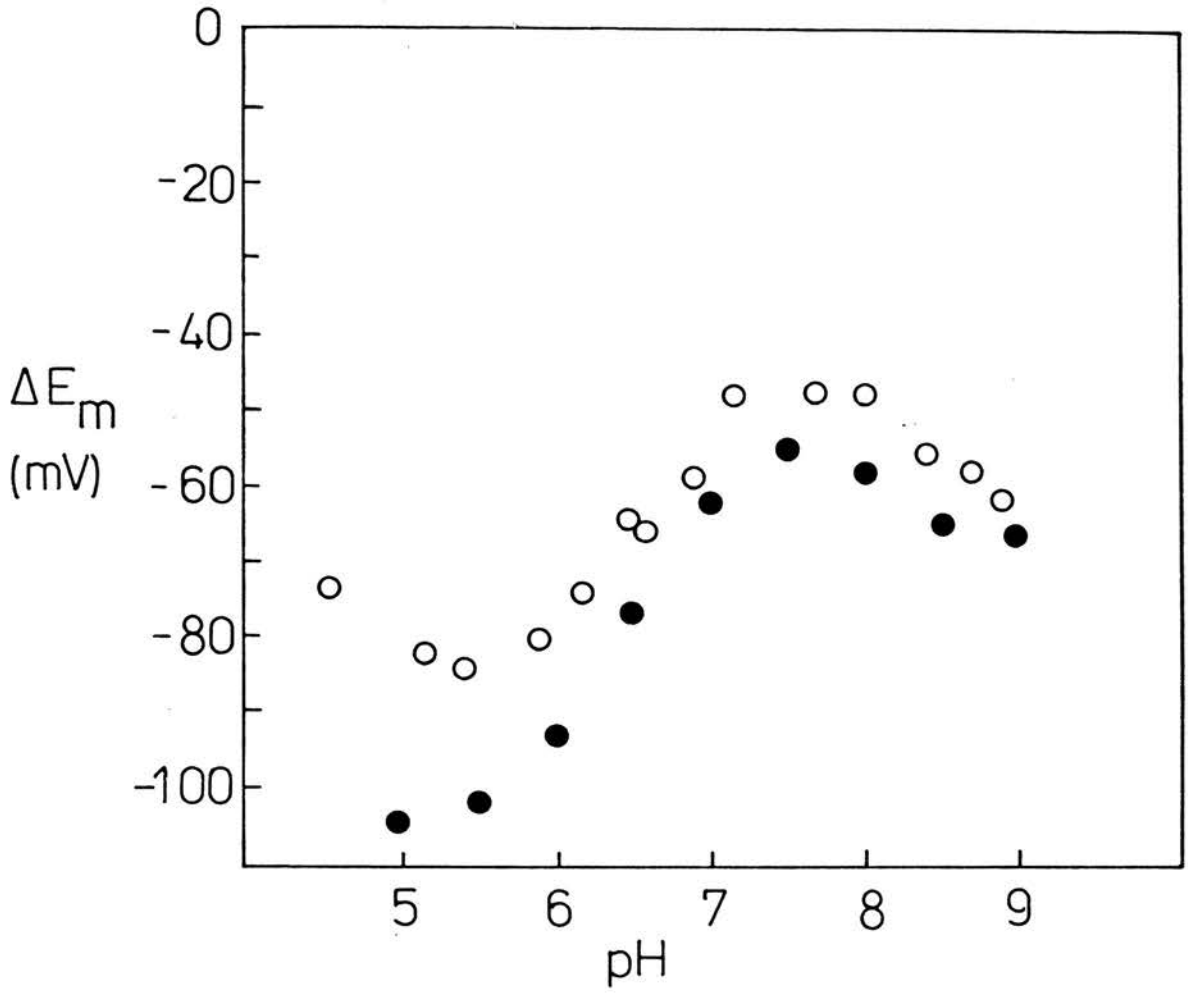

Figure 25: pH Dependence of Redox Potential Equilibrium Between P. stutzeri (221) Cytochrome c-551 and P. aeruginosa Azurin

○ E_m(c-551) - E_m(azurin) calculated from redox equilibria of the type shown in Figure 24. ● E_m(c-551) - E_m(azurin) calculated from separate determinations of midpoint potential in mixtures with ferri-ferrocyanide (the azurin data are taken from Pettigrew et al., 1983).

extent of azurin oxidation/reduction in mixtures with cytochrome c_{551} at different pH values can be measured spectrophotometrically. Figure 24 shows a typical experiment. It is not possible to determine accurately the redox state of the proteins in a cytochrome/azurin mixture because neither protein has an isosbestic point near the absorbance maximum of the other. However, the contribution of azurin to the absorbance at 550nm is small, as is the contribution of cytochrome to the absorbance at 625nm, and so approximate calculations can be made.

ΔE_m (cytochrome-azurin) is plotted against pH in Figure 25 (open circles). The redox potential of P. aeruginosa azurin measured against the ferri-ferrocyanide couple is also pH dependent (see Pettigrew et al., 1983 in Appendix II). The solid circles represent ΔE_m (cytochrome-azurin) calculated from the two sets of redox potential data obtained in the presence of ferri-ferrocyanide. The parallel nature of the ΔE_m versus pH curves is clear evidence that the pH dependence of the cytochrome c_{551} redox potential is not an artifact of pH dependent ferricyanide binding.

B. P.stutzeri 224 and P. mendocina cytochromes c-551

The redox potentials of P. stutzeri 224 and P. mendocina cytochromes c_{551}, measured by the method of mixtures with ferri-ferrocyanide, are plotted against pH in Figures 26 and 27, respectively. In both cases the theoretical curves were fitted using Equation 2. For P. stutzeri 224 cytochrome c_{551}, the best fitting theoretical curve was obtained using pK_O = 7.8 and pK_R = 8.45, and for the P. mendocina cytochrome pK_O and pK_R were assigned values of 7.2 and 8.0.

The E_m data obtained for P. mendocina cytochrome c_{551} ca. pH10 and above suggest a third pK. If this is a real effect then it is not a 695nm band pK since the 695nm band persists unchanged in the ferricytochrome

P.stutzeri 224 cyt.c-551

pKo1 - 7.8
pKr - 8.45

POINT	X	Y
1	4.45	201.5
2	4.65	206.5
3	5.1	203.5
4	5.5	203
5	6.5	200
6	6.25	200.5
7	6.8	202
8	7.05	200.5
9	7.3	198
10	7.55	197
11	7.4	199
12	7.6	191
13	7.65	187
14	8	184.5
15	8.2	181.5
16	8.4	177
17	8.6	173
18	8.8	174
19	9.1	168.5
20	9.45	168
21	9.75	169
22	10	165

Figure 26: E_m versus pH for P. stutzeri (224) Cytochrome c-551

The theoretical curve was obtained using Equation 2 with $\tilde{E}$ = 201mV, pK_O = 7.8 and pK_R = 8.45.

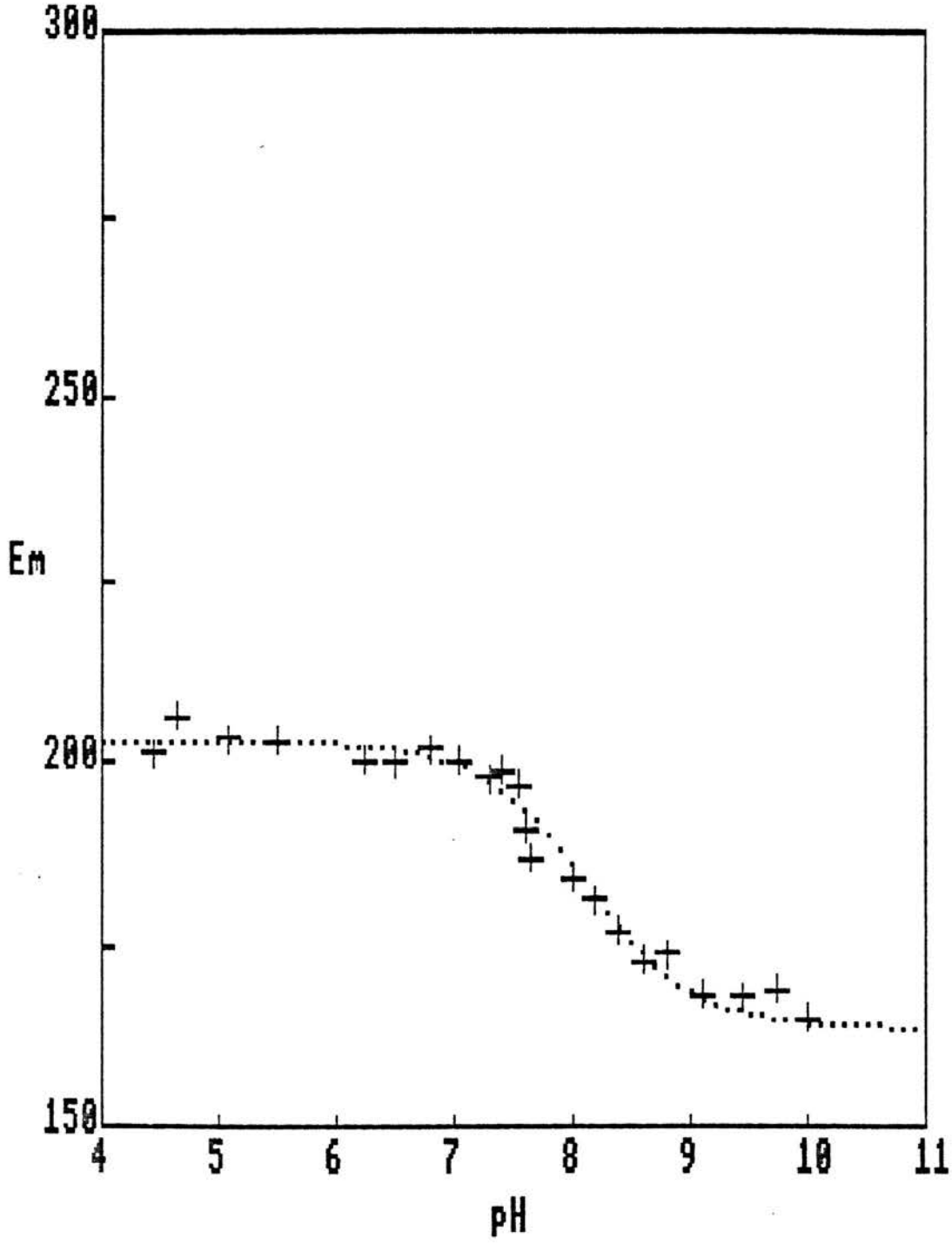
300
250
200
150
Em
4
5
6
7
8
9
10
11
pH

P.mendocina cyt.c-551

pKo1 - 7.2
pKr - 8

POINT	X	Y
1	4.8	270
2	5.25	271
3	6.45	266
4	6.8	263
5	7.2	252
6	7.5	246
7	7.65	245
8	8.15	236
9	8.5	231
10	8.8	225
11	9.3	222
12	9.8	216
13	10.25	209

Figure 27: $\underline{E_m}$ versus pH for P. mendocina Cytochrome c-551

The theoretical curve was obtained using Equation 2 and $\tilde{E}$ = 270mV, pK_O = 7.2 and pK_R = 8.0.

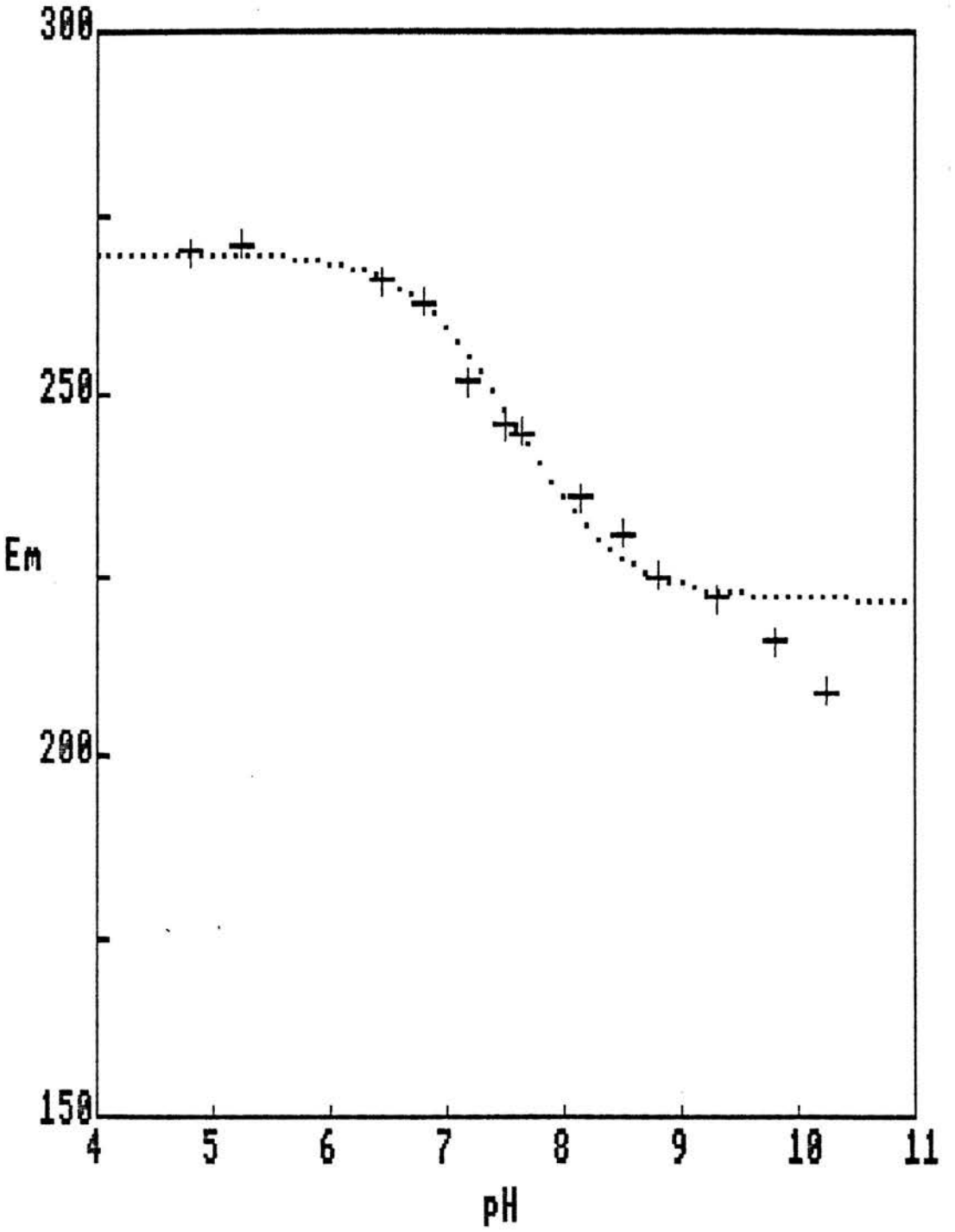
300
250
200
150
Em
4
5
6
7
8
9
10
11
pH

spectrum beyond pH10.95.

C. P. denitrificans and A. vinelandii Cytochromes c-551

The E_m versus pH curves for P. denitrificans and A. vinelandii cytochromes c_{551} are shown in Figures 28 and 29, respectively. Redox potentials were measured by the method of mixtures with ferri-ferrocyanide. In both cases E_m is only very slightly pH dependent, with an overall drop in potential of ca. 20mV between pH5 and 8. The theoretical curves were drawn using Equation 3 (page 29) which covers the case where two ionisations occur in the ferricytochrome (pk_{O1}, pK_{O2}) and one in the ferrocytochrome (pK_{R1}), in the sequence pK_{O1}, pK_{R1}, pK_{O2}. Below pH 9 the data appear to follow the theoretical curves quite convincingly, although in the absence of these curves it is difficult to distinguish any sort of pattern. Apart from two pH points in each case, there is little justification for including pK_{O2} in the theoretical curves. A 695nm band titration has not been performed on the A. vinelandii cytochrome; the 695 nm band of P. denitrificans cytochrome c_{551} begins to titrate ca. pH10 but a pK has not been assigned. In the latter case pK_{O2} may not be a 695nm band pK anyway, since the data appear to level off again ca. pH10.5.

D. C.thiosulphatophilum cytochrome c-555

The redox potential of C. thiosulphatophilum cytochrome c_{555} is significantly lower than the redox potentials of any of the cytochromes c_{551} and cannot be measured in conjunction with the ferri-ferrocyanide couple (this being useful in the range 200-400mV only). For this cytochrome three-point reductive titrations were performed anaerobically using Fe^{2+}/Fe^{3+}EDTA, as described in Chapter II, and E_m calculated from a plot of log ($[cyt]_{ox}/[cyt]_{red}$) against E_h. The E_m versus pH curve of cytochrome c_{555} is shown in Figure 30. The theoretical curve was constructed using Equation 2 (page 28) with pK_O

P.denitrificans cyt.c-551

pKo1 - 6.4
pKr - 6.75
pKo2 - 9.8

POINT	X	Y
1	4.9	272
2	5.6	271
3	5.9	270.5
4	6.3	266.5
5	6.7	261
6	7.05	258
7	7.8	252
8	8.25	253
9	8.5	251
10	8.8	248
11	9	245
12	9.05	243.5
13	9.2	242
14	9.8	236
15	10.1	234.5

Figure 28: E_m versus pH for P. denitrificans Cytchrome c-551

The theoretical curve was obtained using Equation 3 with $\tilde{E}$ = 253mV, pK_{O1} = 6.4, pK_R = 6.75 and pK_{O2} = 9.8.

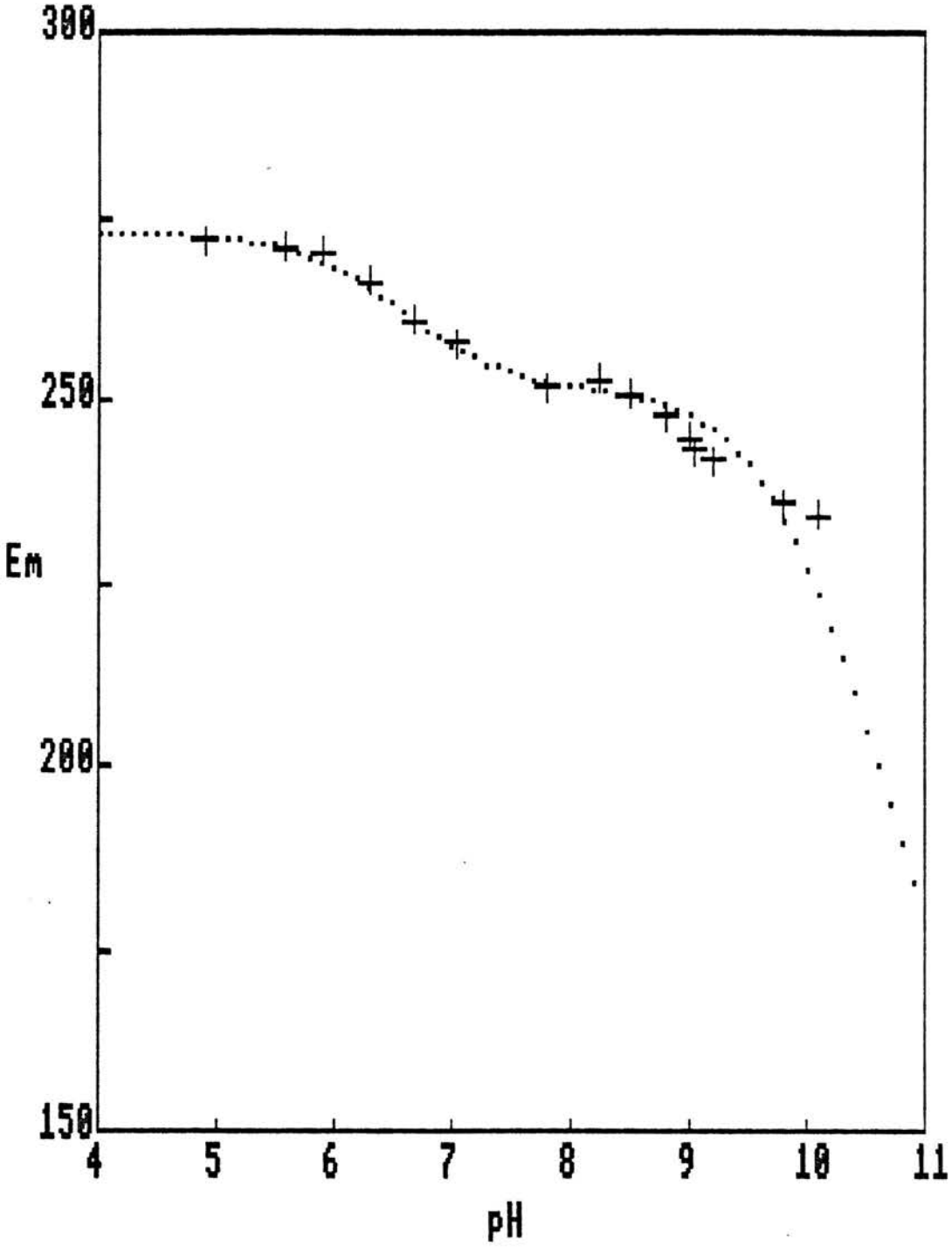
300
250
200
150
Em
4
5
6
7
8
9
10
11
pH

A.vinelandii cyt. c-551

pKo1 - 5.8
pKr - 6.2
pKo2 - 10

POINT	X	Y
1	4.5	286
2	4.6	290.5
3	5	283
4	5.35	279
5	5.9	278.5
6	6.35	271
7	6.5	268
8	6.95	267
9	7.65	260
10	8	266
11	8.4	262
12	8.75	261
13	9.2	259.5
14	9.65	246
15	10.1	244

Figure 29: E_m versus pH for A. vinelandii Cytochrome c-551

The theoretical curve was obtained using Equation 3 with $\tilde{E}$ = 287mV, pK_{O1} = 5.8, pK_R = 6.2 and pK_{O2} = 10.0.

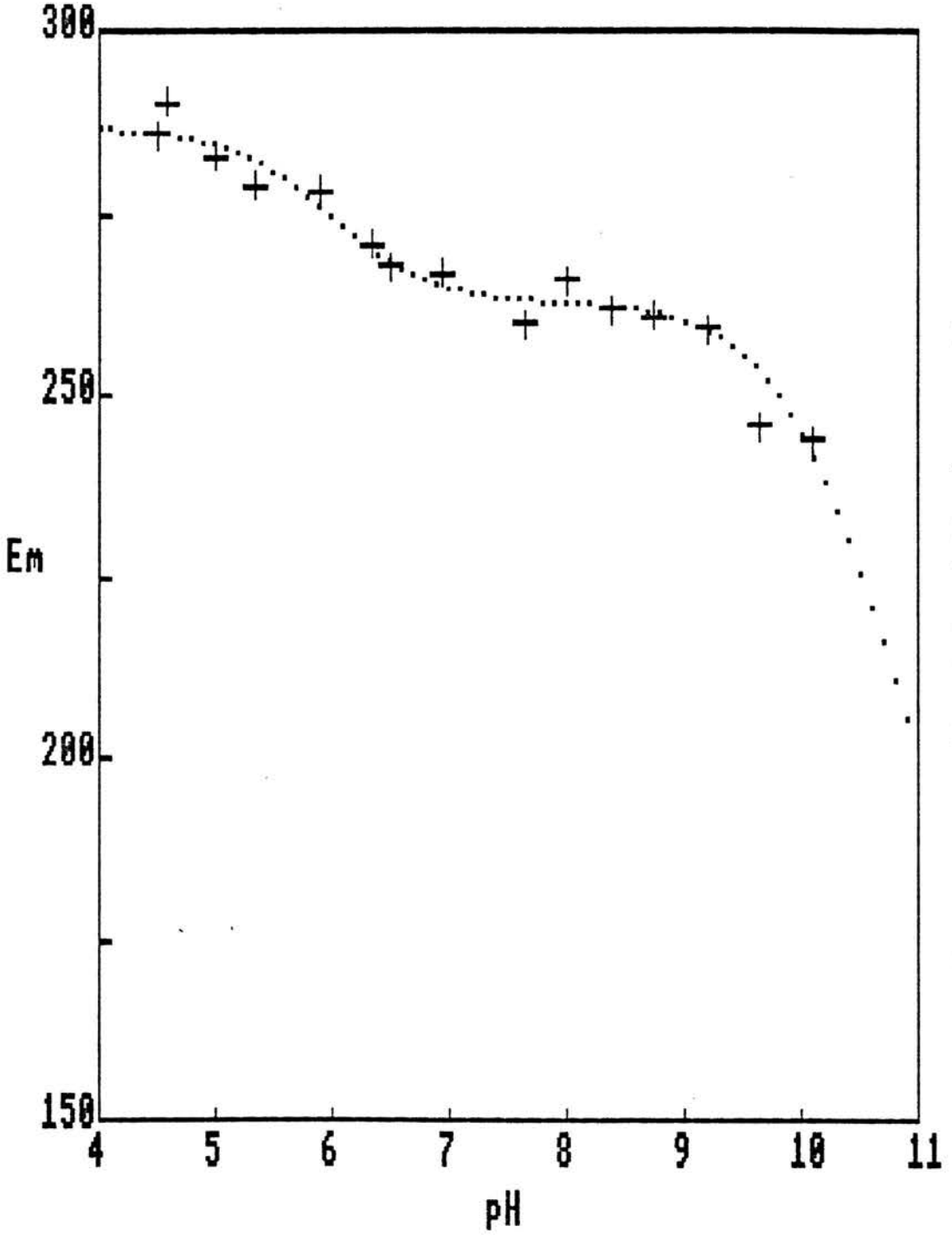
300
250
200
150
Em
4
5
6
7
8
9
10
11
pH

C.thiosulphatophilum c-555

pKo1 - 6.3
pKr - 7.1

POINT	X	Y
1	4.5	189
2	4.95	182
3	5.15	182
4	5.6	180
5	5.9	174
6	6.15	174
7	6.2	165
8	6.4	168
9	6.8	155
10	7	149
11	7.2	149
12	7.35	144
13	7.65	142
14	7.9	143
15	8.2	139
16	8.25	133
17	8.65	139
18	8.9	139

Figure 30: E_m versus pH for C. thiosulphatophilum Cytochrome c-555

The theoretical curve was obtained using Equation 2 with $\tilde{E}$ = 182mV, pK_O = 6.3 and pK_R = 7.1.

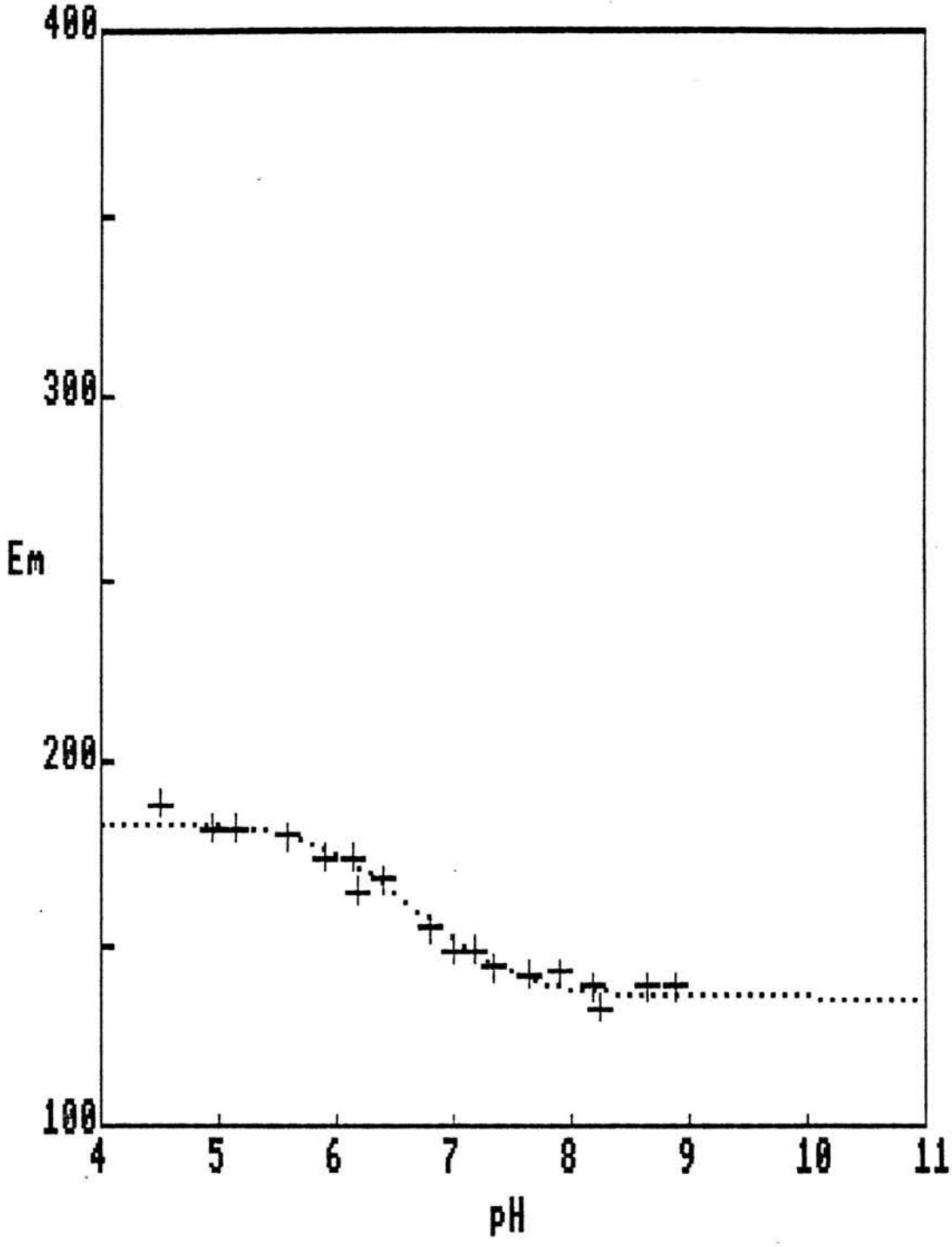
400
300
200
100
Em
4
5
6
7
8
9
10
11
pH

= 6.3 and pK_R = 7.1.

It should be noted here that the bulk of the data shown in Figure 30 were originally obtained by G. Pettigrew (G. Pettigrew, unpublished data) and that the few additional points made by myself were required check that my own preparation behaved similarly for the purposes of subsequent NMR experiments.

D. Comments on Redox Curves

The data for the four Pseudomonas cytochromes c_{551} are collected together in Figure 31 and the E_m versus pH curve of P. aeruginosa cytochrome c_{551} is included (as a dotted line) for comparison. Three of the four cytochromes show similar 2-ionisation E_m versus pH curves to P. aeruginosa cytochrome c_{551}, although in each of these three cases the overall drop in potential is some 20mV less (pK_O and pK_R are closer together) and the pKs both occur about 1 pH unit higher. The P. denitrificans cytochrome has a different E_m versus pH profile in that a third ionisation appears to occur below pH10; pK_{O1} and pK_R are separated by only 0.35 pH units and there is a concomitantly small drop in potential between pH6 and 8. If indeed propionic acid-7 is the group which ionises with pK_O and pK_R in all five cytochromes then the question then arises: why do the pKs vary? One possible explanation is that the tertiary structures of the cytochromes are rather different. However, NMR data to be presented in Chapter V for P. stutzeri 221 and P. mendocina cytochromes c_{551} indicate that their tertiary structures are really very like the structure determined for P. aeruginosa cytochrome c_{551}. On the other hand, it is conceivable that the immediate environment of propionic acid-7 may be quite different in the five cytochromes, even though no gross structural differences are apparent. In this respect, propionic acid-7 may adopt different orientations with respect to the haem (its distance from the haem will affect the separation of pK_O

Figure 31: E_m versus pH Curves for Pseudomonas Cytochromes c-551

● P. denitrificans, ○ P. mendocina, ▲ P. stutzeri (221) and Δ P. stutzeri (224) cytochrome c_{551}; ---- theoretical curve for P. aeruginosa cytochrome c_{551} (see Figure 10).

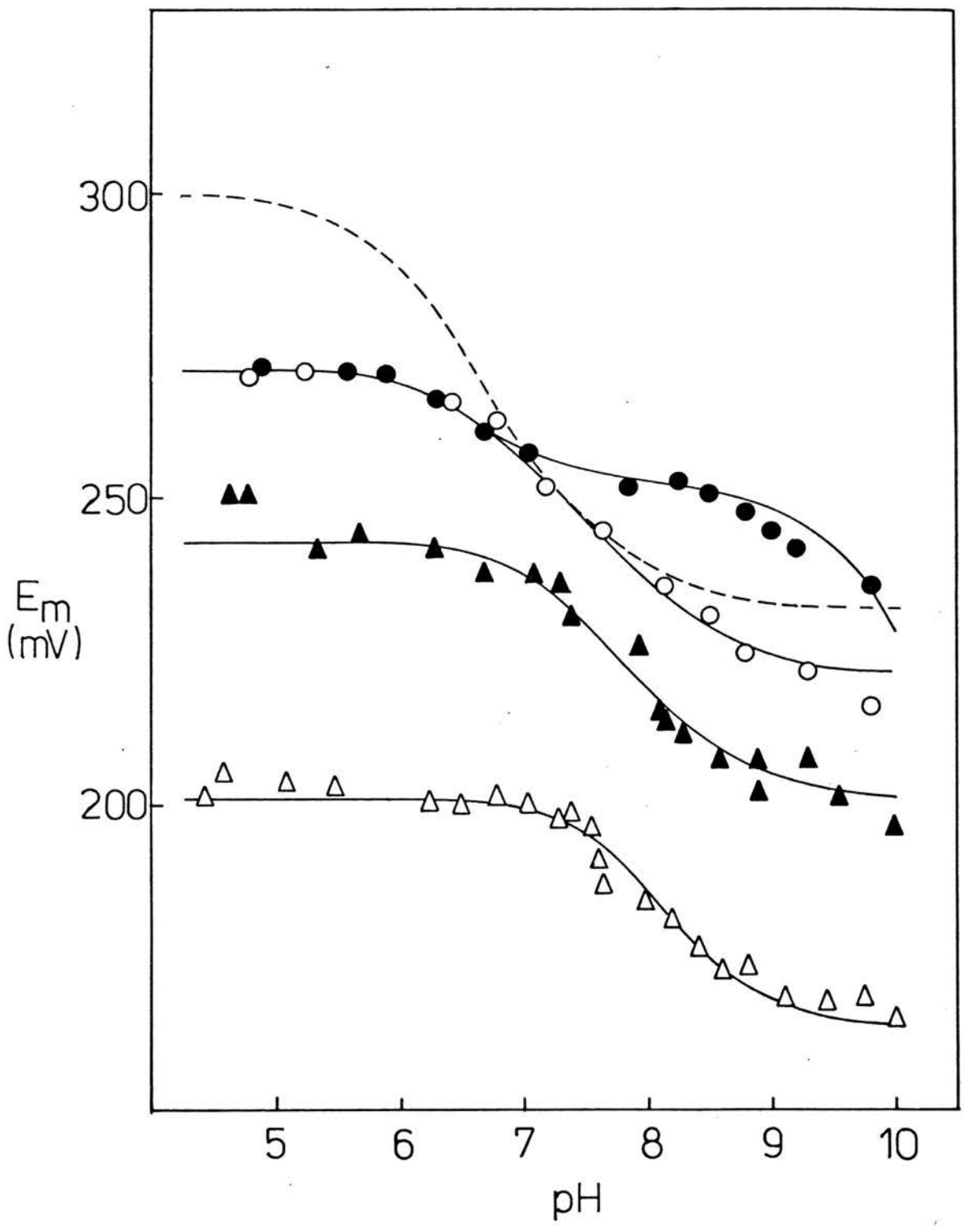
300
250
200
E_m
(mV)
5
6
7
8
9
10
pH

and pK_R) or the propionic acid may be able to form a variety of interactions with amino acids in the polypeptide backbone (the precise interaction may influence the pKs at which it ionises). In the crystal structure of *P. aeruginosa* cytochrome c_{551}, propionic acid-7 is hydrogen bonded to Arg47 and Trp56. Trp56 is conserved in the other four *Pseudomonas* cytochromes discussed here, and the *A. vinelandii* cytochrome, but the residue at sequence position 47 is variable (*P. stutzeri* 221, *P.stutzeri* 224, and *P. mendocina* cytochromes c_{551} have His47, *P. denitrificans* cytochrome c_{551} has Ser47 and the *A. vinelandii* cytochrome has Lys47). The possibility then arises that the nature of the amino acid at sequence position 47 may be important in controlling the pKs at which propionic acid-7 ionises. If this is indeed the case, then it should be possible to predict *how* amino acid 47 will affect the propionic acid pKs. This predictive aspect is considered further in chapter VII (Discussion). Of more immediate importance is the question of whether propionic acid-7 actually *does* ionise in any of the other cytochromes - Chapter V considers the situation with *P. stutzeri* 221 and *P. mendocina* cytochromes c_{551}.

The E_m versus pH curve of *C. thiosulphatophilum* cytochrome c_{555} is similar in shape to the curves obtained for the *Pseudomonas* cytochromes; it shows the same overall drop in potential as the *P. stutzeri* cytochromes although the pKs are more like those observed for *P. aeruginosa* cytochrome c_{551}. It might be speculated that propionic acid-7 is the ionising group in this cytochrome also. The crystal structure of cytochrome c_{555} has been determined to 2.7Å resolution and it clearly has many features in common with the tertiary structure of *P. aeruginosa* cytochrome c_{551}, particularly with regard to the structure at the bottom of the haem crevice (Korzun & Salemme, 1977). A tryptophan occurring at sequence position 34 and a histidine at position 37 may be

structurally analogous to Trp56 and residue 47,respectively, in cytochrome c_{551}. However, the crystal structure is not yet at a sufficient level of refinement to infer hydrogen bonds so it is not known whether either of these amino acids interact with propionic acid-7. The identity of the group ionising with redox state dependent pKs is investigated by NMR in Chapter V.

An interesting aspect of the curves shown in Figure 31 is the differences in level of redox potential amongst the five homologous cytochromes. Kassner (1972a,b) has suggested that the high redox potentials of c-type cytochromes relative to model haem complexes can be accounted for by the non-polar nature of the haem environment; within the hydrophobic interior of a cytochrome molecule, positively charged ferric haem is relatively less stable than ferrous haem (0 net charge), and so the haem has an increased affinity for a reducing electron. As an extension of this proposal, Kassner suggested that for homologous cytochromes of the same size, higher potentials result from the substitution of polar by hydrophobic amino acids in the haem crevice. Figure 31 shows that a substantial difference in the level of redox potential occurs between P. stutzeri 221 and P. stutzeri 224 cytochromes c_{551} - these differ in sequence by 11 amino acids, only 2 of which are considered to be haem contact residues (see Matsuura et al., 1982). Phe27 and Tyr34 in P. stutzeri 221 cytochrome are substituted by Leu27 and Asn34 in the 224 cytochrome. The hydrophobicity indices (i.e. ΔG value for transfer of the side chain from water to ethanol) for Phe27 and Tyr34 show them to be significantly more hydrophobic than Leu or Asn (see Tablel-1 of Schulz & Schirmer, 1979). That a higher potential is observed for P. stutzeri 221 cytochrome c_{551} is thus consistent with Kassner's hypothesis; although a difference of some 40mV relative to the 224 cytochrome seems quite dramatic considering there are only 2 important substitutions, this represents

a very small ΔG value.

E. α-Band Titrations

Moore et al. (1980) observed that the α-band of P. aeruginosa cytochrome c_{551} shifted ca. 2nm to the red and became markedly asymmetric towards alkaline pH. By careful titration of the ferrocytochrome over the pH range 5-9 they were able to show that the changes in the α-band shape and peak maximum could be fitted to a pK of 7.2, this value corresponding exactly with the value assigned to pK_R in the E_m versus pH curve of the cytochrome. Hence, the α-band titration was able to provide direct experimental confirmation of a theoretically derived pK value. Unfortunately, none of the other Pseudomonas cytochromes studied here developed a pronounced asymmetry or shifted to the red at alkaline pH, or at least not on the scale exhibited by P. aeruginosa cytochrome c_{551}. An α-band titration of P. stutzeri 221 cytochrome c_{551} did indicate some minor changes but these were too small to be assigned a pK value. However, C. thiosulphatophilum cytochrome c_{555} behaves similarly to P. aeruginosa cytochrome c_{551} in this respect. Its α-band, although asymmetric already, becomes noticeably more so towards alkaline pH and there is a small, concomitant change in intensity (G. Pettigrew, unpublished data). These changes have been fitted to a pK of 6.8, which is in reasonably good agreement with the pK_R of 7.0 derived from the E_m versus pH curve given the inaccuracies in measuring such small absorbance changes.

The α-band of most Class I c-type cytochromes is essentially symmetric (notable exceptions are C. oncopleti cytochrome c_{557} and E. gracilis cytochrome c_{558}, where the haem is bound to the polypeptide via one thioether linkage only), and the origin of the asymmetry observed in the cytochrome c_{555} α-band is not understood. In this respect, however, the ionisation state of groups

close to the haem can contribute to the asymmetry.

CHAPTER V: NMR EXPERIMENTS

The aim of the NMR studies was to identify a chemical group in each cytochrome which ionises with the redox state dependent pK values predicted from the corresponding redox measurements. The strategy is straightforward: ionisation of a chemical group will perturb the local magnetic environment, thereby causing changes in chemical shift for resonances of adjacent covalently bonded protons; resonances from non-covalently bonded protons which are in close spatial proximity to the ionising group may also be affected. In each oxidation state such shifting resonances will titrate with a pK corresponding to that of the ionising group. If the resonances can be assigned to specific amino acids then it should be possible to locate the ionising group in the protein. The lengthiest part of this procedure is resonance assignment.

NMR data for *P. stutzeri* 221 and *P. mendocina* cytochromes c_{551} are discussed in Section I and *C. thiosulphatophilum* cytochrome c_{555} is discussed in Section II.

N.B. Superscripts in this chapter refer to the notes in Appendix I.

Section I - Pseudomonas cytochromes c-551

For *P. stutzeri* cytochrome c_{551} to be discussed here as many assignments were made as was practicable, before carrying out pH titration experiments. The rationale for doing so was twofold: (i) The cytochrome c_{551} redox potential may be affected by an ionising group through its electrostatic effect on the haem or via an associated conformational change - the more resonances that are assigned then the more likely it is that these two possibilities can be distinguished. (ii) Since a crystal structure is not available for *P. stutzeri* (or *P. mendocina*) cytochrome c_{551} it was important to check that its solution structure closely resembles the *P. aeruginosa* (and *P. mendocina*) cytochrome structure - it is meaningless to compare the effects of an ionising group on redox potential if the tertiary structures of the three cytochromes differ.

Details of the *P. stutzeri* cytochrome resonance assignments are given in Section A, the tertiary structures of *P. stutzeri*, *P. mendocina* and *P. aeruginosa* cytochromes are compared in Section B and the pH titration results for *P. stutzeri* and *P. mendocina* cytochromes c_{551} are presented in Section C.

A. Resonance Assignments for P. stutzeri 221 cytochrome c-551

1. Aromatic assignments - ferricytochrome

The aromatic region of *P. stutzeri* ferricytochrome c_{551} is shown in Figure 32. This cytochrome contains only 7 aromatic amino acids *viz.* 2 tryptophans (Trp56, Trp77), 2 phenylalanines (Phe7, Phe27), 1 tyrosine (Tyr34) and 2 histidines (His16, His47), which contain a total of 28 aromatic amino acid CH protons. From the multiplet patterns of each type of aromatic amino acid shown in Table VIII it can be computed that the aromatic region of the spectrum should contain:

Table VIII: Coupling Patterns for the Aromatic Amino Acids

phenylalanine

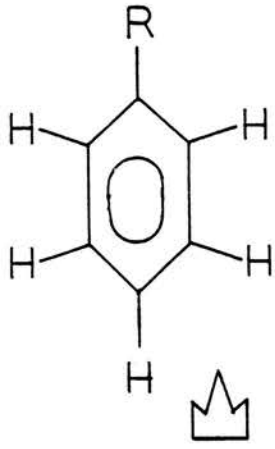

tyrosine

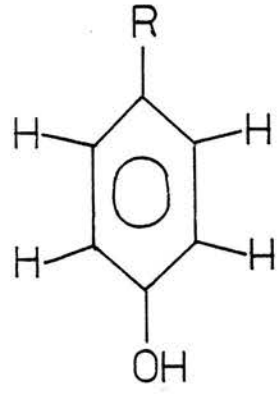

tryptophan

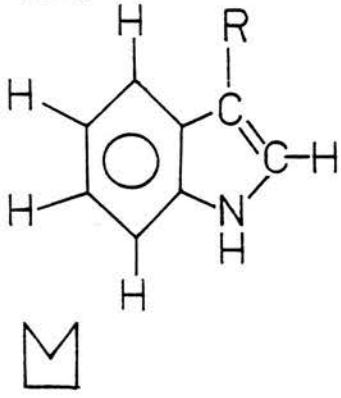

histidine

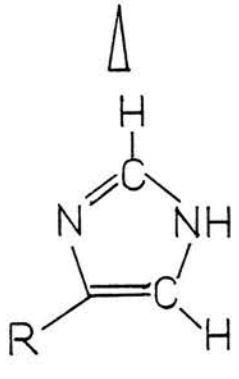

Figure 32: Aromatic Region of the convolution Difference Spectrum of P. stutzeri (221) Ferricytochrome c-551

The spectrum was obtained at pH* 6.5, 27°C. The labelled resonances are: F7 = Phe7, W56 = Trp56 and Y34 = Tyr34

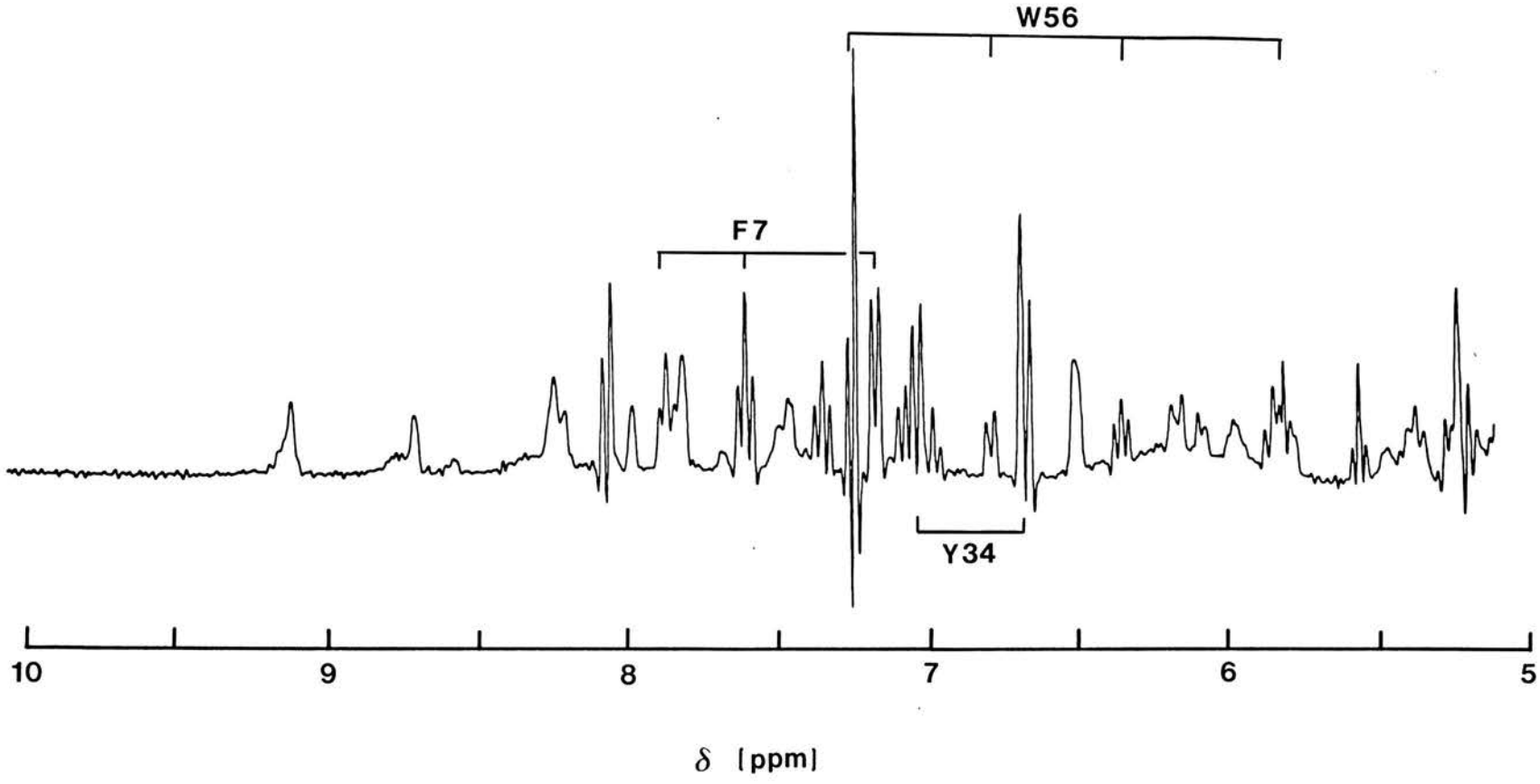
W56
F7
Y34
10
9
8
7
6
5
δ [ppm]

6 x 1-proton singlet
4 x 1-proton doublet
4 x 2-proton doublet
6 x 1-proton triplet
2 x 2-proton triplet

assuming that the ring systems of tyrosine and phenylalanine undergo rapid flipping about the C -C bond[12].

Singlets: one of the two histidines, His16, is the fifth iron ligand and, as such, its two resonances are expected to be shifted upfield, outwith the aromatic region (see Introduction/III). Therefore, only four 1-proton singlets should be observed and these can be seen at 8.68, 7.65, 7.21 and 6.64 ppm. Between pH7 and 9 the resonances at 8.68 and 7.65 ppm have markedly pH dependent chemical shift values (see Section B) and on this basis they are assigned to the C-2 and C-4 resonances of the unliganded histidine, His47. The specific assignment of the tryptophan singlets is discussed later.

Doublets and triplets: doublet and triplet resonances from the same amino acid can be identified by a standard double resonance technique called spin decoupling[3]. In a spectrum containing two coupled doublets (e.g. tyrosine), say, time-shared irradiation of one of them will remove the multiplet splitting of the other so that it appears as a singlet. In the case of a coupled doublet and triplet (e.g. tryptophan) irradiation of the doublet will cause the triplet to collapse to a doublet. Since each aromatic amino acid shows a distinctive pattern of coupled resonances, spin decoupling experiments can be used to distinguish phenylalanine, tryptophan and tyrosine resonances. As an example, Figure 33 shows how the spin system of one of the two phenylalanine residues was assigned: the resolved triplet at 7.65 ppm (a) could arise from either a

Figure 33: Spin-Decoupling Experiments on the Phe7 Spin System

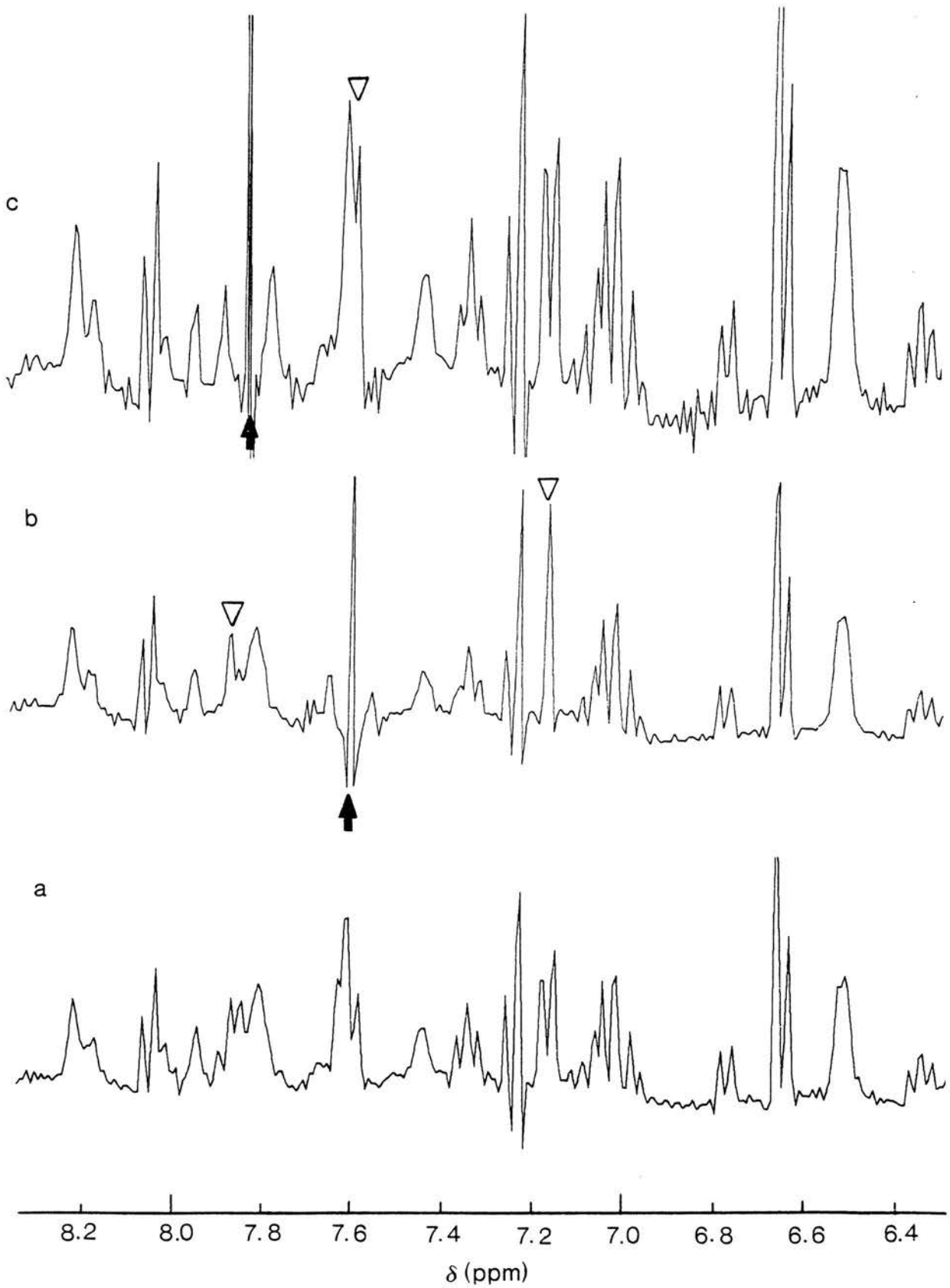
c
b
a
8.2
8.0
7.8
7.6
7.4
7.2
7.0
6.8
6.6
6.4
δ (ppm)

tryptophan or a phenylalanine[4]. Irradiation at this triplet (b) decoupled a doublet to a singlet at 7.15 ppm and also a triplet to a singlet at 7.85 ppm. Subsequent irradiation of the triplet decoupled only the triplet at 7.65 ppm (c). The doublet is therefore the ortho resonance of a phenylalanine, the triplet at 7.65 ppm being the meta resonance and the triplet at 7.85 ppm the para resonance.

A second example is illustrated in Figure 34, which shows the assignment of a set of tryptophan resonances. Irradiation of a doublet at 7.23 ppm decouples a triplet to a doublet at 6.32 ppm (b). Irradiation at the triplet decouples the doublet to a singlet, but also decouples a triplet to a doublet ca. 5.8 ppm (c). This is a region of considerable resonance overlap and in the absolute spectrum the 1-proton triplet collapsing to a doublet is scarcely discernable; it is however quite clear from the difference spectrum (a)-(c) (not shown). Irradiation at 5.8 ppm causes the collapse of its coupled triplet at 6.32 ppm and also of the doublet at 6.76 ppm (d).

With further spin decoupling experiments, the resonances of the second tryptophan and the single tyrosine, Tyr34, were identified. This left only one resonance (a doublet) unassigned in the aromatic region and it was assumed to be the ortho resonance of the second phenylalanine; irradiation at this doublet did not decouple any other resonance in the aromatic region between 5.5 and 10 ppm so it was concluded that the meta and para protons of this phenylalanine have unusually upfield shifted resonances.

Quartets: Two quartets occur in the aromatic region of this cytochrome, one at 6.10 ppm and the other at 5.10 ppm. Irradiation at these quartets causes the collapse of two 3-proton doublets in the aliphatic region, at 1.7 and 1.25 ppm, respectively . From their coupling pattern, these resonances must arise from two alanine (or threonine) residues. Since alanine/threonine α-CH

Figure 34: Spin-Decoupling Experiments on the Trp56 Spin System

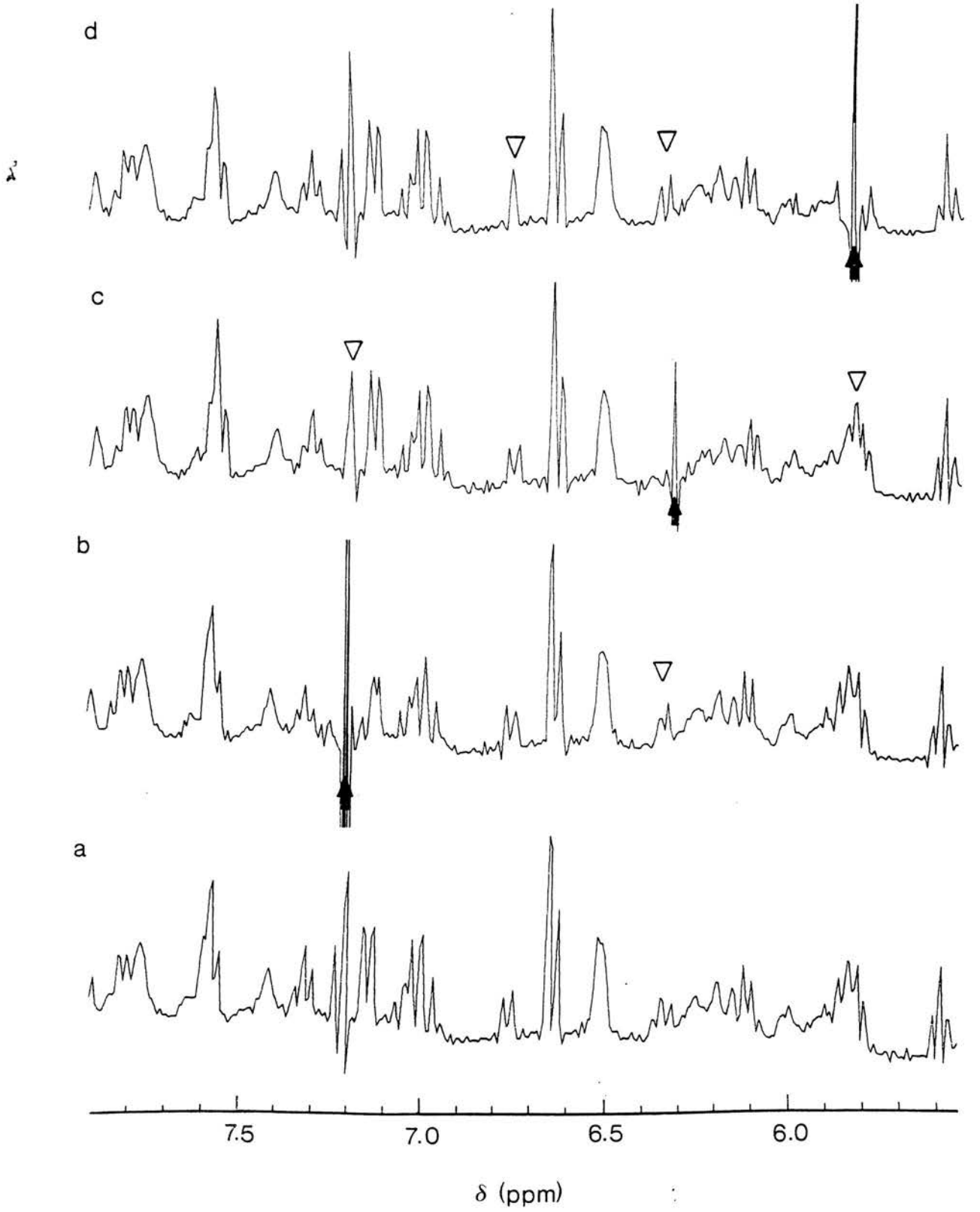
d
c
b
a
7.5
7.0
6.5
6.0
δ (ppm)

resonances normally occur in the aliphatic region from 3-4 ppm, these downfield shifted quartets must experience an unusual environment. They are assigned to Ala13 and Ala14, which occur in the sequence between the two conserved cysteine residues covalently linking haem c to the polypeptide in all c-type cytochromes. Resonances of the two amino acids located between these cysteines in other cytochromes have previously been noted to experience such downfield shifts (Moore & Williams, 1980b).

The first-stage assignments are summarised in Figure 32.

2. Aromatic assignments - ferrocytochrome

The ferrocytochrome aromatic region contains more overlapping resonances than does the ferricytochrome and was consequently more difficult to assign. The aromatic region is shown in Figure 35.

The four singlet resonances are again discernable, but at 8.62, 7.75, 7.35 and 7.03 ppm in this oxidation state. As in the ferricytochrome the His47 singlets are specifically assigned as a result of their pH dependent chemical shifts, the C-2 resonance being that at 8.62 ppm and the C-4 resonance at 7.03 ppm.

The doublet resonances of Tyr34 at 7.29 and 7.52 ppm and the spin systems of one tryptophan and one phenylalanine were assigned by straightforward spin decoupling experiments.

Two peaks, occurring at 6.23 and 5.99 ppm, were each shown to be of 3-proton intensity. Irradiation at 6.23 ppm decoupled a 3-proton doublet to a singlet at 2.41 ppm, and irradiation at 5.99 ppm caused the collapse of a 3-proton doublet at 1.96 ppm. By comparison with other c-type cytochromes (Keller & Wüthrich, 1978a,b), the peaks at 6.23 and 5.99 ppm are assigned to the haem thioether-2 and thioether-4 methine resonances (see Figure 5), their coupled aliphatic resonances being assigned to the methyl protons. However, since the

Figure 35: Aromatic Region of the Convolution Difference Spectrum of P. stutzeri (221) Ferrocytochrome c-551

The spectrum was obtained at pH* 7.7, 27°C. The labelled resoances are: 56, W56 = Trp56; 77, W77 = Trp77, F27 = Phe27; α, β, γ and δ are the meso resonances.

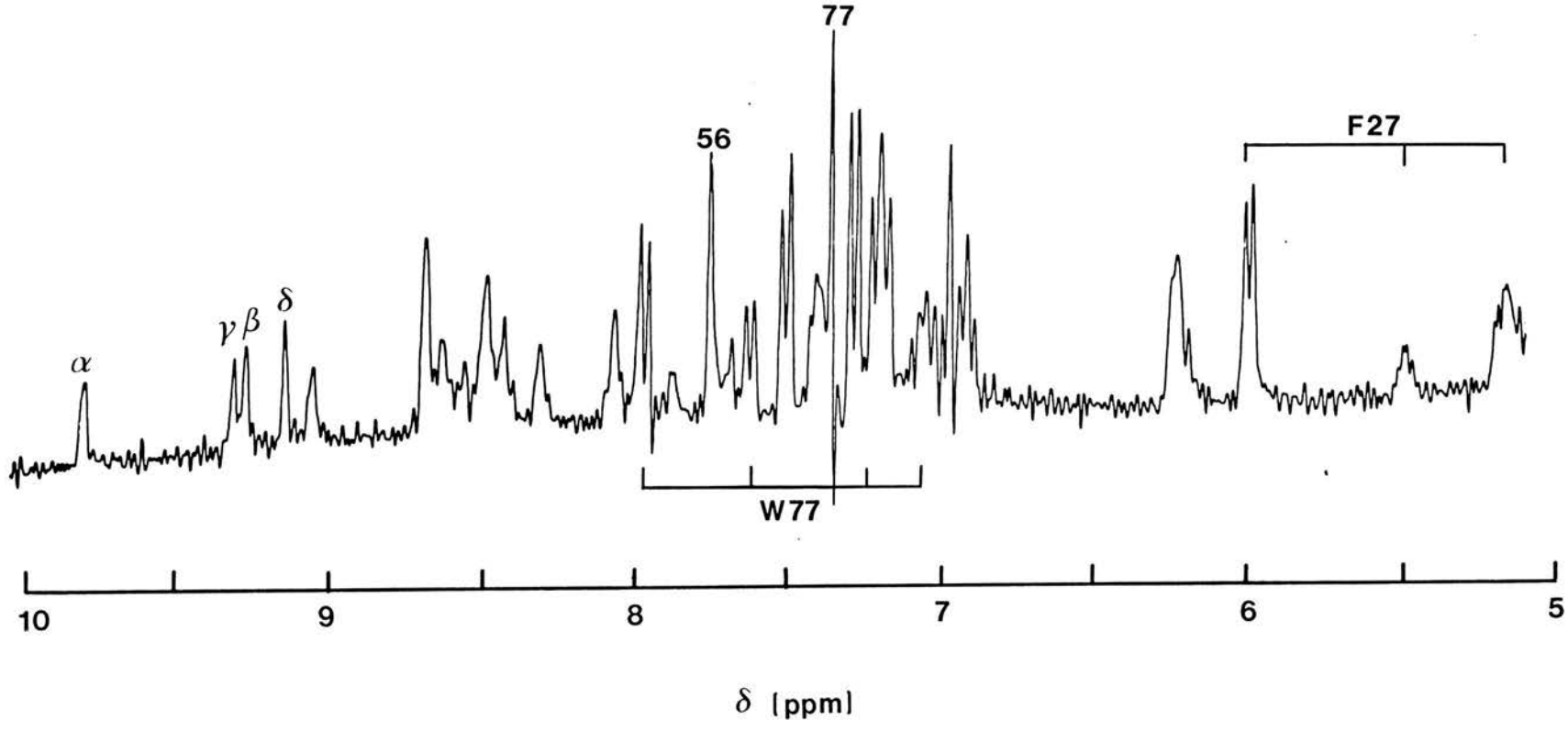
77
56
F27
α
γ β
δ
W77
10
9
8
7
6
5
δ [ppm]

methine resonance accounts for only one proton, each of the two peaks must contain contributions from the second phenylalanine and the second tryptophan. Irradiation at 5.99 ppm also collapses a triplet occurring on the limit of the aromatic region at 5.11 ppm. Irradiation at this triplet decouples a second triplet at 5.47 ppm and also decouples a doublet to a singlet under the 5.99 ppm peak. This family of coupled resonances therefore belongs to the second phenylalanine and so, as in the ferricytochrome, one set of phenylalanine resonances occurs towards the upfield end of the aromatic region. Assignment of the second tryptophan is discussed below.

The ferrocytochrome assignments covered in this section are summarised in Figure 35.

3. Cross-assignment of aromatic resonances and deduction of residue sequence positions

As an aid to specific assignment the chemical shift position of resonances can be correlated between the spectra of the oxidised and reduced cytochrome. With phenylalanine, for instance, this allows us to relate either set of assigned resonances in the ferricytochrome to one of the two sets in the ferrocytochrome. If it transpires that phenylalanine spin system A is much more oxidation state dependent than spin system B then it can be concluded, tentatively, that Phe A is closer to the haem than Phe B (assuming that no conformation changes occur between the two oxidation states). Consideration of the three-dimensional structure may allow Phe A and Phe B to be specifically assigned to the phenylalanines occurring at positions 7 and 27 in the sequence.

If a proton undergoes rapid exchange[5] between two magnetically different environments (e.g. ferri- and ferrocytochrome c), then the chemical shift position for the proton resonance will be intermediate between its position in the ferri- and ferrocytochrome. Its precise chemical shift in mixtures of the two redox states will be a function of the relative amounts of oxidised and

reduced cytochrome present, so that at 1:1 ferricytochrome:ferrocytochrome the resonance will occur midway between its two chemical shift limits.

Figure 36 shows spectra of various mixtures of oxidised and reduced P. stutzeri 221 cytochrome c_{551} obtained by titrating the ferricytochrome with sodium ascorbate. Several resonances can be followed as they shift back to their diamagnetic positions in the ferrocytochrome; some of these are indicated by dotted lines and/or letters. Of particular interest are the resonances labelled e and f. These represent the 1-proton triplets of the tryptophan which remains unassigned in the ferrocytochrome - the titration shows that both these triplets must overlap the thioether-4 methine resonance at 6.23 ppm in the fully reduced state. Certain other resonances cannot be detected in the redox mixtures due to exchange broadening[6] or because of resonance overlap. A few resonances can only be located towards the beginning or end of the titration and in these cases a plot of chemical shift (δ) versus pH can be extrapolated to predict where such resonances should apppear at the other titration limit. This is illustrated in Figure 37. Here it can be seen that a tryptophan doublet at 6.75 ppm in the ferricytochrome is predicted to occur at 7.3 ppm in the ferrocytochrome. There is a resonance at approximately this position in the ferrocytochrome and although its multiplet nature is not clear (see Figure 35, for example), subsequent spin decoupling experiments showed that it is coupled to the tryptophan triplets overlapping the thioether-4 methine resonance. Figure 37 also shows the cross-assignment of one phenylalanine resonance from each of the two spin systems, which allows complete cross-assignment of all the phenyalanine resonances. The doublets of Tyr34 were also cross-assigned.

The conclusions from this experiment are summarised in Figure 38.

Figure 36: Titration of P. stutzeri (221) Ferricytochrome c-551 with Ascorbic Acid

Figures on the left refer to the % ferrocytochrome present. Labelled resonances are: (a) His47 C-2, (b) Trp77 C-4 or C-7, (c) Phe7 ortho, (d) Phe27 ortho, (e) Trp56 C-5 or C-6, (f) Trp56 C-6 or C-5 and (g) Phe27 para.

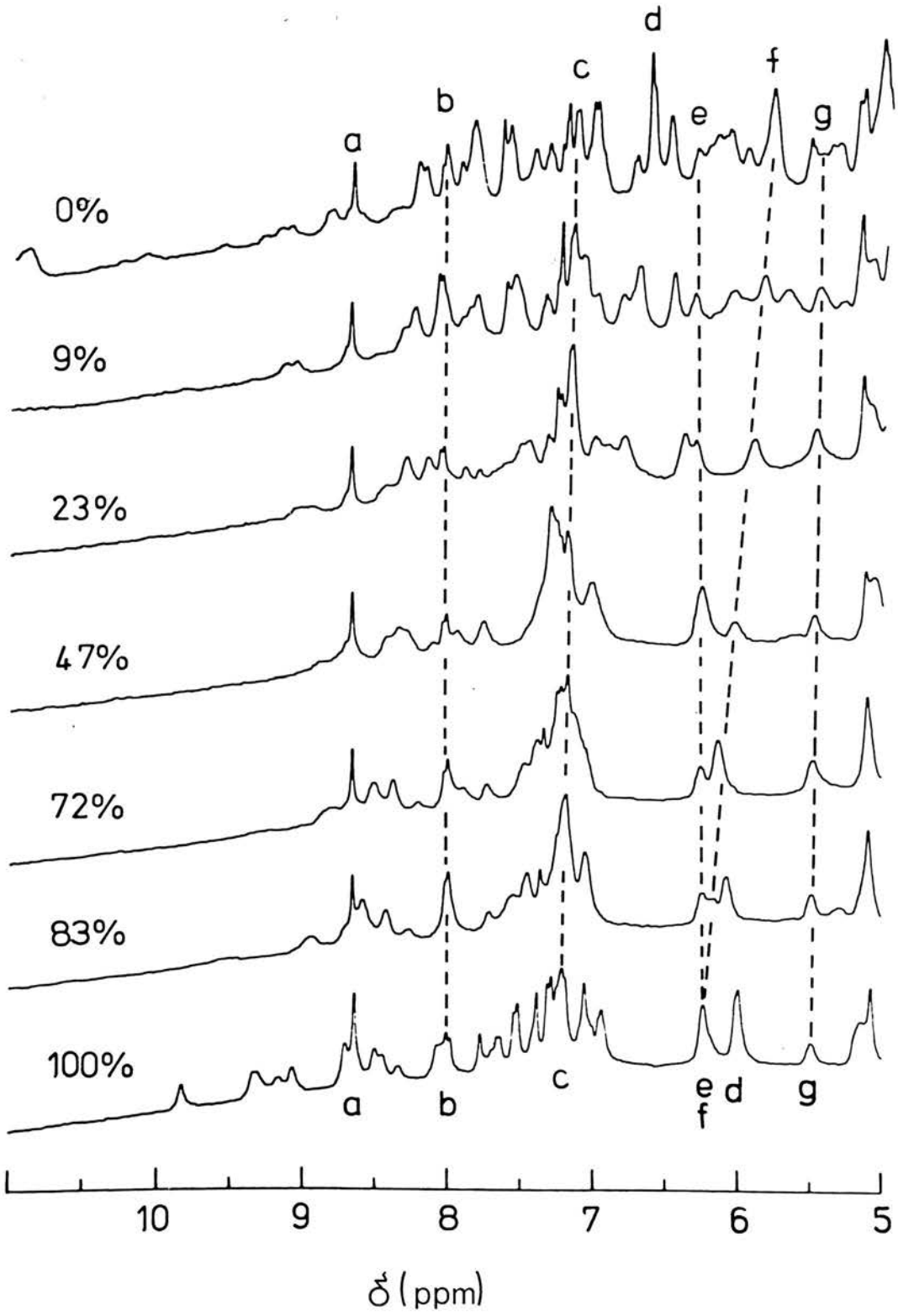
a
b
c
d
e
f
g
0%
9%
23%
47%
72%
83%
100%
10
9
8
7
6
5
δ (ppm)

Figure 37: Chemical Shift (δ) versus pH for the Ascorbate Titration

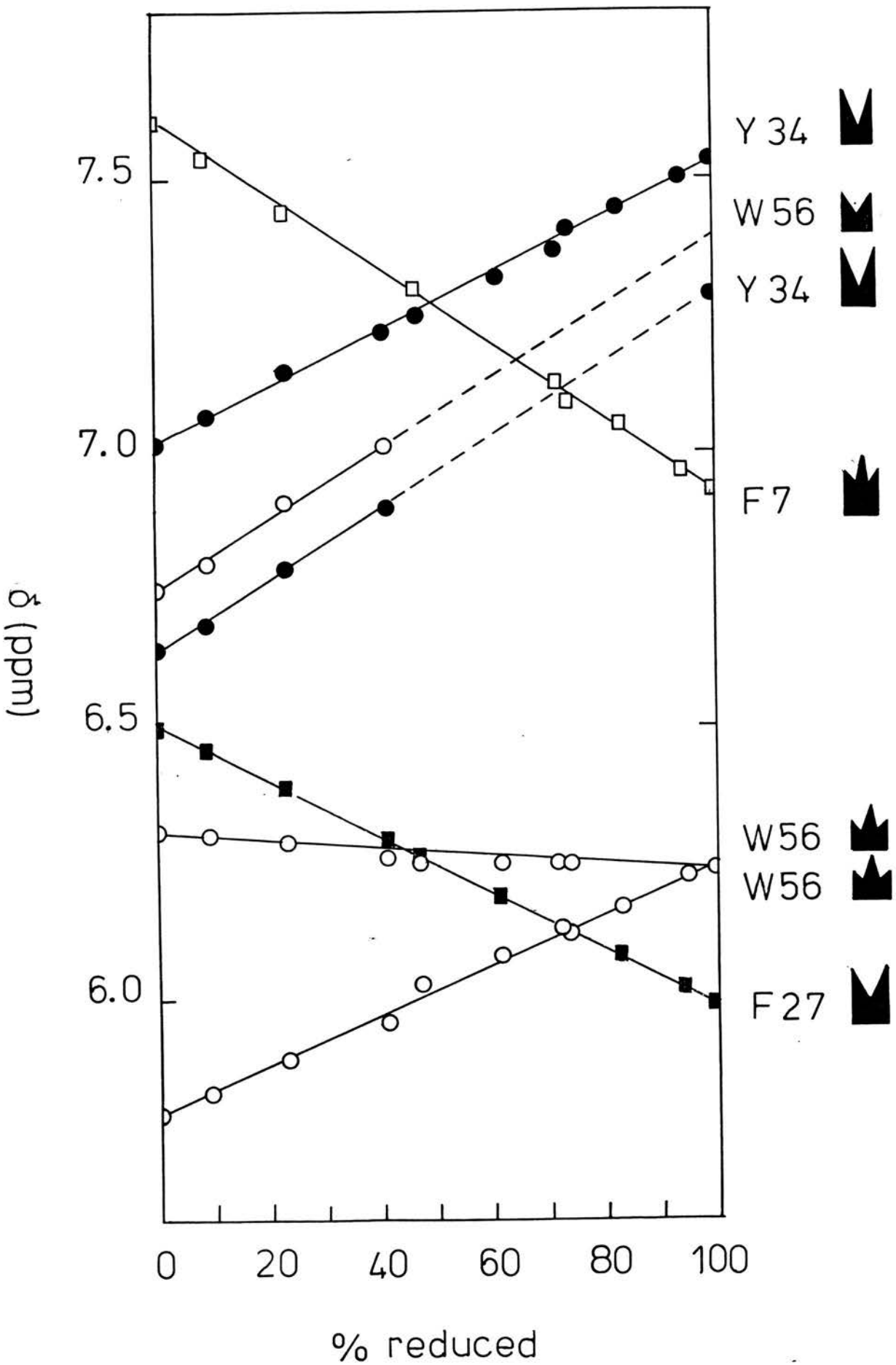
7.5
7.0
6.5
6.0
δ (ppm)
0
20
40
60
80
100
% reduced
Y 34
W 56
Y 34
F 7
W56
W56
F 27

Figure 38: Cross-Assignment of Aromatic Resonances of P. stutzeri (221) cytochrome c-551

Black = His47; Blue = Trp77; Red = Trp56; Orange = Tyr34; Green = Phe7; Brown = Phe27; (Pink = Ala13/14).

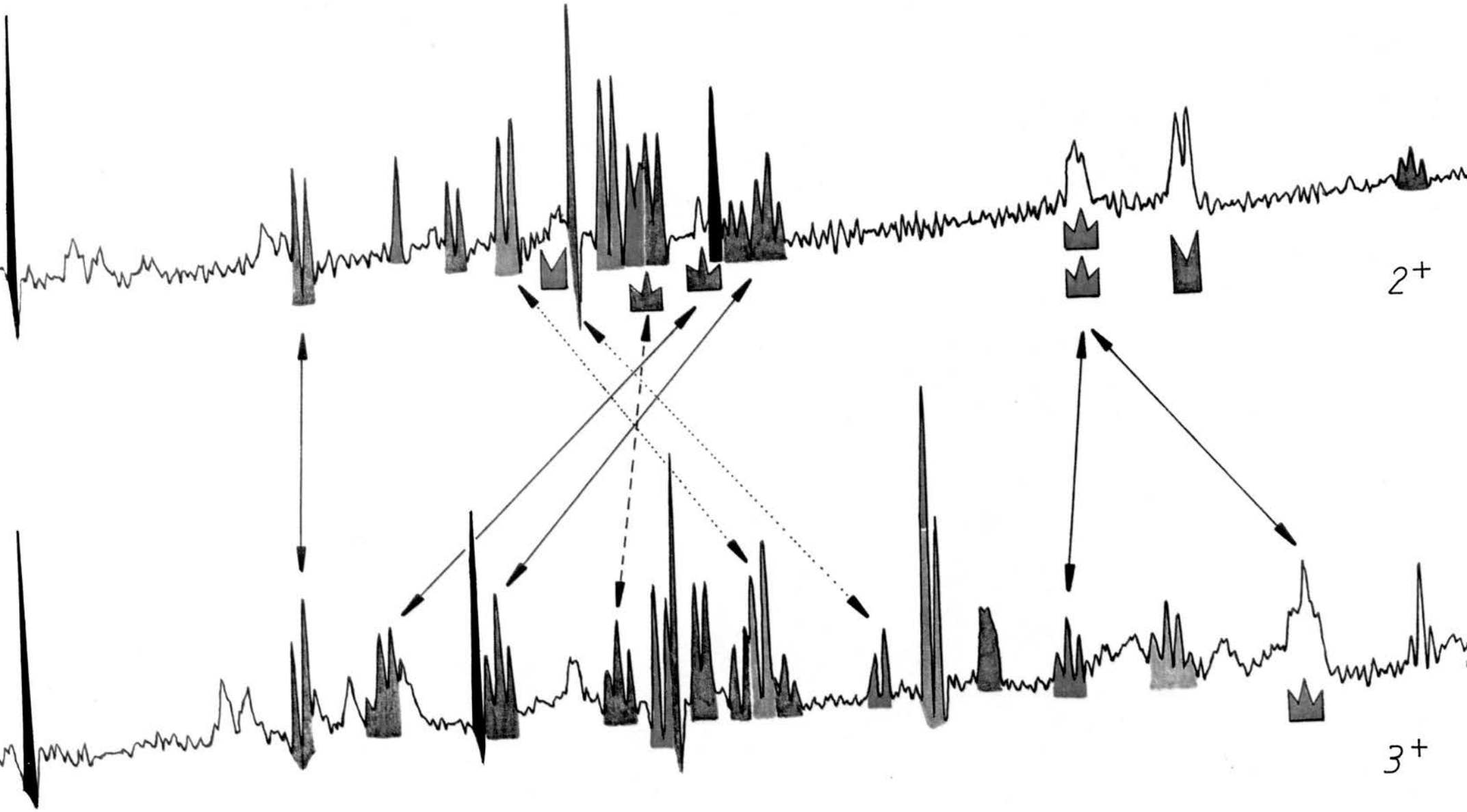
2+
3+

One tryptophan spin system is more oxidation state dependent than the other (although not all of the resonances are affected to the same extent). The two tryptophans of P. stutzeri cytochrome c_{551} occur at identical sequence positions in P. aeruginosa cytochrome c_{551}. In the three-dimensional structure of the latter, Trp56 is hydrogen bonded to a haem propionic acid substituent (Matsuura et al., 1982) whereas Trp77 occurs in a part of the molecule quite remote from the haem - on this basis the tryptophan resonances occurring at 6.76, 5.8, 6.32 and 7.23 ppm in P. stutzeri ferricytochrome c_{551} are assigned to Trp56. The argument extends to the tryptophan singlets as well and so the singlet occurring at 6.64 ppm is assigned to Trp56.

Specific assignment of the two phenylalanines is more difficult; both are affected by change of oxidation state. However, the unusual upfield shifts experienced by one set of phenylalanine resonances suggest their assignment to Phe27. From the three-dimensional structure of P. aeruginosa cytochrome c_{551} it appears that the amino acid occurring at sequence position 27 could be within the shielding region of the haem ring current field[7]. In the P. aeruginosa cytochrome there is a tyrosine at position 27 and its resonances are shifted markedly upfield from the primary position of tyrosine resonances[8] (G.R. Moore, unpublished observations).

These assignments are included in Figure 38.

4. Haem substituent assignments

The ^{1}H NMR spectrum of P. stutzeri ferricytochrome c_{551} is shown in Figure 39. The anomalously large shifts observed for the few resonances between 10 and 40 ppm and between 0 and -20 ppm result from the interaction of their nuclear spins with the unpaired electron of the ferric iron. In paramagnetic molecules unpaired electron spin density can be transferred to individual nuclei by electron spin delocalisation through chemical bonds. In paramagnetic haem c, delocalisation occurs via 5th

Figure 39: ^{1}H NMR Spectrum of P. stutzeri (221) Ferricytochrome c-551

Spectrum obtained at pH* 6.3, 27°C. The labelled resonances are M1, M3, M5 and M8 = haem methyls; P1 and P2 = β-CH_2 protons of haem propionic acid-7; Met = Met61 methyl.

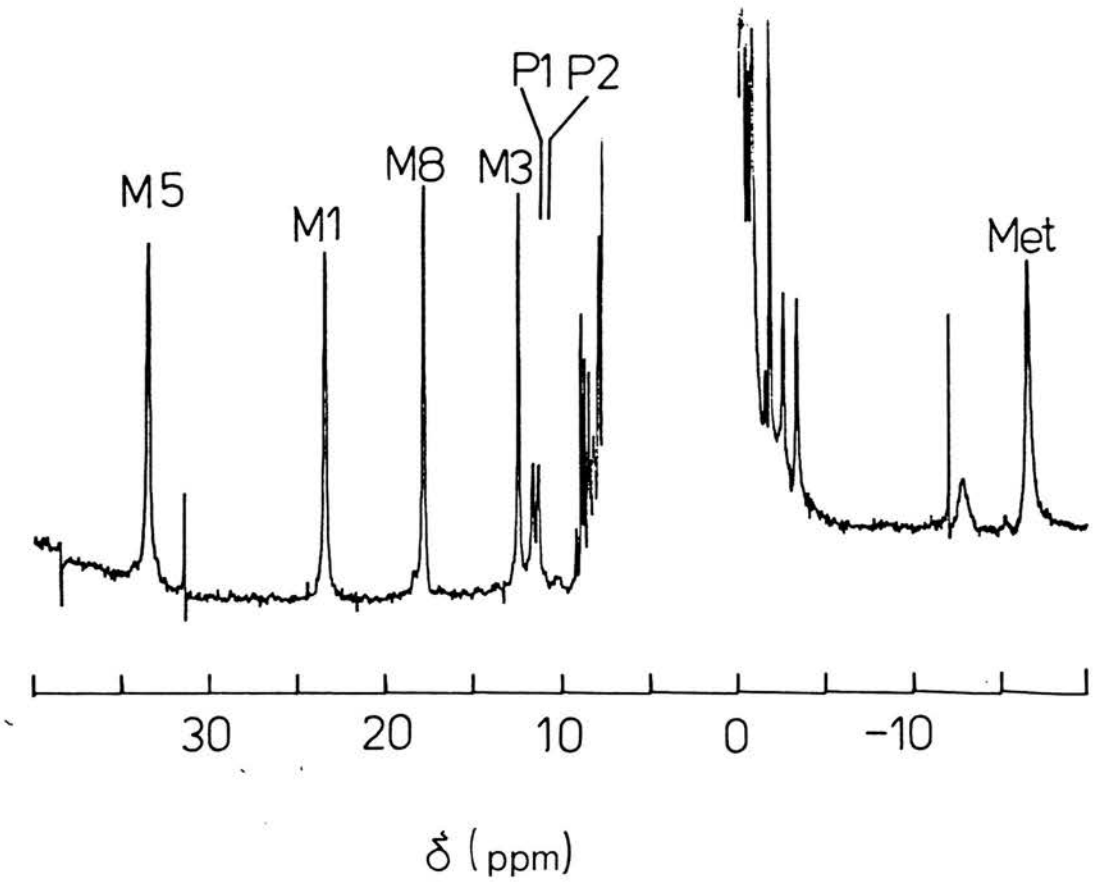
M5
M1
M8
M3
P1
P2
Met
30
20
10
0
-10
δ (ppm)

(histidine) and 6th (methionine) axial ligands and also through the two nitrogen atoms directly bonded to the iron. Since the π-orbital system extends over the entire conjugated porphyrin ring system, spin delocalisation via the nitrogens can produce finite spin densities on every haem atom, including side chain atoms. Hence, the paramagnetically downfield shifted resonances observed in Figure 39 arise from the methyl and propionic acid substituents of the haem.

The four 3-proton intensity resonances at 33.4, 23.4, 17.7 and 12.3 ppm are those of the four methyls occurring at substituent positions 1, 3, 5 and 8 on the haem ring (see Figure 5). These haem methyls have been specifically assigned in P. aeruginosa ferricytochrome c_{551} (Keller & Wüthrich, 1978b). Comparison of the P. stutzeri ferricytochrome spectrum with the P. aeruginosa cytochrome spectrum shows that the methyl chemical shift values are extremely simliar for the two proteins. By analogy with P. aeruginosa cytochrome c_{551}, then, the four methyl resonances are specifically to methyls 5, 1, 8 and 3, respectively (low to high field[1]).

The two 1-proton intensity resonances, P1 and P2, might arise from His16 (the 5th iron ligand) or from the propionic acid substituents. P1 and P2 were assigned on the basis of NOE experiments. A NOE is the change in intensity of one resonance by selective saturation of another resonance[9]. This effect occurs between spin-spin coupled resonances and also between adjacent but non-covalently bonded groups and so NOEs can yield information about the spatial relationship of resonances. Figure 40 shows a NOE experiment involving P1. From the NOE difference spectrum, b, it can be seen that irradiation at P1 gives an NOE to P2 and to a singlet resonance assigned to Trp 56. Since P1 and P2 show a NOE to each other this implies that they are the resonances of two inequivalent β-methylene protons of the same propionic acid, since the propionic acids are not close

Figure 40: Trp56 NOE

Low field region of the ^{1}H NMR spectrum of *P. stutzeri* ferricytochrome c_{551} obtained at pH* 8, 27°C. (A) Conventional spectrum; (B) the NOE difference spectrum obtained upon irradiation of P1 for 0.5 sec prior to acquisition. The labelled resonances are P1 and P2 = the β-CH_2 protons of haem propionic acid-7 and W = Trp56 C-2.

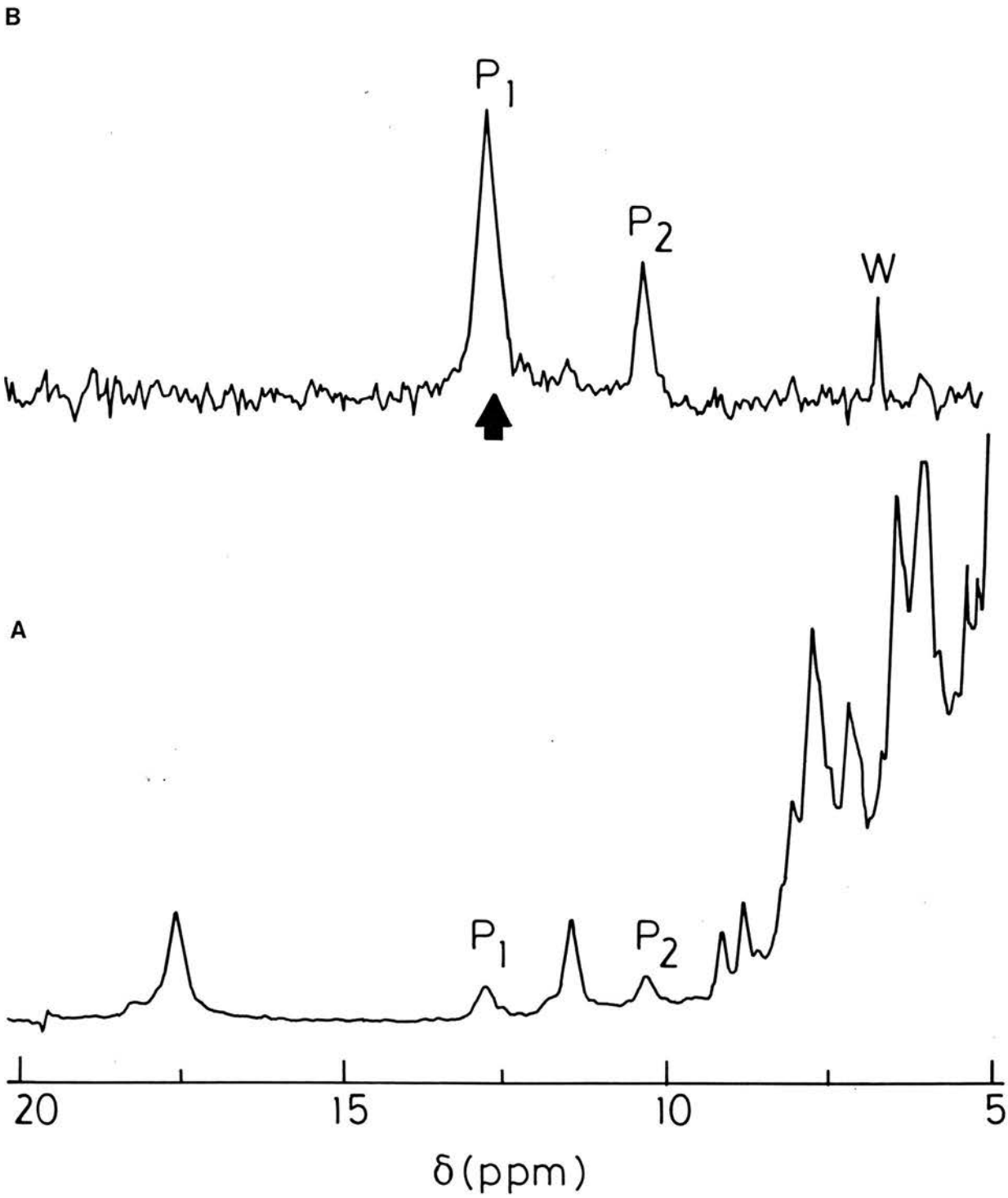
B
P1
P2
W
A
P1
P2
20
15
10
5
δ(ppm)

enough to each other for a through-space NOE to occur between the β-methylene groups. In addition the α-methylene proton resonances do not appear in this downfield region of the spectrum and so a NOE between the α and β protons of the same propionic acid can be discounted. The NOE observed between P1 and the Trp56 resonance allows specific assignment of the α-methylene protons to the propionic acid occurring at substituent position 7 on the haem ring (the "inner" propionic acid), since Trp56 is known to be sufficiently close to the inner propionic acid in P. aeruginosa cytochrome c_{551} to be able to form a hydrogen bond with it. An analogous NOE was observed for P. aeruginosa ferricytochrome c_{551} (G. Moore & F. Leitch, unpublished observations).

In diamagnetic ferrocytochrome c_{551}, the only resolved haem resonances are those of the four meso protons, which occur between 9 and 10 ppm. These are indicated in Figure 35. The rigid structure of the haem ring makes it particularly suited to NOE experiments since the rigidity facilitates NOEs between adjacent but non-covalently bonded protons. Thus, irradiation of any haem ring proton resonance is expected to produce a NOE in the resonances arising from its adjacent protons on the ring. Irradiation of the meso α resonance, for example, will produce NOEs to the resonances of thioether-4 methine group and methyl 5. Because the meso, methyl and thioether protons are asymmetrically distributed around the haem, NOE experiments can be used to assign most of the haem proton resonances. For P. stutzeri ferrocytochrome c_{551} the four meso resonances and the unresolved methyl resonances were specifically assigned by a sequence of NOE experiments similar to those described by Wuthrich for horse cytochrome c and P. aeruginosa cytochrome c_{551} (Keller & Wüthrich, 1978a,b) and so the procedure is not discussed further here.

B. Comparison of P. stutzeri (221) Cytochrome c-551 Resonance Assignments with P. aeruginosa and P. mendocina Assignments

The aromatic amino acid compositions of P. aeruginosa and P. mendocina cytochromes c_{551} are compared with those of both P. stutzeri cytochromes in Table IX. Most of the aromatic assignments have previously been published for P. aeruginosa cytochrome c_{551} (Moore et al., 1977), but unambiguous assignments for the Tyr27 and Phe34 spin sytstems have been made only recently (G. Moore, unpublished data). These aromatic assignments, together with assignments for P. mendocina ferrocytochrome c_{551} (G. Moore, unpublished data), are shown with the P. stutzeri 221 cytochrome data in Table X. Three aromatic residues are conserved between the cytochromes viz. Phe7, Trp56, and Trp77, and in either oxidation state the chemical shift values for the three sets of resonances are very similar. For His47, which occurs in both P. stutzeri 221 and P. mendocina cytochrome c_{551}, the chemical shifts of the C2 and C4 resonances correspond closely between the ferrocytochromes at both low and high pH values. In addition, resonances of Phe27 in P. stutzeri cytochrome c_{551} and of Tyr27 in the P. aeruginosa cytochrome both show anomalous upfield shifts from the primary position of these resonances, indicating that they have similar orientations with respect to the haem. These similarities suggest that the three proteins share a highly conserved tertiary structure even though they have a sequence homology of only 57%. Further support for this comes from comparison of the haem substituent assignments shown in Table XI, from which it is clear that the haem crevice regions are also similar. This latter observation is perhaps not too surprising since the haem crevice is intimately associated with the passage of electrons and is more likely to be conserved than any other region of the molecule. In this respect, Dickerson has listed 13

Table IX: Aromatic Amino Acids Occurring in the Pseudomonas Cytochromes

Source of Cytochrome c-551	Residue					
	7	27	34	47	56	77
P. aeruginosa	Phe	Tyr	Phe	Arg	Trp	Trp
P. stutzeri 221	Phe	Phe	Tyr	His	Trp	Trp
P. stutzeri 224	Phe	Leu	Asn	His	Trp	Trp
P. mendocina	Phe	Leu	Asn	His	Trp	Trp

Table XI: Comparison of Some Haem Substituent Assignments

[a]Assignments made at pH5.5 (27°C). [b]Assignments made at pH6.5 (27°C). [c]Assignments made at pH7.7 (27°C). [d]Assignments made at pH5.7 (27°C).

Resonance	Chemical Shift (ppm)				
	P. aeruginosa cyt. c_{551}		P. stutzeri (221) cyt. c_{551}		P. mendocina cyt. c_{551}
	ferri[a]	ferro[a]	ferri[b]	ferro[c]	ferri[d]
methyl 1	24.3	3.66	23.1	3.72	22.6
methyl 3	13.1	3.74	11.4	3.72	14.1
methyl 5	31.9	3.30	34.4	33.4	31.4
methyl 8	18.0	3.39	17.4	17.7	18.05
meso α	-	9.86	-	9.85	-
meso β	-	9.34	-	9.32	-
meso γ	-	5.98	-	6.00	-
meso δ	-	1.85	-	1.96	-
thioether (2) methine	-	5.98	-	6.00	-
thioether (2) methyl	-	1.85	-	1.96	-
thioether (4) methine	-	6.16	-	6.24	-
thioether (4) methyl	-	2.41	-	2.41	-

Table X: Comparison of Aromatic Resonance Assignments

[a] Assignments made at pH5.5 (27°C). [b]Assignments made at pH6.5 (27°C). [c]Assignments made at pH7.7 (27°C). [d]Assignments made at pH7.0 (57°C).

Resonance	Chemical Shift (ppm)				
	P. aeruginosa cyt. c_{551}		*P. stutzeri* (221) cyt. c_{551}		*P. mendocina* cyt. c_{551}
	ferri[a]	ferro[a]	ferri[b]	ferro[c]	ferro[d]
Trp56					
C-4 or C-7	6.70	7.36	6.76	7.4	7.72
C-5 or C-6	6.02	6.38	5.8	6.23	6.29
C-6 or C-5	6.34	5.81	6.32	6.23	5.74
C-7 or C-4	7.23	7.08	7.23	7.24	7.03
C-2	6.63	7.77	6.64	7.75	7.67
Trp77					
C-4 or C-7	8.16	8.02	8.06	7.99	7.96
C-5 or C-6	7.43	7.28	7.34	7.2	7.24
C-6 or C-5	7.10	7.12	6.96	7.05	7.01
C-7 or C-4	7.22	7.61	7.07	7.65	7.54
C-2	7.13	7.28	7.21	7.34	7.34
Phe7					
ortho	7.01	7.26	7.16	7.18	7.04
meta	6.81	6.94	7.61	6.93	6.69
para	7.15	7.12	7.87	7.05	6.56
Phe27					
ortho	-	-	6.51	6.0	-
meta	-	-	n.d.	5.11	-
para	-	-	5.45	5.47	-
Phe34					
ortho	7.60	7.22	-	-	-
meta	7.60	7.22	-	-	-
para	7.60	n.d.	-	-	-
Tyr27					
ortho or meta	6.40	5.80	-	-	-
meta or ortho	4.98	4.69	-	-	-
Tyr34					
ortho or meta	-	-	6.63	7.29	-
meta or ortho	-	-	7.02	7.52	-
His47					
C-2	-	-	8.68	8.62	8.46
C-4	-	-	7.65	7.03	7.05

residues which are in close contact with the haem in P. aeruginosa cytochrome c_{551} and 10 of these are conserved in the other two cytochromes; interestingly, the 3 variable residues are either adjacent or likely to be hydrogen-bonded to haem propionic acid-7.

Since the immediate environment of the haem is important in determining the level of redox potential (Kassner, 1972,1973), so differing haem environments could possibly have been the basis for the differences in level and pH dependence of redox potential observed for the three cytochromes. However, the assignment comparisons offer no clue as to the origin of these differences.

C. pH Titrations

1. P. stutzeri 221 cytochrome c-551

(a) Ferricytochrome

NMR spectra of P. stutzeri 221 ferricytochrome c-551 were recorded at several pH* values[11]. Figure 41 shows the region between 40 and 10 ppm containing haem substituent resonances. The chemical shift position of two methyl resonances, M5 and M3, and the propionic acid resonances, P1 and P2, are affected by pH and in Figure 42, where chemical shift (δ) is plotted against pH*, these resonances can be seen to titrate with pK*s of 7.5-7.7. Since their resonances shift with pK values close to the pK_O of 7.6 predicted from the redox measurements (see Chapter IV) these protons are presumably near to the ionising group. Therefore, an obvious candidate for the ionising group is haem propionic acid-7.

In the aromatic region of the ferricytochrome spectrum only two resonances have marked pH dependent chemical shifts and these are the C-2 and C-4 proton resonances of His47. Chemical shift versus pH is plotted for these in Figure 43 (curves b and c), the theoretical curves being fitted in both cases using pK* = 7.6. The

Figure 41: ^{1}H NMR Spectrum of P. stutzeri (221) Ferricytochrome c-551 at Various pH Values

Labelling of resonances as for Figure 39.

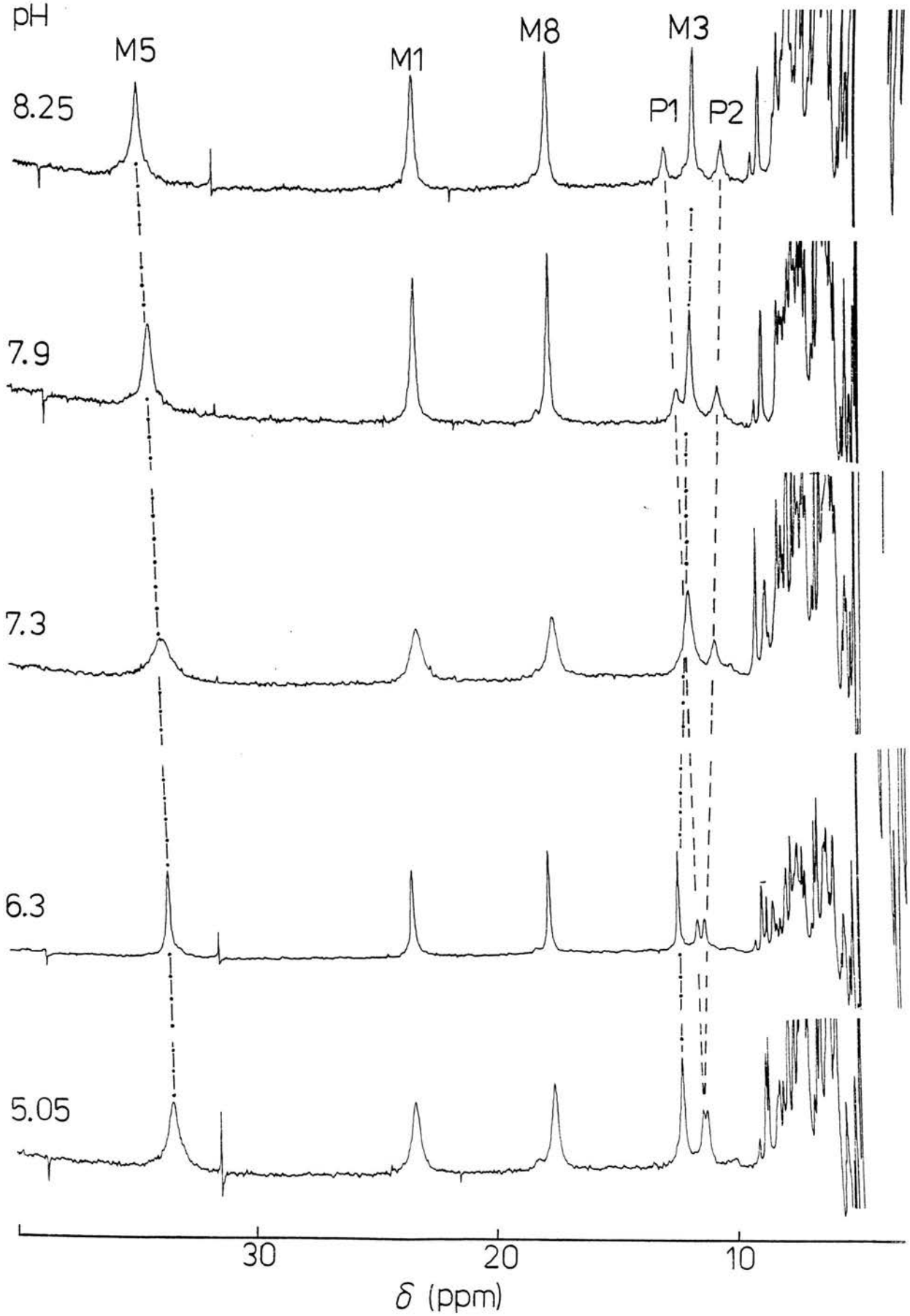
pH
M5
M1
M8
M3
P1
P2
8.25
7.9
7.3
6.3
5.05
30
20
10
δ (ppm)

Figure 42: pH Dependence of Chemical Shift (δ) for Haem Substituent Resonances of P. stutzeri (221) Ferricytochrome c-551

(○, ●, △, ▲, ◇, ◆) represent experimental points. Theoretical curves were calculated with the following pK* values: M5, pK = 7.5; M3, pK = 7.7; P1 and P2, pK = 7.5. Labelling of resonances as for Figure 39.

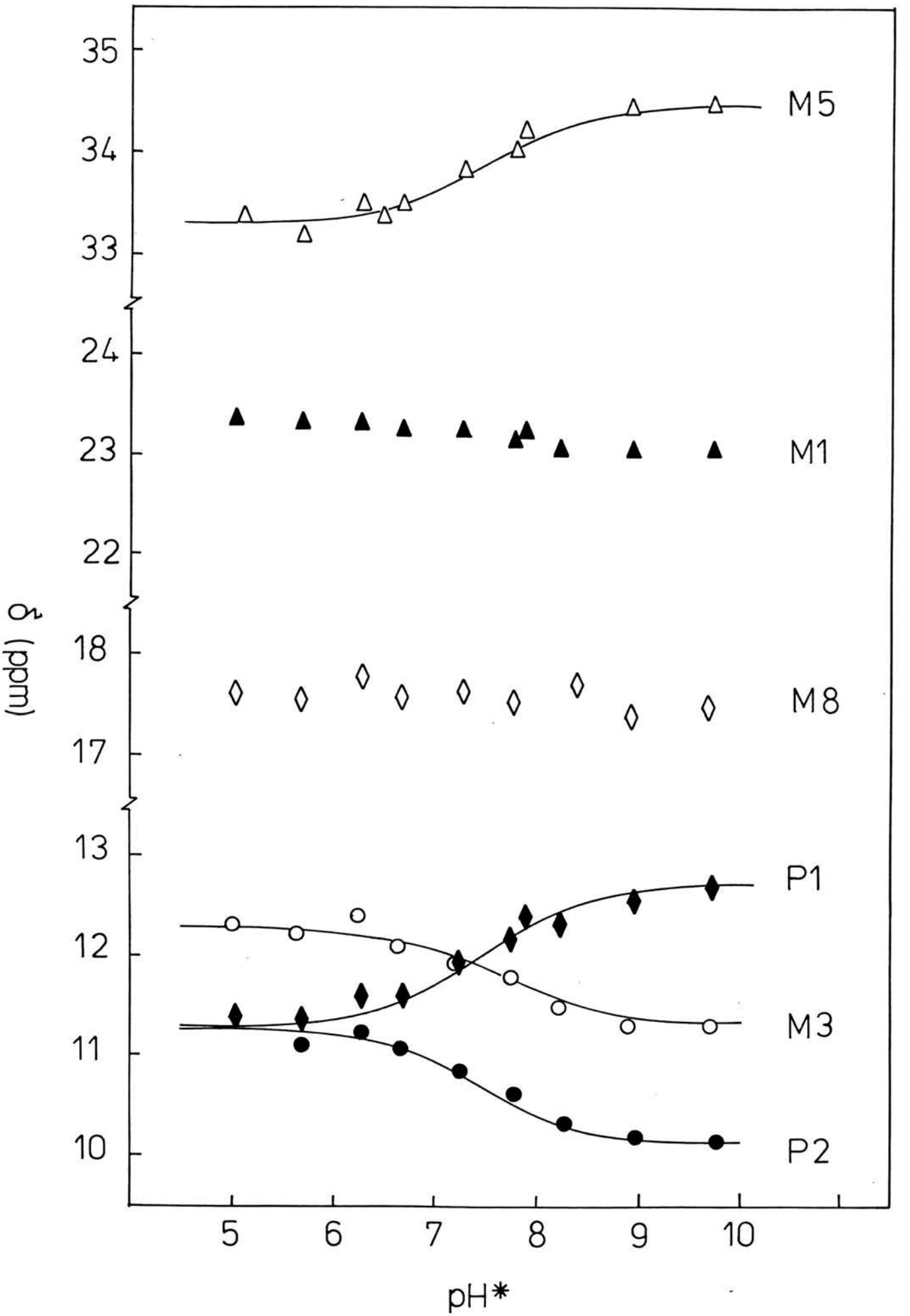
35
34
33
24
23
22
18
17
13
12
11
10
M5
M1
M8
P1
M3
P2
δ (ppm)
5
6
7
8
9
10
pH*

overall shifts of 1.05 ppm for the C-2H resonance and 0.43 ppm for the C-4H resonance are typical for the deprotonation of histidine (Markley, 1974). Both resonances broaden out considerably above pH6.5, although the C-2 resonance sharpens up again beyond pH8.5, and their shift positions can only be followed in non-resolution enhanced spectra[4]. The broadening or disappearance of histidine resonances midway through the course of a pH titration is, however, a common occurrence (for example, see Bachovchin & Roberts, 1978) and can be explained in terms of a relatively slow on-off rate for the imidazolium proton (Sudmeier et al., 1980).

The aromatic region at low and high pH is shown in Figure 44. A few resonances other than those of His47 show small pH dependent chemical shifts (<0.1 ppm), notably the singlet resonance of Trp 56, the Tyr 34 doublet that it overlaps, and the Phe27 ortho resonance, but these shifts are too small to be fitted to theoretical curves.

(b) Ferrocytochrome

The resonances of His47 have marked pH dependent chemical shifts in this oxidation state also but from Figure 43 (curves a and d) it can be seen that their pKs are rather higher; both theoretical curves were fitted using a pK^* value of 8.2. This figure is in good agreement with the predicted value of 8.3 for pK_R. The titrating resonances exhibited the same behaviour as they did in the ferricytochrome, broadening at intermediate pH values. Again the C-2 resonance sharpened at pH>9 while the C-4 resonance remained broad (although it can be seen in the resolution enhanced spectrum, Figure 45(b), at 6.65 ppm because there are no other overlapping resonances in this area).

From Figure 45 (a) and (b), it is clear that the chemical shifts of all other aromatic resonances are virtually independent of pH. Those resonances which showed smallshifts in the ferricytochrome pH titration

Figure 43: pH dependence of Chemical Shift (δ) for His47 C-2 and C-4 Resonances of P. stutzeri (221) Cytochrome c-551

(O, ●) represent experimental points. The theoretical curves were calculated using the following pK^* values: (a) C-2 (ferrocytochrome), pK = 8.2; (b) C-2 (ferricytochrome), pK = 7.6; (c) C-4 (ferricytochrome), pK = 7.6; (d) C-4 (ferrocytochrome), pK = 8.2.

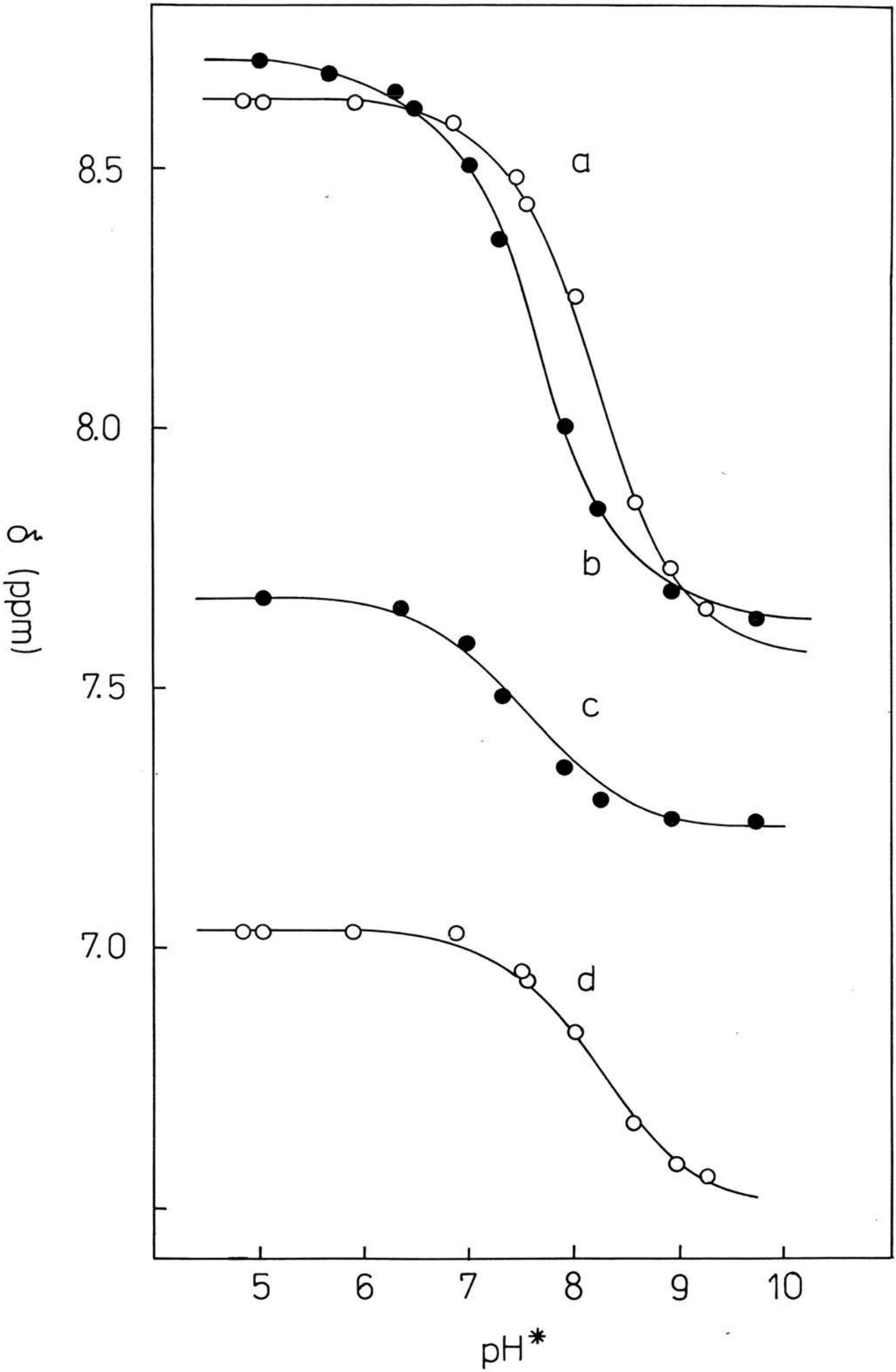
8.5
8.0
7.5
7.0
δ (ppm)
a
b
c
d
5
6
7
8
9
10
pH*

Figure 44: Aromatic Region of the Convolution Difference Spectrum of P. stutzeri (221) Ferricytochrome c-551

(a) pH* 5.05; (b) pH* 8.95.

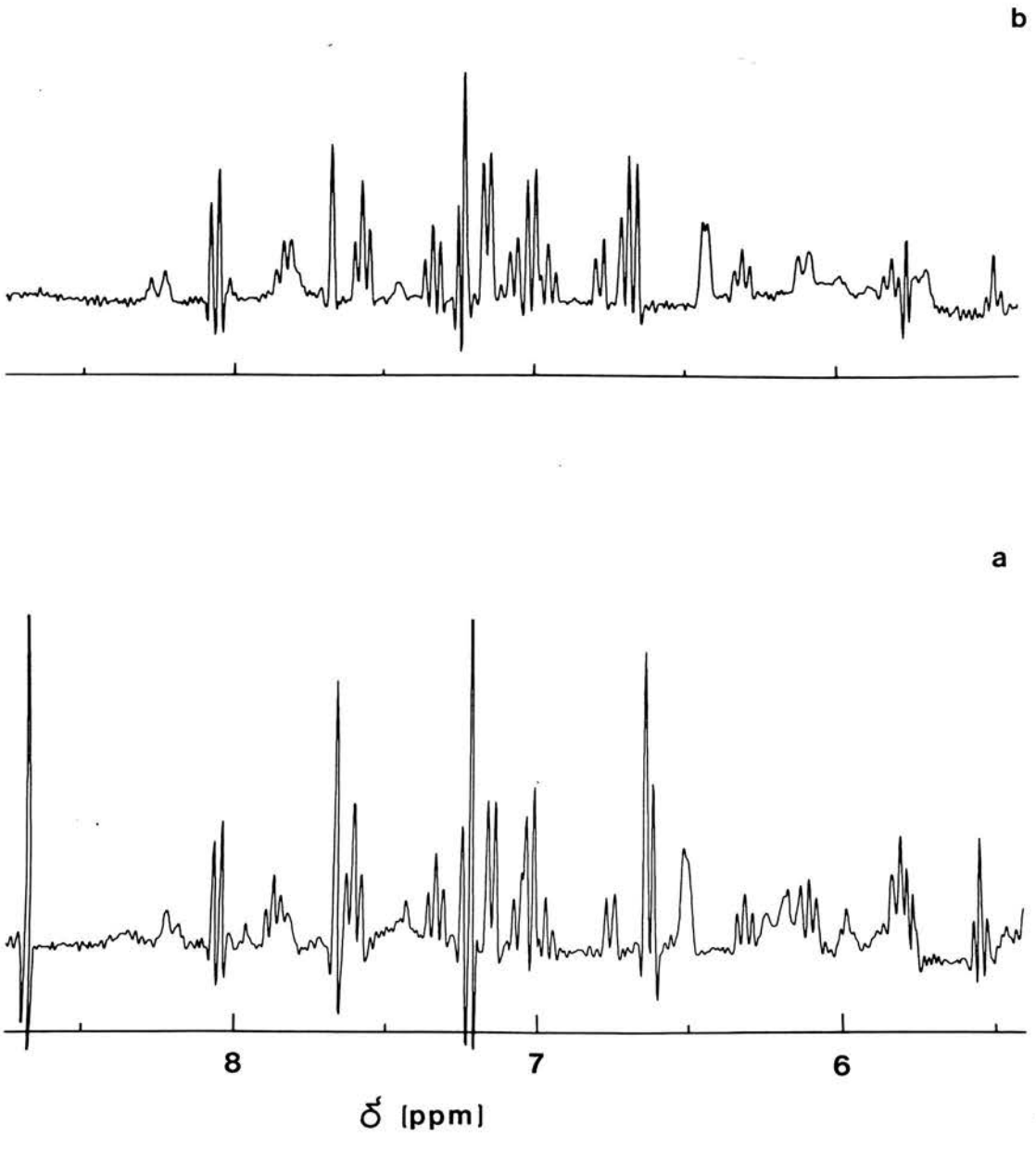
b
a
8
7
6
δ (ppm)

Figure 45: Aromatic Region of the Convolution Difference Spectrum of P. stutzeri (22l) Ferrocytochrome c-55l

(a) pH* 6.85; (b) pH* 8.55.

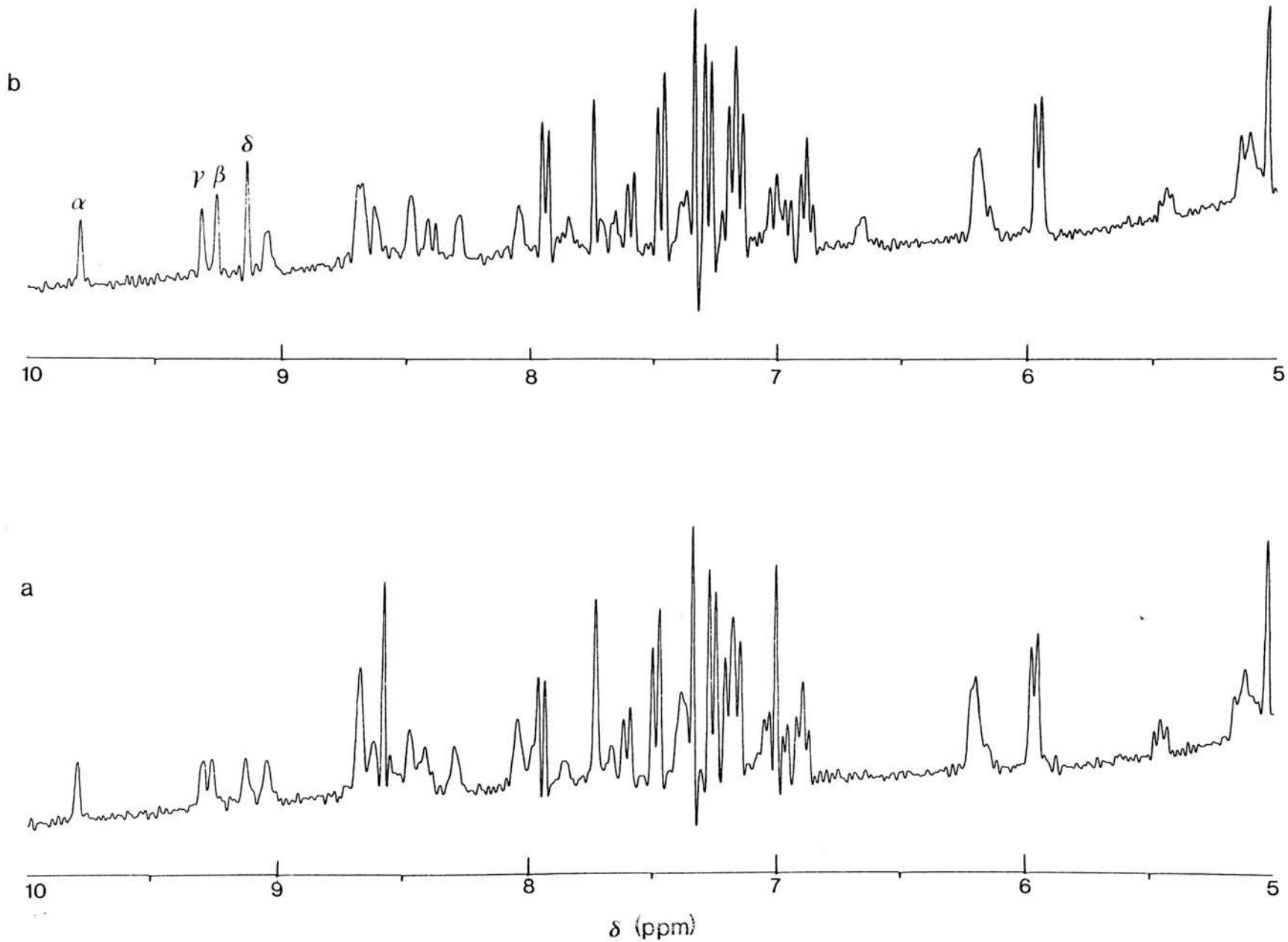
b
α
γ β
δ
10
9
8
7
6
5
a
10
9
8
7
6
5
δ (ppm)

showed even less remarkable shifts in the ferrocytochrome titration. The four haem meso resonances resolved between 9 and 10 ppm were similarly unaffected by pH. In neither the ferrocytochrome nor the ferricytochrome were the upfield shifted Met61 resonances sensitive to pH changes.

(c) Conclusions

The overall impression from the pH titration is that pH changes between pH5 and 9.5 have relatively little effect on the cytochrome structure; despite the fact tht it was possible to look at only a restricted number of resonances it is clear that the ionisations giving rise to pK_O and pK_R are not linked to any major conformational changes.

The C-2 and C-4H resonances of His47 titrate normally although their pK^* is different in the two oxidation states, being ca. 0.5 pH units higher in the ferrocytochrome. Redox state dependent pK values could arise if His47 occupied rather different chemical environments in each of the two oxidation states but this would require some sort of conformational change to take place during electron transfer; there in no crystallographic or NMR data for P. aeruginosa cytochrome c_{551} which suggests a redox state associated conformational change and given that the P. stutzeri cytochrome behaves similarly it would seem an unlikely explanation for the redox state dependent pKs. Since Arg47 is hydrogen bonded to haem propionic acid-7 in P. aeruginosa cytochrome c_{551} and is therefore relatively close to the haem, then His47 in P. stutzeri cytochrome c_{551} may be close enough to the haem be influenced by its net charge. From electrostatic considerations, it could be argued that histidine would ionise with a lower pK in the ferricytochrome since the haem carries a net charge of +1 in this oxidation state (neutral histidine would therefore be favoured). Deprotonation of the histidine would be less important in the ferrocytochrome, which carries 0 net charge.

Some haem methyl and propionic acid resonances showed pH dependent chemical shifts in the ferricytochrome (none of these resonances is resolved in the ferrocytochrome), titrating with the same pK as the histidine resonances in this oxidation state. Since the chemical shifts of P1, P2 and the haem methyl resonances cannot be followed in the ferrocytochrome pH titration then it is not possible to say whether the pK affecting these resonances is redox state dependent. The pH effects on these resonances were in many ways similar to the effects observed during pH titration of P. aeruginosa cytochrome c_{551}; for this cytochrome it was suggested that one of the haem propionic acid substituents ionises (see Introduction/III).

In summary then, the P. stutzeri cytochrome c_{551} pH titrations show that certain haem substituent resonances and the His47 resonances have pH dependent chemical shifts. In the ferricytochrome, these resonances titrate with the pK_O value of 7.6 predicted from the redox measurements. The His47 resonances titrate with a higher pK in the ferrocytochrome, this value agreeing with the predicted pK_R of 8.3. The identity of the ionising group which affects the redox potential is unclear from these data alone. His47 would appear to be the obvious candidate given that it shows redox state dependent pKs. However, propionic acid-7 is also a possibility, especially since P. aeruginosa cytochrome c_{551}, which lacks His47, is affected in a similar way by pH changes. It was suggested above that His47 and propionic acid-7 have a close spatial relationship. The possibility then arises that the resonances of either species might be indirectly influenced by ionisation of the other. Thus four situations might apply (i) propionic acid-7 ionises (ii) His47 ionises (iii) propionic acid-7 and His47 ionise but only one of these ionisations affects the redox potential (iv) propionic acid-7 and His47 ionise and both ionisations contribute to the fall in redox

potential. In the latter two cases it is proposed that the propionic acid ionises with the same pK as His47 in the ferrocytochrome (i.e. $pK_R = 8.3$).

2. P. mendocina cytochrome c-551

(a) Ferricytochrome

The pH titration of P. mendocina ferricytochrome c_{551} was similar in most respects to the P. stutzeri ferricytochrome titration. Four methyl (M5,1,8,3) and two propionic acid (P1,2) resonances are resolved between 40 and 9.5 ppm and of these M5, M3, P1 and P2 have pH dependent chemical shifts. From the plot of chemical shift against pH^*, Figure 46, it can be seen that all four resonances shift to about the same extent as their counterparts in the P. stutzeri ferricytochrome titration (compare Figure 42). One interesting difference is that P1 and P2 shift towards each other and overlap at high pH in the P. mendocina cytochrome titration, whereas they overlap at low pH and then shift apart in the P. stutzeri titration; this would indicate a different environment for the propionic acid resonances in the two proteins. The data are fitted to theoretical curves using $pK^* = 7.5$. This is the same value found for the titrating resonances in P. stutzeri cytochrome c_{551} but it does not agree so well with the pK_O value predicted from the redox measurements on P. mendocina cytochrome c_{551} (see Chapter IV).

(b) Ferrocytochrome

The ferrocytochrome pH titration was incomplete since some reoxidation of the cytochrome occurred at high pH^*, the subsequent electron exchange causing a marked deterioration in spectral quality. However, the only shifting resonances appear to be those of His47, and their pK^* in this oxidation state is greater than the ferricytochrome pK^* by at least 0.3 pH units - this can be deduced from the plot of δ versus pH^* for the C-2 resonance (Figure 47).

Figure 46: pH Dependence of Chemical Shift (δ) for Haem Substituent Resonances of P. mendocina Ferricytochrome c-551

The labelled resonances are: M1, M3, M5 and M8 = haem methyls, P1 and P2 = β-CH_2 resonances of haem propionic acid-7. The theoretical curves were calculated using the following pK^* values: M5, pK = 7.5; M3, pK = 7.7; P1 and P2, pK = 7.6.

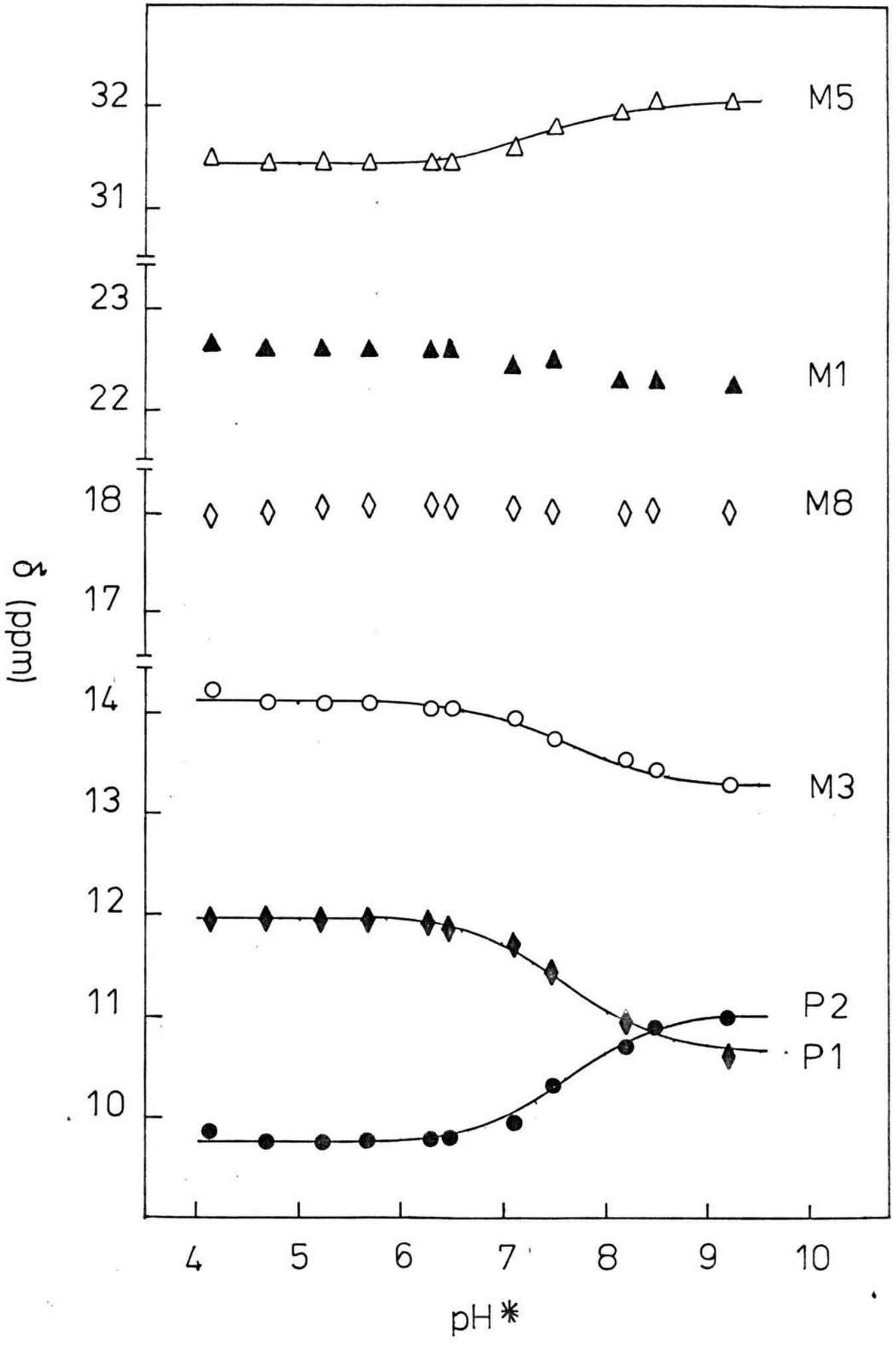
32
31
23
22
18
17
14
13
12
11
10
M5
M1
M8
M3
P2
P1
δ (ppm)
4
5
6
7
8
9
10
pH*

Figure 47: pH Dependence of Chemical Shift (δ) for the His47 C-2 and C-4 Resonances of P. mendocina Cytochrome c-551

The theoretical curves were calculated using the following pK^* values: (a) C-2 (ferricytochrome), pK = 7.5; (b) C-4 (ferricytochrome), pK = 7.5. O are points for an incomplete titration of the C-2 resonance in the ferrocytochrome.

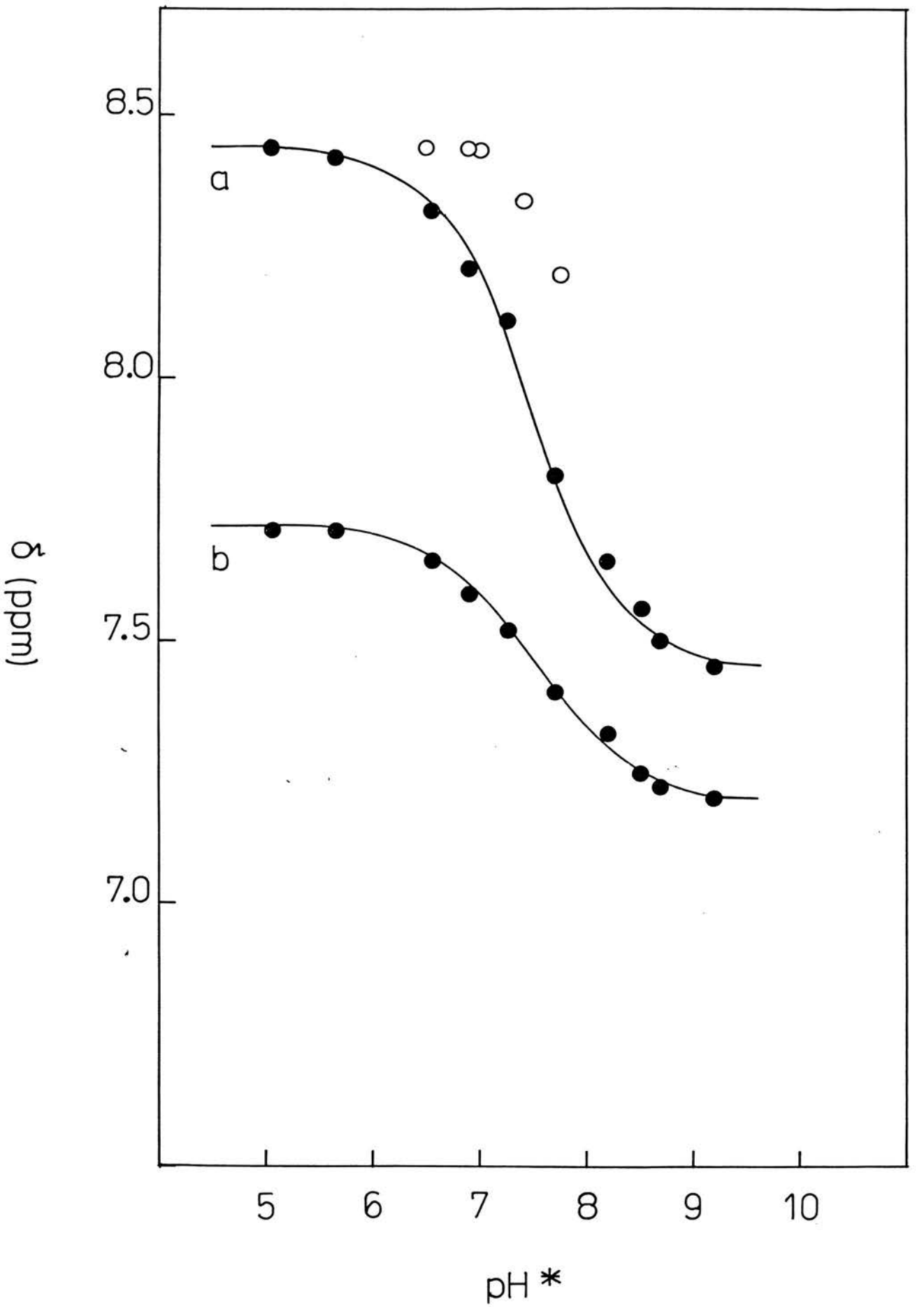
8.5
8.0
7.5
7.0
δ (ppm)
a
b
5
6
7
8
9
10
pH *

(c) Conclusions

From consideration of the resonances which shift and the extent to which they shift, P. mendocina cytochrome c_{551} behaves more like P. stutzeri cytochrome c_{551} than the P. aeruginosa cytochrome.

Section II - C. thiosulphatophilum Cytochrome c-555

A. Assignments

(i) Aromatic resonances

Cytochrome c_{555} contains 7 aromatic amino acids *viz.* 1 tryptophan (Trp34), 4 tyrosines (Tyr1,10,53 and 80) and 2 histidines (His18 [the 5th iron ligand] and His37). Thus three singlet resonances should be observed in the NMR spectrum. In the ferricytochrome, singlet resonances occur at 8.80, 8.01 and 7.78 ppm (see Figure 52). The chemical shift of the resonance at 8.01 ppm is independent of pH, but the other two resonances shift upfield between pH6 and 8 and are assigned to His37 on this basis. The resonance at 8.01 ppm is thus the Trp34 singlet. In the ferrocytochrome, two singlet resonances are resolved at 7.86 and 7.37 ppm and five more occur downfield between 9 and 10 ppm (see Figure 54). Four of the downfield shifted singlets arise from the *meso* protons, while the fifth is the His37 C-2H resonance, as evidenced by its pH dependent chemical shift. The pH dependence of chemical shift also allowed assignment of the singlet at 7.86 ppm to His37 C-4H, and so the Trp34 singlet must be that at 7.37 ppm.

Apart from two coupled doublets which have been assigned to Tyr1, no other assignments have been made in either oxidation state. The Tyr doublets were specifically assigned on the basis of their pH dependent chemical shifts, as discussed below.

(ii) Haem substituent and axial ligand resonances

Figure 48 shows the hyperfine shifted resonances of ferricytochrome c_{555}. The single upfield shifted methyl resonance at -2.8 ppm could arise from Met60 or from a methionine, leucine, isoleucine or valine in the polypeptide backbone. However, the ϵ-CH_3 resonance of the axially liganded methionine is typically the most upfield shifted resonance in the ferricytochrome spectrum of

Figure 48: ^{1}NMR Spectrum of C. thiosulphatophilum Ferricytochrome c-555

The labelled resonances are: M1, M2, M3 and M4 = haem methyls (not specifically assigned); P1-P7 = unassigned 1-/2-proton intensity resonances; Met? = methyl resonance tentatively assigned to the axial ligand, Met60.

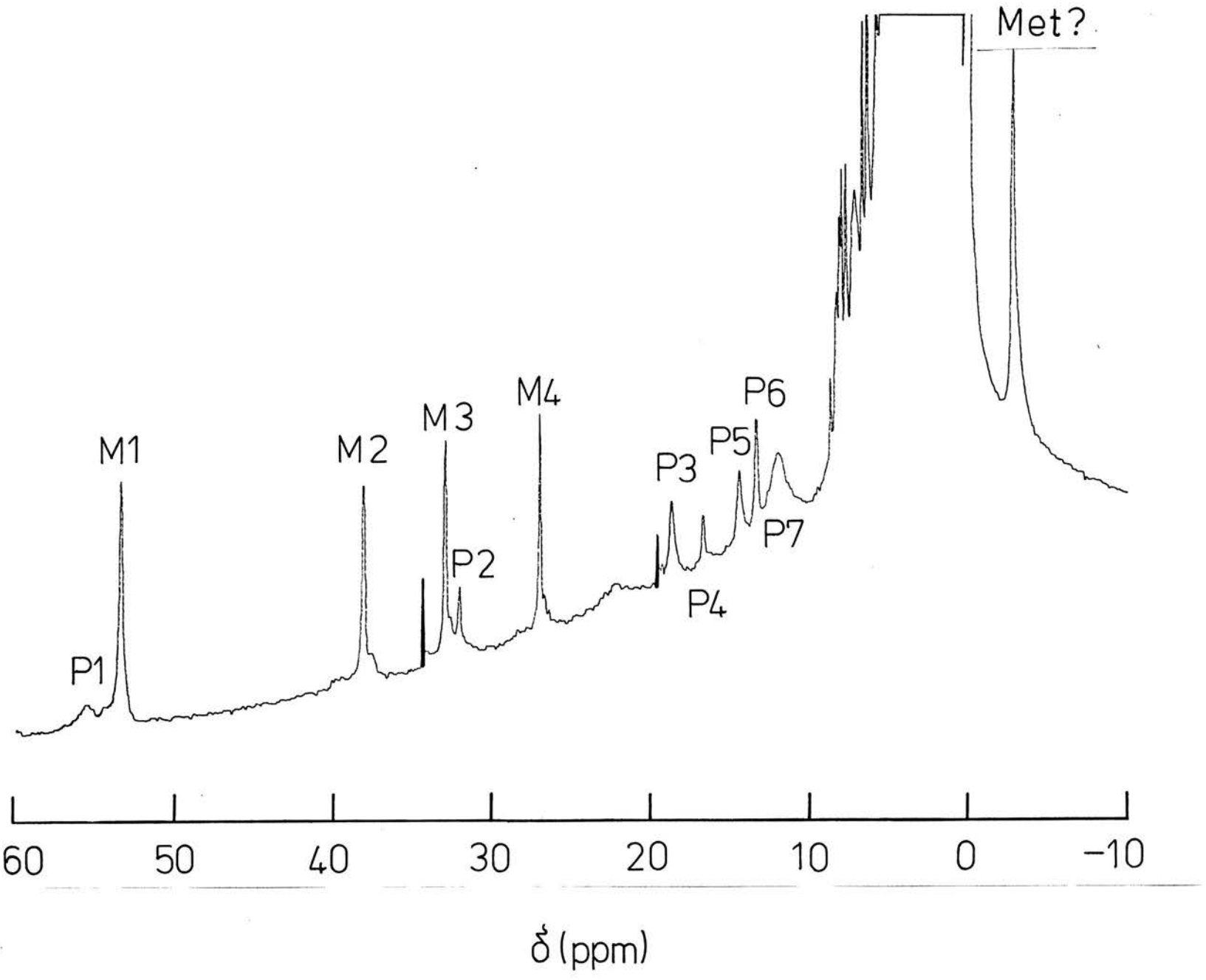
Met?
M1
M2
M3
M4
P1
P2
P3
P4
P5
P6
P7
60
50
40
30
20
10
0
−10
δ (ppm)

Class I c-type cytochromes, although in horse cytochrome c, R. rubrum cytochrome c_2 and P. aeruginosa cytochrome c_{551} this resonance occurs between -15 and -20 ppm. The hyperfine shift experienced by this methyl resonance in cytochrome c_{555} is clearly much smaller. Some of the Met60 resonances have been assigned in the ferrocytochrome and in this oxidation state their chemical shifts are similar to the shifts of corresponding methionine ligand resonances in other c-type cytochromes, implying that the orientation of Met60 relative to the haem is not significantly different in cytochrome c_{555}. Nor does the crystal structure indicate aything unusual about the mode of haem liganding (Korzun & Salemme, 1978). The anomalous hyperfine shift of the Met60 resonance must therefore be a reflection of the unpaired electron spin density distribution in ferricytochrome c_{555}. Presumably this is markedly different from the distribution in the other c-type cytochromes which have been studied to date (see Introduction).

The methyl resonance M1 is shifted anomalously downfield - in other Class I c-type cytochromes, the most hyperfine shifted haem methyl resonance occurs typically ca. 30-40 ppm. In the high spin Class II c-type cytochrome, R. rubrum cytochrome c′, the haem methyl resonances occur between 60 and 80 ppm (Emptage et al., 1981), and in this respect cytochrome c_{555} appears to exhibit some high spin character. The presence of a small proportion of of high spin cytochrome might also account for the Met60 methyl shift.

Seven other resonances (P1-P7) occur between 10 and 60 ppm. Resonances P6 and P7 each appear to be of 2-proton intensity, the remainder being 1-proton intensity. These presumably include the β-CH_2 resonances of propionic acids-6 and -7 but they have not been assigned.

In ferrocytochrome c_{555}, the four meso resonances

occur at 10.11, 9.79, 9.72 and 9.56 ppm but they have not been specifically assigned.

B. pH Titrations

(a) Ferricytochrome c-555

The downfield region of ferricytochrome c_{555} spectrum containing hyperfine shifted haem substituent resonances is shown at three pH values in Figure 49. The chemical shifts of the two methyl resonances M1 and M4 are sensitive to changes in pH, the resonances shifting overall by 2.5 and 2 ppm respectively. The titration curves for these two resonances are included in Figure 50, where theoretical curves have been fitted to the experimental data using $pK^*=6.2$. M1 and M4 broaden markedly during the titration, their linewidths being maximal ca. pH6.2. Of the other resonances, P1, P2, P4 and P7 also have pH dependent chemical shifts. P1 shows the most dramatic overall shift, moving upfield by ca. 6 ppm (low to high pH) - this resonance remains very broad throughout the titration. P2, P4 and P7 show overall shifts of about 2 ppm. All four peaks titrate with the same pK as the two methyl resonances, as can be seen in Figure 50. The chemical shift of the Met60 methyl resonance is independent of pH.

The aromatic region of the ferricytochrome spectrum is shown at various pH values in Figure 51. The two singlet resonances assigned to His37 shift overall by 0.9 and 0.5 ppm, these values being quite typical for an ionising histidine residue (Markley, 1974). Chemical shift is plotted against pH^* in Figure 52, where the theoretical curves were fitted using $pK^*=6.3$. Other pH associated changes in the aromatic spectrum are very minor. The coupled doublets assigned to Tyr1 each shift by ca. 0.05 ppm but with a noticeably higher pK^* than the histidine resonances (see Figure 52). Here, the theoretical curves were fitted using $pK^*=7.7$ - this pK is typical for the N-terminal amino group in proteins (see

Figure 49: ^{1}H NMR Spectrum of C. thiosulphatophilum Ferricytochrome c-555 at Various pH Values

Labelling of resonances as for Figure 48.

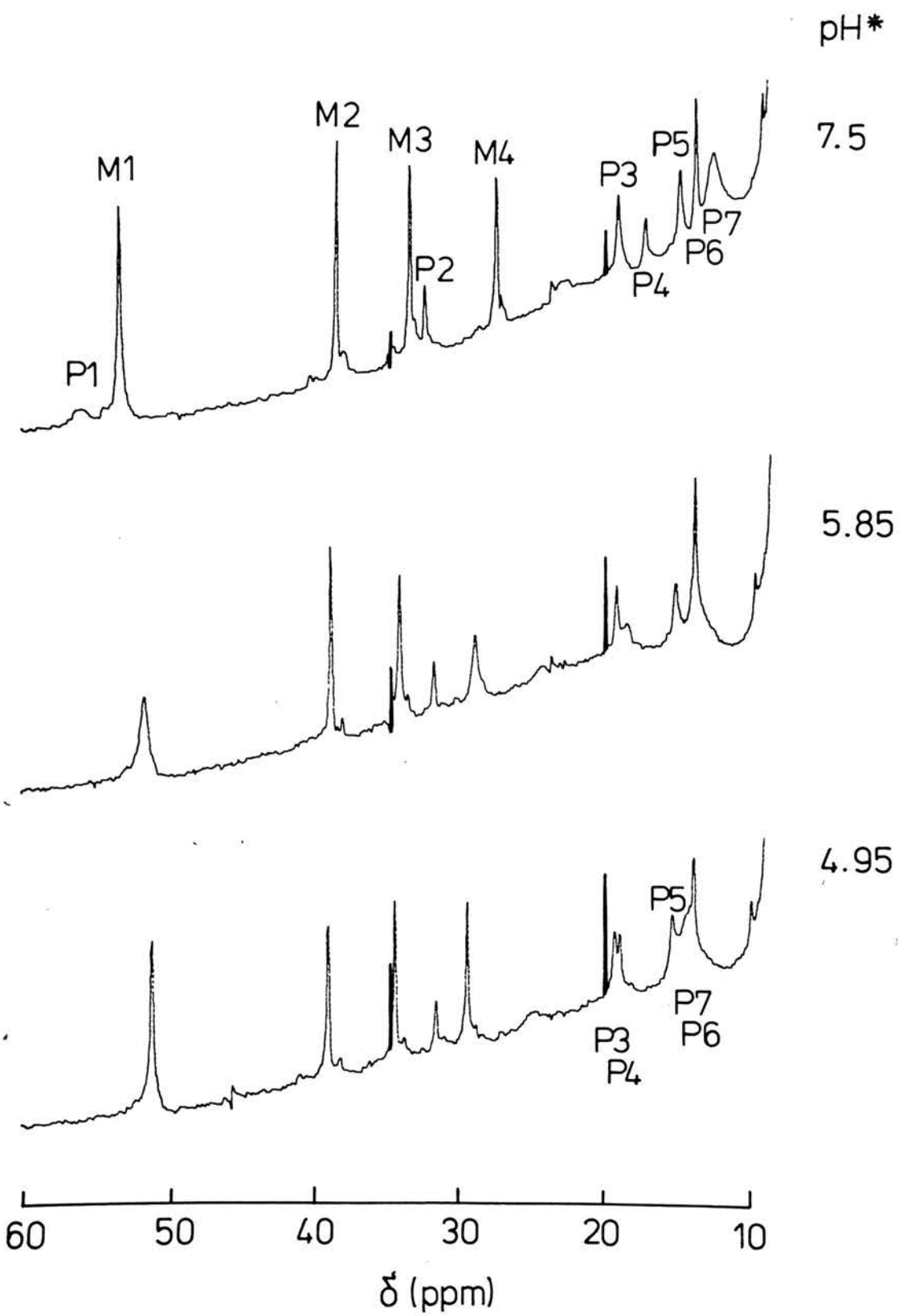
pH*
7.5
M1
M2
M3
M4
P1
P2
P3
P4
P5
P6
P7
5.85
4.95
60
50
40
30
20
10
δ (ppm)

Figure 50: pH Dependence of Chemical Shift (δ) for Haem Substituent Resonances of C. thiosulphatophilum Ferricytochrome c-555

Labelling of resonances as for Figure 48. The theoretical curves were all fitted using $pK^{*} = 6.2$.

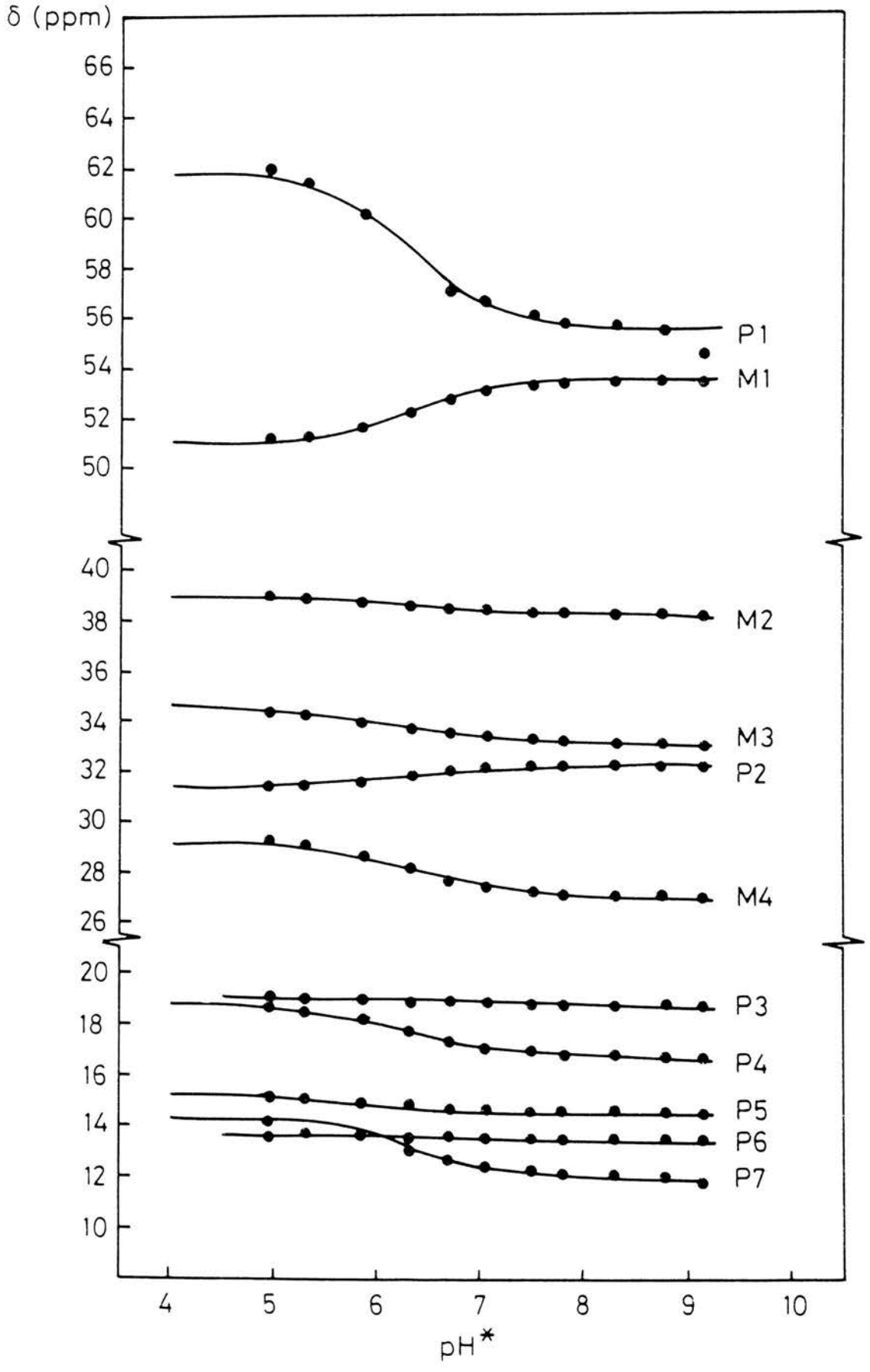
δ (ppm)
66
64
62
60
58
56
54
52
50
40
38
36
34
32
30
28
26
20
18
16
14
12
10
P1
M1
M2
M3
P2
M4
P3
P4
P5
P6
P7
4
5
6
7
8
9
10
pH*

Figure 51: The Aromatic Region of the ^{1}H NMR Spectrum of C. thiosulphatophilum Ferricytochrome c-555 at Various pH Values

Labelled resonances are: H = His37 C-2 and C-4; Y = Tyr1.

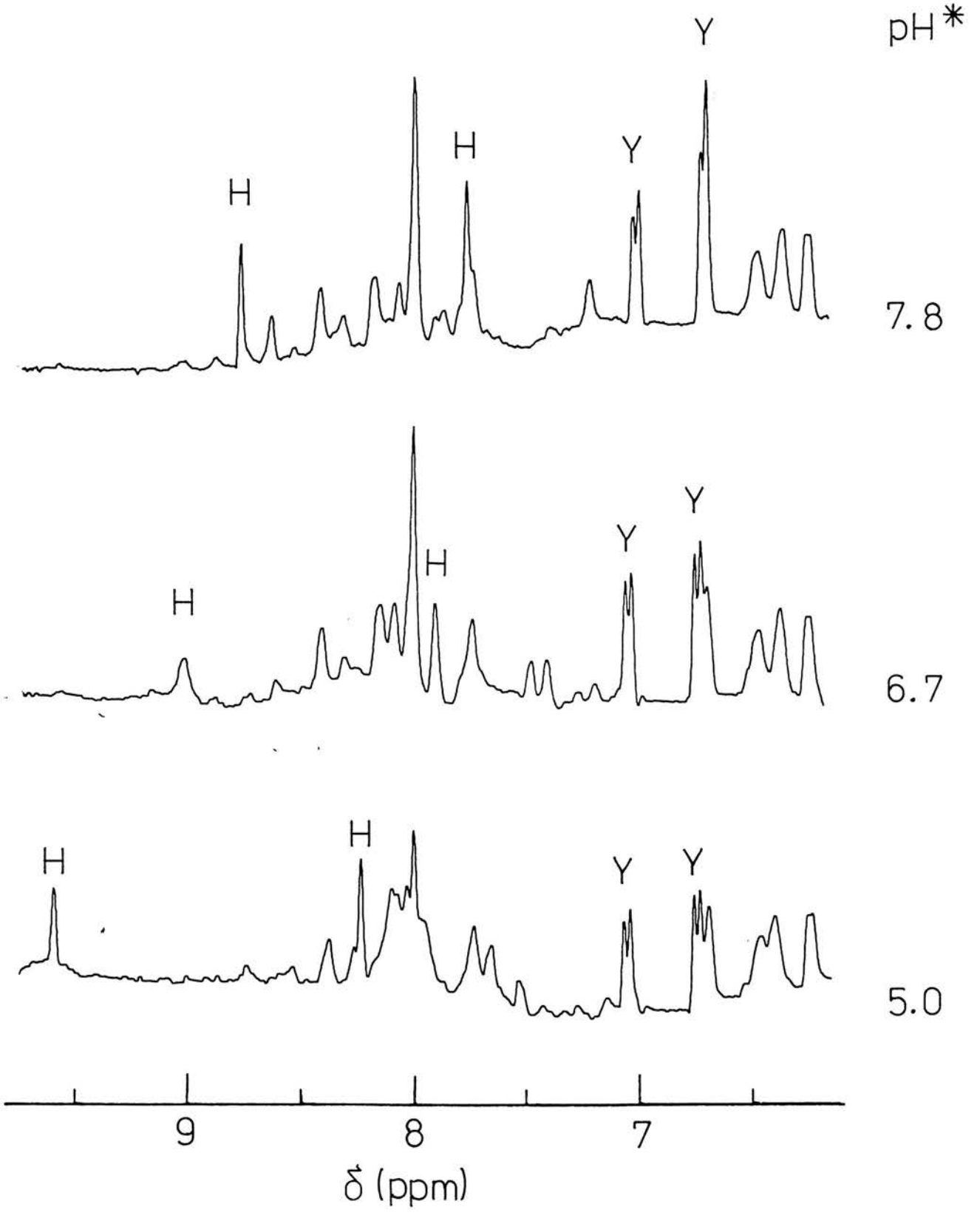
pH*
Y
H
H
Y
7.8
H
H
Y
Y
6.7
H
H
Y
Y
5.0
9
8
7
δ (ppm)

Figure 52: pH Dependence of Chemical Shift (δ) for the Aromatic Resonances of C. thiosulphatophilum Ferricytochrome c-555

The theoretical curves were fitted using pK^{*} = 6.3 (His37) and pK^{*} = 7.7 (Tyr1).

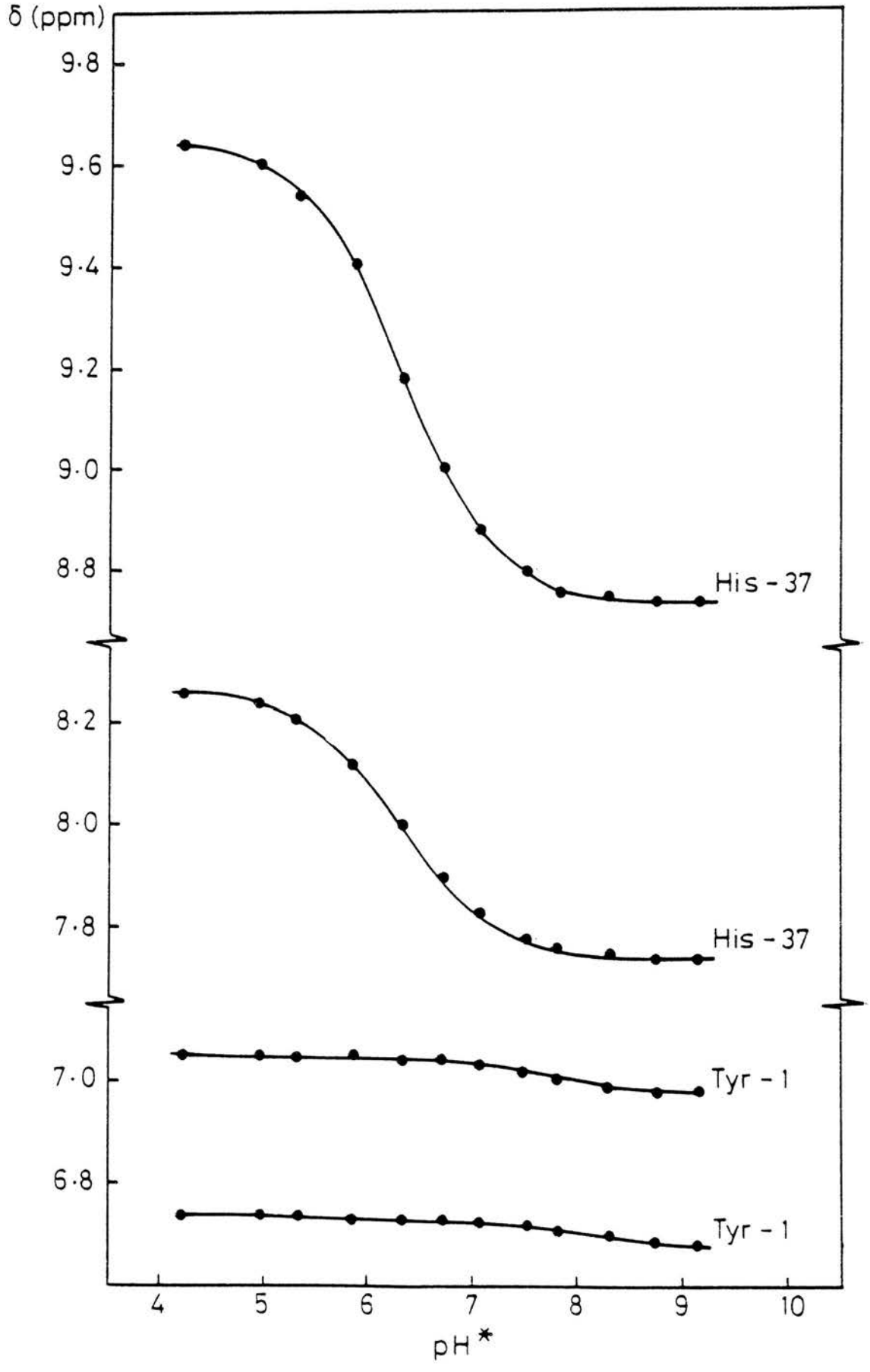
δ (ppm)
9·8
9·6
9·4
9·2
9·0
8·8
His - 37
8·2
8·0
7·8
His - 37
7·0
Tyr - 1
6·8
Tyr - 1
4
5
6
7
8
9
10
pH*

Figure 53: The Aromatic Region of the ^{1}H NMR Spectrum of C. thiosulphatophilum Ferrocytochrome c-555 at Various pH Values

The labelled resonances are: H = His37 C-2 and C-4; m = meso (not specifically assigned).

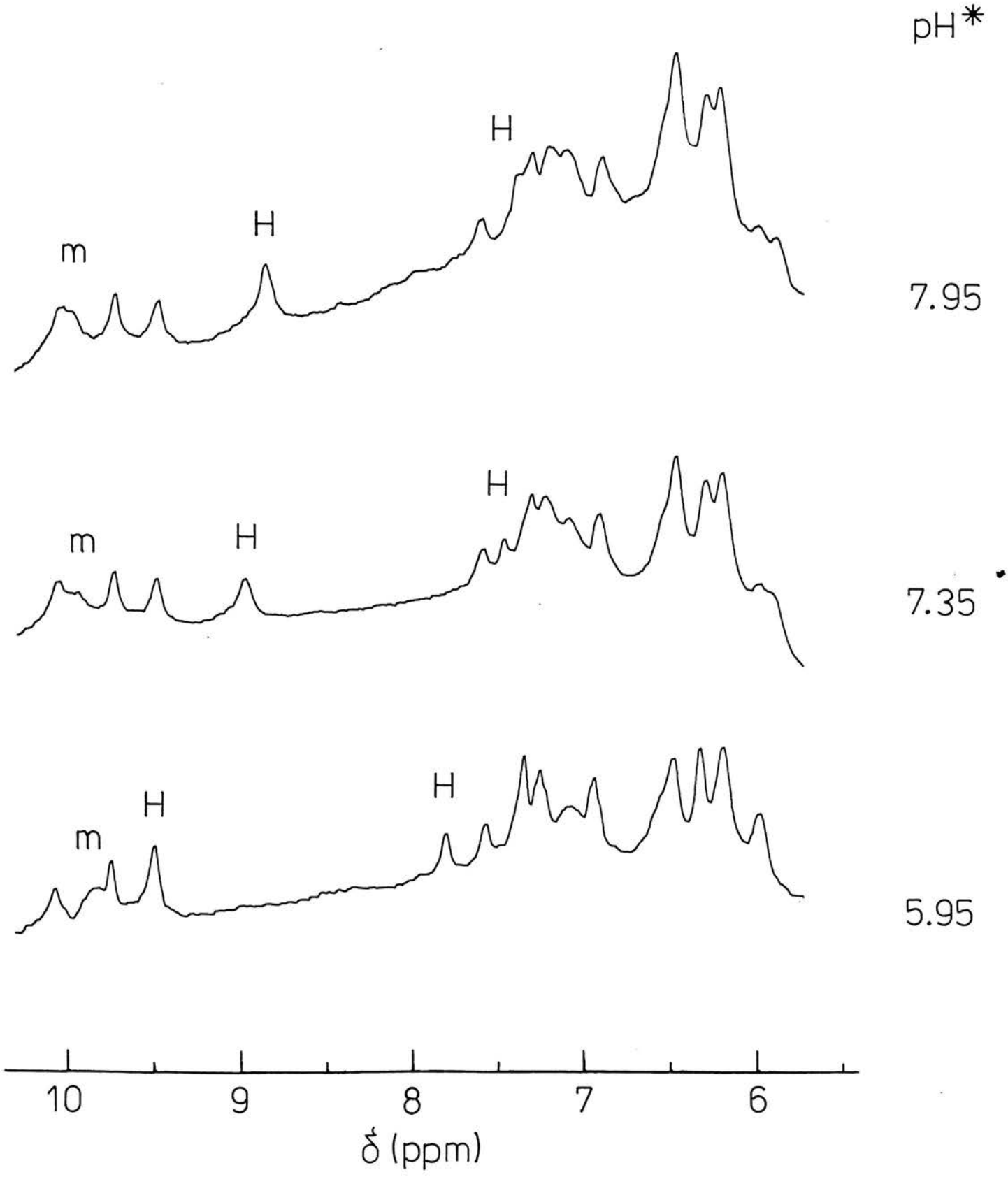
pH*
m
H
H
7.95
m
H
H
7.35
m
H
H
5.95
10
9
8
7
6
δ (ppm)

Figure 54: pH Dependence of Chemical Shift (δ) for the Aromatic Resonances of C. thiosulphatophilum Ferrocytochrome c-555

The theoretical curves were fitted using $pK^{*} = 7.0$.

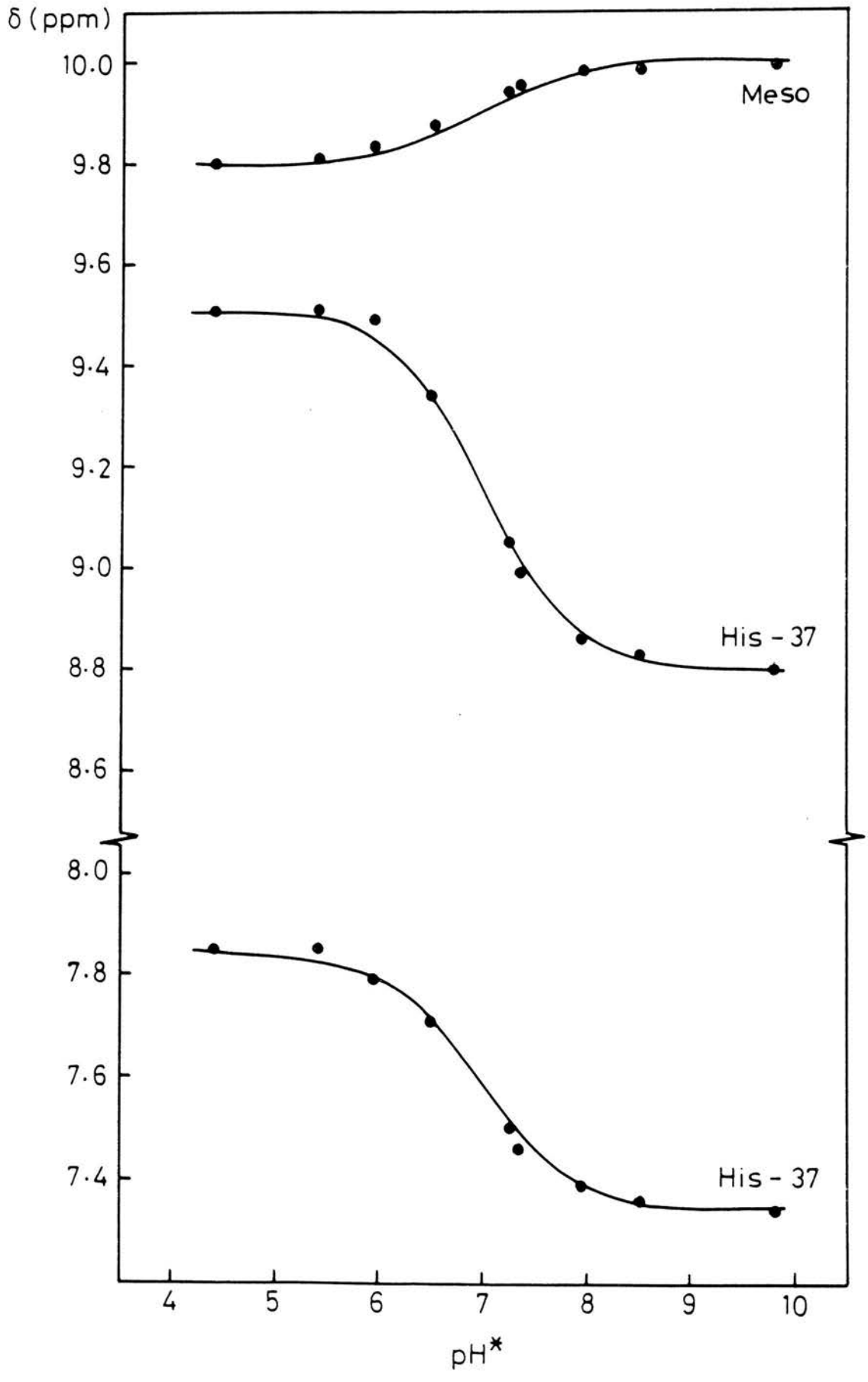
δ (ppm)
10.0
9.8
9.6
9.4
9.2
9.0
8.8
8.6
8.0
7.8
7.6
7.4
Meso
His - 37
His - 37
4
5
6
7
8
9
10
pH*

Schulz & Schirmer, 1979), and it was for this reason that these tyrosine doublets were assigned to Tyr1.

(b) Ferrocytochrome c-555

Some spectra from the ferrocytochrome pH titration are shown in Figure 53. Since many of the aromatic resonances are rather broad the spectra have not been resolution enhanced, allowing for more accurate determination of chemical shift values. Three resonances were clearly affected by pH changes, these being the C-2H and C-4H singlets of His37 and one of the haem meso resonances. All three titrated with the same pK^* value of 7.0, as shown in Figure 54. The overall shift of 0.75 ppm for the C-2H singlet is rather smaller than expected, although the C-4H resonance titrated normally.

There are a few other resonances which have slightly pH dependent chemical shifts, an example being the peak at 7.05 ppm (pH5.95), and these also appear to be associated with a pK^* value of approximately 7. Since most resonances remain unassigned these changes were uninterpretable in terms of an ionising group.

C. Conclusions and comparison with Pseudomonas cytochromes

The pH titrations of the two redox states of cytochrome c_{555} gave qualitatively similar changes in the NMR spectra to those observed for P. stutzeri 221 cytochrome c_{551}; no major pH induced structural changes occurred between pH5 and 9 but a limited number of residues showed small pH dependent changes in their chemical shift positions. The chemical shifts of some haem substituent resonances and the resonances of an unliganded histidine were affected by a pK^* of 6.3 in the ferricytochrome and a pK of 7^* in the ferrocytochrome. The pK^* values agree extremely well with the pKs predicted from redox measurements on cytochrome c_{555} (see Chapter IV).

The X-ray crystallographic structure of cytochrome

c_{555} shows that His37 is located in a region of the polypeptide chain which forms the bottom of the haem crevice, and that it is close to the propionic acid groups (Korzun & Salemme, 1978). Unfortunately, the crystal structure is not yet at a level of resolution where the precise interactions of His37 with the propionic acid groups and other amino acids can be distinguished, but it is conceivable that His37 is hydrogen bonded to propionic acid-7. Although the sequence alignment for cytochrome c_{555} and P. stutzeri 221 cytochrome c_{551} show that His37 and His47 are not homologous, they may well be structurally analogous. The NMR data presented above show that His37, like His47, is titratable and therefore relatively accessible to solvent. As with His47, the C-4H resonance of His37 has a much more oxidation state dependent chemical shift position than the C-2H resonance indicating that these histidine residues are orientated similary with respect to the haem.

In ferricytochrome c_{555}, there are more haem substituent resonances resolved between 10 and 60 ppm than in the cytochromes c_{551}. Apart from the two methyl resonances, four 1/2-proton peaks were affected by pH. The overall shifts of P2, P4 and P7 were of a similar magnitude to the shifts observed for the propionic acid resonances in P. stutzeri 221 cytochrome c_{551}. P1 showed a much bigger overall shift, more like the shift observed for the propionic acid resonances of P. aeruginosa cytochrome c_{551}. As in the Pseudomonas cytochromes, only two of the four methyl resonances are affected by pH titration of ferricytochrome c_{555}, their overall shifts being of a comparable magnitude. The NMR data obtained for cytochrome c_{555} are at least consistent with the proposal that propionic acid-7 ionises in this cytochrome also, even though the evidence for this rests on the pH dependent behaviour of a number of unassigned haem substituent resonances.

In ferrocytochrome c_{555} one of the meso resonances shows a pronounced pH dependent chemical shift which can be assigned a pK. Although a haem meso resonance could be observed to shift in pH titrations of P. stutzeri and P. aeruginosa ferrocytochromes c_{551}, the overall shift in both cases was too small for it to be fitted to a pK, and so it was not possible to show that haem substituent resonances are affected by pK_R. With cytochrome c_{555} there is clear evidence that a redox state dependent pK affects haem substituent resonances.

CHAPTER VI: CHEMICAL MODIFICATION EXPERIMENTS

A. Modification of Histidine Residues in Proteins with Ethoxyformicanhydride

Ethoxyformic anhydride (EFA) reacts with histidine residues in proteins to yield an N-ethoxyformylated derivative, as shown below.

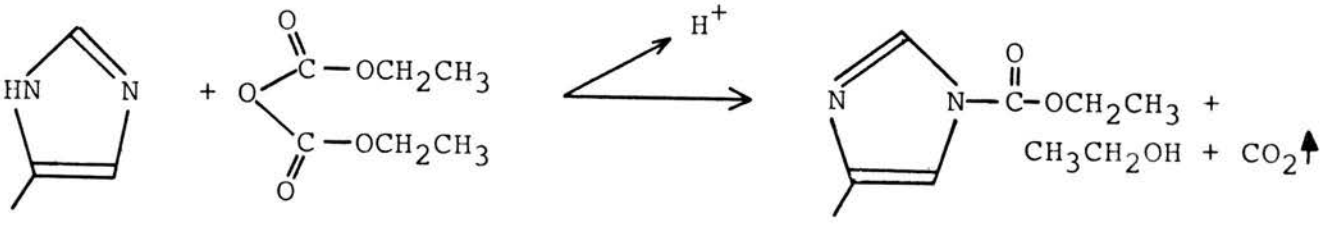

The reaction is accompanied by an increase in absorbance at 230-245 nm and this can be used to quantitate the extent of reaction using a difference extinction coefficient of $\Delta\epsilon = 3.2 \times 10^3\ M^{-1}cm^{-1}$ at 240 nm (Ovadi et al., 1967).

The model compound N-ethoxyformylimidazole has a half-life in water of about 2hr at pH2, 55hr at pH7 and 18 min at pH10 (Melchior & Fahrney, 1970); generally speaking the lability of N-ethoxyformyl derivatives of proteins precludes the isolation of modified peptides, except under very mild conditions.

Although EFA has a high degree of specificity for accessible histidine residues there are a number of reports in the literature of its reactions with other nucleophilic residues in proteins e.g. the active site serine of chymotrypsin (Melchior & Fahrney, 1970), tyrosine groups in thermolysin (Burstein et al., 1974) and the α-amino group of pepsin (Melchior & Fahrney, 1970). Rósen et al. (1970) have also proposed that EFA

can modify a tryptophan in the hydrophobic interior of bovine serum albumin. Fortunately, modification of both tyrosine and tryptophan is associated with distinct spectral changes in addition to an absorbance change ca. 240 nm, but some caution clearly has to be exercised in interpreting results.

Under conditions of large excess, EFA can react to form di-ethoxyformylhistidine, which has a higher extinction coefficient at 240 nm than the mono-ethoxyformylated species; clearly this could lead to an overestimate of the number of histidine residues modified. Mild hydroxylamine treatment will deacylate the mono-substituted histidine but not the di-substituted species and so residual absorbance at 240 nm after hydroxylamine treatment of a modified protein is indicative of di-ethoxyformylation. Morris & McKinley-McKee (1972) have recommended that the molar excess of EFA to histidine should be less than 30 to avoid formation of di-ethoxyformylhistidine.

B. Modification of Horse Cytochrome c with EFA

Since P. stutzeri 221 cytochrome c_{551} was available in relatively limited amounts, horse cytochrome c was used for preliminary modification studies with EFA. This cytochrome has three histidine residues, at positions 18, 26 and 33 in its sequence (Margoliash et al., 1961). His18 is the 5th iron ligand and, as such, is buried in the centre of the protein, but His26 and His33 occur towards the surface and might be expected to be accessible to modifying reagents.

(i) Choice of conditions

Since the hydrolysis rate of ethoxyformylimidazole is minimal at pH6 (Melchior & Fahrney, 1970) and since EFA reacts with the deprotonated form of histidine (Holbrook & Ingram, 1973), then the optimum pH for modification is in the range pH6-7 (assuming that the histidine undergoing modification has a typical pK value

of ~7). Additionally, as the reaction of EFA with histidine produces a proton, then the modification should be carried out in a well-buffered solution. For horse cytochrome c and P. stutzeri 221 cytochrome c_{551} the above requirements were met by using 10mM sodium phosphate, pH7.0 as the reaction medium.

(ii) Modification

In line with the recommendations of Morris & McKinley-McKee, modification of cytochrome c was attempted with a 15x excess of EFA over cytochrome i.e.5x excess with respect to the histidine content of this protein. Figure 55(a) shows the U.V. absorption spectrum of the cytochrome during the course of modification; the fractional absorbance change at 240nm is plotted against time in Figure 55(b). The reaction was complete after about 30 min, at which point ΔA_{240} corresponded to 0.9 mole histidine modified per mole cytochrome. The time course for modification is not first order, since a plot of $A_\infty - A_t$ against time is non-linear; this is probably due to the fact that EFA is unstable in aqueous solution. The total absorbance change at 240nm represents the formation of ethoxyformylhistidine only, since there were no other spectral changes indicating that tyrosine or tryptophan had been modified. The formation of di-ethoxyformylhistidine is unlikely under the conditions used, although it was not possible to test for its presence by the normal procedure of hydroxylamine treatment since hydroxylamine reduces cytochrome c (there are very large redox state associated spectral changes ca. 240 nm which swamp any effect of hydroxylamine on EFA-modified histidine).

Modification causes the appearance of an absorbance minimum at 315nm, which is coincident with the absorption band of reduced cytochrome c. Modification must therefore affect the redox state of cytochrome c in some way, but this point was not investigated further.

Figure 55: Chemical Modification of Horse Cytochrome c with Ethoxyformic Anhydride

(a) Spectral changes associated with the modification. (b) Fractional change in absorbance at 240nm as a function of time.

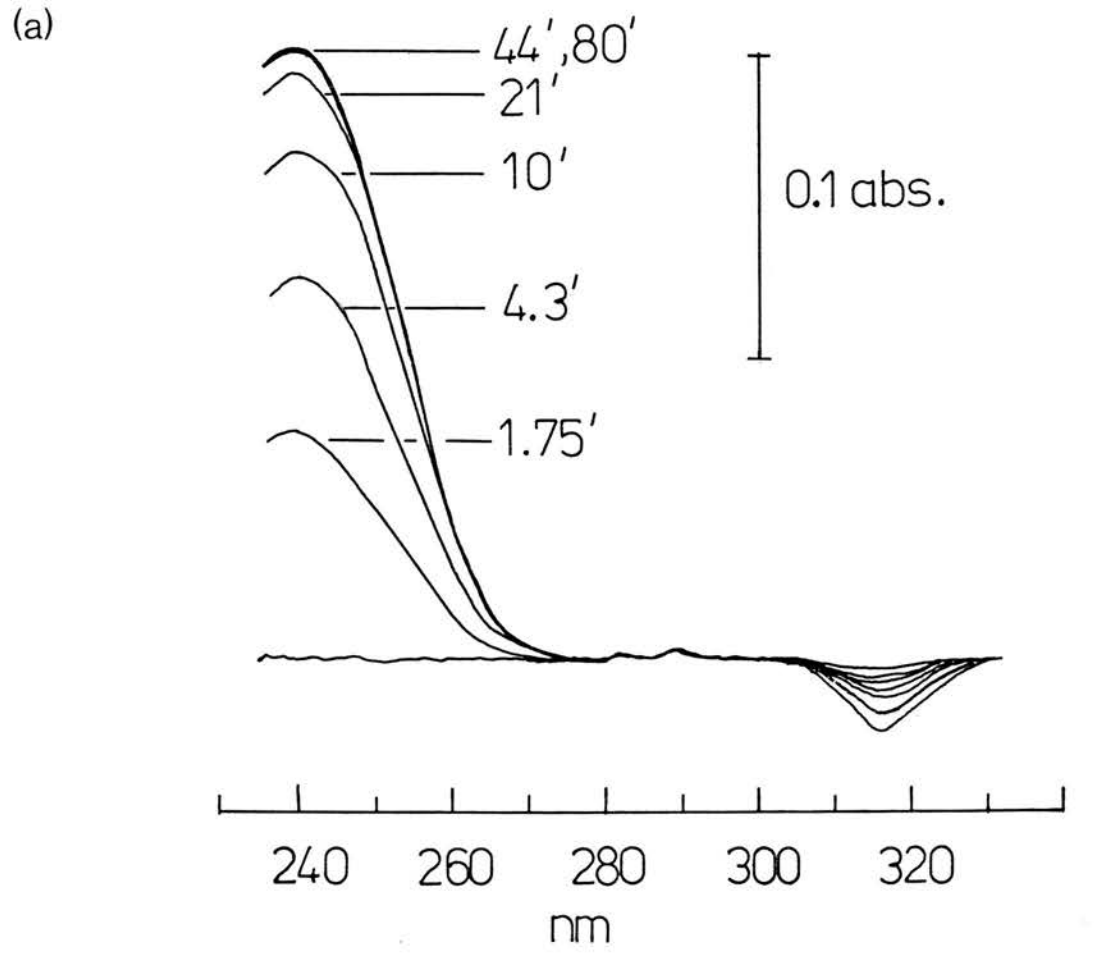
(a)
44',80'
21'
10'
4.3'
1.75'
0.1 abs.
240
260
280
300
320
nm

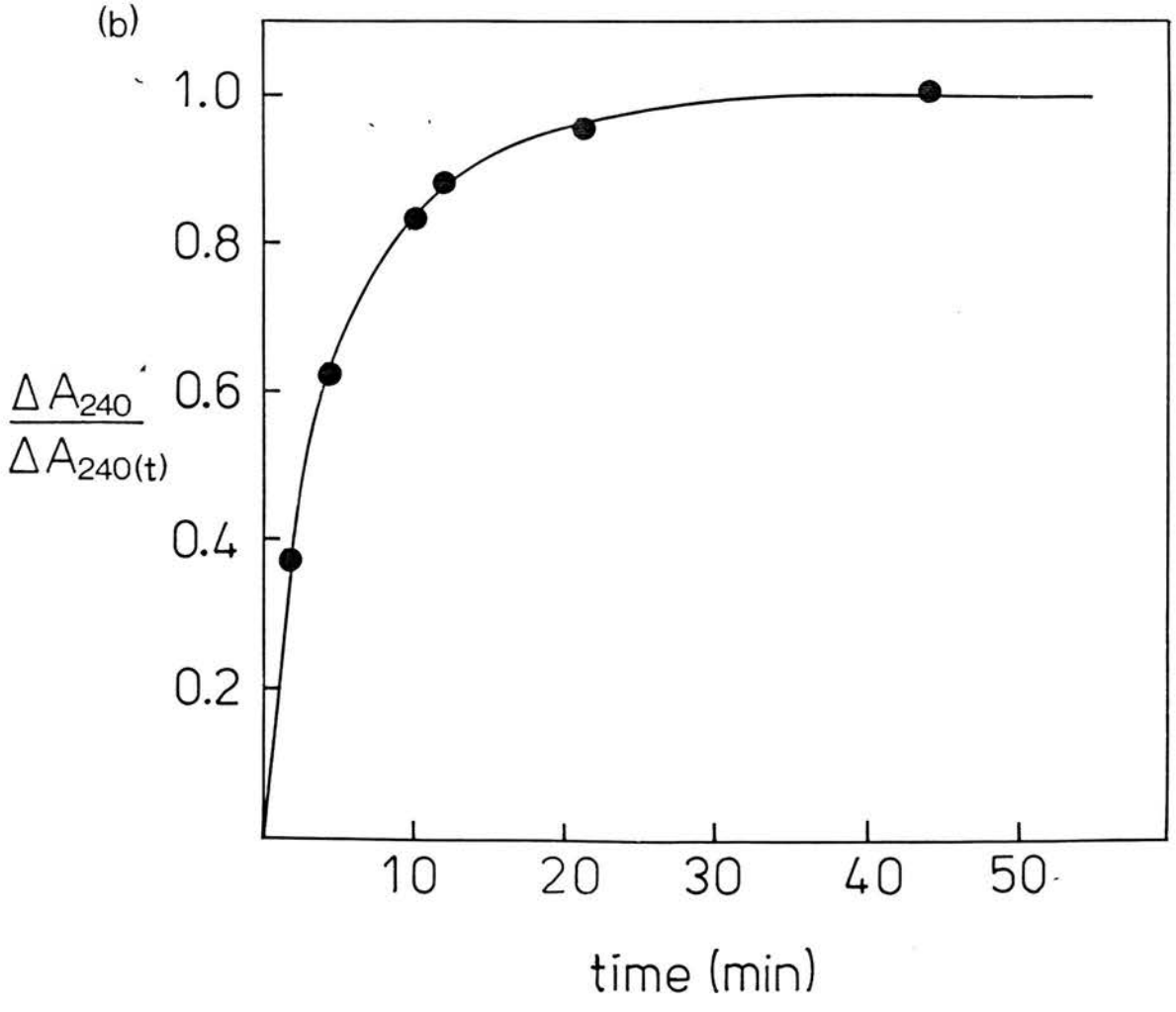
(b)
1.0
0.8
0.6
0.4
0.2
ΔA240 / ΔA240(t)
10
20
30
40
50
time (min)

(iii) Redox potential measurements

The redox potential of cytochrome c, modified as described above, was measured against the ferro-ferricyanide couple at a number of different pH values. The data are compared in Figure 56 with redox potential data obtained in a parallel experiment for the unmodified cytochrome. The modification has two effects on redox potential: (i) there is an overall drop of 20-30mV (ii) it becomes slightly pH dependent, falling by about 10mV between pH 5 and 8.

(iv) Comments

Since approximately 1 histidine residue/molecule cytochrome c was modified in these experiments then it is pertinent to ask which one. His18 seems an unlikely candidate, being in the centre of the protein. On the other hand, from consideration of the crystal structure (Dickerson et al., 1971) it is not obvious why His33 or His26 should be exclusively modified, since both are relatively exposed on the surface of the protein. However, two pieces of information argue for it being His33 which is ethoxyformylated under these conditions. (i) Attempts to carboxymethylate horse cytochrome c with bromoacetate resulted in only 1 histidine, His33, being modified; there were no concomitant changes in the visible spectrum. All histidines could be carboxymethylated in the presence of 8M urea but this complete carboxymethylation caused very large spectral changes, including the loss of the α and β absorption bands in the ferrocytochrome (Stellwagen, 1966). Therefore, in the native protein His26 is not accessible to bromoacetate and modification of His33 does not significantly perturb the cytochrome tertiary structure. (ii) ^{1}H NMR data show that resonances assigned to His33 titrate with pK=6.5 whereas those assigned to His26 only begin to titrate at pH values below 3.5 (Cohen & Hayes, 1974). Together, (i) and (ii) indicate that His26 has a rather unusual environment (which is not immediately

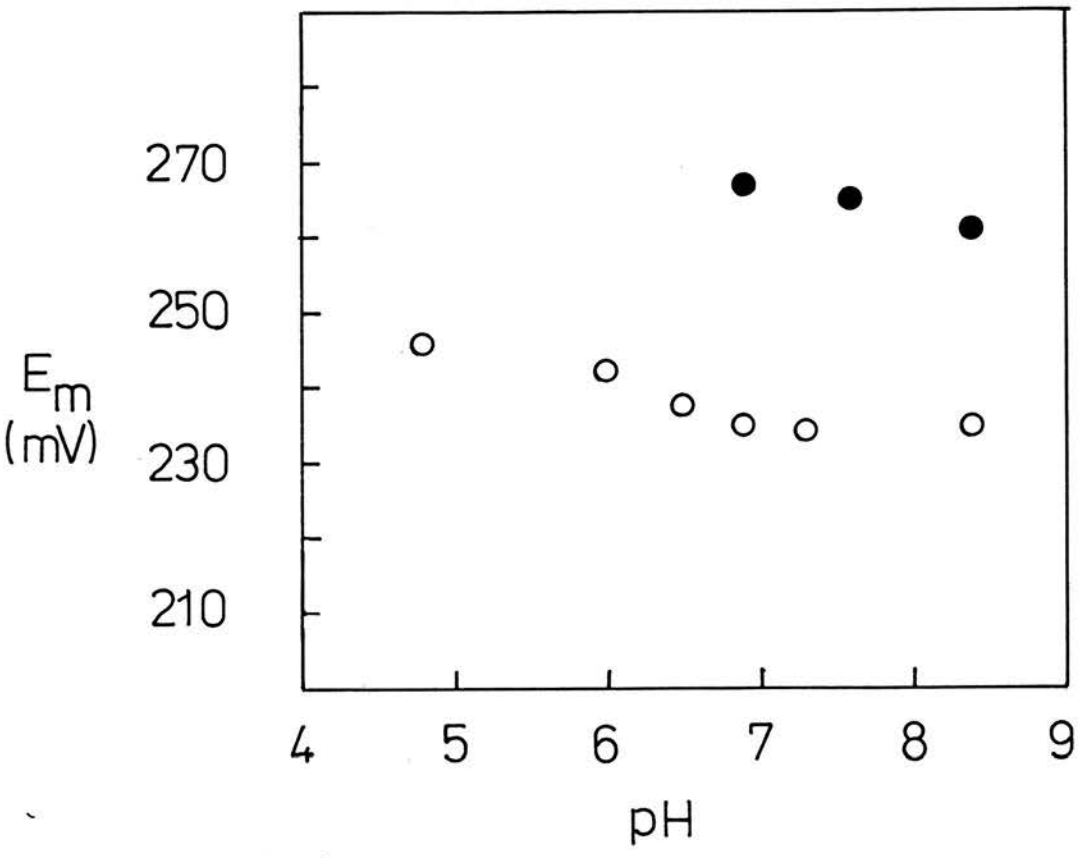

Figure 56: E_m versus pH for Ethoxyformylated Horse Cytochrome c

● Redox potential measured before ethoxyformylation. o Redox potential measured after ~1 mol histidine modified/mol cytochrome.

evident from the crystal structure) and that it is probably not ethoxyformylated under the mild conditions used here.

How does ethoxyformylation lead to an overall decrease in the cytochrome redox potential? Since redox potential is a sensitive monitor of molecular integrity then one explanation might be that modification causes a localised conformational rearrangement (this would not necessarily be reflected in the visible spectrum). An alternative explanation is based on an observation made by Vanderkooi et al. (1973a) that the redox potential of cytochrome c bound to the mitochondrial membrane is some 45mV lower than that measured for the cytochrome free in solution. This observation was rationalised by proposing that ferricytochrome c binds to the membrane with a greater avidity than ferrocytochrome c, and affinity constant measurements show that this is indeed the case (Vanderkooi et al., 1973b). If His33 were involved in binding to membranes then modification with an ethoxyformyl group might affect the redox potential in a similar way i.e. by stabilising the ferricytochrome with respect to the ferrocytochrome. The origin of the small pH dependent effect in this context is not clear.

C. Chemical Modification of P. stutzeri 221 Cytochrome c-551 with EFA

In order to determine the relative importance of His47 and haem propionic acid-7 for the pH dependence of redox potential observed for P. stutzeri 221 cytochrome c_{551} an attempt was made to chemically modify His47 with EFA.

(i) Modification

The same excess of EFA over cytochrome was used as for cytochrome c, although the P. stutzeri cytochrome contains only 2 histidines so the excess relative to the histidine content of the protein was 7.5x rather than 5x. The effects of modification on the U.V. spectrum are

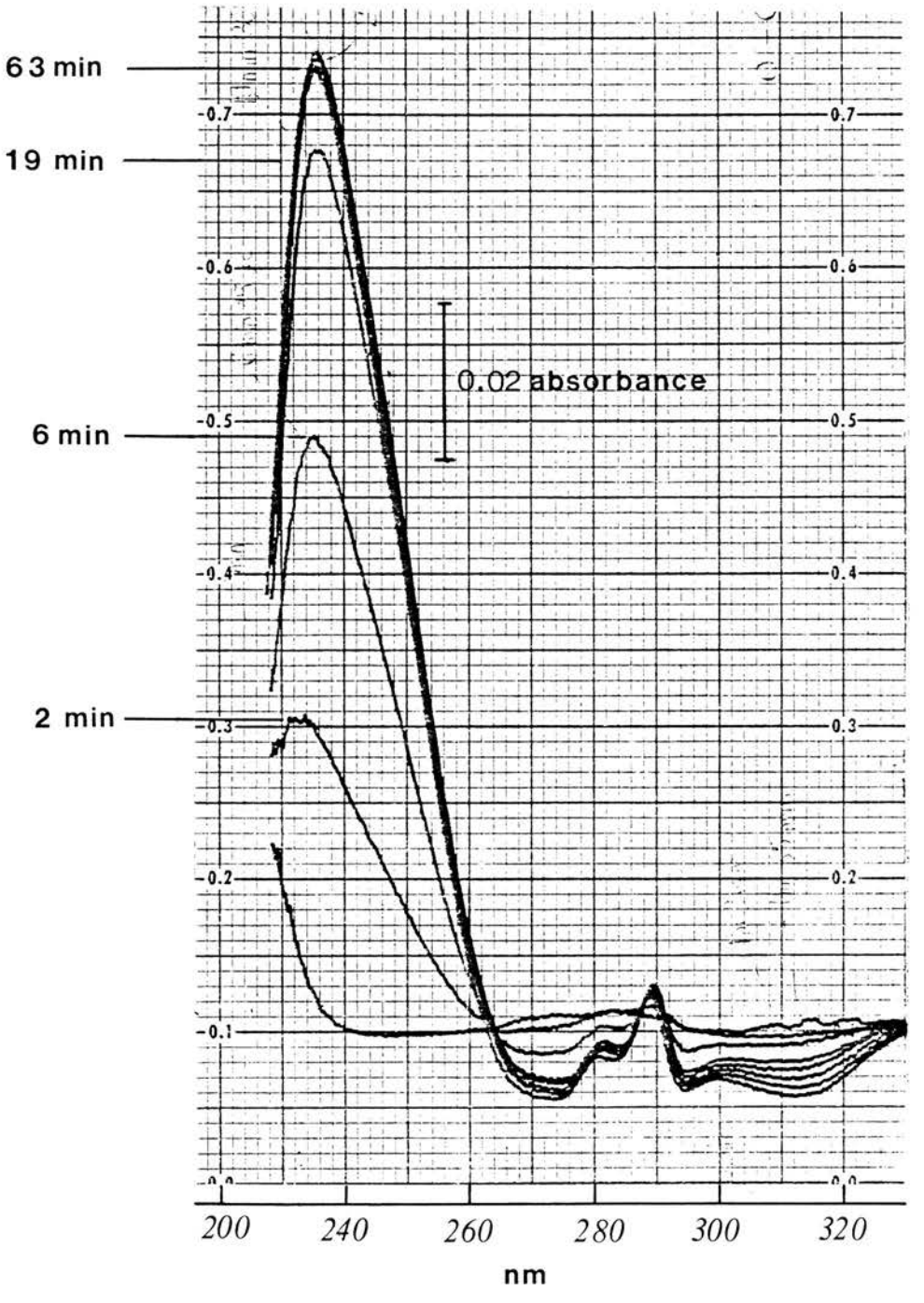

Figure 57: Chemical Modification of P. stutzeri (221) Cytochrome c-551 with Ethoxyformic Anhydride

shown in Figure 57. The absorbance maximum of ethoxyformylhistidine is near 236 nm in this cytochrome, and using $\Delta\epsilon_{240}$ = 3200 $M^{-1}cm^{-1}$ a value of 1.3 mole histidine modified/mole cytochrome is obtained. There are, however, other changes in the U.V. region which may complicate the absorbance change at 236 nm; the maxima at 280 and 290 nm which develop in parallel to that at 236 nm are suggestive of the perturbation of another aromatic amino acid. Figure 58(a) shows the spectral changes associated with the ethoxyformylation of tyrosine in thermolysin (A) and in a model tyrosine system (B) - the spectra show quite clearly that it is not tyrosine which is being modified in P. stutzeri cytochrome c_{551}. Figure 58(b) shows that the ethoxyformylation of tryptophan in a model system also causes a decrease in absorption between 270 and 300nm, and so the spectral changes observed with cytochrome c_{551} do not appear to be associated with modification of either of these amino acids. Alternatively, in view of the parallel nature of the absorbance changes at 236 nm and 270-300 nm, and in view of the possibility that His47, like Trp56, might be hydrogen bonded to propionic acdi-7, then the maxima at 280 and 290 nm could be due to an alteration in the environment of Trp56. This alteration may be brought about by the ionisation of propionic acdi-7 as the histidine modification proceeds, which would be the case if the propionic acid pK is atypically high because of an interaction with His47. Assuming that the environment of Trp56 is perturbed by the ethoxyformylation of His47, then this will complicate the absorbance change at 236 nm, since tryptophan absorbs here. The calculation of 1.3 mole histidine modified/ mole cytochrome may be an overestimate if this perturbation causes in increase in Δ absorbance at 236 nm.

Redox potential measurements

Following modification as described above, the redox potential of the P. stutzeri cytochrome was measured by the method of mixtures with ferro-ferricyanide. The

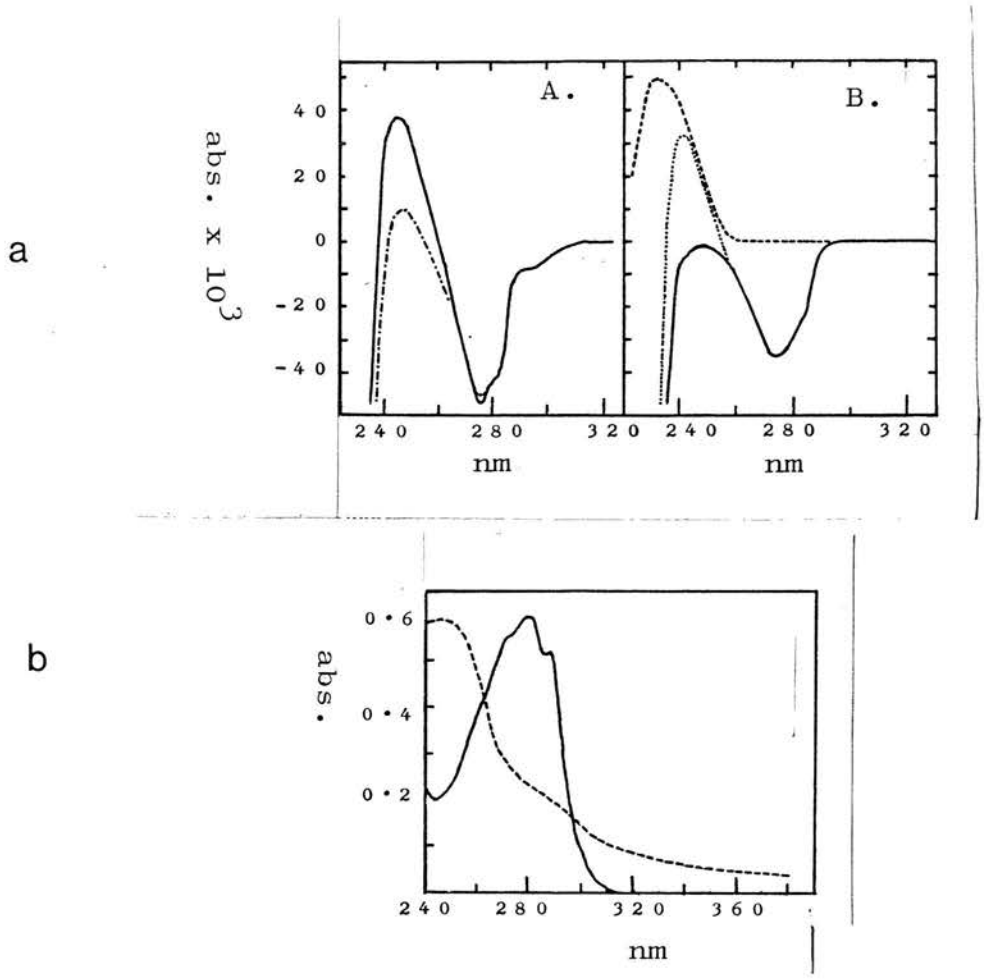

Figure 58: Spectral Changes Associated with Ethoxyformylation of Tyrosine and Tryptophan

(a) Tyrosine: A, difference spectrum of thermolysin after modification by ethoxyformic anhydride (broken line is spectrum after treatment with hydroxylamine); B, spectral changes after treatment of N-acetyl-L-tyrosine ethyl ester (solid line) and imidazole (broken line) with ethoxyformic anhydride - the dotted line is the algebraic sum of the other two lines [from Burstein et al., 1974]. (b) Tryptophan: U.V. spectrum of acetyltryptophan before (solid line) and after (broken line) reaction with ethoxyformic anhydride [from Rosen et al., 1970].

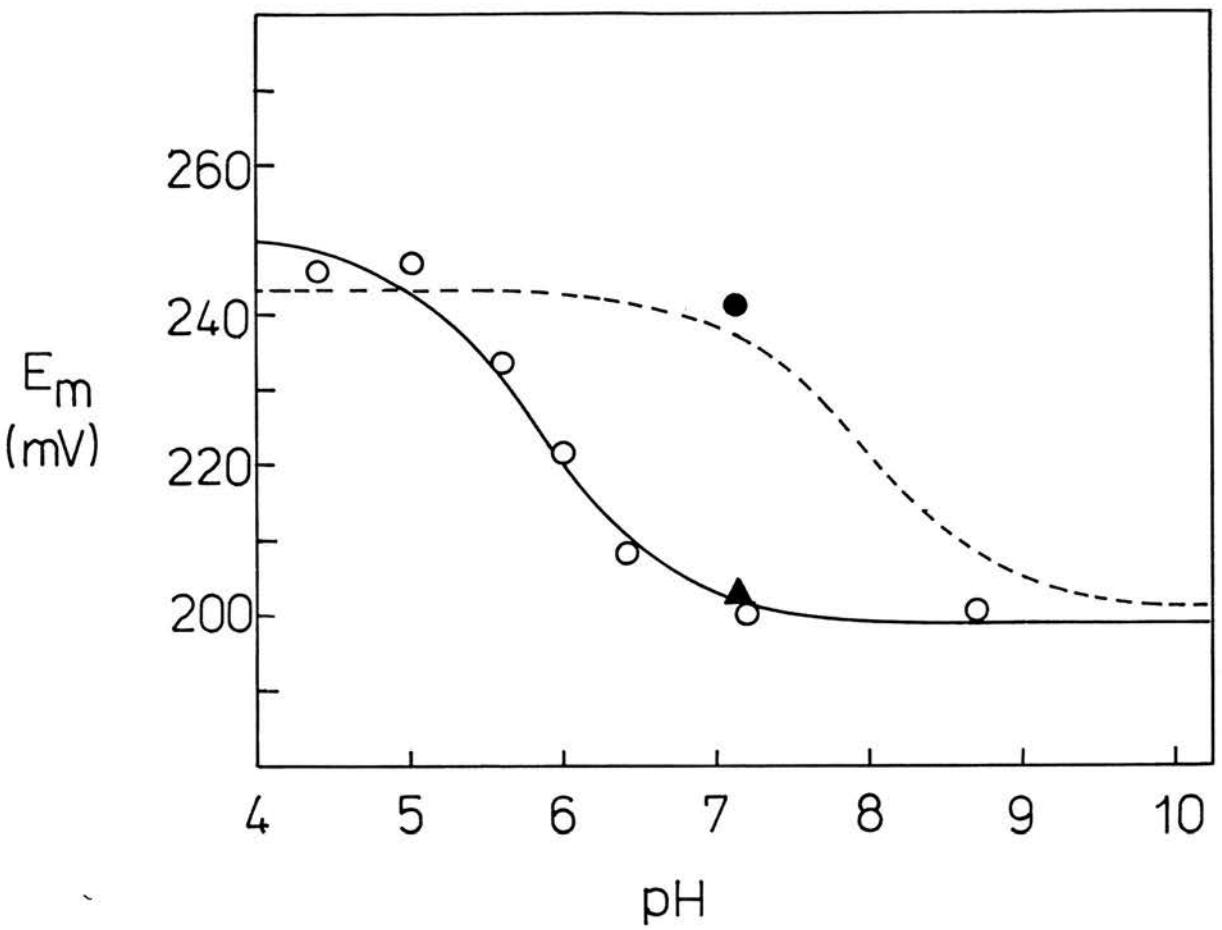

Figure 59: E_m versus pH for P. stutzeri (221) Cytochrome c-551 After Modification with Ethoxyformic Anhydride

● Redox potential measured before modification. ○ Redox potential measured shortly after modification. ▲ Redox potential measured ca. 8 hr after modification. The solid line is the theoretical curve obtained from Equation 2 using pK_O = 5.45 and pK_R = 6.3. The broken line is the theoretical curve previously obtained for the unmodified cytochrome (see Figure 23).

results are shown in Figure 59, which also includes the theoretical curve calculated previously (see Chapter IV) for the redox potential measurements on unmodified cytochrome. The difference is striking - for the ethoxyformylated protein the theoretical curve has pK values of 5.45 and 6.3 i.e. approximately 2 pH units below the pK values for the unmodified cytochrome. However, the redox potential of both forms is nearly identical at high and low pH, which is a good indication that modification has not induced any significant structural alteration in the protein.

Comments and conclusions

The central observation is that modification of approximately 1 histidine residue in P. stutzeri cytochrome c_{551} causes a change in the pH dependence profile of its redox potential. Two questions may now be posed: (i) which histidine gets modified and (ii) how can this affect the pH dependence of redox potential? With regard to the first question, this cytochrome has only 2 histidine residues, His16 and His47. His16 is the 5th axial ligand to the haem iron and is therefore buried in the centre of the molecule; His47 occurs towards the surface of the protein and of the two is more likely to be accessible to EFA. However, two other arguments support the proposal that it is His47 which gets modified. Firstly, ethoxyformylation of His16 would impair its function as an iron ligand and consequent upon that there would large changes in the visible spectrum - no such changes were observed. Secondly, treatment of P. aeruginosa cytochrome c_{551} with EFA under the same condition as used for the P. stutzeri cytochrome caused no absorbance increase ca. 240 nm (see section E below) - P. aeruginosa cytochrome c_{551} has only 1 histidine in its sequence, viz. His16.

How does ethoxyformylation affect redox potential? Presumably, an interaction between His47 and propionic acdi-7 is disrupted upon modification. This allows the

propionic acid to titrate with "typical" pK values of 5.45 and 6.3. Assuming that ethoxyformyl-His47 does not ionise in the pH range 5-8 (see section F) then the pH dependence of redox potential observed for the modified cytochrome must be entirely due to the propionic acid ionisation. This then implies that the propionic acid ionises in the unmodified cytochrome also, thereby causing the fall in redox potential. The experiment does not exclude the possibility, however, that in the unmodified cytochrome the ionisation of His47 also contributes to the pH dependence of redox potential.

D. Attempted Modification of P. aeruginosa Cytochrome c-551 with EFA

P. aeruginosa cytochrome c_{551} was treated with an equivalent excess of EFA to that used for the P. stutzeri cytochrome modification. After one hour there was no change in the U.V. absorbance such as would indicate the ethoxyformylation of histidine, or of tyrosine or tryptophan. Addition of twice as much EFA had no effect on the spectrum either. The redox potential of the cytochrome measured after this exposure to EFA was the same as that of the untreated cytochrome (to within 5mV at pH7.0).

It is therefore concluded that His16 is not modifiable with EFA. P. aeruginosa cytochrome c_{551}, like the P. stutzeri cytochrome, has tryptophan at position 56 in its sequence so this experiment tends to support the conclusion reached above that Trp56 in P. stutzeri cytochrome c_{551} does not get ethoxyformylated and that modification of His47 indirectly perturbs the environment of Trp56.

E. The pK of N-Ethoxyformylimidazole

In chemically modifying His47 the aim was to introduce a chemical group onto the imidazole ring to disrupt the His47-propionic acid-7 interaction. However,

since the modified cytochrome c_{551} also exhibits a pH dependent redox potential, the pKs could be interpreted as being due to the ionisation of ethoxyformyl-His47. It was therefore necessary to check that N-ethoxyformylhistidine does not ionise in the pH range 5-9.

Since it contains an electron withdrawing carbonyl group, N-ethoxyformylated histidine is expected to have a lower pK than histidine. From consideration of the pH profile for the rate of hydrolysis of modified imidazole, Melchior & Fahrney (1970) deduced that the N-ethoxyformylimidazolium ion should have a pK_a of 3.6; this value can easily be checked by NMR. Figure 60 shows the ^1H NMR spectrum obtained after reacting imidazole with an equimolar amount of EFA. Five resonances are observed, of which three are the C-2H, C-4H and C-5H resonances of EFA-modified imidazole. At a molar ratio of EFA:imidazole of 1:1 there is apparently insufficient EFA to completely modify all the imidazole and so the C-2H and the equivalent C-4H + C-5H resonances of free imidazole also appear in the spectrum. Figure 61 shows the pH profile of these resonances. Theoretical curves for three of these resonances were drawn using a pK^* value of 3.6. For the other two resonances i.e. those of free imidazole, pK^* is >7.

This experiment was performed with imidazole in preference to histidine since the α-amino group of histidine is susceptible to modification by EFA. However, as histidine has a lower pK than imidazole the pK of N-ethoxyformylhistidine is expected to be less than 3.6. Thus the pK of ethoxyformyl-His47 should not contribute to the pH effects on cytochrome c_{551} redox potential observed above pH5.

F. The NMR Spectrum of P. stutzeri 221 Cytochrome c-551 after Chemical Modification with EFA

The structural effects on P. stutzeri cytochrome

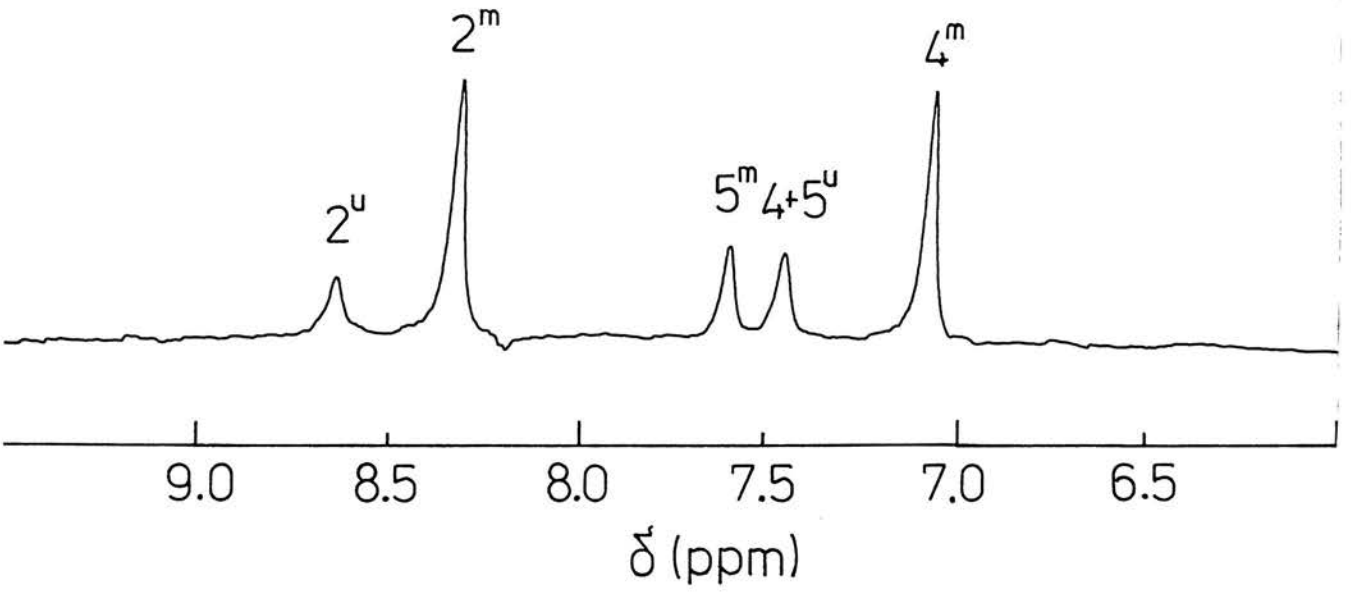

Figure 60: ^{1}H NMR Spectrum of Ethoxyformylimidazole

The labelled resonances are: 2^{m}, 4^{m}, 5^{m} - the C-2, C-4 and C-5 resonances of ethoxyformylimidazole; 2^{u}, $4+5^{u}$ - the C-2 and equivalent C-4/C-5 resonances of free imidazole.

Figure 61: pH Dependence of Chemical Shift (δ) for the Resonances of Ethoxyformylimidazole and Imidazole

○ Ethoxyformylimidazole. ● Imidazole. The solid lines are theoretical curves fitted using $pK^{*} = 3.6$.

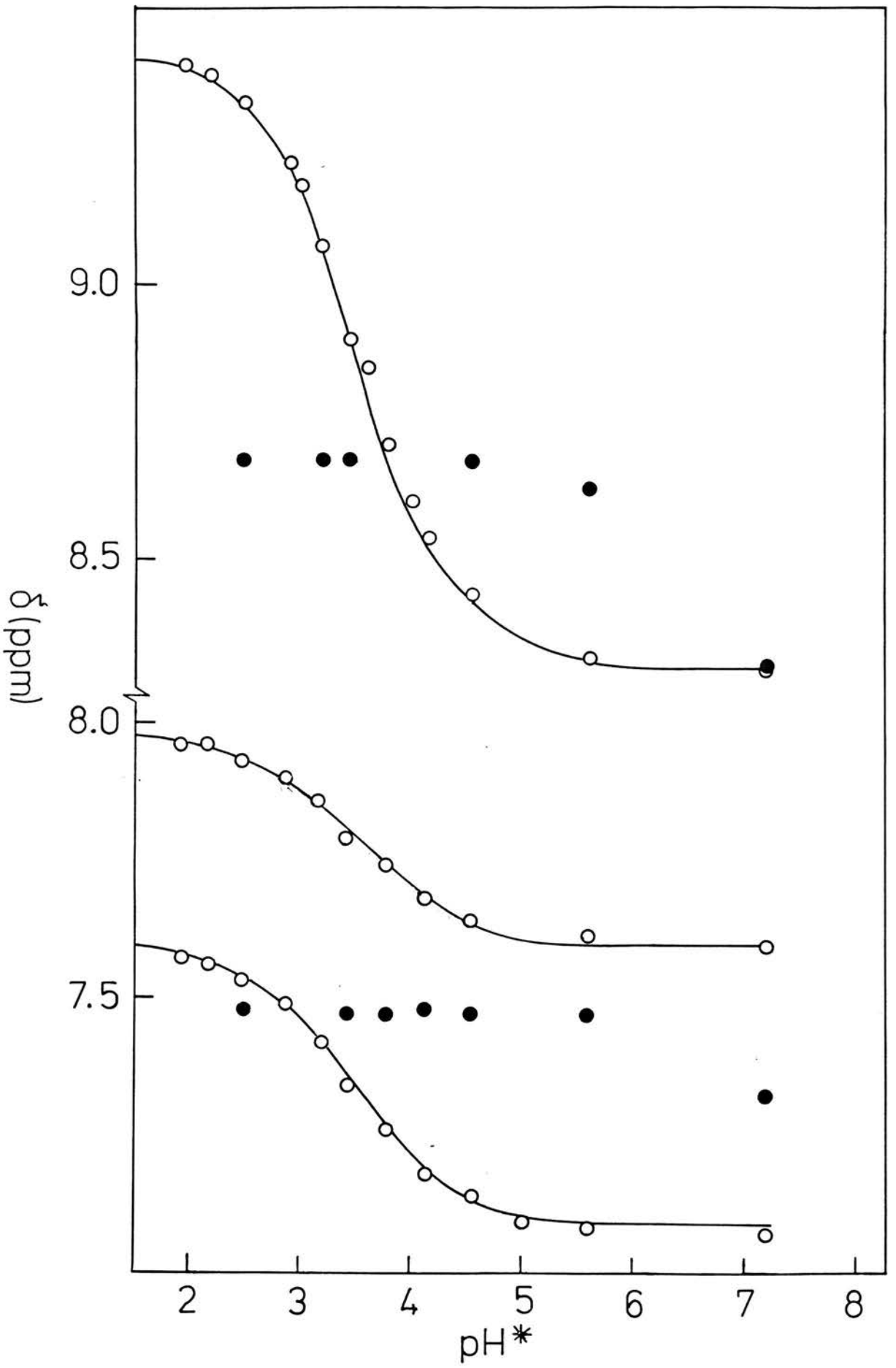
9.0
8.5
8.0
7.5
δ (ppm)
2
3
4
5
6
7
8
pH*

c_{551} resulting from chemical modification with EFA can be assessed from its NMR spectrum.

The spectrum of the modified ferricytochrome is similar to the spectrum of the unmodified protein with regard to the chemical shifts of the haem methyl and Met61 resonances. The downfield shifted haem substituent resonances are shown at three pH values in Figure 62 - these spectra can be compared with those obtained prevoiusly for the unmodified cytochrome (Figure 41). The most obvious difference between the two sets of spectra is the poorer quality of the modified cytochrome spectra. This effect is indicative of protein aggregation, but it is not clear how ethoxyformylation of His47 could cause aggregation. If δ is plotted against pH for the resonances of the modified cytochrome (Figure 63) and the curves then compared with those in Figure 42, a number of differences become apparent. (i) In modified cytochrome c_{551}, M1 and M8 have very pH dependent chemical shifts, while the chemical shifts of M5 and M3 are relatively insensitive to pH changes. In the unmodified cytochrome the opposite is true, with M5 and M3 having the more pH dependent chemical shifts (ii) M1 and M8 in the modified protein show larger values of $\Delta\delta$ than do M5 and M3 in the unmodified cytochrome. However, despite these differences in pH dependent behaviour, the chemical shifts of the four methyls in the two species are virtually identical at high pH (>8). This indicates that the chemical modification of His47 does not drastically perturb the haem environment but suggests that the haem methyl resonance shifts could be affected in a minor way by disruption of the His47-propionic interaction.

In the unmodified cytochrome the pH dependent shifts of the propionic acid-7 β-CH_2 resonances were taken as evidence that this propionic acid ionises. In the modified cytochrome spectra only one other resonance apart from the methyls can be discerned between 10 and 40 ppm.; it has not been assigned but its chemical shift at

Figure 62: ^{1}H NMR Spectrum of Modified P. stutzeri (221) Cytochrome c-551 at Various pH Values

The labelled resonances are: M1, M3, M5 and M8 = haem methyls; P? = 1-proton resonance tentatively assigned to a propionic acid-7 β-CH_2 proton.

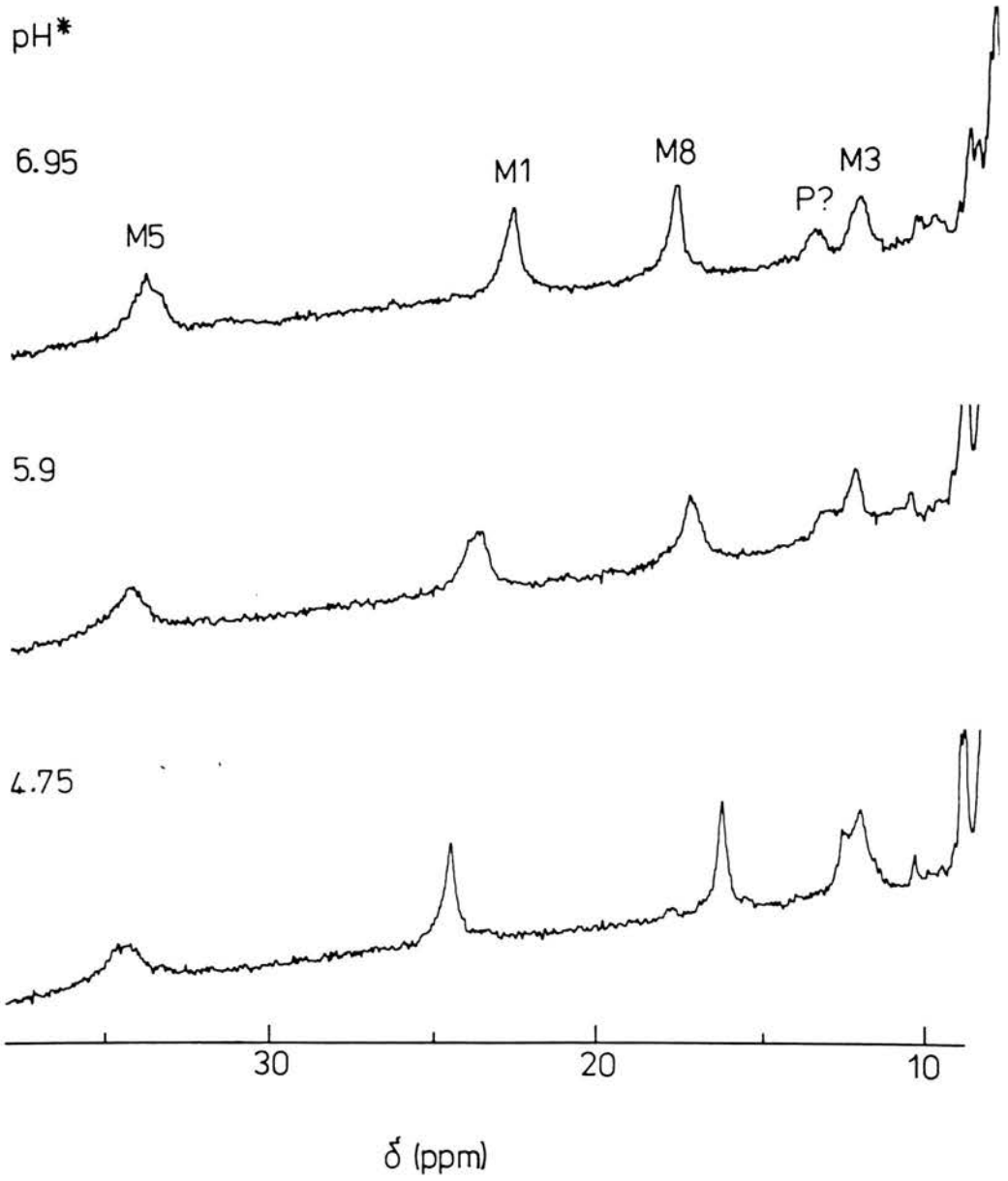
pH*
6.95
M5
M1
M8
P?
M3
5.9
4.75
30
20
10
δ (ppm)

Figure 63: pH Dependence of Chemical Shift (δ) for the Haem Substituent Resonances of Modified P. stutzeri (221) Ferricytochrome c-551

Labelling of resonances as for Figure 62. The theoretical curves were fitted using $pK^{*} = 5.8$.

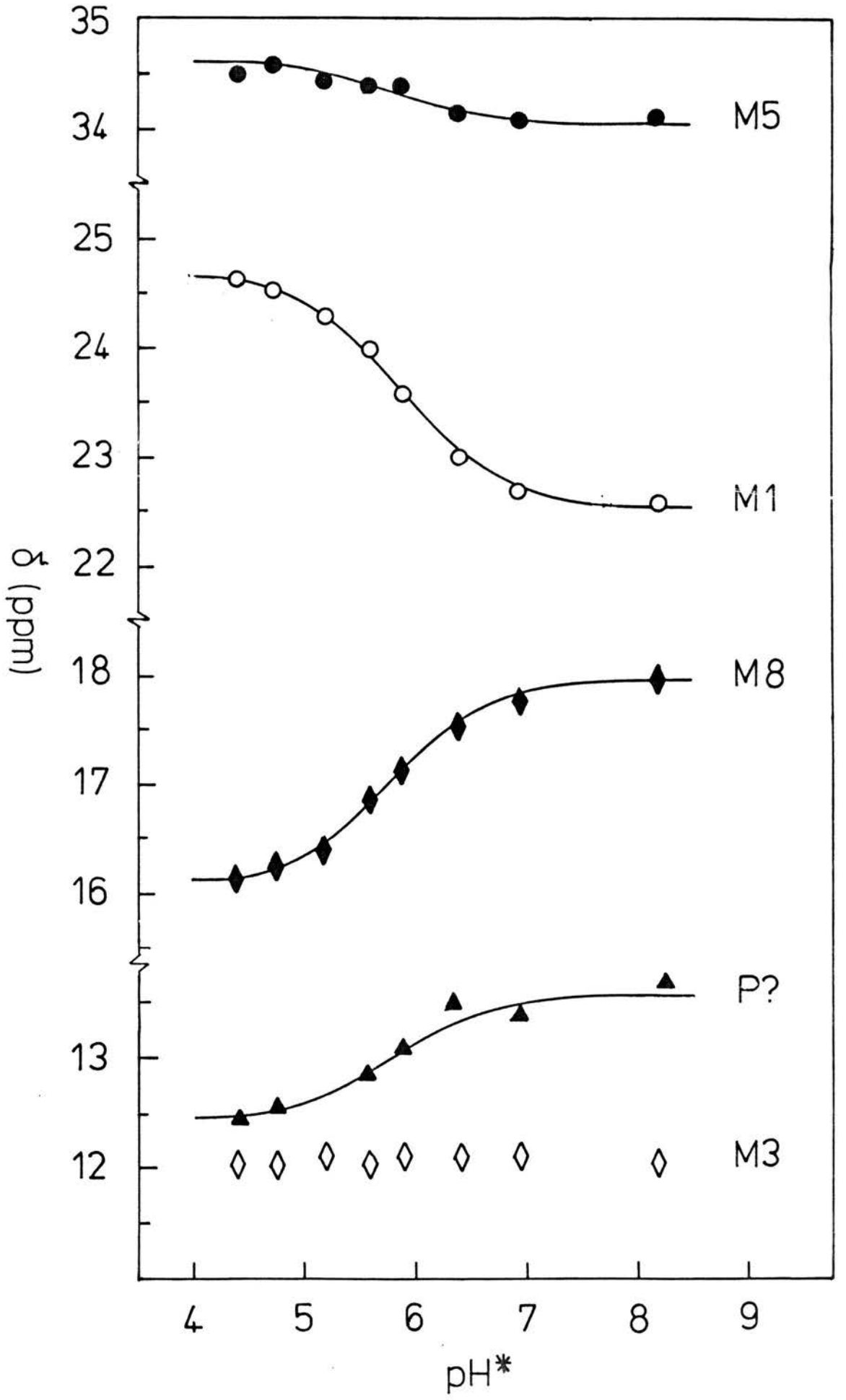
35
34
25
24
23
22
18
17
16
13
12
δ (ppm)
M5
M1
M8
P?
M3
4
5
6
7
8
9
pH*

high pH is quite similar to that of P1 in the unmodified cytochrome and is therefore assumed to be one of the propionic acid-7 resonances. This resonance, designated P? in Figure 62, titrates with a value of $\Delta\delta$ comparable to the propionic acid resonances in the unmodified cytochrome but, like the methyls, with pK^*_O = 5.8. Given that ethoxyformyl-His47 does not ionise in the pH range 4.4-9.0 then this pK is attributable to the ionisation of propionic acid-7. The pK^*_O value of 5.8 compares reasonably well with the value of 5.45 predicted from the redox measurements described above.

In the aromatic region of the modified cytochrome spectrum, the poor quality of the spectra obscured the coupling pattern of most resonances. However, the only resonances of much interest were the C-2H and C-4H singlets of ethoxyformyl-His47 and, with the help of a Hahn spin echo pulse sequence, singlets can usually be distinguished quite easily. A singlet resonance was clearly discernable at 8.25 ppm in the ferricytochrome and 8.4 ppm in the ferrocytochrome. This singlet has the approximate chemical shift expected for the C-2H resonance of deprotonated ethoxyformylhistidine, as judged from Figure 61. Titration of the cytochrome over the pH^* range 4.4 to 8.2 produced virtually no change in the chemical shift of this resonance in either oxidation state. No singlet resonance with a chemical shift comparable to the C-4H resonance of ethoxyformylimidazole was observable in the NMR spectrum of either oxidation state during pH titration.

These limited data on the histidine resonances are at least consistent with the proposal that ethoxyformyl-His47 does not ionise in the pH range over which the modified cytochrome redox potential is pH dependent.

CHAPTER VII: DISCUSSION

NOTE: The work presented in the Results chapters have concentrated on data for the Pseudomonas cytochromes c_{551}. However I was also involved in some of the experimental work covering a broader area, some of which is published in the papers of Appendix II (Pettigrew et al., 1983; Moore et al., 1983). I will be putting the cytochrome c_{551} work in the context of this broader survey and will clearly indicate experiments which I myself performed and those which were performed by others.

1. The Interaction Between His47 and Propionic Acid-7 in P. stutzeri Cytochrome c-551

In P. stutzeri 221 cytochrome c_{551} four pieces of evidence suggest that His47 may interact with haem propionic acid-7: (i) For most proteins which contain a titratable histidine, the pK value for the histidine is ca. 6-7 (Markley, 1974); in P. stutzeri 221 cytochrome c_{551}, the pK of His47 lies outwith this range in both oxidation states (pK_O = 7.6, pK_R = 8.3), indicating some kind of environmental perturbation. (ii) The substituent propionic acids of isolated haem c titrate with pK ~ 5. Ionisation of propionic acid-7 is likely to be less favourable within the hydrophobic interior of a cytochrome molecule, the propionate anion being a destabilising influence, and so its pK in situ may be greater than 5 (but see page 226). However, pK values of 7.6 and 8.3 are rather higher than might be expected. (iii) pK values of 5.45 and 6.3 were observed for propionic acid-7 upon modification of His47. (iv) His47 and propionic acid-7 ionise with the same redox state dependent pKs.

Since Arg47 in P. aeruginosa cytochrome c_{551} is hydrogen bonded to propionic acid-7, then it is likely

that His47 of P. stutzeri 221 cytochrome c_{551} is sufficiently close to propionic acid-7 to be involved in a hydrogen bonding interaction. An appropriate hydrogen bonding scheme should be able to explain the conjoint ionisation of His47 and the propionic acid and the anomalously high pK values of both species. Two types of hydrogen bonding scheme can be envisaged, involving either one proton (Figure 64 B,C) or two protons (Figure 64 A). The following arguments strongly support a one-proton scheme. Firstly, if Equation 2 (page 28) is re-written to incorporate two deprotonations occurring with the same pK then the equation becomes

$$E_m = \tilde{E} + \frac{RT}{nF} \ln \frac{[H^+]^2 + K_R[H^+] + K_R^2}{[H^+]^2 + K_O[H^+] + K_O^2} \qquad \text{Equation 4}$$

Figure 65 shows that if the values of pK_O and pK_R used with equation 2 to generate curve (a) are substituted in Equation 4, then a much steeper curve, curve (b), is obtained. Curve (a) is the theoretical curve which gave the best fit to the P. stutzeri 221 cytochrome c_{551} redox data and it is clear that the data points do not lie along curve (b). By selecting values of $pK_O = 7.8$ and $pK_R = 8.1$ it is possible to produce a theoretical curve with Equation 4 which gives a good fit to the same redox data but ΔpK_{red-ox} is reduced from 0.7 to 0.3 pH unit. However, the NMR pH titration data yielded pKs that were very close to the redox pKs obtained using Equation 2, and ΔpK_{red-ox} was identical.

A second argument in favour of a one proton scheme is simply that it is easier to understand how His47 and the propionic acid could be affected by the same deprotonation. With a two proton scheme such as that shown in Figure 64 A, deprotonation of one group need not necessarily lead to deprotonation of the other with the same pK; it may be that after the first deprotonation event one or both of the two groups reorientate and thereby cause the second deprotonation, but this

Figure 64: Possible Hydrogen Bonding Schemes Between His47 and Propionic Acid-7

(A) two-proton scheme; (B) loss of hydrogen-bonded proton; (C) loss of non-hydrogen bonded His proton (D and E) cytochrome modified with ethoxyformic anhydride (R = ethoxyformyl).

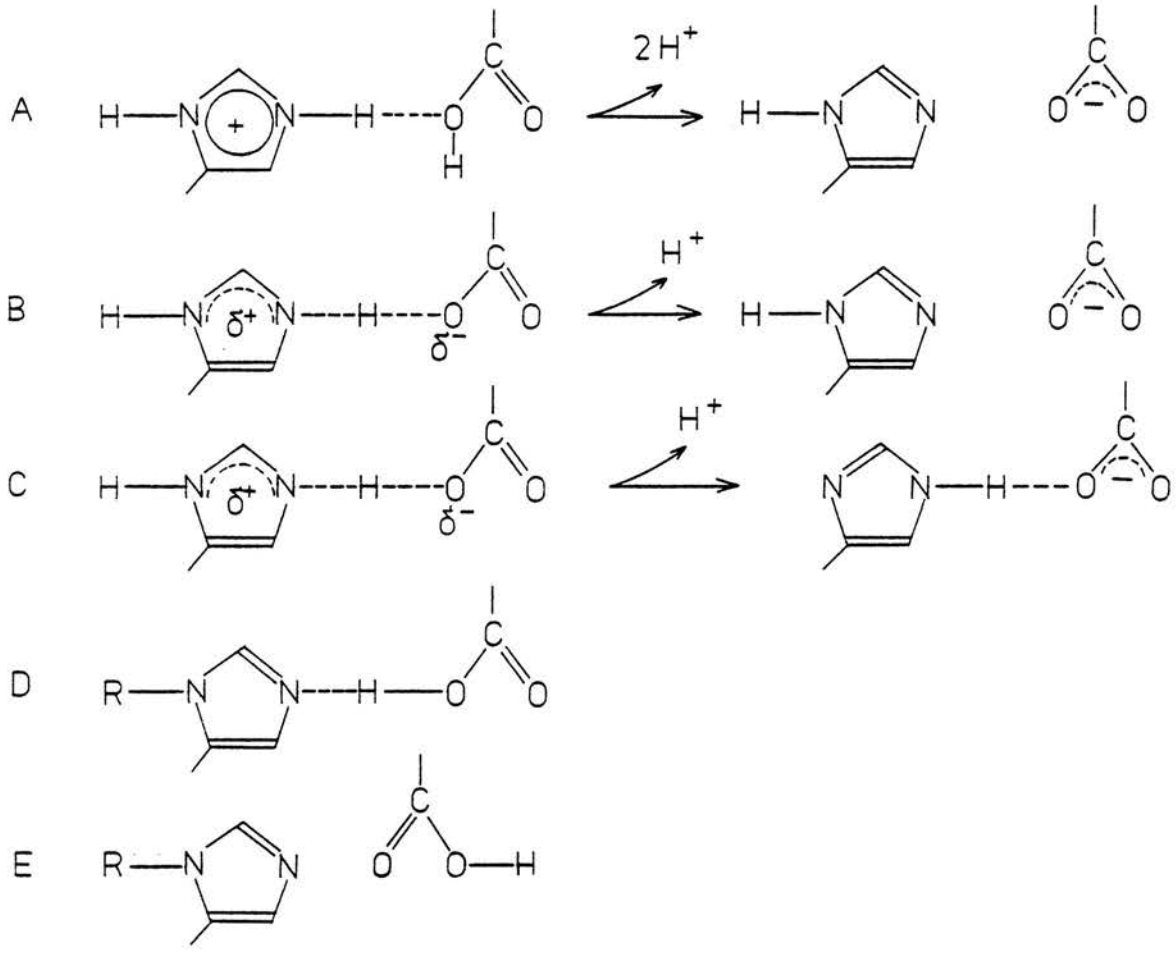

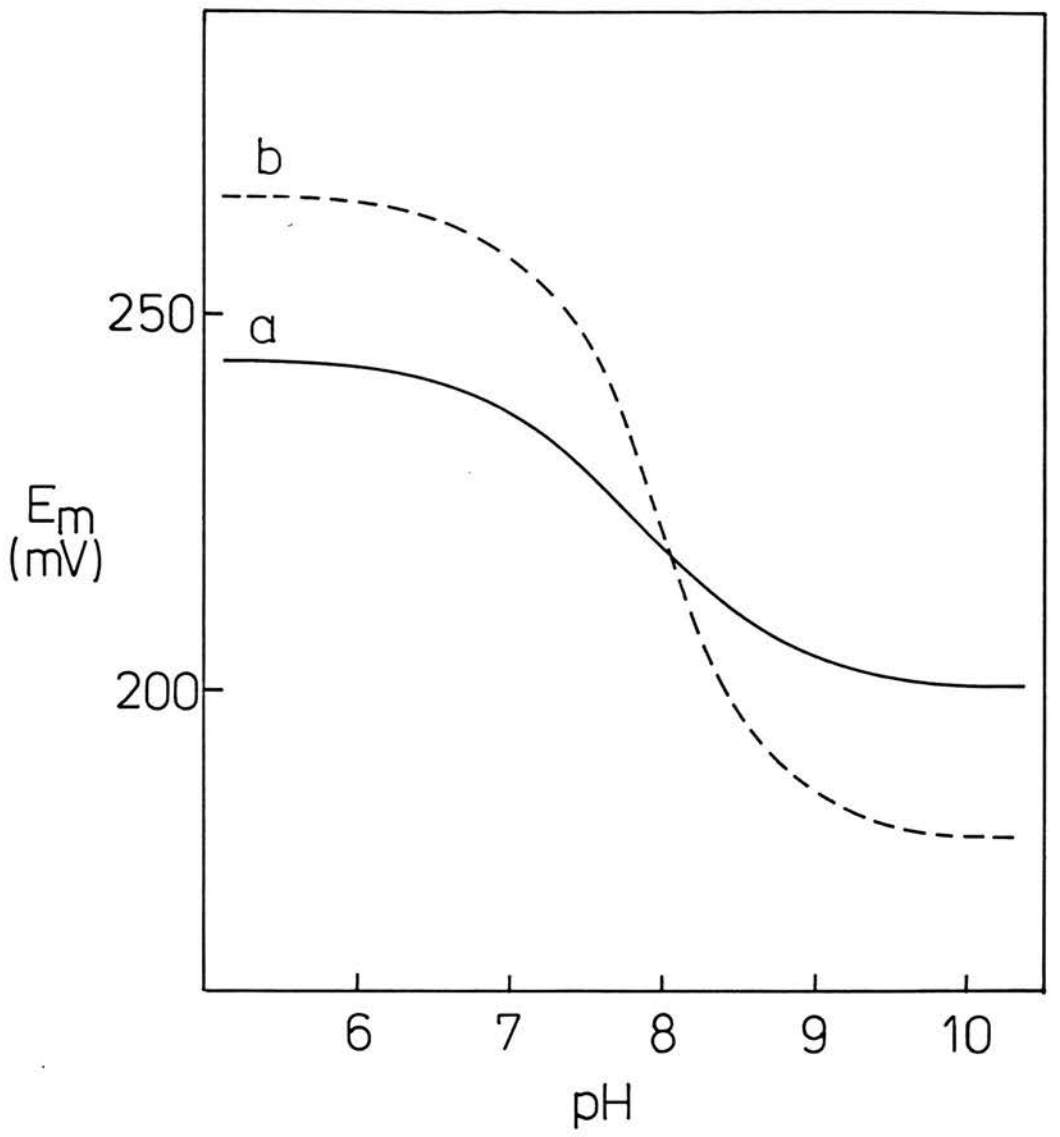

Figure 65: E_m versus pH Curves for Ionisations Involving One and Two Protons

(a) One proton case: the theoretical curve was constructed using Equation 2 and pK_O = 7.6 and pK_R = 8.3. (b) Two proton case: the theoretical curve was constructed using Equation 4 and the same pKs as in (a).

introduces a level of complexity that can be avoided by thinking in terms of a one proton scheme.

Several different possibilities exist for hydrogen bonds involving one proton, of which only two are shown in Figure 64. In (B), the proton to be lost is involved in the hydrogen bond. In (C), the proton lost is not involved in the hydrogen bond, but as a result of the histidine deprotonation, the proton in the hydrogen bond is attracted more strongly to the histidine. In this respect the latter scheme is analogous to the currently accepted form of the His-Asp-Ser catalytic triad of the serine proteases (Bachovchin et al., 1981; Steitz & Shulman, 1982). With the composite schemes (B) and (C) both groups carry a partial charge at low pH, but following loss of a proton, fully charged propionate and neutral histidine are generated. The use of the word "ionisation" to describe the events occurring at pK_O/pK_R is inappropriate in this context (especially since histidine is neutral above the pK) and "deprotonation" is used in preference.

An attempt was made to distinguish which of schemes (B) and (C) operate in P. stutzeri cytochrome c_{551}. Robillard & Shulman (1972, 1974) observed a broad resonance at low field (17.25 ppm)in the ^1H NMR spectrum of chymotrypsin in H_2O, which they assigned to the Asp-His hydrogen bonded proton. This resonance persisted in the spectrum over the pH range 5-9.5 but shifted to a new upfield position with pK=7.5. A -NH proton resonance is observed in H_2O only when its rate of exchange with H_2O is slowed sufficiently for it to be observed - this means a residence time of >3 msec, which is likely if the proton in question is hydrogen-bonded. If a low-field resonance could be observed to titrate with the appropriate pK values in the NMR spectrum of P. stutzeri cytochrome c_{551} in H_2O, then it is likely that scheme (C) operates; the resonance would be expected to disappear at alkaline pH if scheme (B) obtained. However, a single

attempt to do this experiment showed no sign of a low-field titratable resonance, so nothing further could be deduced on the precise nature of the hydrogen bonding scheme.

Possible interactions between chemically modified His47 and propionic acid-7 are shown in (D) and (E) of Figure 64. Modification ensures that His47 is neutral above pH4. Since the NMR pH titration data indicated that His47 resonances are unaffected by ionisation of the propionic acid in modified cytochrome c_{551} then scheme (E) is the more likely. The presence of an ethoxyformyl group on His47 may sterically hinder the formation of a hydrogen bond.

2. Interaction of Propionic Acid-7 with Amino Acid 47 in Other Cytochromes c-551

P. stutzeri 221 cytochrome c_{551} and *P. aeruginosa* cytochrome c_{551} show markedly different E_m versus pH profiles, the pK_O and pK_R values of the latter being lower by about 1 pH unit. In both cytochromes, however, it appears that propionic acid-7 becomes deprotonated with a redox state dependent pK and that this event is partially or wholly responsible for the fall in redox potential at alkaline pH (see Section 5 below). It seems not unreasonable, then, to propose that ionisation of propionic acid-7 is responsible for the pH dependence of E_m of all the cytochromes c_{551} discussed in Chapter IV. If this is so then it is pertinent to ask why the pK values of propionic acid -7 should vary so much between the cytochromes. The unusual interaction of His47 with the propionic acid in *P. stutzeri* 221 cytochrome c_{551}, and the effect that chemical modification of His47 had upon pK_O and pK_R for this cytochrome, suggested that the amino acid at sequence position 47 in the cytochromes c_{551} might be important in modulating the pK values at which propionic acid-7 ionises. With this as a working hypothesis, it was hoped that values of pK_O and pK_R could

be predicted simply by considering the identity of amino acid 47. For instance, it might be expected that A. vinelandii cytochrome c_{551}, which has Lys47, will show similar pK values to P. aeruginosa cytochrome c_{551}.

Table XII summarises the pK_O and pK_R values observed for each cytochrome and the amino acid at position 47 in the sequence. Data are also included for the more distantly related cytochrome c_{555} from C. thiosulphatophilum which contains His37 at a position sequentially analogous to residue 47 of the cytochromes c_{551}.

If amino acid 47 does influence the pKs at which propionic acid -7 ionises then the following comments can be used as a guide to predicting pK_O and pK_R values. (i) All cytochromes which contain His47 should show similar pKs to those observed for P. stutzeri 221 cytochrome c_{551}. (ii) Given that P. stutzeri cytochrome c_{551} pKs are raised through an unusual hydrogen bonding interaction with His47 then it is predicted that the propionic acid pKs will be lower in all cytochromes in which His47 is substituted by another amino acid. (iii) Substitution by Arg or Lys may additionally tend to favour a lower pK for propionic acid-7 in both oxidation states, since the positive charge carried by these amino acids will stabilise the propionate anion. In instances where His47 is replaced by an uncharged but hydrogen bonding amino acid the pKs are more difficult to predict since their values will depend on the type of hydrogen bonding interaction formed.

The separation of pK values between the two oxidation states, ΔpK_{R-O}, is also of interest. This number is expected to be ca. 1 for all cytochromes, the rationale being that if it is the same group which ionises in all the cytochromes (i.e. propionic acid-7) then, given their structural homology, the redox state imposed separation of its pK values should be similar in each cytochrome.

Table XII: Summary of pK and ΔpK Values for Cytochromes c-551

Source of Cytochrome c_{551}	Residue 47	Residue 56	pK_O	pK_R	ΔpK_{red-ox}
P. aeruginosa	Arg	Trp	6.2	7.3	1.1
P. stutzeri 221	His	Trp	7.6	8.3	0.7
P. stutzeri 224	His	Trp	7.8	8.45	0.65
P. mendocina	His	Trp	7.2	8.0	0.8
P. denitrificans	Ser	Trp	6.4	6.75	0.35
A. vinelandii	Lys	Trp	5.8	6.2	0.4
C. thiosulphatophilum cytochrome c_{555}			6.3	7.0	0.7

The above considerations do not unfortunately lead to consistently successful prediction either of pK values or of ΔpK. As Table XII shows, *A. vinelandii* cytochrome c_{551} has quite different pKs from *P. aeruginosa* cytochrome c_{551} despite the seemingly conservative substitution of Lys for Arg; more strikingly, though, ΔpK is reduced from 1.1 to 0.35 by this substitution. *C. thiosulphatophilum* cytochrome c_{555} has low pKs compared to the *P. stutzeri*/*mendocina* cytochromes, despite NMR data which indicates that a similar type of interaction occurs between His37 and propionic acid-7 in this cytochrome. Additionally, ΔpK is considerably less than 1 for *P. denitrificans* cytochrome c_{551}; this value is similar to that observed for the *A. vinelandii* cytochrome, despite the fact the *P. denitrificans* cytochrome c_{551} has Ser47 and the *A. vinelandii* cytochrome contains Lys.

On the other hand, *P. stutzeri* 221, *P. stutzeri* 224 and *P. mendocina* cytochromes c_{551} show similar pKs, as expected if they all contain His47, and these three cytochromes, as well as *C. thiosulphatophilum* cytochrome c_{555}, show approximately the same value of ΔpK. Although cytochrome c_{555} pKs are lower than expected on the basis that His37 interacts with propionic acid-7 in an analogous way to His47 in *P. stutzeri*/*P. mendocina* cytochromes c_{551}, this may be a consequence of a rather different tertiary structure in the region of propionic acid-7 (the X-ray structure of this cytochrome has not yet been solved at sufficiently high resolution to allow detailed structural comparisons with *P. aeruginosa* cytochrome $_{551}$).

Thus the identity of amino acid 47 does not *per se* allow successful prediction of pK values. Three cytochromes clearly do not behave as expected *viz.* *C. thiosulphatophilum* cytochrome c_{555} (because its pKs are lower than predicted) and *A. vinelandii* and *P. denitrificans* cytochromes c_{551} (because ΔpK is

anomalously small). Although the cytochrome c_{555} pKs can be rationalised in terms of structural differences, ΔpK observed for the A. vinelandii and P. denitrificans cytochromes c_{551} is so different as to suggest some redox state dependent ionisation other than that of propionic acid-7 in these proteins (see below). However, the identity of amino acid 47 in these two cytochromes does not reveal why propionic acid-7 should not ionise.

ΔpK may be influenced by two factors (i) distance of the ionising group from the haem (ii) relative stabilisation of the ion in the ferri- and ferrocytochrome - neighbouring charged groups might provide additional stabilisation of the ion in both oxidation states and thus mask the redox state imposed separation of pKs. In the limited context of the six homologous cytochromes discussed above (cytochrome c_{555} excluded) ΔpK is not expected to vary much for the former reason, since propionic acid-7 occurs essentially at a fixed distance from the haem (although different orientations relative to the haem are possible). The latter reason may go some way towards explaining differences in ΔpK, but it is possible that the particularly low values observed for the A. vinelandii and P. denitrificans cytochromes are explained by the fact that it is not propionic acid-7 which ionises. In Section 5 below it is proposed that in these two cytochromes a histidine residue is deprotonated with redox state dependent pKs; the small ΔpK value would thus be explained by the relative remoteness of histidine from the haem compared to propionic acid-7.

3. Ionisations Affecting Redox Potential in the Cytochromes c-2 and Mitochondrial Cytochromes c

The work described above has shown that the ionisation states of propionic acid-7 and a histidine residue influence the redox potential of the cytochromes c_{551}. As mentioned in the Introduction, the Pseudomonas

cytochromes c_{551} differ from their larger mitochondrial and bacterial homologues (*viz.* the cytochromes c_2) mainly through deletion of a loop of polypeptide which shields the bottom of the haem crevice. Although there is some compensatory polypeptide chain rearrangement to close off the haem crevice, more of the haem is left exposed to solvent in the cytochromes c_{551} than in the bigger proteins. Propionic acid-6 and (to a lesser extent) propionic acid-7 are relatively accessible to solvent for this reason. The question then arises as to whether the pH *in*dependence of redox potential observed for some of the bacterial cytochromes c_2 and the mitochondrial cytochromes might be a consequence of the fact that propionic acid -7 is buried in these proteins and cannot ionise over the physiological pH range. If this were the case, however, an explanation would be required for why a few cytochromes c_2 and, as will be seen, two mitochondrial cytochromes c, have pH *dependent* redox potentials. One possibility is that a histidine residue ionises with redox state dependent pKs.

Cytochromes c-2: On page *33*, the cytochromes c_2 were discussed in terms of those which show a Type 1 redox potential versus pH curve and those which have a Type 2 curve. The midpoint potentials of cytochromes showing Type 1 curves are essentially independent of pH over the physiological pH range since pK_{O2} is generally ca. 8.5 or greater. For those cytochromes which show a Type 2 curve (i.e. pK_{O1}, pK_R, pK_{O2}) two subgroups can be distinguished - the first group has $\Delta pK_{R-O1} \simeq 1$ and the second has $\Delta pK \simeq 0.4$. *R. rubrum* and *Rm. vannielii* cytochromes c_2 belong to the first of these subgroups, and *Rps. sphaeroides*, *Rps. palustris* and *Rps. viridis* cytochromes c_2 belong to the second.

Pettigrew et al. (1978) proposed that for the cytochromes with Type 2 curves pK_{O1} and pK_R arise from the redox state dependent ionisaton of propionic acid-7. In Type 1 cases, the presence of a nearby arginine

residue (Arg38) was proposed to stabilise the negative charge produced by ionisation of propionic acid-7 and to thereby mask the redox state imposed separation of its pK value. These proposals were based on the observation that the absence of Arg38 in two of the cytochromes with Type 2 curves (R. rubrum and Rm. vannielii cytochromes) was associated with the most pronounced separation of pK_{O1} and pK_R. However, there are cytochromes c_2 which contain Arg38 but also show Type 2 curves. Subsequently obtained data showing that propionic acid-7 does not ionise in Rps. viridis cytochrome c_2, which has a pH dependent redox potential, led us to modify the proposals made by Pettigrew et al. as follows: (i) the presence of Arg38 in a cytochrome will cause propionic acid-7 to ionise with very low pKs (<5, say) (ii) in R. rubrum and Rm. vannielii cytochromes, which lack Arg38, propionic acid-7 ionises at more typical pK values ($pK_O \sim 6$, $pK_R \sim 7$) (iii) in cytochromes which show Type 2 curves but which contain Arg38, the species which ionises with redox state dependent pKs is His39. (This work is described in Moore et al., 1984 - see Appendix II.)

Thus, in NMR spectra of R. rubrum and Rm. vannielii cytochromes c_2, where Arg 38 is replaced by Gln or Asn, the propionic acid resonances are expected to have pH dependent chemical shifts. In NMR spectra of all other cytocromes c_2 which contain Arg38, propionic acid resonances are expected to have pH independent chemical shifts; however, for Rps. viridis and Rps. globiformis cytochromes c_2, which have histidine at sequence position 39, resonances of His39 should titrate with the pK_O and pK_R values observed in the corresponding E_m versus pH curve. Figure 66 shows the ^1H NMR spectra obtained for Rm. vannielii and Rps. capsulata ferricytochromes c_2 at various pH values. Resonances marked P1, P2 and P3 have been assigned by Moore to the propionic acid groups of these cytochromes. For Rm. vannielii cytochrome c_2 they shift with $pK_O^* = 6.3$. As anticipated, their chemical

shifts are not affected by pH in the Rps. capsulata cytochrome.

NMR spectra of the His39 containing cytochrome, Rps. viridis cytochrome c_2 showed the His resonances titrating with $pK^* = 6.8$ in the ferricytochrome and $pK^* = 7.1$ in the ferrocytochrome. The chemical shifts of the propionic acid resonances were independent of pH (data of G. Moore). In order to confirm that the redox state dependent ionisation of His39 does indeed influence the redox potential of this and other His39 containing cytochromes, an attempt was made to chemically modify His39 with ethoxyformicanhydride. The effect of histidine modification on the redox potential of Rps. viridis cytochrome c_2 is shown in Figure 67 (data of F. Leitch). If the redox state dependent ionisation of His39 is the cause of the pH dependence of E_m observed between pH5 and 9, then modification of His39 is expected to abolish the pH dependence. Although ΔpK_{R-O1} is small for the unmodified cytochrome (i.e. the fall in E_m is not very pronounced), it is clear from Figure 67 that ethoxyformylation of His39 eliminates pH effects on E_m below pK_{O2}.

Our conclusions from this joint work can be summarised as:

Cytochrome c-2	Sequence	E_m vs. pH Curve	Ionisation
R. capsulata	-Arg38-Thr39-	Type 1	none
Rps. viridis	-Arg38-His39-	Type 2	His39
Rm. vannielii	-Gln38-Lys39-	Type 2	propionic acid

Thus from the identity of amino acids 38 and 39 in the sequence of any cytochrome c_2 it ought to be possible to predict those cytochromes which will have Type 2 E_m versus pH curves. However there is an additional level of complexity: some cytochromes, for example, Rps. sphaeroides cytochrome c_2, contain Arg38 but not His39 and yet show Type 2 curves. Such cytochromes contain at

Figure 66: ^{1}H NMR Spectrum of Rps. capsulata and R. vannielii Ferricytochromes c-2 at Various pH Values

(a) Rps. capsulata ferricytochrome c_2; (b) R. vannielii cytochrome c_2. The labelled resonances are: S = methionine ligand methyl resonance, M1-M4 = Haem methyl resonances, P1-P3 = 1-proton resonances proposed to come from haem propionic acids. [Data of G. Moore.]

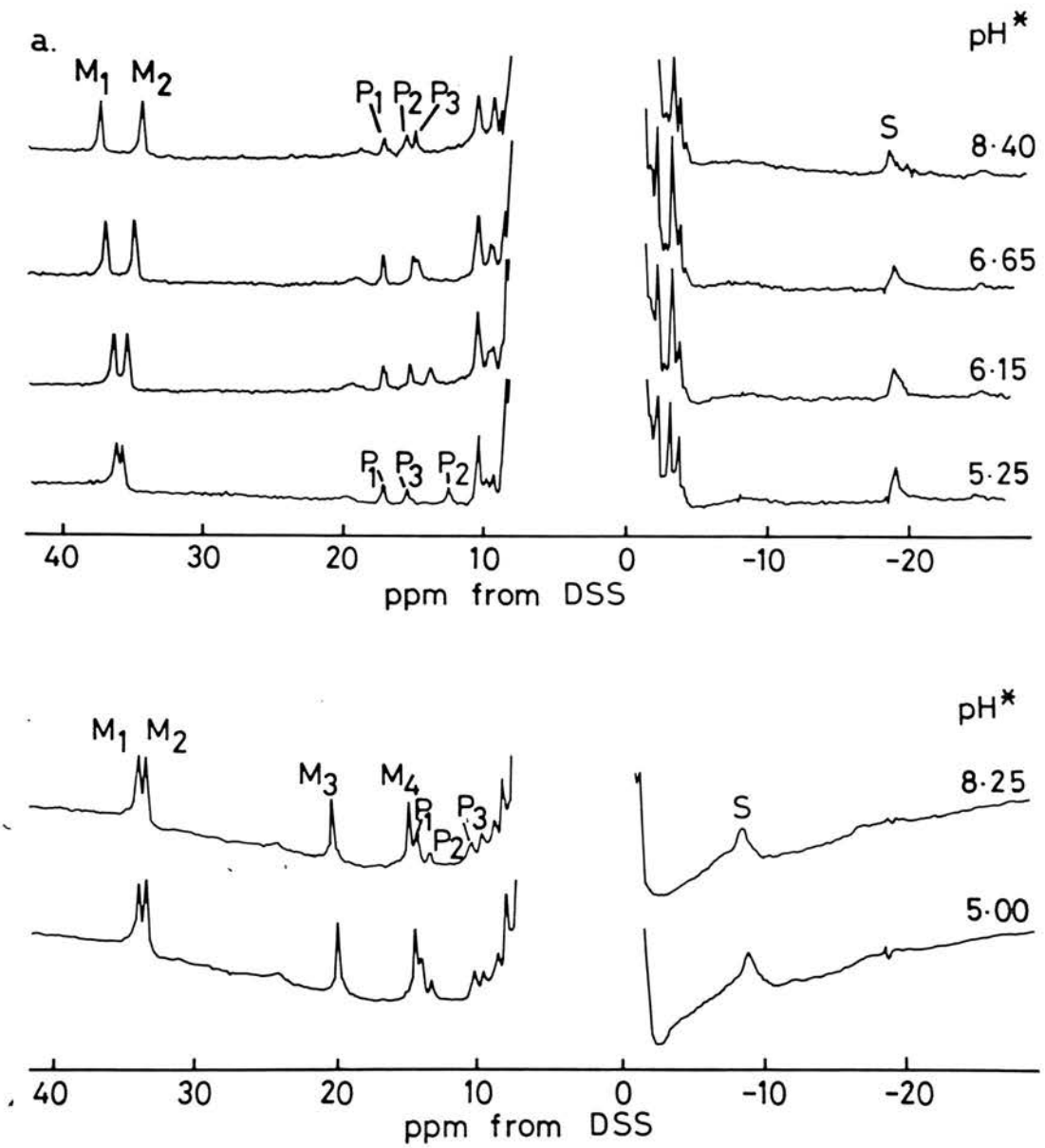
a.
pH*
M1 M2
P1 P2 P3
S
8·40
6·65
6·15
P1 P3 P2
5·25
40 30 20 10 0 -10 -20
ppm from DSS
pH*
M1 M2
M3
M4
P1 P3
P2
S
8·25
5·00
40 30 20 10 0 -10 -20
ppm from DSS

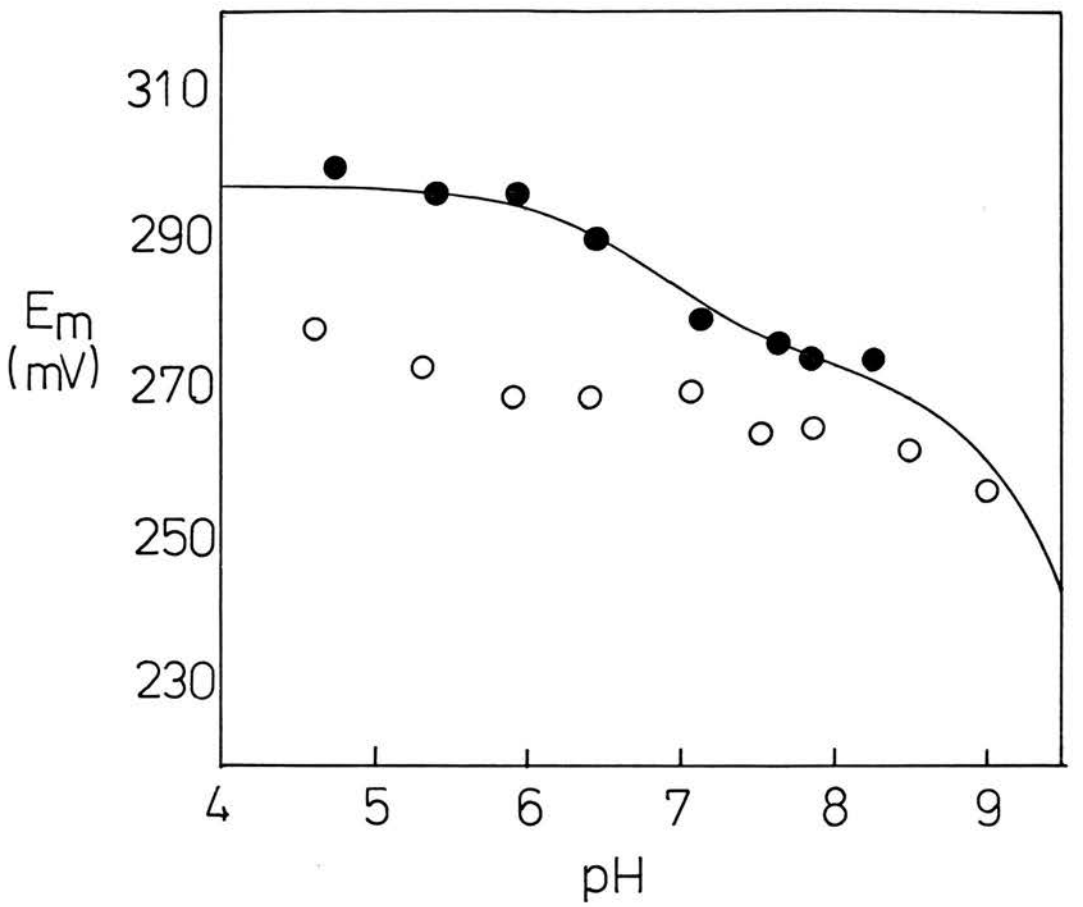

Figure 67: The Effect of Histidine Modification on the pH Dependence of Redox Potential of Rps. viridis Cytochrome c-2

● Midpoint potential determined before modification with ethoxyformic anhydride; the solid line is the theoretical curve obtained from Equation 3 using pK_{O1} = 6.7, pK_R = 7.1 and pK_{O2} = 9.2. ○ Midpoint potential determined after modification of His39 with ethoxyformic anhydride.

least one unliganded histidine residue (His75, His111 in Rps. sphaeroides cytochrome c_2) which may well ionise with redox state dependent pKs, although this has not yet been demonstrated. On the other hand, there are cytochromes which contain unliganded histidine residues (apart from His39) and show Type 1 curves. Therefore, Type 2 curves can be successfully predicted only if Arg38 is absent or His39 is present.

Mitochondrial cytochromes c: The mitochondrial cytochromes c are more closely related in sequence to the cytochromes c_2 than to any other group of bacterial cytochromes; indeed, some cytochrome c_2 sequences show more homology with mitochondrial cytochromes than with other members of the cytochrome c_2 group. In view of this structural continuum between the two cytochrome classes, some of the comments made on the nature of ionising groups in the cytochromes c_2 should be applicable to the mitochondrial cytochromes.

All the cytochromes c which have been sequenced (some 70 or so) contain Arg38, and the few which have been studied by redox potentiometry show Type 1 E_m versus pH curves. We predicted that any mitochondrial cytochrome which contains His39 should show a Type 2 E_m versus pH curve. Only three cytochromes have histidine at sequence position 39, viz. Saccharomyces cerevisae, Candida crusei and Crithidia oncopelti cytochromes c. Figure 68 shows the E_m versus pH curves obtained for the S. cerevisae and C. oncopelti cytochromes (data of G. Pettigrew and F. Leitch). Both are Type 2. The dotted lines have been drawn to emphasize the effect of pK_{O1} and pK_R on the redox potential of each cytochrome; since ΔpK_{R-O1} is small, the drop in potential between the two pKs is not very marked and it is largely obscured by the proximity of pK_{O2} to pK_R. Redox potential measurements have not yet been made on the C. crusei cytochrome.

In conclusion: For the mitochondrial cytochromes c and the photosynthetic bacterial cytochromes c_2, the

Figure 68: pH Dependence of Redox Potential for Mitochondrial Cytochromes

(a) S. cerevisae cytochrome c; the solid line is a theoretical curve constructed from Equation 3 with pK_{O1} = 6.9, pK_R = 7.3 and pK_{O2} = 8.3 (data of F. Leitch). (b) C. oncopelti cytochrome c_{557}; the solid line is a theoretical curve constructed from Equation 3 with pK_{O1} = 6.6, pK_R = 7.0 and pK_{O2} = 8.0 (data of G. Pettigrew). The broken line in (a) is for a single ionisation with pK_{O2} = 7.85; in (b) the broken line is for a single ionisation with pK_{O2} = 7.55.

A.

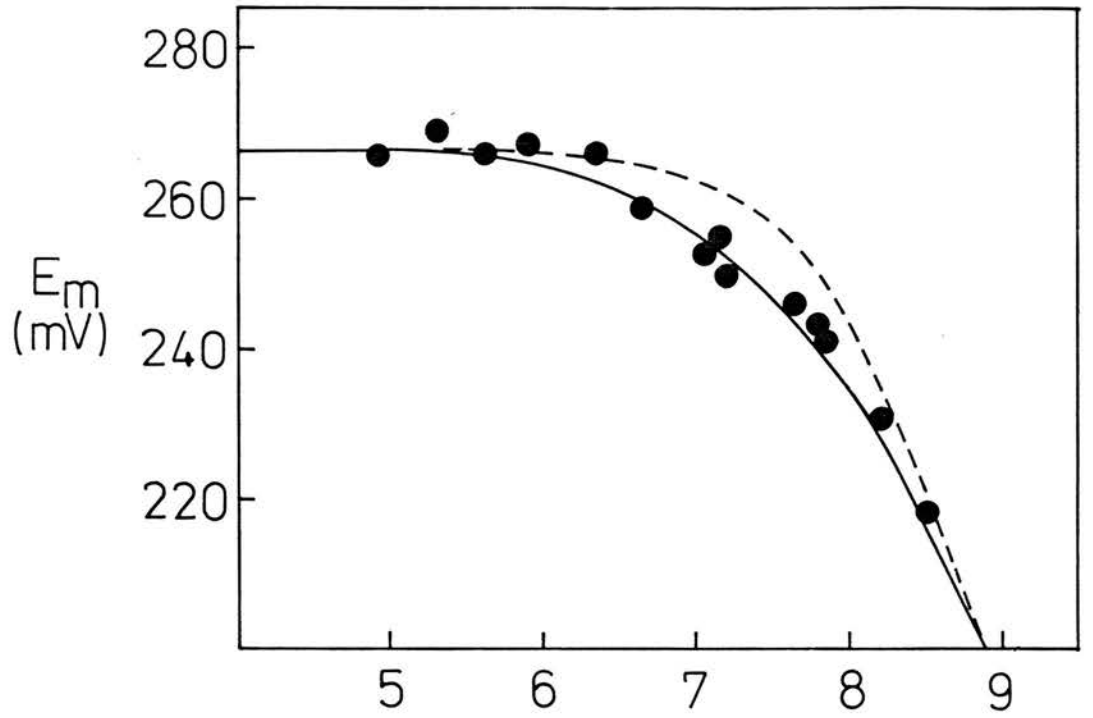

B.

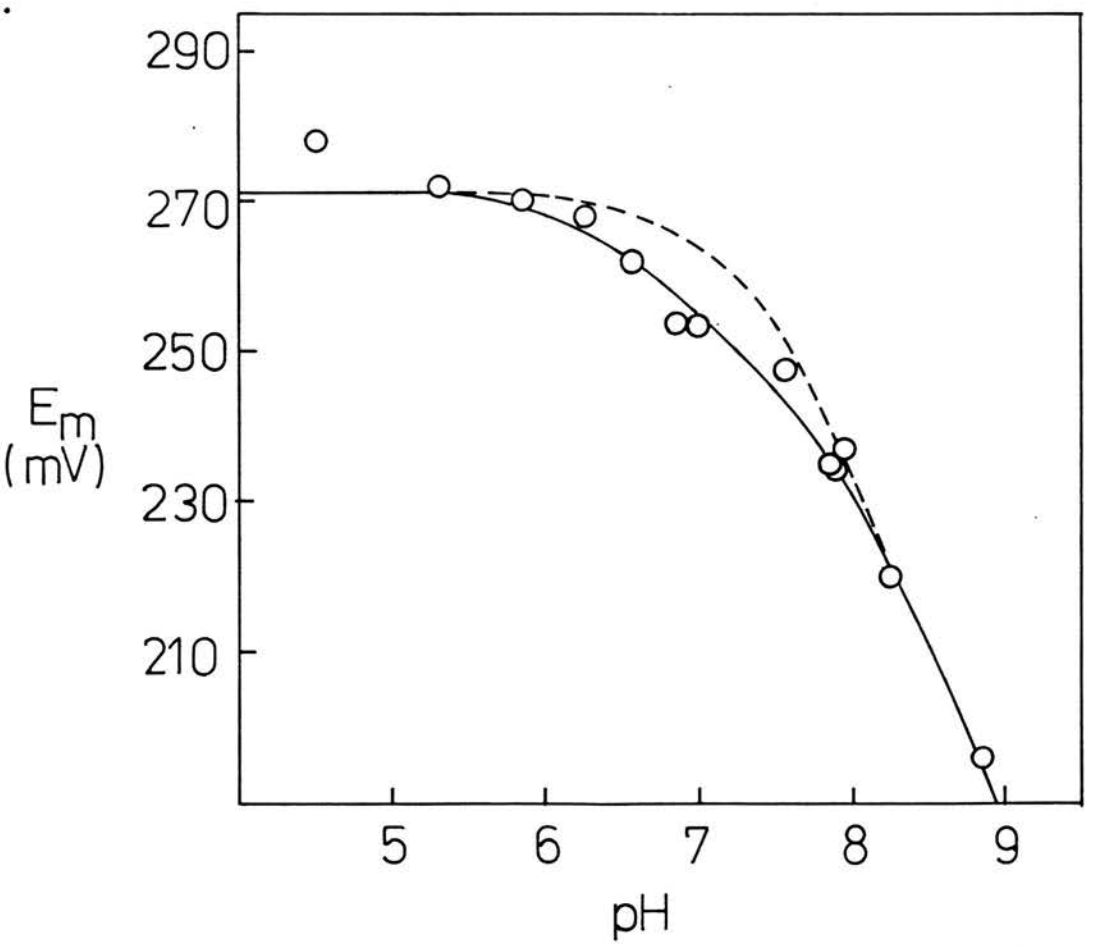

presence of Arg38, which is adjacent to propionic acid-7, causes the propionic acid to ionise with low pKs. For those cytochromes which show pKs within the physiological pH range, the ionising group is (i) propionic acid-7, in cases where Arg38 is substituted by Asn or Gln (ii) His39, when present in the sequence, or (iii) an unliganded histidine residue other than His39. It should be possible to predict the type of E_m versus pH curve expected for most cytochromes c/c_2 simply by considering the amino acids occurring at sequence positions 38 and 39. It is not however possible to predict the cases where an unliganded histidine residue other than His39 will affect redox potential - for example, neither His26 nor His33 in horse cytochrome c have redox state dependent pKs, yet His49 in Rps. palustris cytochrome c_2 apparently does.

4. Summary of Ionisations Affecting Redox Potential

Table XIII summarises pK_O (or pK_{O1}), pK_R and ΔpK values for the various cytochromes discussed above which show pH dependence of redox potential between pH5 and 8.5. The nature of the group ionising at pK_O (or pK_{O1}) and pK_R has been established in the cases indicated (*) and is predicted for the rest. For all the cytochromes, Δ pK assumes one of three values, approx. 0.4, 0.7 or 1. Each of these three values is typically associated with one type of ionisation viz. histidine ($\Delta pK \simeq 0.4$), propionic acid ($\Delta pK \simeq 1$) or histidine + propionic acid ($\Delta pK \simeq 0.7$).

Only for Rps. viridis cytochrome c_2 has the ionisation of histidine been experimentally established as the sole redox state dependent ionisation. However, in view of our successful prediction of pH dependent redox potentials for the C. oncopelti and S. cerevisiae cytochromes, His39 is almost certainly the ionising group in these cases also. Rps. sphaeroides cytochrome c_2 and P. denitrificans and A. vinelandii cytochromes c_{551} are

Table XIII: Summary of Ionisations Which Affect Redox Potential.

Cytochrome	pK_O	pK_R	ΔpK	Ionising Group
[1]*S. cerevisae* cyt c	6.9	7.3	0.4	histidine
[1]*C. oncopelti* cyt c_{557}	6.6	7.0	0.4	histidine
[2]*Rps. sphaeroides* cyt c_2	6.1	6.4	0.3	histidine
[3]*Rps. viridis* cyt c_2	6.7	7.1	0.4	histidine*
P. denitrificans cyt c_{551}	6.4	6.75	0.35	histidine
A. vinelandii cyt c_{551}	5.8	6.2	0.4	histidine
C. thiosulphatophilum cyt $_{555}$	6.3	7.0	0.7	histidine + propionic acid*
P. stutzeri 221 cyt c_{551}	7.6	8.3	0.7	histidine + propionic acid*
P. stutzeri 224 cyt c_{551}	7.8	8.45	0.65	histidine + propionic acid
P. mendocina cyt c_{551}	7.2	8.0	0.8	histidine + propionic acid*
[3]*R. rubrum* cyt c_2	6.2	7.0	0.8	propionic acid
[2]*Rm. vannielii* cyt c_2	6.3	7.4	1.1	propionic acid*
[4]*P. aeruginosa* cyt c_{551}	6.2	7.3	1.1	propionic acid*

*Ionising group has been established experimentally. pK_O and pK_R values were obtained from: (1) Moore et al. (1984), (2) Pettigrew et al. (1975), (3) Pettigrew et al. (1978), (4) Moore et al. (1980).

proposed to have ionising histidine residues solely on the basis that their ΔpK values are ~0.4. Rps. sphaeroides cytochrome c_2 contains 2 unliganded histidine residues (His75, 111) and P. denitrificans and A. vinelandii cytochromes c_{551} each contain 1 (His43 and His81, respectively), so the proposal is at least feasible. In the case of the cytochromes c_{551}, the presence of an ionising histidine group is particularly questionable in view of the fact that propionic acid-7 ionises in the other Pseudomonas cytochromes studied. Although His43 in P. denitrificans cytochrome c_{551} is quite close to the haem, His81 in A. vinelandii cytochrome c_{551} occurs at the end of the C-terminal helix and is as remote from the haem as it conceivably could be. That both cytochromes show the same ΔpK value is therefore rather surprising. In the absence of any NMR data on these two cytochromes c_{551}, the assignment of pK_O and pK_R to histidine must remain highly speculative.

For the cytochromes which have ΔpK~0.7, it has been shown that histidine and propionic acid-7 are both deprotonated with the same pKs. The fact that ΔpK is less than pK for propionic acid-7 ionisation but greater than pK for histidine ionisation is consistent with a complex deprotonation event involving both species.

Finally, the largest ΔpK values, and so the most pronounced effects on E_m, are observed for cytochromes in which propionic acid-7 ionises. It is not intended here that the apparent link between ΔpK and the nature of the ionising group should be over-emphasized. As has been discussed already, ΔpK reflects not only the nature of the ionising group but also its distance from the iron and the degree of charge shielding it experiences. The next section gives a physical explanation for how propionic acid and histidine ionisations affect E_m and discusses on a more quantitative basis the reason why histidine ionisations affect E_m to a lesser extent.

5. The Structural Basis for pH Effects on Redox Potential

The redox potential of any system is a measure of its ability to accept (or donate) electrons. A compound with a high redox potential is a good electron acceptor (poor electron donor), which essentially means that the system has a greater tendency to exist in its reduced state than its oxidised state. In structural terms, this means that the reduced form is stabilised relative to the oxidised form. Thus the redox potential of a system can be viewed in terms of the relative stabilities of its two redox forms.

The general shapes of the different types of E_m versus pH curve have already been discussed in terms of ionisable groups which influence redox potential but, as yet, no mention has been made of how mechanistically these ionisations perturb E_m.

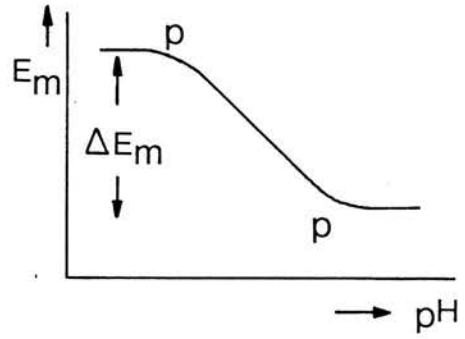

For Type 2 curves, for instance, it would be useful to explain in structural terms the fall in E_m between pK_{Ol} and pK_R. A decrease in E_m could be explained, on the basis of the foregoing discussion, by a relative stabilisation of the ferricytochrome with respect to the ferrocytochrome. Since ferrous haem c carries 0 net charge (protoporphyrin IX being a dianion) whereas ferric haem c carries a net charge of +1 then the electrostatic interaction of ionisable groups with the haem may contribute to the relative stabilisation of one cytochrome oxidation state over the other. Thus, for cytochromes in which propionic acid-7 ionises, a fall in redox potential will occur because the propionate anion

preferentially stabilises the ferricytochrome structure through electrostatic interaction with the positively charged ferric haem. In those cytochromes where histidine ionises, loss of the histidine proton at alkaline pH will also tend to stabilise the ferricytochrome (or, vice versa, the presence of the imidazolium cation at acidic pH will tend to destabilise the ferricytochrome with respect to the ferrocytochrome).

Moore (1983) showed that for those cytochromes in which propionic acid-7 ionises, the propionic acid-7: ferric haem electrostatic energy of interaction, calculated from ΔE_m, agrees with values predicted using Coulomb's law.

$\Delta G_{el}(emp)$, the empirical electrostatic interaction free energy, can be calculated from

$$\Delta G_{el}(emp) = -nF\Delta E_m$$

ΔE_m is the difference in redox potential between fully protonated and fully deprotonated states. For Rm. vannielii cytochrome c_2 and P. aeruginosa cytochrome c_{551}, for example, ΔE_m is 65 mV. If this value is used in the above equation, $\Delta G_{el}(emp)$ is computed to be $-6.27 kJ.mol^{-1}$.

A theoretical electrostatic interaction free energy, $\Delta G_{el}(theor)$, is calculated from Coulomb's law,

$$\Delta G_{el}(theor) = \frac{1347\ q_1.q_2}{\epsilon.D} \qquad kJ.mol^{-1}$$

where q_1 is the charge on the haem iron (0 or +1 net), q_2 is the charge on the propionic acid (0 or -1), D is the distance between charges, in Å, and ϵ is the effective dielectric constant. D is in the order of 10-15Å for the haem iron-propionate distance in these cytochromes; while the value of ϵ is uncertain Moore has shown that for a charge product of -1, ϵ values in the range 10-40 give $\Delta G_{el}(theor)$ values of -13.5 to -2.2 $kJ.mol^{-1}$.

Thus, the experimentally determined interaction free

energy (ΔG_{el}[emp]), obtained from ΔE_m, falls within the range of theoretical (ΔG_{el}[theor]) values calculated above using likely numbers for ϵ. An implicit assumption in both types of calculation is that no conformational change is associated with the fall in E_m, an assumption which appears to be justified since the theoretical and measured values agree well. (However, considerable uncertainty necessarily surrounds the range of ΔG(theor) values calculated given that ϵ is not a measurable quantity.) These data can therefore be taken as evidence that electrostatic interactions between ferric haem c and its propionic acid side chains can influence the redox potential of cytochromes.

For those cytochromes in which a histidine residue (only) ionises, ΔE_m values are consistently smaller than for cytochromes where propionic acid-7 ionises. With Rps. viridis cytochrome c_2, ΔE_m is 23 mV and the corresponding ΔG_{el}(emp) value is -2.22 kJ.mol^{-1}. Consideration of the Coulomb's law equation indicates that larger values of either D or ϵ, or both, would account for a lower value of ΔG_{el}(emp). As Moore has pointed out, the ionisable histidine residue in these cytochromes probably occurs near the molecular surface in all cases, so D is certainly likely to be larger than for the propionic acid-7: iron interaction; by the same token, however, ϵ is also likely to be greater if a surface residue is involved.

For the four cytochromes where it is proposed that a partially charged histidine and partially charged propionic acid-7 exist below pK_o, ΔE_m is 40-45 mV, and ΔG_{el}(emp) 3.86-4.34 kJ.mol^{-1}. Like cases where propionic-7 alone ionises, 1 full charge is associated with the deprotonation event. However, ΔG_{el}(theor) may be different in the two situations because the terms D and ϵ are different.

(cont.)

6. Biological Considerations

(i) Do the pKs occur in vivo?

Brandt et al. (1966) showed that the pK_O of 9 observed in the E_m versus pH curve of horse cytochrome c (see page 30) can be considered to result from an ionisation with pK=11 and a coupled conformational change with pK=-2. In a similar way, Prince & Bashford (1979) showed that the pK_{O2} of 8.0 observed in the E_m versus pH curve of Rps. sphaeroides cytochrome c_2 is a composite pK resulting from an ionisation occurring with pK>11 and a slow coupled conformational change. In the case of Rps. sphaeroides cytochrome c_2 Prince & Bashford claim that the conformational change is suppressed upon binding of the cytochrome to chromatophore membranes and that the redox potential in vivo is independent of pH between 7 and 11. However, it should be stressed here that the studies of Brandt et al. and Prince & Bashford are concerned with the "695 band pK" which occurs at alkaline pH in all Class I c-type cytochromes. Since this pK is associated with loss of the 695nm absorption band from ferricytochrome spectra, it has been attributed to breakage of the iron-methionine bond (see page 30). It clearly has a different origin from the pKs occurring between pH5 and 8 in the cytochromes considered above (since these pKs do not affect the 695nm band) and so it has not been discussed hitherto.

We carried out an analysis of the pKs observed for Rm. vannielii cytochrome c_2 (pK_{O1}=6.3, pK_R=7.4, pK_{O2}=9.4). In a series of pH jump experiments, solutions of the ferricytochrome in ferricyanide at pH5 were rapidly reduced with buffers containing ferrocyanide. For final pH values below pH8.5 the kinetics of reduction were fast and monophasic, but above pH8.5 the kinetics of reduction were biphasic with an initial rapid reduction being followed by a much slower oxidation. With the latter measurements, E_m calculated at the end of the fast phase was higher than E_m calculated at the end of the

slow phase; at pH9.6, for instance, the two values differed by ca.20mV (work described in Moore et al., 1984 - see Appendix II). The biphasic kinetics observed above pH8.5 indicate that a slow conformational change affects redox potential at alkaline pH; E_m calculated at the end of the fast phase is higher because measurement was made before the conformational change took place. Thus pK_{O2} is associated with a conformation change but pK_{O1} and pK_R are not.

Although suppression of the 695nm band pK in vivo could be a widespread phenomenon amongst the c-type cytochromes, given that they all interact closely with a coupling membrane, it is the pKs which occur between pH5 and 8 (and do not involve a conformational change) that may be of physiological importance. Considerable effort has been expended (by this author) in trying to assess whether the P. aeruginosa cytochrome c_{551} pKs occur under in vivo conditions i.e. when bound to a membrane. Two types of experiment were attempted, which involved binding cytochrome c_{551} either to artificial phospholipid membranes or to washed P. aeruginosa respiratory membranes. All attempts to bind the cytochrome to phospholipid membranes were unsuccessful, probably because this cytochrome, like most bacterial cytochromes, has an acidic isoelectric point and will experience charge repulsion from the negatively charged phospholipid vesicles. Binding experiments with respiratory membranes proved to be impracticable since the membranes contain an integral cytochrome which absorbs at the same α-band maximum as cytochrome c_{551} (redox potential measurements rely on being able to estimate spectrophotometrically the extent of cytochrome c_{551} reduction). In this context it is appropriate to point out that Prince & Bashford (1979) also claim that pK_{O1} and pK_R (as well as pK_{O2}) of Rps. sphaeroides cytochrome c_2 are not observed for the cytochrome bound to chromatophore membranes - their redox potential analyses, however, overlook the presence of a

cytochrome in the chromatophore membrane which absorbs at 550nm (see page 6), and their data are therefore incorrect. Thus, the question of whether such pKs affect the redox potential of cytochromes *in vivo* remains open.

Unlike the 695nm band pK, where it is easy to envisage that binding to a membrane could could suppress a conformational change, there is no obvious reason, at least in cases where a buried propionic acid residue is involved, why pK_{O1} and pK_R should be affected by membrane binding. The bacterial cytochromes studied here are soluble (periplasmic) proteins and their association with the cytoplasmic membrane is unclear. Probably all are reduced by a membrane-bound donor, however, and some are also oxidised by a membrane bound system (e.g. cytochrome c_2) so some association with the membrane must occur. Perhaps an alternative approach to assessing the *in vivo* significance of pK_O and pK_R would be to crosslink a cytochrome and its soluble oxidase (e.g. cytochrome c_{551} and cytochrome cd_1 and measure the rate of electron transfer at different pH values.

(ii) The physiological implications for pH dependence of redox potential

Given that the redox potentials of many c-type cytochromes *in vivo* are pH dependent over the physiological pH range then it is pertinent to ask how this might affect their function. A change in redox potential span available between the cytochrome and its redox partners may result in an increase or decrease in the rate of electron transfer via the cytochrome. Changes in pH could therefore control the rate of electron transport through the respiratory chain to which the cytochrome belongs - fluctuations in pH at respiratory membranes are an integral part of the now generally accepted chemiosmotic hypothesis. There is at least one report in the literature of a system where the rate of electron transfer is regulated by pH changes at the periplasmic surface of a membrane. Hashimoto & Nishimura

(1981) showed that the rate of electron transfer in the photosynthetic membranes of Chromatium vinosum was regulated by H^+ concentration at the surface region of the periplasmic side of the membrane. They stressed that the internal pH of the periplasmic space, rather than the pH difference or the difference in electrochemical potential of $[H^+]$ across the membrane, was the major factor determining the rate of re-reduction of the integral membrane cytochrome, cytochrome c_{555}. They further suggested that an electron donor to cytochrome c_{555} located on the periplasmic side of the photosynthetic membrane may be involved in the rate limiting step - the immediate reductant of cytochrome c_{555} is a soluble cytochrome c_{551} (van Grondelle et al., 1977). Knaff et al. (1980) have shown that this cytochrome c_{551} may be structurally related to P. aeruginosa cytochrome c_{551} (although no sequence data is available yet). It would be of interest to examine any pH dependence of redox potential of this cytochrome and the effect of pH on its oxidation by cytochrome c_{555}.

If a cytochrome with a pH dependent redox potential occurs at the branchpoint of an electron transport pathway then pH induced changes in its redox potential might serve to control the flux of electrons through each branch. Branched electron transport pathways are fairly common in bacteria. In this respect, there is a multiplicity of possible electron donors and acceptors for cytochrome c_{551} in denitrifying pseudomonads (see Figure 1) so it seems likely that pH could dictate its interaction with these.

As a final note, an interesting observation which argues for the physiological importance of the pH dependence of redox potential, at least in cytochrome c_{551}, is this. Wood demonstrated that the copper protein azurin is functionally interchangeable with cytochrome c_{551} in P. aeruginosa (P. Wood, unpublished data). We have shown that the redox potential of azurin is also pH

dependent and that the shape of its E_m versus pH curve almost exactly parallels that observed for cytochrome c_{551} (data described in Pettigrew et al., 1983 - see Appendix II).

(iii) The c-type cytochromes as scalar models for proton pumping proteins

The chemiosmotic hypothesis proposes that the energy liberated in electron transfer is transduced into an electrochemical proton gradient across a membrane. Although it is now widely agreed that redox energy is transduced in this way, the molecular mechanism which couples electron transport to vectorial proton translocation across the membrane remains obscure. Two general forms of coupling mechanism have been distinguished, direct and indirect. The former is represented by Mitchell's concept of the redox loop where the redox chain bends back on itself to give rise to alternating hydrogen and electron carriers (Figure 69a). Coupling between scalar redox processes and vectorial proton translocation is thus envisaged as a purely physical consequence of the molecular arrangement of the redox chain in the membrane. In the latter, indirect scheme (Figure 69b), H^+ is not directly bound to the (H^+ transferring) redox centre during translocation but to some other site the function of which is linked to the redox reaction.

Both mitochondrial cytochrome c oxidase and cytochrome c reductase have been proposed to pump protons by an indirect mechanism, where electron transfer at the redox centre is conformationally coupled to protolytic events in the surrounding polypeptide chain(s), in an analogous way to the Bohr effects in haemoglobin (Papa, 1976; Wikström & Krab, 1979). The work described above on the soluble c-type cytochromes, however, suggests that proton pumping in these complexes could be essentially electrostatic in origin. It is thus proposed that the redox state imposed separation in pK values of a group

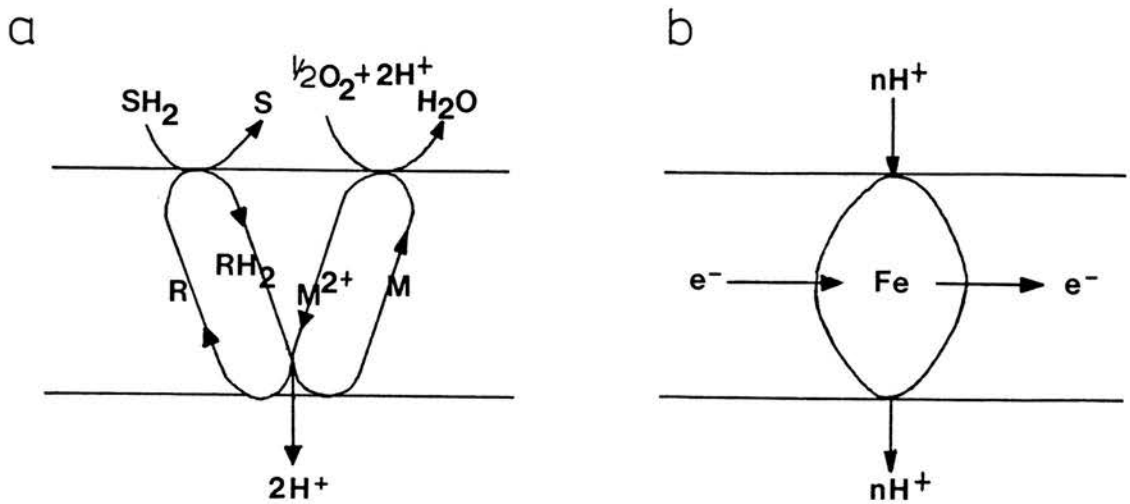

Figure 69: Mechanisms for the Conversion of the Free Energy of Redox Reactions to A Transmembrane Electrochemical Proton Gradient

(a) Mitchell´s redox loop. (b) Vectorial proton pumping. [Taken from Papa, 1976]

close to one of the redox centres in each complex will give rise to proton-coupled electron transfer in the pH range between pK_O and pK_R. Consistent with this hypothesis is the observation that both cytochrome c reductase and cytochrome c oxidase comprise subunits with pH dependent redox potentials. Wilson et al. (1972a) measured E_m over the pH range 6-8.5 for the high and low potential haem components of cytochrome c oxidase and found that E_m for the high potential haem (haem a) is pH dependent by -60mV/pH unit above pH7 i.e. $pK_O = 7$. With cytochrome c reductase, the E_m versus pH curve of cytochrome b_T shows a pK_O value of 6.7 (Wilson et al., 1972b). (Two other components of cytochrome c reductase, viz. the Rieske Fe-S protein and cytochrome c_1, have pH dependent redox potentials, but only above pH8.5 [Prince & Dutton, 1976; King, 1983]).

The c-type cytochromes with pH dependent redox potentials do not pump protons in the sense that cytochrome c oxidase or reductase do, since this is a vectorial, transmembrane effect. Rather, they are "scalar" models for how the multienzyme complexes might generate/take-up protons in association with redox state changes. Within the membrane, these simple redox state-linked protolytic effects must be interconnected with some translocational or reorientation step to account for vectorial proton pumping (von Jagow & Engel, 1980 and see Wikström et al, 1981).

APPENDIX I

Notes on NMR Terminology and Methods

1. The chemical shift parameter, δ, is defined as,

$$\delta(\text{ppm}) = \frac{\nu_{ref} - \nu_I}{\nu_o} \times 10^6$$

where ν_I is the resonance frequency of any proton, ν_{ref} that of the reference compound (normally DSS) and ν_o is the operating frequency of the spectrometer. Consideration of this equation indicates that the number of Hz/ppm must increase with ν_o if δ is to remain constant at all operating frequencies. Therefore, increasing the operating frequency of the spectrometer will improve spectral resolution by reducing resonance overlap.

2. The magnetically anisotropic character of an aromatic π-bond system produces an unsymmetrical magnetic field operating through space, which either opposes or augments the applied fields in the vicinity of neighbouring protons, as shown in Figure 70. The arrows indicate that the anisotropic effect opposes the applied field in the region above and below the ring while it augments the applied field in the region outside the perimeter of the ring. Thus all protons directly attached to the aromatic ring system of tyrosine, phenylalanine, tryptophan and histidine experience a deshielding ring current effect.

3. The multiplet structure observed in a high resolution spectrum is due to spin-spin coupling between neighbouring covalently bonded protons. The magnetic field experienced by a proton is affected by the various spin orientations of an adjacent proton(s), which has approximately equal probability of adopting either a high energy (spin = +1/2) orientation, opposing the applied magnetic field, or a low energy (spin = -1/2) orientation

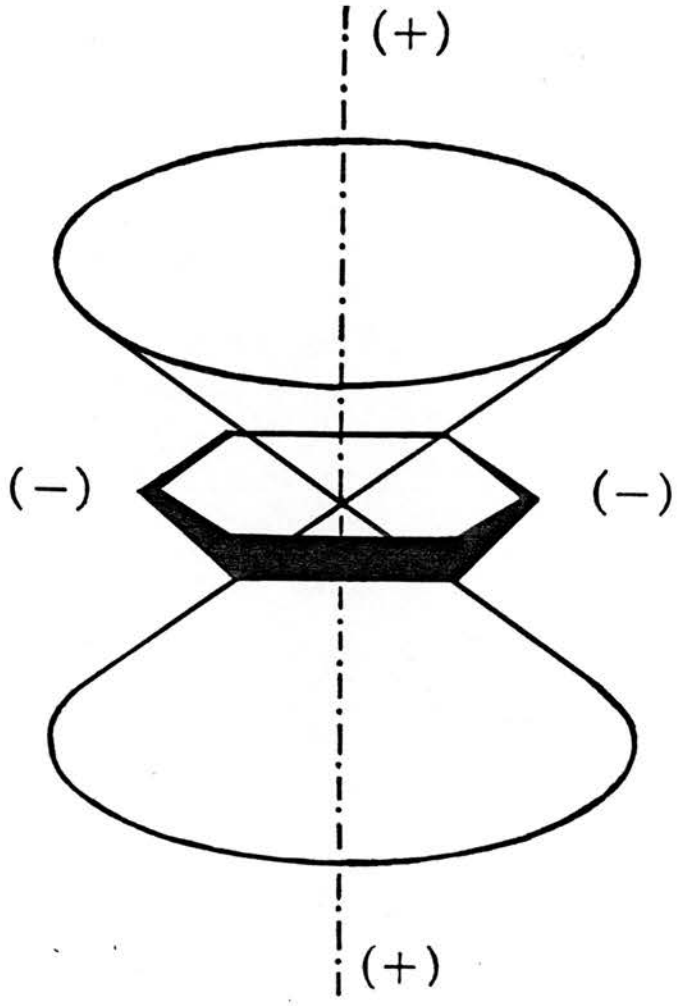

Figure 70: Ring Current Field for a Benzene Ring

The cone separates the shielding (+) and deshielding (-) regions.

which augments the applied magnetic field. All that is necessary, then, to eliminate the effect of spin-spin coupling between two protons is to cause one of them to undergo rapid and continuous transitions between its available energy states. The other proton sees only the average of the orientations, and its multiplet structure collapses. In order to make one of the coupled protons undergo these rapid transitions it is necessary to irradiate it steadily at its resonance (Larmor) frequency; the resonance of the other proton is simultaneously scanned. Irradiation during data accumulation is called time-shared irradiation and this particular double resonance technique is known as spin decoupling.

Generally, a doublet will collapse to a singlet upon irradiation at its coupled resonance, and a triplet will normally collapse to a doublet when one of its two coupled resonances are irradiated. However, in the case of the para triplet of a phenylalanine ring which is freely flipping (see note 12), irradiation of the meta triplet resonance will cause the para triplet to decouple to a singlet.

4. In Fourier transform NMR spectroscopy, a protein NMR spectrum is initially obtained in the form of a free induction decay (FID) which is a collection of exponentially decaying sine waves resulting from simultaneous excitation of all the nuclei in the protein (Figure 71a). The FID is a time domain function and it is converted to a frequency domain function (i.e. a conventional NMR spectrum) by Fourier transformation (Figure 71b). Mathematical manipulation of the FID before transformation can improve the quality of information inherent in it - if, for example, the FID is multiplied by a function which decays exponentially, the result is an increase in the signal-to-noise ratio in the spectrum, albeit at the expense of an increase in effective linewidth. This process is termed convolution. Quite

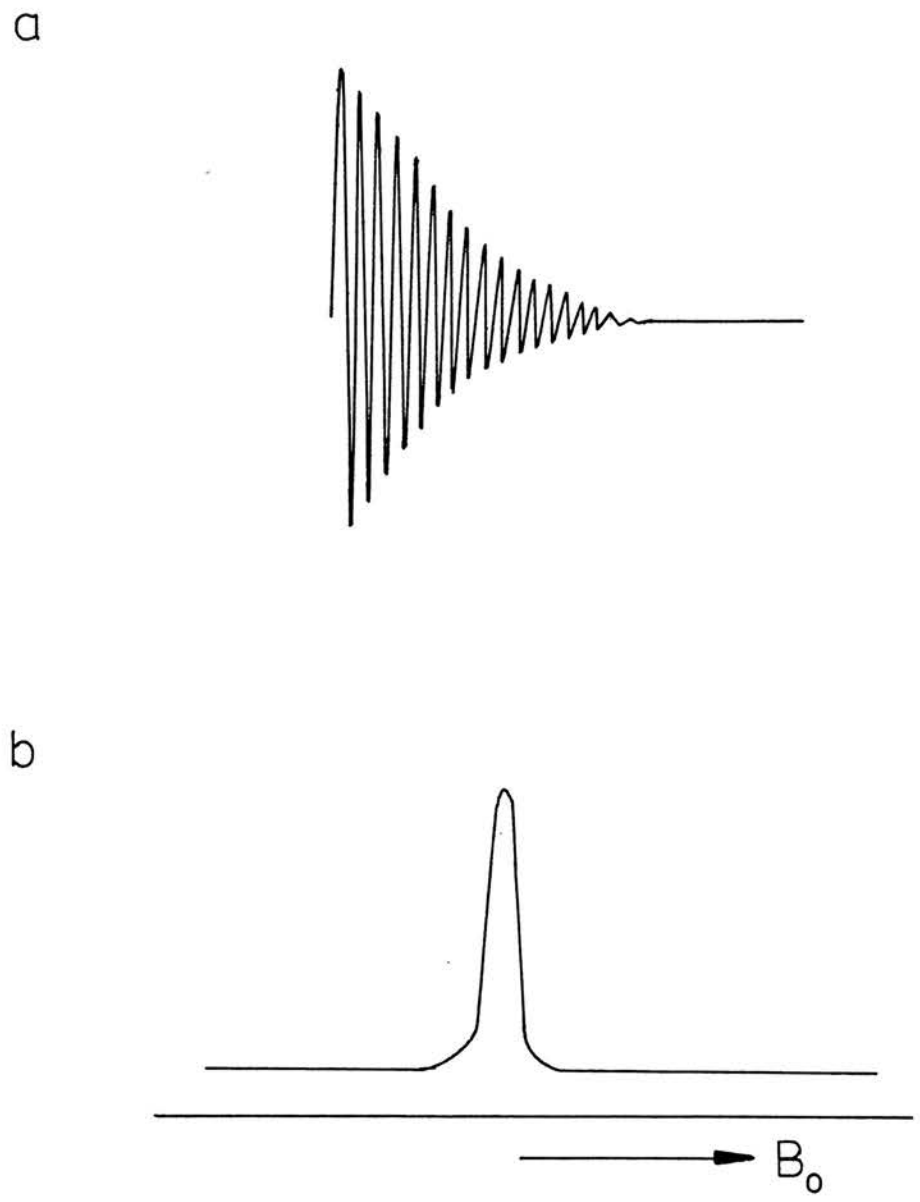

Figure 71:

(a) Free induction decay of a single resonance. (b) the corresponding NMr spectrum.

dramatic resolution enhancement of the NMR spectrum can then be obtained by subtracting the normal spectrum from the convolution broadened spectrum. This is shown in Figure 72, a and b. A less desirable aspect of convolution difference is that peaks which are broad in the normal spectrum do not appear in the difference spectrum. Furthermore, relative resonance intensities are largely meaningless (and the number of protons under any peak must be calculated by integration of the corresponding peak in the normal spectrum).

5. There are a number of rate processes which can affect an NMR spectrum; these include interconversion between two different molecular forms of a protein, and electron exchange in cytochrome molecules. A proton may then find itself in one of two magnetically inequivalent environments at any point in time. In such instances the rate of exchange of the proton between sites, compared to the difference in its resonance chemical shift position in each site, determines the character of the NMR spectrum. There are two limiting cases, called fast and slow exchange. In the fast exchange limit, the proton is jumping so rapidly compared with the difference in its resonance frequencies (chemical shifts) in the two environments, that it experiences, on the NMR time scale, the average of the two environments. Therefore, a single peak is observed at the average resonance position. In the slow exchange limit the proton sees only one of the two environments and hence two separate resonances are observed. These limits are illustrated in Figure 73a, where a proton exchanges between two equally populated sites A and B at a rate defined by k. Situations 1 and 5 represent the slow and fast exchange limits. Figure 73b shows the effect of changing the fractional population in sites A and B in the fast exchange limit, using the same rate constant as for curve 4 in Figure 73a; the resonance appears at an intermediate position determined by the relative populations in sites A and B.

Figure 72: Mathematical Manipulation of the Free Induction Decay

(a) 1, normal FID; 2, same FID after convolution (i.e. multiplication by a factor which decreases exponentially); 3, difference FID (1-2). (b) 1, spectrum corresponding to FID 1 above; 3, resolution enhanced spectrum corresponding to FID 3 above.

a

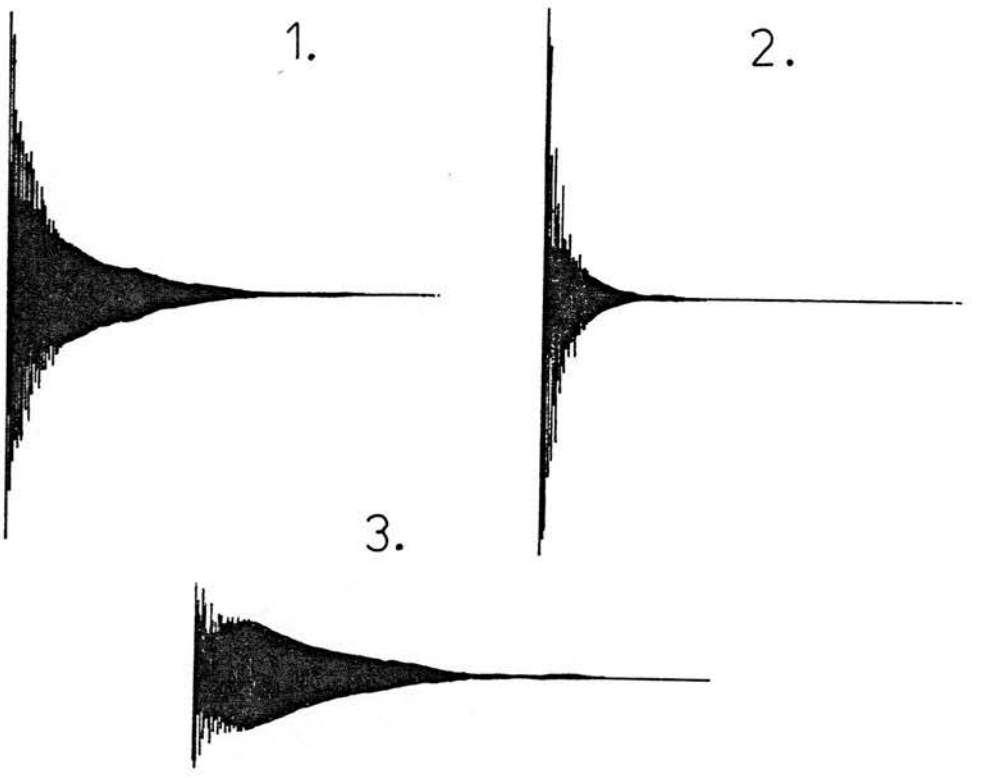

b

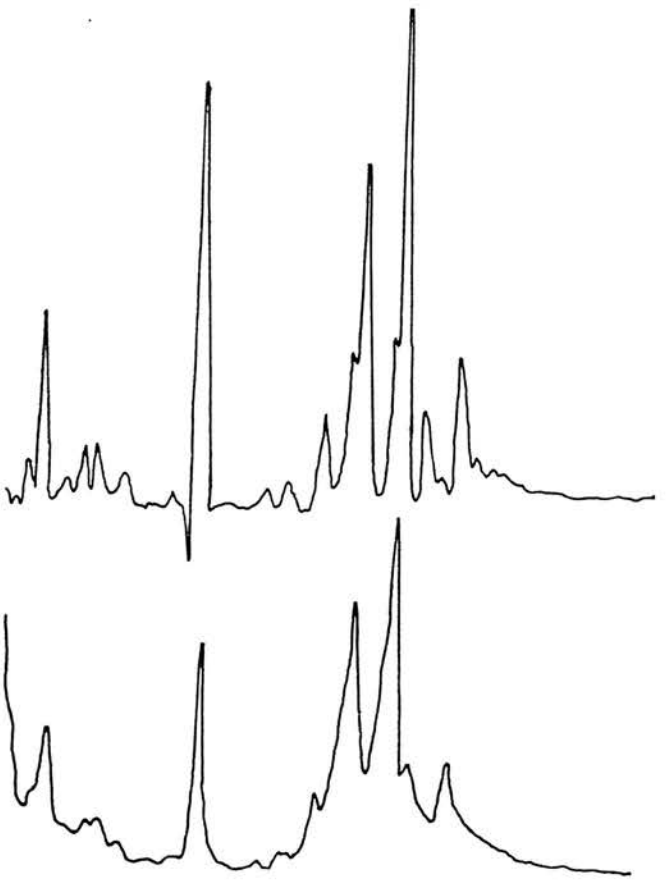

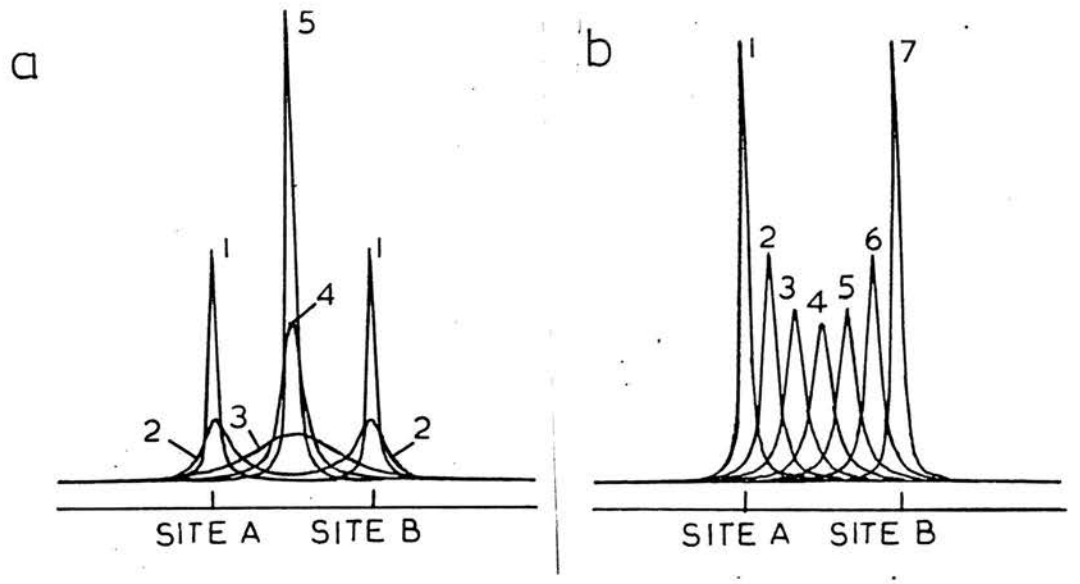

Figure 73: NMR Lineshape for Chemical Exchange Between Two Sites

The two sites are separated by $_{AB}$ = 100Hz and the inherent linewidths of both A and B are 5.0 Hz. (A) With P(opulation)$_A$ = P_B = 0.5 and (1) k = 0.314 sec^{-1} (2) k = 31.4 sec^{-1} (3) k = 220 sec^{-1} (4) k = 1.57 x $10^3 sec^{-1}$ (5) k = 3.14 x $10^6 sec^{-1}$.(B) With k = 1.57 x $10^3 sec^{-1}$ and (1) P_B = 0.010 (2) P_B = 0.166 (3) P_B = 0.333 (4) P_B = 0.5 (5) P_B = 0.677 (6) P_B = 0.833 (7) P_B = 0.99.

For a cytochrome, sites A and B may represent the environment of a proton in the ferri- and ferrocytochromes, where k is the rate of electron exchange. In the titration of P. stutzeri ferricytochrome c_{551} with reductant, the appearance of the partially reduced spectra indicated fast electron exchange; a bimolecular rate constant of $2.67+0.5 \times 10^6$ $M^{-1}s^{-1}$ (27^oC, pH6.5) was calculated.

6.

$$A \underset{k}{\overset{k}{\rightleftharpoons}} B$$

If species A and B are in fast exchange then the exchange contribution to the linewidth of a resonance in a 1:1 mixture of A and B can be approximated to:

$$\delta\nu_{1/2} = \frac{2\pi (\delta_A - \delta_B)^2}{k}$$

where k is the first order rate constant, $\delta\nu_{1/2}$ is the resonance linewidth measured at half height, and δ_A and δ_B are the chemical shifts of the resonance in species A and species B, respectively (Wüthrich, 1976). This equation says that for a system in fast exchange the linewidth of a resonance is primarily determined by the magnitude of $\delta_A - \delta_B$. By reference to Figure 38, it can be seen that the chemical shifts of some aromatic resonances in P. stutzeri cytochrome c_{551} are much more oxidation state dependent than others i.e. $\delta_A - \delta_B$ is larger. For example, the meta and para resonances of Phe7 and the doublets of Tyr34 shift much more than the triplet resonances of Trp77. At a 1:1 ratio of ferricytochrome:ferrocytochrome, then, the Phe7 resonances will be considerably broader than the Trp77 resonances. In convolution difference spectra many of these broad resonances are not detectable.

7. When placed in an external magnetic field, the haem ring behaves essentially like the ring systems of aromatic amino acids in generating an unsymmetrical local magnetic field (see note 2 and Figure 70). The resonances

The resonances of the haem substituent protons therefore experience downfield shifts. The iron ligands, His and Met, are located perpendicular to the haem plane and occur within the shielding region of the haem ring current field - their resonances are thus expected to be upfield shifted. Amino acids in the polypeptide backbone which are in close contact with the haem may also experience its ring current effects and their resonances will be upfield or downfield shifted from their primary positions depending on the orientation of each amino acid relative to the plane of the haem.

8. The term "primary position" applies to the chemical shift observed for an amino acid resonance when the amino acid occurs in a random coil protein or a small peptide. In the spectrum of a native protein, a resonance may be displaced from its primary position due to the proximity of other parts of the molecule (which can influence the local magnetic field of the amino acid). This displacement is called its secondary shift.

9. The NOE experiment is another example of a double resonance method (see note 3) where two radiofrequency pulses are applied to a system i.e. the standard 90° observation pulse and a pulse to perturb a selected proton spin system. Unlike spin decoupling, however, the perturbing pulse in NOE experiments is applied for a period before data accumulation. The nuclear Overhauser effect is defined as the change in intensity of a resonance signal of one proton, caused by saturation of the signal from another proton by irradiation at its resonance frequency. The phenomenological basis for the effect has been discussed by Noggle & Schirmer (1971) and no explanation is attempted here. NOEs can be observed between spin-spin coupled resonances and also between resonances of non-covalently bonded protons which are in close proximity. With regard to the latter case, the intensity change observed is inversely proportional to

the interproton distance raised to the 6th power, and so protons which are not in van der Waals contact are unlikely to give any effect.

10. The hyperfine shift of a resonance, δ_{HF}, is the difference in chemical shift observed for the resonance between the ferri- and ferrocytochrome. It may be expressed as the sum of two components:

$$\delta_{HF} = \delta_{pc} + \delta_c$$

where δ_{pc} is the pseudocontact shift which arises from dipolar electron-proton coupling and δ_c is the contact shift arising from the interaction of the nuclear spin with the unpaired electron density of the paramagnetic iron. (This definition assumes that there is no conformation change between the two oxidation states and thus no change in the diamagnetic contribution to the shift [δ_d]. In fact δ_d does change for the haem resonances of cytochrome c, even though there is no conformation change - this is because of differences in bonding due to the net charge difference in the two oxidation states.)

δ_{pc} is a through-space effect whereas δ_c is a through-bond effect and so the latter effect contributes to δ_{HF} for axial ligand and haem substituent resonances only. Since δ_c is given by

$$\delta_c = \frac{hA}{h\nu_I} \cdot \frac{g_B}{} \cdot s(s+1) \cdot \frac{1}{3kT}$$

and since A, the hyperfine coupling constant, is expressed as

$$A = (B_o + B_z \cos^2\eta) \cdot Q_c^{\pi}$$

where B_o and B_z are constants, η is the angle between the C-H bond of the proton considered and the normal to the haem plane, and Q_c is the integrated electron spin density localised on the π orbital of the haem ring carbon atom to which the substituent group is attached, then it can be seen that variation in η can affect the contact shift for the C-H resonance of a haem substituent group. For the propionic acid β-CH_2 resonances, δ_{pc} is

small compared to δ_C and so pH dependent variations of and Q_C^{π} may dominate δ_{HF} (Wüthrich, 1976).

11. Glasoe & Long (1960) measured the pH values of standard acid and base solutions prepared in either H_2O or ^2H_2O, using a number of different types of glass electrode. They concluded that,

$$p^2H = pH + 0.4$$

However, Li et al. (1961) noted that isotope effects on the pK value of histidine appear to be equal and opposite in sign to the isotope effect at the glass electrode. The pH and pK values quoted in this thesis are denoted pH^* and pK^* to indicate that the values are uncorrected for the isotope effect at the electrode. The pK^*_{ox} and pK^*_{red} values obtained by NMR , however, agree with those obtained from the redox experiments.

12. The ring systems of both tyrosine and phenylalanine can flip about the C_β-C_γ bond , the flip rate dictating the appearance of the NMR spectrum. With tyrosine, for example, the two <u>ortho</u> protons become equivalent when the flip rate is fast, as do the two <u>meta</u> protons, and an AA´BB´ spectrum (i.e. two 2-proton doublets) is observed. With slow flipping, an ABCD type spectrum (i.e. four 1-proton singlets) results, and at intermediate flip rates the resonances are too broad to be observed.

REFERENCES

Almassy, R.J. & Dickerson, R.E. (1978) Proc. Nat. Acad. Sci 75, 2674-2678

Ambler, R.P. (1976) C.N.R.S. Int. Symp. Electron Transport in Microorganisms, Marseille.

Ambler, R.P. in "From Cyclotrons to Cytochromes" (1980) A.B. Robinson & N.O. Kaplan (Eds.) Academic Press, New York.

Ambler, R.P. & Murray, S. (1973) Biochem. Soc. Trans. 1, 162-164.

Ambler, R.P. & Taylor, E. (1973) Biochem. Soc. Trans. 1, 111-113.

Ambler, R.P. & Wynn, M. (1973) Biochem. J. 131, 485-498.

Bachovchin, W.W. & Roberts, (1978) J. Am. Chem. Soc. 100, 8041-8047.

Bachovchin, W.W., Kaiser, R., Richards, J.H. & Roberts, J.D. (1981) Proc. Nat. Acad. Sci. 78, 7323-7326.

Barber, D., Parr, S.R. & Greenwood, C. (1976) Biochem. J. 157, 431-438.

Bates, R.G. (1954) Electrometric pH Determinations (page 208), Wiley, New York.

Bergey's Manual of Determinative Bacteriology (8th Ed., 1974) R.E. Buchanan & N.E. Gibbons, Eds., Williams & Wilkins, Baltimore, MD.

Bosshard, H.R. (1981) J. Mol. Biol. 153, 1125-1149.

Boswell, A.P., Eley, C.G.S., Moore, G.R., Robinson, M.N., Williams, G., Williams, R.J.P., Neupert, W.J. & Hennig, B. (1982) Eur. J. Biochem. 124, 289-294.

Bowyer, J.R., Tierney, G.V. & Crofts, C.R. (1979) FEBS Lett. 101, 207-212.

Brandt, K.G., Parks, P.C. Czerlinski, G.H. & Hess, G.P. (1966) J. Biol. Chem. 241, 4180-4185.

Brautigan D.L., Feinberg, B.A., Hoffman, B.M., Margoliash, E., Peisach, J. & Blumberg, W.E. (1977) J. Biol. Chem. 252, 574-582.

Brunori, M., Greenwood, C. & Wilson, M.T. (1974) Biochem. J. 137, 113-116.

Burstein, Y., Walsh, K.A. & Neurath, H. (1974) Biochemistry 13, 205-210.

Butler, J., Davies, D.M. & Sykes, A.G. (1981) J. Inorg. Biochem. 15, 41-53.

Campbell, W.H., Orme-Johnson, W.H. & Burris, R.H. (1973) Biochem. J. 135, 617-630.

Campbell, I.D., Dobson, C.M., Williams, R.J.P. & Xavier, A.V. (1973) J. Magn. Res. 11, 172-181.

Carlson, C.A., Ferguson, L.P. & Ingraham, J.L. (1982) J. Bacteriol. 151, 162-171.

Chao, Y-H., Bersohn, R. & Aisen, P. (1979) Biochemistry 18, 774-779.

Clark, W.M. (1960) Oxidation Reduction Potentials of Organic Systems, Williams & Wilkins, Baltimore MD.

Clegg. R.A. (1976) Biochem. J. 153, 533-541.

Cohen, J.S. & Hayes, M.B. (1974) J. Biol. Chem. 249, 5472-5477.

Davenport, H.E. & Hill, R. (1952) Proc. R. Soc. Lond B 139, 327-345.

Davis, L.A., Schejter, A. & Hess, G.P. (1974) J. Biol. Chem. 249, 2624-2632.

Dickerson, R.E. (1980) Scientific American 242/3, 98-110.

Dickerson, R.E. & Timkovich, R. (1975) The Enzymes 11, 395-544.

Dickerson, R.E., Takano, T., Eisenberg, D., Kallai, O.B., Samson, L., Cooper, A. & Margoliash, E. (1971) J. Biol. Chem. 246, 1511-1535.

Doudoroff, M., Contopolou, R., Kunisawa, R. & Palleroni, N.J. (1974) Int. J. Sys. Bacteriol. 24, 294-300.

Dutton, P.L. (1974) Biochim. Biophys. Acta 346, 165-212.

Dutton, P.L., Petty, K.M., Bonner, H.S. & Morse, S.D. (1975) Biochim. Biophys. Acta 387, 536-556.

Eley, C.G.S., Moore, G.R., Williams, G. & Williams, R.J.P. (1982) Eur. J. Biochem. 124, 295-303.

Ellfolk, N. & Soininen, R. (1970) Acta Chem. Scand. 24, 2126-2136.

Emptage, M.H., Xavier, A.V., Wood, J.M., Alsaadi, B.,

Moore, G.R., Pitt, R.C., Williams, R.J.P., Ambler, R.P. & Bartsch, R.G. (1981) Biochemistry 20, 58-64.
Forget, P. (1974) Eur. J. Biochem. 42, 325-332
Glasoe, P.D. & Long, F.A. (1960) J. Phys. Chem. 64, 188-190.
Gudat, J.C., Singh, J. & Wharton, D.C. (1973) Biochim. Biophys. Acta 292, 376-390.
Gupta, R.K. & Koenig, S.H. (1971) Biochem. Biophys. Res. Comm. 45, 1134-1143.
Haddock, B.A. & Jones, C.W. (1977) Bacteriol. Rev. 41, 47-99.
Hanania, G.I.H., Irvine, D.H., Eaton, W.A. & George, P. (1967) J. Phys. Chem. 71, 2022-2030.
Harbury, H.A. (1957) J. Biol. Chem. 225, 1009-1023.
Hashimoto, K. & Nishimura, M. (1981) J. Biochem. 89, 909-917.
Holbrook, J.J. & Ingram, V.A. (1973) Biochem. J. 131, 729-738.
Horio, T., Higashi, T., Yamanaka, T., Matsubara, H. & Okunuki, K. (1961) J. Biol. Chem. 236, 944-951.
Kassner, R.J. (1972) Proc. Nat. Acad. Sci. 69, 2263-2267.
Kassner, R.J. (1973) J. Am. Chem. Soc. 95, 2674-2677.
Keller, R.M. & Wüthrich, K. (1978a) Biochim. Biophys. Acta 533, 195-208.
Keller, R.M. & Wüthrich, K. (1978b) Biochem. Biophys. Res. Comm. 83, 1132-1139.
Keller, R.M., Wüthrich, K. & Pecht, I. (1976) FEBS Lett. 70, 180-184.
Kihara, H., Saigo, S., Nahatani, H., Hiromi, K., Ikeda-Saito, M. & Iizuka, T. (1976) Biochim. Biophys. Acta 430, 225-243.
King, T.E. (1983) Adv. Enzym. 54, 267-360.
Knaff, D.E., Whetstone, R. & Carr, J.W. (1980) Biochim. Biophys. Acta 590, 50-58.
Kodama, T. & Mori, T. (1969) J. Biochem. 65, 621-628.
Kodama, T. & Shidara, S. (1969) J. Biochem. 65, 351-360.
Kolthoff, I.M. & Auerbach, C. (1952) J. Am. Chem. Soc.

74, 1452-1456.
Korzun, Z.R. & Salemme, F.R. (1977) Proc. Nat. Ac. Sci. 74, 5244-5247.
Kuronen, T., Saraste, M. & Ellfolk, N. (1975) Biochim. Biophys. Acta 393, 48-54.
Laemmli, U.K. (1970) Nature 277, 680-685.
Lenhoff, H.M. & Kaplan, N.O. (1956) J. Biol. Chem. 220, 967-982.
Levine, B.A., Moore, G.R., Ratcliffe, G.R. & Williams, R.J.P. (1979) Int. Rev. Biochem. 24, 77-141.
Li, N.C., Tang, P. & Mathur, R. (1961) J. Phys. Chem. 65, 1074-1076.
Liu, M-C., Payne, W.J., Peck, H.D. & LeGall, J. (1983) J. Bacteriol. 154, 278-286.
MacGregor, C.H. (1974) J. Biol. Chem. 249, 5321-5327.
Mandel, M. (1966) J. Gen. Micro. 43, 273-293.
Margalit, R. & Schejter, A. (1973) Eur. J. Biochem. 32, 492-499.
Margoliash, E., Nisonoff, A. & Reichlin, M. (1970) J. Biol. Chem. 245, 931-939.
Margoliash, E., Smith, E., Kreil, G. & Tuppy, H. (1961) Nature 192, 1121-1127.
Markley, J.L. (1974) Acc. Chem. Res. 8, 70-80.
Matsushita, K., Shinagawa, E. Adachi, O. & Ameyama, M. (1982) FEBS Lett. 139, 255-258.
Matsuura, Y., Takano, T. & Dickerson, R.E. (1982) J. Mol. Biol. 156, 389-409.
Melchior, W.B. & Fahrney, D. (1970) Biochemistry 9, 251-258.
Meyer, T.E. (1970) Ph.D. Thesis, University of California (San Diego).
Meyer, T.E., Bartsch, R.G., Cusanovich, M.A. & Mathewson, J.H. (1968) Biochim. Biophys. Acta 153, 854-861.
Miller, W.G. & Cusanovich, M.A. (1975) Biophys. Struct. Mech. 1, 97-111.
Moore, G.R. (1983) FEBS Lett. 161, 171-175.
Moore, G.R. & Pettigrew, G.W. (1984) "Structure and

Function of c-Type Cytochromes" (in preparation).
Moore, G.R. & Williams, R.J.P. (1980a) Eur. J. Biochem. 103, 493-502.
Moore, G.R. & Williams, R.J.P. (1980b) Eur. J. Biochem. 103, 503-512.
Moore, G.R. & Williams, R.J.P. (1980c) Eur. J. Biochem. 103, 513-521.
Moore, G.R. & Williams, R.J.P. (1980d) Eur. J. Biochem. 103, 523-532.
Moore, G.R. & Williams, R.J.P. (1980e) Eur. J. Biochem. 103, 533-541.
Moore, G.R., Pitt, R.C. & Williams, R.J.P. (1977) Eur. J. Biochem. 77, 53-60.
Moore, G.R., Pettigrew, G.W., Pitt, R.C. & Williams, R.J.P. (1980) Biochim. Biophys. Acta 590, 261-271.
Morris, D.L. & McKinley-McKee, J. (1972) Eur. J. Biochem. 29, 515-520.
Nisonoff, A., Reichlin, M. & Margoliash, E. (1970) J. Biol. Chem. 245, 940-946.
Noggle, J.H. & Schirmer, R.E. (1971) The Nuclear Overhauser Effect, Academic Press, New York.
Ovadi, J., Libor, S. & Elödi, P. (1967) Acta Biochem. Biophys. Acad. Sci. Hung. 2, 455-458.
Palleroni, N.J., Doudoroff, M. & Stanier, R.Y. (1970) J. Gen. Micro. 60, 215-231.
Papa, S. (1976) Biochim. Biophys. Acta 456, 39-84.
Pecht, I. & Rosen, P. (1973) Biochem. Biophys. Res. Comm. 50, 853-858.
Pettigrew, G.W., Aviram, I & Schejter, A. (1976) Biochem. Biophys. Res. Comm. 68, 807-813.
Pettigrew, G.W., Aviram, I. & Schejter, A. (1975) Biochem. J. 149, 155-167.
Pettigrew, G.W., Bartsch, R.G., Meyer, T.E. & Kamen, M.D. (1978) Biochim. Biophys. Acta 503, 509-523.
Pettigrew, G.W., Meyer, T.E., Bartsch, R.G. & Kamen, M.D. (1975) Biochim. Biophys. Acta 430, 197-208.
Prince, R.C. & Bashford, C.L. (1979) Biochim. Biophys.

Acta 547, 447-454.
Prince, R.C. & Dutton, P.L. (1976) FEBS Lett. 65, 117-119.
Prince, R.C. & Dutton, P.L. (1977) Biochim. Biophys. Acta 459, 573-577.
Redfield, A.G. & Gupta, R.K. (1971) Cold Spring Harbour Sym. Quant. Biol. 36, 405-411.
Robillard, G. & Shulman, R.G. (1972) J. Mol. Biol. 71, 507-511.
Robillard, G. & Shulman, R.G. (1974) J. Mol. Biol. 86, 519-540.
Rodkey, F.L. & Ball, E.G. (1950) J. Biol. Chem. 182, 17-28.
Rosen, C., Gejvall, T. & Andersson, L. (1970) Biochim. Biophys. Acta 221, 207-213.
Sawyer, L., Jones, C.L., Damas, A.M., Harding, M.M., Gould, R.O. & Ambler, R.P. (1981) J. Mol. Biol. 153, 831-835.
Schulz, G.E. & Schirmer, R.H. (1979) Principles of Protein Structure, Springer-Verlag, New York.
Senn, H. & Wüthrich, K. (1983a) Biochim. Biophys. Acta 746, 48-60.
Senn, H. & Wüthrich, K. (1983b) Biochim. Biophys. Acta 743, 69-81.
Senn, H., Eugster, A. & Wüthrich, K. (1983) Biochim. Biophys. Acta 743, 58-68.
Senn, H., Keller, R.M. & Wüthrich, K. (1980) Biochem. Biophys. Res. Comm. 92, 1362-1369.
Silvestrini, M.C., Brunori, M., Wilson, M.T. & Darley-Usmar, V.M. (1981) J. Inorg. Biochem. 14, 327-338.
Spackman, D.H. (1963) Fed. Prc. Fed. Am. Soc. Exp. Biol. 22, 244.
Steitz, T. & Shulman, R.G. (1982) Ann. Rev. Biophys. Bioengineer. 11, 419-444.
Stellwagen, E. & Cass, R.D. (1975) J. Biol. Chem. 250, 2095-2098.

Stellwagen, E. (1966) Biochem. Biophys. Res. Comm. 23, 29-33.

Sudmeier, J.L., Evelhoch, J.L. & Jonsson, N.B-H. (1980) J. Magn. Res. 40, 377-390.

Swank, R.T. & Burris, R.H. (1969) Biochim. Biophys. Acta 180, 473-489.

Takano, T. & Dickerson, R.E. (1981) J. Mol. Biol. 153, 75-119.

Theorell, H. & Akeson, A. (1941) J. Am. Chem. Soc. 63, 1804-1811.

Van Grondelle, R., Duysens, L.N.M., Van Der Wel, J.A. & Van Der Wal, H.N. (1977) Biochim. Biophys. Acta 461, 188-201.

Vanderkooi, J., Erecinska, M. & Chance, B. (1973a) Arch. Biochem. Biophys. 154, 531-540.

Vanderkooi, J., Erecinska, M. & Chance, B. (1973b) Arch. Biochem. Biophys. 154, 219-229.

Velick, S.F. & Strittmater, P. (1956) J. Biol. Chem. 221, 265-275.

Von Jagow, G. & Engel, W.D. (1980) FEBS Lett. 111, 1-5.

Wikström, M.F.K. & Krab, K. (1979) Biochem. Soc. Trans. 7, 880-887.

Wikström, M.F.K., Krab, K. & Saraste, M. (1981) Ann. Rev. Biochem. 50, 623-655.

Wilson, M.T. & Greenwood, C. (1971) Eur. J. Biochem. 22, 11-18.

Wilson, D.F., Erecinska, M., Leigh, J.S. & Koppelman, M. (1972b) Arch. Biochem. Biophys. 151, 112-121.

Wilson, D.F., Lindsay, J.G. & Brocklehurst, E.S. (1972a) 256, 277-285.

Wood, P.M. (1978) FEBS Lett. 92, 214-218.

Wood, P.M. (1980a) Biochem. J. 189, 385-391.

Wood, P.M. (1980b) Biochem. J. 192, 761-764.

Wood, P.M. & Willey, D.L. (1980) FEMS Microbiol. Lett. 7, 273-277.

Wood, F.E., Post, C.B. & Cusanovich, M.A. (1977) Arch. Biochem. Biophys. 184, 586-595.

Wüthrich, K. (1970) Structure & Bonding 8, 53-121.
Wüthrich, K. (1976) NMR in Biological Research: Peptides and Proteins, North-Holland, Amsterdam.
Yang, T.Y. & Jurtshuk, P. (1978) Biochim. Biophys. Acta 502, 543-548

APPENDIX II

Biochimica et Biophysica Acta, 725 (1983) 409–416
Elsevier

BBA 41413

THE EFFECT OF IRON-HEXACYANIDE BINDING ON THE DETERMINATION OF REDOX POTENTIALS OF CYTOCHROMES AND COPPER PROTEINS

G.W. PETTIGREW [a], F.A. LEITCH [a] and G.R. MOORE [b]

[a] *Department of Biochemistry (Veterinary Unit), Royal Dick School of Veterinary Studies, University of Edinburgh, Edinburgh EH9 1QH and* [b] *Laboratory of Inorganic Chemistry, University of Oxford, Oxford OX1 3QR (U.K.)*

(Received June 28th, 1983)

Key words: Cytochrome; Copper protein; Redox potential; Azurin; Ligand binding; Iron hexacyanide

The midpoint redox potentials of *Pseudomonas aeruginosa* cytochrome *c*-551 and *Rhodopseudomonas viridis* cytochrome c_2 were measured as a function of pH in the presence of *Euglena* cytochrome *c*-558 and the results compared with those obtained in the presence of ferro-ferricyanide. The pattern of pH dependence observed for the two bacterial cytochromes was the same whether it was measured by equilibrium with another redox protein or with the inorganic redox couple. Thus, the pH dependence of redox potential is not a consequence of pH-dependent ligand binding. The midpoint potential of *Ps. aeruginosa* azurin was measured as a function of pH using both ferro-ferricyanide mixtures and redox equilibrium with horse cytochrome *c* or *Rhodopseudomonas capsulata* cytochrome c_2. In this case also the pattern of pH dependence obtained did not vary with the redox system used and it closely resembled that of *Ps. aeruginosa* cytochrome *c*-551. This is consistent with the observation that the equilibrium between cytochrome *c*-551 and azurin is relatively independent of pH. An equation was derived which described pH-dependent ligand binding and which can produce theoretical curves to fit the experimental pH dependence of redox potential for both cytochrome and azurin. However, the pronounced effect on such curves produced by varying the ligand association constants, and the insensitivity of the experimental data to changes in ionic strength, suggest that ligand binding effects do not account for the pH dependence of redox potential.

Introduction

The ferro-ferricyanide couple has been widely used in the determination of redox potentials of high-potential electron-transfer proteins [1–4] and ferricyanide is commonly used as a mediator in the anaerobic titration of unfractionated systems and oxidases [5–8]. Yet it has become clear that ferricyanide binds to horse cytochrome *c* [9–12] and if differential binding occurred for the two redox states then a perturbation of redox potential would be observed according to the equation derived by Dutton [13]:

$$E_m = E_{m(NL)} + \frac{0.06}{n} \log \frac{1 + K_R[L]}{1 + K_o[L]} \quad (1)$$

where $E_{m(NL)}$ is the midpoint potential in the absence of ligand and K_R and K_o are association constants for the binding of ligand (L) to the protein.

In our studies of bacterial cytochrome *c* a principal interest has been the pH dependence of redox potential and we have interpreted this in terms of ionisations in the protein which are influenced by the redox state of the haem. We have recently distinguished two groups of cytochromes in this respect, one of which is characterised by the redox-linked ionisation of a haem propionic acid and is exemplified here by *Pseudomonas* cytochrome *c*-551 [14,15], while the second group is characterised by a redox-linked deprotonation of a

histidine and is represented here by *Rhodopseudomonas viridis* cytochrome c_2 [16,17]. However, the possibility exists that the apparent pH dependence is due simply to differential binding of ferricyanide to protonated and unprotonated forms of the proteins and that this pH dependence would disappear if the redox potential could be determined by another method.

Such an explanation has been proposed by Lappin et al. [18] for *Ps. aeruginosa* azurin on the basis of the variations in the pH dependence of redox kinetics using different redox agents. These authors propose that with appropriate redox agents the midpoint potential of azurin would be independent of pH. If this is true for azurin it may also hold for *Ps. aeruginosa* cytochrome *c*-551, since the redox equilibrium between the two is known to be relatively pH independent [19,20].

In this paper we present evidence that the pH dependence of redox potential observed for some *c*-type cytochromes and azurin is not due to pH-dependent ligand binding.

Methods

Preparation of redox proteins

Azurin ($A_{625}/A_{280} = 0.5$) and cytochrome c-551 ($A_{550(red)}/A_{280} = 1.15$) were prepared from cells of *Ps. aeruginosa* and cytochrome *c*-551 ($A_{551(red)}/A_{280} = 1.35$) was prepared from *Ps. stutzeri* strain 221 essentially as described by Ambler [21,22]. *Euglena gracilis* cytochrome *c*-558 was purified as described by Pettigrew et al. [23] and cytochrome c_2 from *Rhodopseudomonas capsulata* strain *St. Louis* was prepared essentially as described by Bartsch [24]. Horse cytochrome *c* (type VI) was from Sigma.

Measurement of redox potentials using ferri-ferrocyanide mixtures

Midpoint redox potentials were determined by spectrophotometric examination of the redox state of the protein on a Cary 219 spectrophotometer in ferri-ferrocyanide solutions of known potential [25,4]. Buffers used were 3.3 mM in acetate, phosphate Tris or borate and the pH was determined at the redox equilibrium before addition of dithionite. Under these conditions, with an ionic strength contribution of 5 mM from the 0.5 mM ferrocyanide and 2–10 mM from the buffers, the ferri-ferrocyanide midpoint potential can be taken from Fig. 1 in Ref. 25. Some experiments were carried out in the presence of 0.1 M NaCl and under these conditions the midpoint potential of ferri-ferrocyanide was taken as 430 mV [3,26]. This should be regarded as an approximate figure as our conditions are not those described in these references, but the absolute value of E_m does not affect the relative pH-dependent patterns that we wish to emphasise.

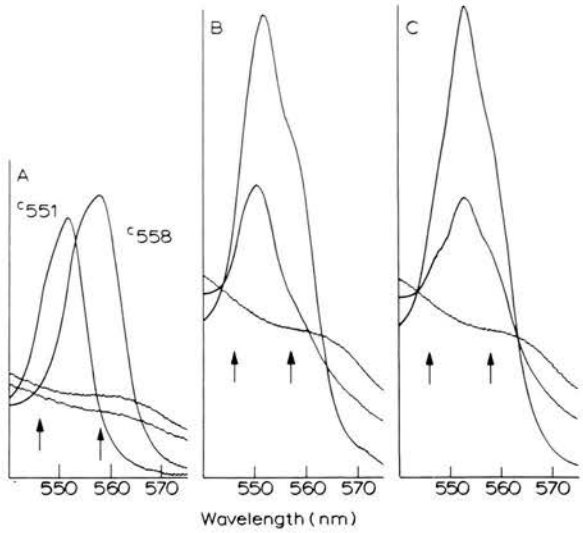

Fig. 1. Determination of the redox potential of *Ps. aeruginosa cytochrome c*-551 by mixture with *Euglena* cytochrome *c*-558. (A) Visible spectra of the oxidised and reduced forms of cytochromes *c*-551 and *c*-558. Arrows indicate isosbestic points at 546 nm (for cytochrome *c*-558) and 558 nm (for cytochrome *c*-551) at pH 8. (B, C) Spectra at redox equilibria after the addition of ferricyanide and after the addition of dithionite to a mixture of ferrocytochrome *c*-551 and ferricytochrome *c*-558 in $3.3 \cdot 10^{-3}$ M acetate, pH 5.17 (B), and $3.3 \cdot 10^{-3}$ phosphate, pH 7.91 (C). Arrows indicate isosbestic points for the individual cytochromes.

Measurement of redox potentials using mixtures with Euglena cytochrome c-558

Ps. aeruginosa cytochrome *c*-551, or cytochrome c_2 from *Rps. viridis* was reduced by millimolar ascorbate and excess reductant removed by passage through Sephadex G-25 (fine) equilibrated in 10 mM NaCl, 0.5 mM EDTA, 0.5 mM sodium phosphate, pH 7. A redox equilibrium was estab-

lished and spectrophotometrically recorded after mixing ferrocytochrome *c*-551 or c_2 with ferricytochrome *c*-558 in 3.3 mM acetate, phosphate, Tris or borate buffer. Two examples of such equilibria are shown in Fig. 1. After measurement of pH, a crystal of ferricyanide was added to achieve complete oxidation followed by a few grains of sodium dithionite for complete reduction. In the case of cytochrome *c*-551 and *c*-558 shown in Fig. 1, measurements at 546 nm (an isosbestic point for the cytochrome *c*-558) allow calculation of the redox state of cytochrome *c*-551 and, conversely, measurements at 557–558 nm (an isosbestic point for cytochrome *c*-551, the exact position of which was dependent on the pH) allow calculation of the redox state of cytochrome *c*-558.

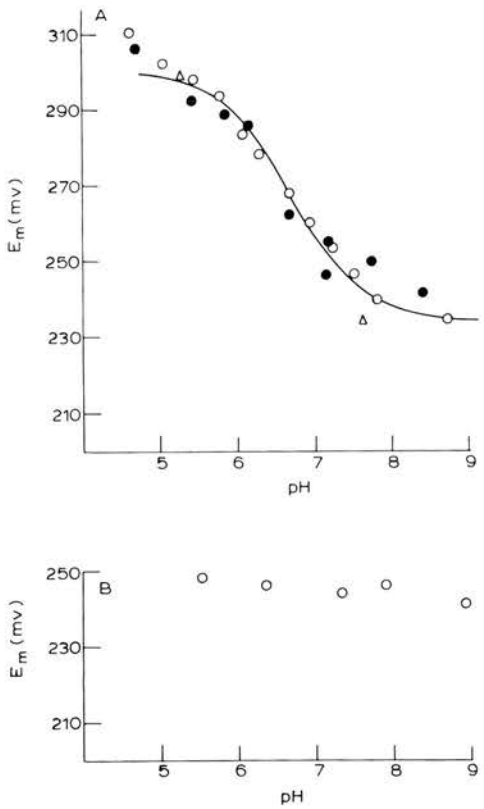

Fig. 2(A). The pH dependence of redox potential of *Ps. aeruginosa* cytochrome *c*-551. Cuvettes contained $2.5 \cdot 10^{-6}$ M cytochrome *c*-551 in $3.3 \cdot 10^{-3}$ M acetate, phosphate, tris or borate buffer. (○) Midpoint potentials measured in $5 \cdot 10^{-4}$ M ferrocyanide and $1.7 \cdot 10^{-5}$ M ferricyanide. (●) Midpoint potentials measured by mixture with $2 \cdot 10^{-6}$ M *Euglena* cytochrome *c*-558. (△) Midpoint potentials measured anaerobically in the presence of 10^{-5} M diaminodurol and a combination Pt/Ag/AgCl electrode. The solid line is a theoretical curve defined by Eqn. 2 with $pK_{ox} = 6.3$ and $pK_{red} = 7.2$ [15]. (B). The pH-independent redox potential of *Euglena* cytochrome *c*-558. At redox equilibrium the cuvettes contained $2.5 \cdot 10^{-6}$ M cytochrome *c*-558, $5 \cdot 10^{-4}$ M ferrocyanide, $8.3 \cdot 10^{-6}$ M ferricyanide and $3.3 \cdot 10^{-3}$ M acetate, phosphate, Tris or borate buffers.

After mixing, spectra were always recorded twice, immediately and after 1 min, to ensure stable redox equilibria had been achieved. From determination of the redox equilibrium constant the difference between the midpoint potentials of cytochrome *c*-558 and its partner in the mixture could be calculated. The midpoint potential of cytochrome *c*-558 was independently determined in ferri-ferrocyanide solutions to be 245 mV with very little variation with pH (Fig. 2B).

Measurement of redox potentials in mixtures of cytochromes and azurin

It is not possible to determine accurately the redox state of the proteins in a cytochrome/azurin mixture because neither protein has an isosbestic point near the peak maximum of the other. However, the contribution of azurin to absorbance at 550 nm is small, as is the contribution of cytochrome to absorbance at 625 nm. The redox state of each protein could therefore be approximately calculated and any pH dependence of equilibria studied.

Ferrocytochrome *c* from horse, *Rps. capsulata* or *Ps. aeruginosa* was mixed with Cu(II)-azurin in 3.3 mM acetate, phosphate, Tris or borate buffer and redox equilibrium, ferricyanide-oxidised and dithionite-reduced spectra were recorded on the Cary 219 spectrophotometer.

Results

The pH dependence of redox potential of Ps. aeruginosa cytochrome c-551

The midpoint potential of *Euglena gracilis* cytochrome *c*-558 measured using mixtures of ferri- and ferrocyanide was essentially independent of pH between pH 5 and 9 (Fig. 2B). A stable redox equilibrium between this cytochrome and *Ps. aeruginosa* cytochrome *c*-551 was rapidly established in the absence of hexacyanide by mixing ferrocytochrome *c*-551 with ferricytochrome *c*-558 and the midpoint potential of the cytochrome *c*-551

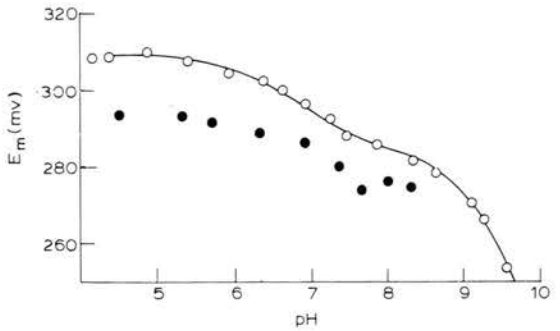

Fig. 3. The pH dependence of redox potential of *Rps. viridis* cytochrome c_2. (○) Results obtained in the presence of $5 \cdot 10^{-4}$ M ferrocyanide and $1.7 \cdot 10^{-5}$ M ferricyanide, 10^{-3} M acetate, phosphate, Tris or glycine buffers [16]. The solid line is a theoretical curve defined by the equation $E_m = E + (0.06/n) \log\{([H^+]^2 + K_R[H^+])/([H^+]^2 + K_{01}[H^+] + K_{01}K_{02})\}$, derived using the procedures of Clark [26] with $pK_{01} = 6.7$, $pK_R = 7.1$ and $pK_{02} = 9.2$. (●) Midpoint potentials measured by mixture with *Euglena* cytochrome *c*-558. The cuvette contained $2 \cdot 10^{-6}$ M cytochrome *c*-558, $2.5 \cdot 10^{-6}$ M cytochrome *c*-551, 0.1 M NaCl and $3.3 \cdot 10^{-3}$ M acetate, phosphate or Tris buffer.

was calculated from the mixed spectra (Fig. 1) assuming E_m(*c*-558) = 245 mV [23]. The derived pH dependence of E_m for cytochrome *c*-551 is shown in Fig. 2A and compared with published results obtained in the presence of ferri-ferrocyanide.

The midpoint potential of cytochrome *c*-551 was also determined using diaminodurol and a Pt/Ag/AgCl combination electrode with the results shown in Fig. 2A. $Ru(CN)_6^{4-}$ or $Co(CN)_6^{3-}$ (final conc. 0.5 mM) had no effect on the redox equilibrium in these experiments.

The pH dependence of redox potential of Rps. viridis cytochrome c_2

Stable redox equilibria were established at different pH values by mixing ferrocytochrome c_2 from *Rps. viridis* and ferricytochrome *c*-558 from *Euglena gracilis*. Midpoint potentials were calculated for the cytochrome c_2 assuming E_m(*c*-558) = 245 mV and these are shown in Fig. 3 in comparison with published results obtained in the presence of ferri-ferrocyanide. It was necessary to conduct the experiments in the presence of 100 mM NaCl because in the absence of added salt the variations in ionic strength for phosphate buffer at different pH values led to perturbations of redox potential superimposed on those caused by pH differences alone. This effect was much less pronounced for the original measurements with ferri-ferrocyanide [16], where the dominant components of ionic strength are the hexacyanides themselves.

The pH dependence of redox potential of Ps. aeruginosa azurin

The midpoint potential of azurin was measured by single point mixtures with known ferri-ferrocyanide concentrations at different pH values and under two conditions of total ionic strength. An extinction coefficient of 3.5 $mM^{-1} \cdot cm^{-1}$ at 625 nm for azurin [19] was used in calculations. This figure is controversial but application of the highest literature value of 5.9 $mM^{-1} \cdot cm^{-1}$ [18] made very little difference to the calculated potentials. Theoretical curves were constructed using the equation:

$$E_m = \tilde{E} + \frac{0.06}{n} \log \frac{K_{red} + [H^+]}{K_{ox} + [H^+]} \qquad (2)$$

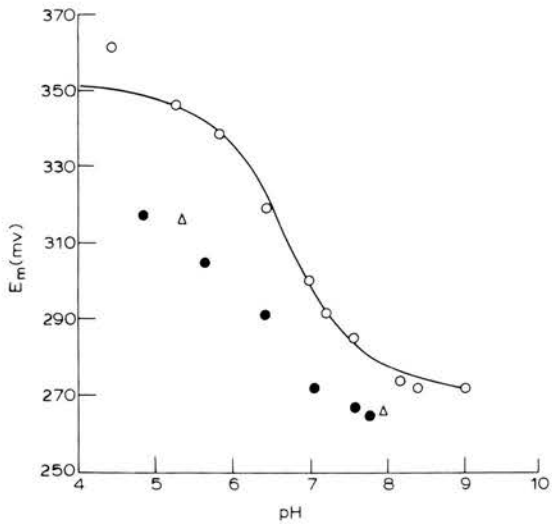

Fig. 4. The pH dependence of redox potential of azurin. The cuvette contained $5 \cdot 10^{-6}$ M azurin. (○) Midpoint potentials measured in $5 \cdot 10^{-4}$ M ferrocyanide and $3.3 \cdot 10^{-5}$ M ferricyanide, $3.3 \cdot 10^{-3}$ M acetate, phosphate, Tris or borate buffer. The solid line is a theoretical curve defined by Eqn. 2 with $pK_0 = 6.1$ and $pK_R = 7.4$. (●, △) Midpoint potentials measured by mixture with horse cytochrome *c* (●) and *Rps. capsulata* cytochrome c_2 (△) (each $2.5 \cdot 10^{-6}$ M) in $2 \cdot 10^{-3}$ M acetate, phosphate or Tris buffers.

in which K_{ox} and K_{red} are proton dissociation constants for a group in the two redox states and $\tilde{E}$ is the midpoint potential at acid pH [15]. Midpoint potentials were also calculated from equilibrium mixtures of horse cytochrome *c* and azurin, and *Rps. capsulata* cytochrome c_2 and azurin (Fig. 4). These cytochromes have pH-independent redox potentials [4] and thus pH-dependent redox equilibria with azurin must be due to pH dependence of the azurin itself. The rate of reaction of ferrocytochrome *c* with Cu(II)-azurin was very dependent on the nature of the cytochrome. That with horse cytochrome *c* was very slow ($t_{1/2} = 45$ s at pH 5 and 29 s at pH 7.4), while those with *Rps. capsulata* cytochrome c_2 and *Ps. aeruginosa* cytochrome *c*-551 were too rapid to measure without rapid reaction techniques.

The redox equilibrium of *Ps. aeruginosa* cytochrome *c*-551 and azurin was measured at several pH values (Fig. 5) and expressed as a difference in midpoint potentials in Fig. 6A. Comparison with such differences calculated from ferri-ferrocyanide experiments on the separate proteins (Fig. 6A) indicates that the equilibrium is essentially independent of pH and that ferri-ferrocyanide does not perturb this equilibrium.

A similar analysis for *Ps. stutzeri* cytochrome *c*-551 and *Ps. aeruginosa* azurin is shown in Fig. 6B. As we report elsewhere [14] pK_0 and pK_R in *Ps. stutzeri* cytochrome *c*-551 are shifted to pH 7.6 and 8.3, respectively. This leads to a mismatch in

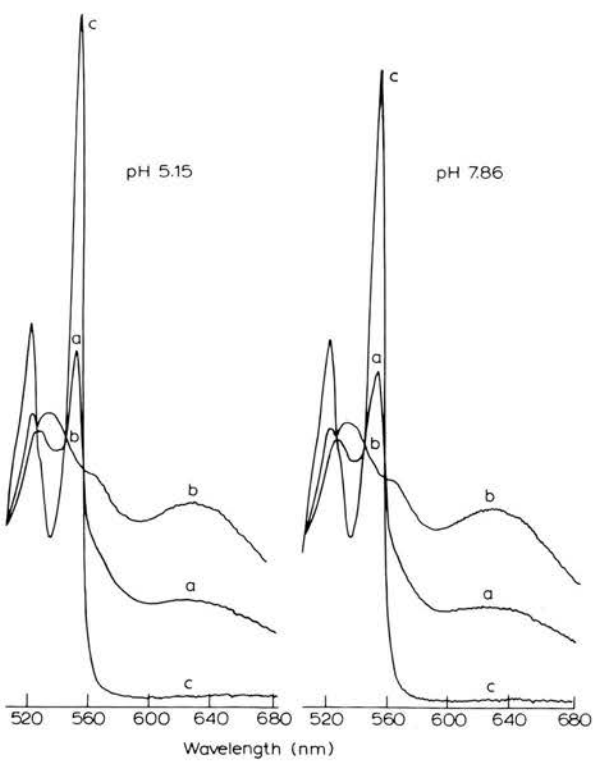

Fig. 5. The redox equilibrium of *Ps. aeruginosa* cytochrome *c*-551 and azurin. The cuvette contained $3 \cdot 10^{-3}$ M cytochrome *c*-551 and $5 \cdot 10^{-3}$ M azurin in $3.3 \cdot 10^{-3}$ M acetate, pH 5.15, or phosphate, pH 7.86. (a) Redox equilibrium achieved by adding ferrocytochrome *c*-551 to Cu II azurin. (b) Ferricyanide oxidised. (c) Dithionite reduced.

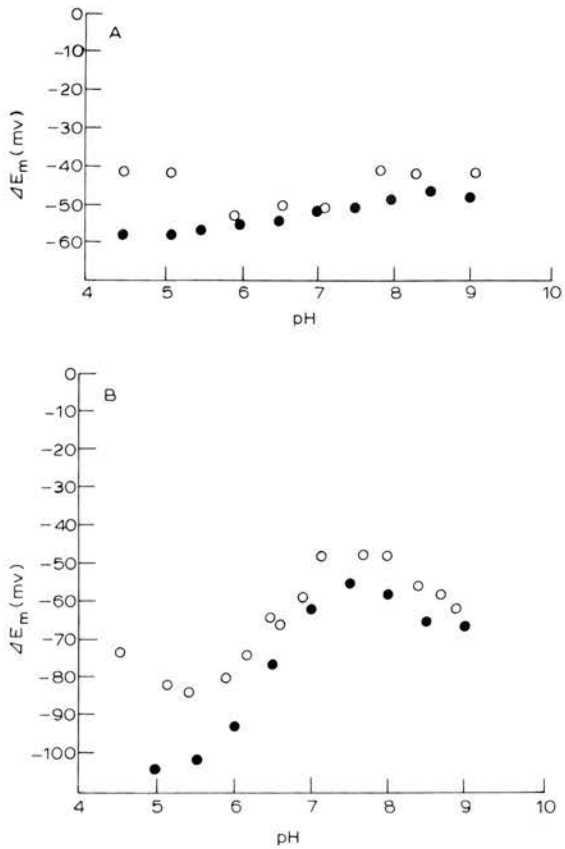

Fig. 6. pH dependence of the equilibria between *Ps. aeruginosa* cytochrome *c*-551 and *Ps. aeruginosa* azurin (A) and *Ps. stutzeri* cytochrome *c*-551 and *Ps. aeruginosa* azurin (B). (●) E_m (*c*-551) $- E_m$(azurin) calculated from separate determinations of midpoint potential in the presence of ferri-ferrocyanide. Data for (A) are from Figs. 2A and 4. Data for (B) appear elsewhere [14] and from Fig. 4. (○) E_m (*c*-551)$- E_m$ (azurin) calculated from redox equilibria of the type shown in Fig. 5.

the pH-dependent patterns of the cytochrome and the azurin and a pH-dependent equilibrium is observed which reflects the pH dependence of the azurin below pH 7.5 and the pH dependence of the cytochrome above this pH.

A Nernst equation incorporating pH-dependent ligand binding

The treatment of Dutton [13] describing the effect of ligand binding on redox potential can be extended to include pH-dependent ligand binding. If the simplifying assumption is made that a negative ligand such as ferri- or ferrocyanide binds only to the protonated state of the protein the following equilibria have to be taken into account:

$$\text{ox} + H^+ \rightleftharpoons \text{ox H},\ K_{OH} = \frac{[\text{ox H}]}{[\text{ox}][H^+]}$$

$$\text{red} + H^+ \rightleftharpoons \text{red H},\ K_{RH} = \frac{[\text{red H}]}{[\text{red}][H^+]}$$

$$\text{ox H} + L \rightleftharpoons \text{ox HL},\ K_{OL} = \frac{[\text{ox HL}]}{[\text{ox H}][L]}$$

$$\text{red H} + L \rightleftharpoons \text{red HL},\ K_{RL} = \frac{[\text{red HL}]}{[\text{red H}][L]}$$

Considering these, Eqn. 3 can be derived:

$$E_m = E_{m(NL)} + \frac{0.06}{n} \log \frac{1 + K_{RH}[H^+] + K_{RL}K_{RH}[H^+][L]}{1 + K_{OH}[H^+] + K_{OL}K_{OH}[H^+][L]} \qquad (3)$$

Using Eqn. 3 a theoretical curve was produced to fit the experimental data for cytochrome *c*-551 (the data for azurin can be fitted to the same equation using the same parameters – not shown). K_{OH} was set equal to K_{RH} so that the redox potential was not affected by differential proton binding in the two redox states, and the curve is therefore due to ligand binding effects only. With the parameters $K_{OH} = K_{RH} = 1.8 \cdot 10^6\ M^{-1}$, $[L] = 5 \cdot 10^{-4}$ M, $K_{RL} = 2.3 \cdot 10^4\ M^{-1}$ and $K_{OL} = 0$ the theoretical curve is that shown in Fig. 7. This of course is not a unique solution but it serves to demonstrate three important points. Firstly, in the absence of other evidence the experimental data can equally well be fitted by a pH-dependent ferri-ferrocyanide binding treatment as by a differential proton binding treatment (cf. Eqn. 2 and Fig. 2A). Secondly, the pK_R value (6.25) required to fit the experimental data to a pH-dependent ligand binding model is very different from the pK_R value (7.2) required for the H^+ binding model of Eqn. 2. Thirdly, a factor of 10 increase or decrease in K_{RL} or [L] produces dramatic changes in the theoretical curve (Fig. 7). We would expect that K_{RL} would be sensitive to ionic strength and therefore the pH dependence of redox potential of azurin and cytochrome *c*-551 was also measured in 0.1 M NaCl. Although the level of redox potential at a particular pH was altered, the pH-dependent pattern remained the same. In particular, the fall in mid-

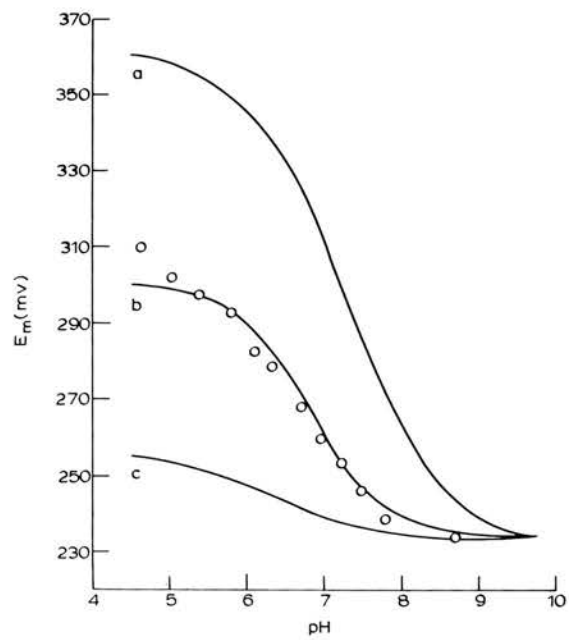

Fig. 7. Theoretical curve for pH dependent ligand binding. Solid lines were constructed from the equation:

$$E_m = E_{m(NL)} + \frac{0.06}{n} \log \frac{1 + K_{RH}[H^+] + K_{RL}K_{RH}[H^+][L]}{1 + K_{OH}[H^+] + K_{OL}K_{OH}[H^+][L]}$$

(Eqn. 3)

with the parameters defined in the text. All curves have $K_{OH} = K_{RH} = 1.8 \cdot 10^6\ M^{-1}$ and $[L] = 5 \cdot 10^{-4}$ M (the ferrocyanide concentration used in redox potential measurements). K_{OL} is set at 0 and K_{RL} is varied between $2.3 \cdot 10^5\ M^{-1}$ (a), $2.3 \cdot 10^4\ M^{-1}$ (b) and $2.3 \cdot 10^3\ M^{-1}$ (c). (○) Experimental points for *Ps. aeruginosa* cytochrome *c*-551 obtained in the presence of ferri-ferrocyanide (from Fig. 4).

point potential between pH 5 and pH 9 was not altered in the way predicted for a decline in K_{RL} at high ionic strength.

It might be argued that a more reasonable model would assign a value to K_{OL} greater than zero. When this was done with $K_{OL} = 10^4$, $K_{RL} = 1.5 \cdot 10^5$ a fall in E_m with pH of the correct magnitude was obtained from Eqn. 3. However, a pK_R of 5.5 was required in order to fit the experimental data, which is even further removed from the pK of 7.2 required for the H^+ binding model. If K_{OL} and K_{RL} were then raised or lowered to the same degree the theoretical curves shifted markedly above or below the experimental results.

Discussion

The patterns of pH dependence of redox potential for *Ps. aeruginosa* cytochrome *c*-551 are virtually identical whether the potential is measured by the ferri-ferrocyanide method at two different ionic strengths, the cytochrome *c*-558 mixture method or the diaminodurol method. To produce such effects by pH-dependent ligand binding would require that these very different redox agents have identical binding affinities for the cytochrome *c*-551. This is so unlikely that we therefore favour an explanation based on a single ionisable group, the pK of which differs in the two redox states, that difference being imposed by the electrostatic influence of the haem [4]. This interpretation is strongly supported by the pH dependence of the NMR spectrum and visible spectrum of cytochrome *c*-551 in the two redox states. From these studies, values of pK_{ox} and pK_{red} were independently derived which agree with those deduced from the redox potential analysis [15].

In the case of cytochrome c_2 from *Rps. viridis*, the pH dependence of redox potential [16] was consistent with a much smaller imposed separation of pK values ($pK_{ox} = 6.7$; $pK_{red} = 7.1$) and the only spectroscopic indicators of pH dependence were the proton resonances of a histidine residue ($pK_{ox} \simeq 6.8$, $pK_{red} \simeq 7.1$) [17]. Eley et al. [12] have shown that a histidine can form a pH-dependent binding site for ferricyanide in mitochondrial cytochrome *c* and therefore it was important to examine the pH dependence of redox potential of *Rps. viridis* cytochrome c_2 in the absence of ferri-ferrocyanide. The results of Fig. 3 indicate that under such conditions the pH dependence of redox potential is still observed. We therefore conclude that the deprotonation of histidine in *Rps. viridis* cytochrome c_2 results directly in the pH dependence of redox potential without pH-dependent ligand binding.

In their work on the pH dependence of kinetics of oxidation and reduction of azurin, Lappin et al. [18] found that ferricyanide oxidation of azurin was influenced by a group on the protein with a pK of 7.1 and ferrocyanide reduction by a group with a pK of 6.1. However, the kinetics of oxidation by tris[4,7-di(phenyl-4-sulphonate)-1,10-phenanthroline] Co(III) were pH independent and Lappin et al. predicted that the redox potential of azurin measured in the presence of this reagent would be independent of pH.

We have confirmed their observation that the redox potential of azurin measured in the presence of ferri-ferrocyanide is markedly pH dependent, but we observed a similar pH dependence in the presence of either horse cytochrome *c* or *Rps. capsulata* cytochrome c_2 as the redox partner in the absence of ferri-ferrocyanide (Fig. 4). Also we found that the equilibrium constant for *Ps. aeruginosa* cytochrome *c*-551/azurin mixtures was essentially independent of pH in agreement with previous work [19,20]. In view of the established pH dependence of cytochrome *c*-551 this implies a matching pH dependence for azurin. Because of the alkaline shift in pK_0 and pK_R in the case of *Ps. stutzeri* cytochrome *c*-551 such a matching is not obtained and the equilibrium constant in this case exhibits a pH dependence predictable from the separate patterns of pH dependence of the cytochrome and the azurin. Finally, the pattern of pH dependence of the azurin iron hexacyanide equilibrium was not affected by raising the ionic strength. These results appear to preclude pH-dependent ligand binding as the factor defining pH dependence of redox potential of azurin.

We therefore conclude that the pH dependence of redox potential for *Ps. aeruginosa* azurin may be interpreted in a similar way to that for cytochrome *c*-551. The difference in the electrostatic environment in the two redox states imposes a separation of pK values for a group on the protein in the vicinity of the redox centre. Our results suggest a group with a pK_{ox} of 6.1 and pK_{red} of

7.4, values in reasonable agreement with the kinetically derived pK_{ox} of 6.1 and pK_{red} of 7.1 [18]. Such an electrostatic explanation may be an oversimplification in the case of azurin because the deprotonation event (at least in the reduced protein) appears to be coupled to a conformational change. It has been shown that deprotonation of His-35 with a $pK_{red} \approx 7$ causes local structural rearrangements in the vicinity of the Cu and it may be this structural change rather than electrostatic interactions that lead to stabilisation of the oxidised protein with respect to the reduced form [27–29].

The pH independence of the kinetics of oxidation of azurin by tris[4,7-di(phenyl-4-sulphonate)-1,10-phenanthroline] Co(III) [18] might be a result of complications introduced by the pH-dependent conformational change of azurin. A minimal reaction scheme is:

$$\begin{array}{ccc} \mathrm{Az(I)} & \overset{k_f}{\underset{k_b}{\rightleftharpoons}} & \mathrm{Az^*(I)+H^+} \\ k_o \downarrow & & \\ \mathrm{Az(II)} & & \end{array}$$

where k_f and k_b are the rate constants for the conformational change in the reduced azurin (Az(I) and Az*(I), resp.) and k_o the oxidation rate constant.

If $k_f \gg k_b$ the pH-jump kinetic experiment used by Lappin et al. [18] does not detect the conformational change when $k_o \gg k_f$, conditions which apply to the oxidation of Az(I) by ferricyanide. However the oxidation of Az(I) by the substituted cobalt reagent is very slow and in this case k_o may be less than k_f with the consequence that the rate equation would include a term for the conformational change.

Acknowledgements

We are indebted to Drs. R.G. Bartsch and T.E. Meyer for providing the facilities and expertise for the growth of *Rps. viridis* and *Rps. capsulata.* We are grateful to Professors M. Brunori, A.G. Sykes and R.J.P. Williams and to Drs. G.W. Canters, H.A.O. Hill, N.A. Kitchen and M.T. Wilson for many helpful discussions. G.W.P. would like to dedicate this paper to the memory of the late Professor G.S. Boyd, who was a constant example and encouragement to him. G.R.M. thanks the SERC for an Advanced Fellowship and G.W.P. and F.A.L. thank the SERC and the Wellcome Trust for financial support.

References

1 Velick, S.F. and Strittmatter, P. (1956) J. Biol. Chem. 221, 265–275
2 Margalit, R. and Schejter, A. (1973) Eur. J. Biochem. 32, 492–499
3 O'Reilly, J.E. (1973) Biochim. Biophys. Acta 292, 509–515
4 Pettigrew, G.W., Meyer, T.E., Bartsch, R.G. and Kamen, M.D. (1975) Biochim. Biophys. Acta 430, 197–208
5 Dutton, P.L., Wilson, D.F. and Lee, C.P. (1970) Biochemistry 9, 5077–5082
6 Wilson, D.F., Erecinska, M., Leigh, J.S. and Koppelman, M. (1972) Arch. Biochem. Biophys. 151, 112–121
7 Dutton, P.L. and Jackson, J.B. (1972) Eur. J. Biochem. 30, 495–510
8 Reid, G.A. and Ingledew, W.J. (1979) Biochem. J. 182, 465–472
9 Butler, J., Davies, D.M. and Sykes, A.G. (1981) J. Inorg. Biochem. 15, 41–53
10 Miller, W.G. and Cusanovich, M.A. (1975) Biophys. Struct. Mech. 1, 97–111
11 Stellwagen, E. and Cass, R.D. (1975) J. Biol. Chem. 250, 2095–2098
12 Eley, C.G.S., Moore, G.R., Williams, G. and Williams, R.J.P. (1982) Eur. J. Biochem. 124, 295–303
13 Dutton, P.L. (1974) Biochim. Biophys. Acta 346, 165–212
14 Leitch, F.A., Moore, G.R. and Pettigrew, G.W. (1983) Biochemistry, in press
15 Moore, G.R., Pettigrew, G.W., Pitt, R.C. and Williams, R.J.P. (1980) Biochim. Biophys. Acta 590, 261–271
16 Pettigrew, G.W., Bartsch, R.G., Meyer, T.E. and Kamen, M.D. (1978) Biochim. Biophys. Acta 503, 509–523
17 Moore, G.R., Leitch, F.A. and Pettigrew, G.W. (1983) Biochim. Biophys. Acta, submitted for publication
18 Lappin, A.G., Segal, M.G., Weatherburn, D.C., Henderson, R.A. and Sykes, A.G. (1979) J. Am. Chem. Soc. 101, 2302–2306
19 Silvestrini, M.C., Brunori, M., Wilson, M.T. and Darley-Usmar, V.M. (1981) J. Inorg. Biochem. 14, 327–338
20 Rosen, P. and Pecht, I. (1976) Biochemistry 15, 775–786
21 Ambler, R.P. (1963) Biochem. J. 89, 341–349
22 Ambler, R.P. and Brown, L.H. (1967) Biochem. J. 104, 784–825
23 Pettigrew, G.W., Leaver, J.L., Meyer, T.E. and Ryle, A.P. (1975) Biochem. J. 147, 291–302
24 Bartsch, R.G. (1971) Methods Enzymol. 23, 344–363
25 Hanania, G.I.H., Irvine, D.H., Eaton, W.A. and George, P. (1967) J. Phys. Chem. 71, 2022–2030
26 Clark, W.M. (1960) in Oxidation Reduction Potentials of Organic Systems, Williams and Wilkins, Baltimore
27 Hill, H.A.O., Leer, J.C., Smith, B.E. and Storm, C.B. (1976) Biochem. Biophys. Res. Commun. 70, 331–338
28 Ugurbil, K. and Bersohn, R. (1977) Biochemistry 16, 3016–3023
29 Adman, E.T., Canters, G.W., Hill, H.A.O. and Kitchen, N.A. (1982) FEBS Lett. 143, 287–292

Biochimica et Biophysica Acta, 764 (1984) 331–342
Elsevier

BBA 41465

CHARACTERISATION OF IONISATIONS THAT INFLUENCE THE REDOX POTENTIAL OF MITOCHONDRIAL CYTOCHROME *c* AND PHOTOSYNTHETIC BACTERIAL CYTOCHROMES c_2

GEOFFREY R. MOORE [a], DAVID E. HARRIS [b], FIONA A. LEITCH [c] and GRAHAM W. PETTIGREW [c]

[a] *The Inorganic Chemistry Laboratory, University of Oxford, South Parks Road, Oxford OX1 3QR,* [b] *Laboratory of Molecular Biophysics, University of Oxford, South Parks Road, Oxford OX1 3PS and* [c] *Department of Biochemistry, Royal Dick School of Veterinary Studies, Summerhall, Edinburgh EH9 1QH (U.K.)*

(Received August 12th, 1983)

Key words: Cytochrome c; Redox potential; Ionization; NMR

Several cytochromes c_2 from the Rhodospirillaceae show a pH dependence of redox potential in the physiological pH range which can be described by equations involving an ionisation in the oxidised form (pK_o) and one in the reduced form (pK_r). These cytochromes fall into one of two groups according to the degree of separation of pK_o and pK_r. In group A, represented here by the *Rhodomicrobium vannielii* cytochrome c_2, the separation is approx. one pH unit and the ionisation is that of a haem propionic acid. Members of this group are unique among both cytochromes c_2 and mitochondrial cytochromes *c* in lacking the conserved residue Arg-38. We propose that the role of Arg-38 is to lower the p*K* of the nearby propionic acid, so that it lies out of the physiological pH range. Substitution of this residue by an uncharged amino acid leads to a raised p*K* for the propionic acid. In group B, represented here by *Rhodopseudomonas viridis* cytochrome c_2, the separation between pK_o and pK_r is approx. 0.4 pH unit and the ionisable group is a histidine at position 39. This was established by NMR spectroscopy and confirmed by chemical modification. Only a few other members of the cytochrome c_2/mitochondrial cytochrome *c* family have a histidine at this position and of these, both *Crithidia* cytochrome *c*-557 and yeast cytochrome *c* were found to have a pH-dependent redox potential similar to that of *Rps. viridis* cytochrome c_2. Using Coulomb's law, it was found that the energy required to separate pK_o and pK_r could be accounted for by simple electrostatic interactions between the haem iron and the ionisable group.

Introduction

The cytochromes c_2 of photosynthetic bacteria are a family of small monomeric and monohaem proteins that are structurally similar to the mitochondrial cytochrome *c* family. Ambler et al. [1] have classed the two families together on the basis of the similarities in their amino-acid sequences, and by these criteria some cytochromes c_2 more closely resemble mitochondrial cytochrome *c* than they do other cytochromes c_2. X-ray crystallographic and NMR spectroscopic studies of members of both cytochrome families confirm that their structures, and their haem environments in particular, are very similar [2–5]. There is also a marked functional similarity. Mitochondrial cytochrome *c* transfers electrons from cytochrome c_1 to cytochrome oxidase in the respiratory chain [6], a function also performed by some cytochromes c_2 [7,8]. Cytochrome c_2 has also been shown to act as the immediate electron donor to photo-oxidised bacteriochlorophyll in some bacteria [8].

Despite the structural and functional similarities, the two cytochrome families differ in one fundamental property: their redox potentials. Whereas in the pH range 5–8 the redox potentials

of mitochondrial cytochromes *c* are 260 ± 20 mV and are generally considered to be pH-independent [9], those of the cytochromes c_2 vary from 290 to 400 mV and some are markedly pH-dependent [10,11].

Pettigrew et al. [11] distinguished two patterns of pH dependence: one involving a single pK in the oxidised form, which correlated with loss of the 695 nm band of that form, and the other involving three pK values, one in the reduced form and two in the oxidised form in the sequence pK_{o1}, pK_r and pK_{o2}. pK_{o2} involved loss of the 695 nm band, indicating that the iron coordination was changed. The degree of separation of pK_{o1} and pK_r defined the appearance of the redox potential-pH curves obtained in the physiological pH range and they varied from the very pronounced pH dependence of *Rhodomicrobium vannielii* cytochrome c_2 ($pK_{o1} = 6.3$; $pK_r = 7.4$) to the slight pH dependence of *Rhodopseudomonas viridis* cytochrome c_2 ($pK_{o1} = 6.7$; $pK_r = 7.1$).

The present paper investigates the nature of the ionisations affecting the haem in these cytochromes and proposes a structural basis for their variable effects on redox potential. We also comment on the results of Prince and Bashford [12], who suggested such ionisations are not physiologically relevant because, they proposed, binding of the cytochrome c_2 to the bioenergetic membrane suppresses a conformation change coupled to the ionisation, thus leading to pH independence of redox potential.

Materials and Methods

Preparation of cytochromes

Cells of *Rm. vannielii* (ATCC 17100), *Rps. viridis* (NTHC 133) and *Rhodopseudomonas capsulata* SL (ATCC 11166) were grown as described by De Klerk et al. [13] in the laboratory of Professor M.D. Kamen (University of California at San Diego). The cytochromes c_2 from these organisms were purified according to the procedures of Bartsch [14] and Meyer [15]. Cytochrome *c*-557 from *Crithidia oncopelti* and cytochrome *c* from *Saccharomyces cerevisiae* (DCL, Kirkliston, West Lothian, U.K.) were purified in described by Pettigrew et al. [16] and cytochrome c_2 from *Rhodopseudomonas globiformis* was a kind gift from Dr. T.E. Meyer (University of California, San Diego).

N^{ϵ}-Acetimidylated fragments of horse cytochrome *c* were prepared as described by Harris and Offord [17] and Harris [18]. Complexes composed of residues (1–38) + (39–104) and (1–37) + (39–104) were formed by mixing solutions of the two fragments to the point where no further change was observed in the Soret peak [18].

Redox potential determinations

Single point measurements in the presence of known concentrations of ferri- and ferrocyanide were made as previously described [10]. The midpoint potential for ferri-ferrocyanide was taken from Fig. 1 of Ref. 19 according to the conditions of total ionic strength. The redox state of the cytochrome was determined by spectrophotometry in the region of the α-band on a Cary 219 spectrophotometer. In a few cases, full oxidative titrations were performed as described in the caption to Fig. 8.

The complexes formed using fragments of horse cytochrome *c* were autoxidisable and had midpoint potentials out of the useful range of the ferri-ferrocyanide couple. For these systems three-point reductive titrations were performed in an anaerobic cuvette constantly bubbled with argon. The Fe-EDTA couple was used as a redox buffer and to mediate electron transfer between the cytochrome and the platinum pin of a combination Pt-Ag|AgCl electrode (Russell pH Ltd., Auchtermuchty, U.K.) inserted into the cuvette. Stirring was achieved by a Teflon-coated 'cell stirrer' (Bel-Art), following a stirring magnet fitted in the sample compartment of a Unicam SP1800 spectrophotometer. The cuvette contained 0.05 M sodium acetate, sodium phosphate, Tris-HCl or glycine-NaOH buffers, 0.5 mM ferric ammonium sulphate and 10 mM EDTA. The cytochrome complexes (5 μM) were progressively reduced in the cuvette by the addition of small volumes of 0.5 mM ferrous ammonium sulphate, and the state of reduction and the ambient potential were recorded after each addition. Complete reduction was finally achieved by addition of a few crystals of sodium dithionite after opening the cuvette and measuring the pH. The standard potential of the Ag|AgCl reference was taken as 198 mV [20] and this was periodically checked using the Fe-EDTA couple

($E_m = 110$ mV at pH 5; Ref. 21). Data plotted according to the Nernst equation gave slopes close to 60 mV except for a few points near pH 9. This may be a consequence of the known instability of the Fe-EDTA chelate at high pH [22].

pH-jump stopped-flow kinetics

The progress of cytochrome reduction after rapid mixing of an unbuffered cytochrome solution and a buffer containing ferrocyanide was monitored at 550 nm in an Applied Photophysics stopped-flow spectrophotometer. The pH of the solution after mixing was measured.

Modification of histidine

Conditions based on those of Miles [23] were used. Diethylpyrocarbonate (Sigma) was diluted in acetonitrile and the concentration of active reagent was determined by the absorbance change produced in a 10 mM imidazole solution ($\epsilon_{230} = 3$ $mM^{-1} \cdot cm^{-1}$). Five equal aliquots of reagent were added at approximately hourly intervals to a solution of 45 μM cytochrome in 20 mM sodium phosphate pH 7.0 to give an excess of 14 mol per mol cytochrome and a final concentration of acetonitrile of 1%. The progress of reaction was followed by difference spectroscopy at 238 nm (equal volumes of acetonitrile being added to the reference cuvette). Once a level of histidine modification of 1 mol per mol had been achieved ($\Delta\epsilon_{238}$ $= 3.2$ $mM^{-1} \cdot cm^{-1}$), the cytochrome was passed through a column of Sephadex G-25 (fine) equilibrated in 10 mM NaCl/0.5 mM sodium phosphate (pH 7.0).

NMR spectroscopy

Cytochrome samples were prepared for NMR spectroscopy by passage through Sephadex G-25 packed into a Pasteur pipette and equilibrated in 10 mM NaCl/0.5 mM sodium phosphate (pH 7.0) in ^2H_2O (Merck, Sharp and Dohme). Cytochrome concentrations were in the range 2–3 mM. The pH values of solutions in the NMR experiments were monitored by a glass electrode (Radiometer) which was inserted directly into the NMR tubes. The pH was adjusted by addition of small aliquots of concentrated NaO^2H or ^2HCl in ^2H_2O. pH values quoted for NMR experiments are direct meter readings, and since they are not corrected for any isotope effect, they are denoted pH*.

^{1}HNMR spectra were obtained using a Brucker 270 MHz or Brucker 300 MHz spectrometer. Chemical shifts are quoted in parts per million (ppm) downfield from the methyl resonance of 2,2-dimethyl-2-silapentane-5-sulphonate. 1,4-Dioxan was used as the internal reference.

Results

Subdivision of the cytochrome c_2 on the basis of pH dependence of redox potential

On the basis of NMR experiments described later, we can distinguish three subdivisions of the cytochromes c_2 which we call groups A, B and C. Group A includes only *Rm. vannielii* and *Rhodospirillum rubrum* cytochromes c_2. Their pH dependence of redox potential (Fig. 1) can be described in terms of two ionisations in the oxidised protein (pK_{O1} and pK_{O2}) and one ionisation in the reduced protein (pK_r). The relevant equation (Ref. 10), derived using the methods of Clark [24], is:

$$E_m = \tilde{E} + \frac{RT}{nF} \ln\left(\frac{[H^+]^2 + K_r[H^+]}{[H^+]^2 + K_{O1}[H^+] + K_{O1}K_{O2}} \right) \quad (1)$$

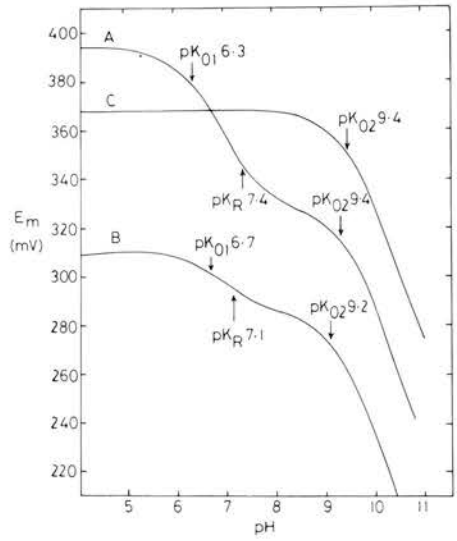

Fig. 1. The pH dependence of the redox potentials of (A) *Rm. vannielii* cytochrome c_2; (B) *Rps. viridis* cytochrome c_2; (C) *Rps. capsulata* cytochrome c_2. The lines are theoretical curves required to fit the experimental data published in Refs. 10 and 11. Curves A and B are defined by Eqn. 1 with the pK values shown and curve C is defined by Eqn. 2.

These cytochromes are characterised by having an asparagine or glutamine in place of Arg-38 [1] and by having a large separation of pK_{O1} and pK_r (approx. 1 pH unit).

Group B includes, amongst others, *Rps. viridis* cytochrome c_2. Their pH dependence of redox potential can also be described by the three-ionisation model and Eqn. 1 (Fig. 1), but pK_{O1} and pK_r are separated by approx. 0.5 pH unit only. Cytochromes of this group contain Arg-38, and at least one non-liganded histidine at the rear of the molecule [1–3].

Group C is represented here by *Rps. capsulata* cytochrome c_2 and horse cytochrome *c*. These exhibit a simple pH dependence of redox potential (Fig. 1) influenced only by pK_{O2} which is common to all cytochromes *c*. The relevant equation is:

$$E_m = \tilde{E} + \frac{RT}{nF}\ln\left(\frac{[H^+]}{[H^+]+K_{O2}}\right) \qquad (2)$$

Cytochromes of this group contain Arg-38.

Group A – structural basis for pH dependence of redox potential

NMR studies of Rm. vannielii cytochrome c_2. The pH dependence of the ^{1}H-NMR spectra of the ferri- and ferrocytochrome were examined. The spectrum of the ferricytochrome (Fig. 2) exhibits the distinctively downfield-shifted resonances arising from the haem substitutent groups found for all low-spin *c*-type cytochromes [4,25,26]. Three of these are methyl resonances (M1–M3). M1 was shown by double-resonance techniques to come from haem methyl-8, in agreement with the horse cytochrome *c* pattern [25]. The fourth haem methyl was not resolved. M1 and M2 shifted with pH with a pK_a of 6.3 (Fig. 3).

Three single proton resonances (P1–P3) were also resolved in the downfield region of the spectrum (Fig. 2). These arise from either the histidine ligand [27] or haem propionates [28]. One-proton intensity resonances in this region have been rigorously assigned to the β-CH_2 protons of the haem propionate substituents of *Pseudomonas* cytochromes *c*-551 [21] and horse cytochrome *c* (Moore, G.R. and Williams, G., unpublished data), and we similarly assign P2 and P3 to a haem propionate in *Rm. vannielii* cytochrome c_2 for the following reasons. Firstly, these single proton resonances occur in the same spectral region as those of horse cytochrome *c* and *Pseudomonas* cytochromes *c*-551 [26,28,29] with the extreme downfield shift indicating that the group involved must be part of the haem or its protein ligands. Secondly, in the *Pseudomonas* cytochromes, propionate resonances shift with pH to the same extent as P3 [26,30]. Thirdly, the pH dependence of the haem methyl resonances of the two cytochromes *c* are similar. In contrast, in systems (such as bisimidazole ferric porphyrins [31] and *Escherichia coli* cytochrome *b*-562; see Moore, G.R., Mathews, F.S. and Williams, R.J.P., unpublished data) where it is known that imidazole ligand ionisations occur, all the downfield-shifted haem and ligand resonances shift upfield as the imidazole ionises to imidazolate, with many of the resonances shifting by approx. 10 ppm.

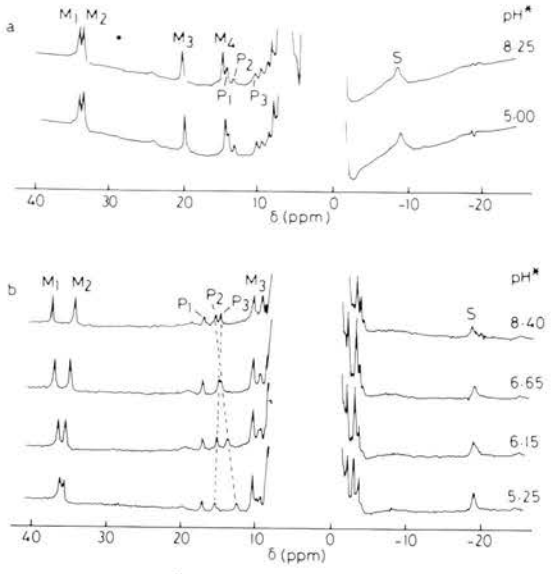

Fig. 2. 270 MHz·^{1}H NMR spectra of (a) *Rps. capsulata* ferricytochrome c_2 and (b) *Rm. vannielii* ferricytochrome c_2. The cytochromes are approx. 3 mM in ^2H_2O at 27°C and pH* was adjusted by the addition of ^{2}HCl or NaO^{2}H. The resonance nomenclature is: S, the methionine ligand methyl resonance; M1–M4, the haem methyl resonances; P1–P3, single-proton resonances that are proposed to come from haem propionates.

The methyl resonance of the methionine ligand of *Rm. vannielii* ferricytochrome c_2 experiences a small shift with pH which can be approximately fitted to a curve with pK_a of 6.3 (Fig. 3), in

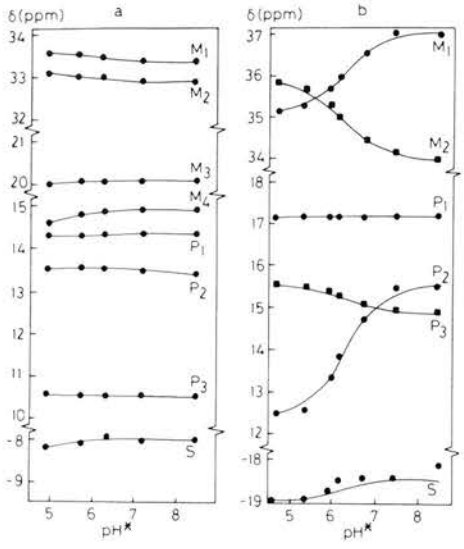

Fig. 3. The pH* dependence at 27°C of the chemical shifts of selected resonances of (a) *Rps. capsulata* ferricytochrome c_2 and (b) *Rm. vannielii* ferricytochrome c_2. The curves of M1, M2, P2, P3 and S in (b) are theoretical curves for an ionisation with pK_a of 6.3.

agreement with the pK_a observed for resonances M1, M2, P2 and P3. The continued presence of this methionine resonance at pH 8 demonstrates

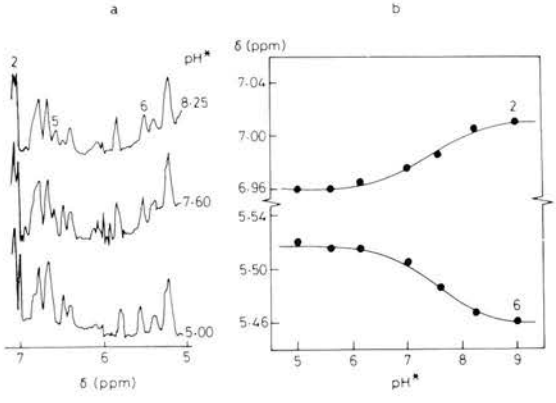

Fig. 4. The pH* dependence of resonances of Trp-59 of *Rm. vannielii* ferrocytochrome c_2. (a) Parts of the aromatic regions of the resolution enhanced 300 MHz·^{1}H-NMR spectra of approx. 2 mM ferrocytochrome c_2 in ^2H_2O at 27°C. Resonances marked 2, 5 and 6 come from the C-2, C-5 and C-6 protons, respectively of Trp-59. (b) The pH* dependence of the C-2 and C-6 resonances of Trp-59 at 27°C. The dots (●) are experimental points and the lines are theoretical curves drawn with a pK_a of 7.4.

that the coordination structure of the iron remains intact in the pH region in which pK_{O1} and pK_r lie. Also, the sharpness of the haem resonances throughout the titration (linewidths of approx. 30 Hz) shows that the rates associated with the ionisation are not lower than 10^4 s^{-1}, which precludes any associated conformational change involving the iron coordination or large movements of the main chain and amino acid side-chains.

The pH dependence of *Rm. vannielii* ferrocytochrome c_2 in ^2H_2O at 27°C was studied over the pH* range from 5.0–9.0. None of the resolved haem resonances (which included the haem methyl-8 resonance at 2.01 ppm) or the methionine ligand resonances shifted. However, the C-2, C-5 and C-6 resonances of the single tryptophan, which were identified by standard methods [5], were found to shift with pH* with a pK_a of 7.4 (Fig. 4). The tryptophan C-7 resonance did not shift and the C-4 resonance was not resolved. A number of unassigned resonances shifted with the pK_a of 7.4, but these shifts were less than 0.05 ppm. As with the ferricytochrome, these small changes in the spectrum indicate that the pK_a of 7.4 is not associated with a large conformational change.

We propose that the pK_a is due to the ionisation of the inner haem propionic acid (propionate-7) for the following reasons. Firstly, we have argued that the pK_a of 6.3 which perturbs the spectrum of ferricytochrome c_2 is due to a haem propionate, and a very similar pattern of pK_o and pK_r has been ascribed to the ionisation of a propionic acid in *P. aeruginosa* cytochrome *c*-551 [26,30]. Secondly, from the X-ray crystal structures of tuna cytochrome *c* [3] and *Rsp. rubrum* cytochrome c_2 [2], it is known that Trp-59 is hydrogen-bonded to propionate-7. Thus, the resonances of Trp-59 would be likely to be affected by ionisation of the propionic acid.

Kinetics of reduction of Rm. vannielii ferricytochrome c_2 in pH-jump experiments. Solutions of *R. vannielii* ferricytochrome c_2 ($2 \cdot 10^{-5}$ M) and ferricyanide (10^{-4} M) at pH 5 were rapidly mixed with buffers ($5 \cdot 10^{-3}$ M) containing ferrocyanide ($5 \cdot 10^{-4}$ M). For final pH values below 8.5, the kinetics of reduction were fast and monophasic (Fig. 5B), while above pH 8.5 kinetics of reduction were biphasic, with an initial rapid reduction followed by a much slower oxidation (Fig. 5C). Mid-

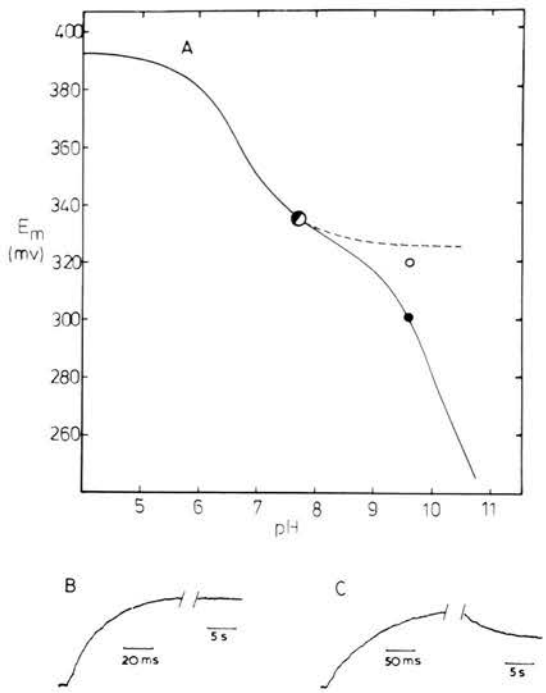

Fig. 5. The redox potential of *Rm. vannielii* cytochrome c_2, measured after the fast and slow phases of ferrocyanide reduction after pH jump. (A) ●, midpoint potential after completion of the slow phase of ferrocyanide reduction; ○, midpoint potential after completion of the fast phase of ferrocyanide reduction. The solid line is defined by Eqn. 1 and the parameters $pK_{O1} = 6.3$, $pK_r = 7.4$, $pK_{O2} = 9.4$ and $\tilde{E} = 392$ mV. The broken line is the extension of the theoretical curve for $pK_{O1} = 6.3$ and $pK_r = 7.4$ in the absence of pK_{O2}. (B) Ferricytochrome c_2 ($2 \cdot 10^{-5}$ M) and ferricyanide (10^{-4} M) in unbuffered solution at pH 5 was rapidly mixed with ferrocyanide ($5 \cdot 10^{-4}$ M) in $5 \cdot 10^{-3}$ M phosphate buffer to give a final pH of 7.7 and the progress of reduction monitored on an oscilloscope. (C) Ferricytochrome c_2 ($2 \cdot 10^{-5}$ M) and ferricyanide (10^{-4} M) in unbuffered solution at pH 5 was rapidly mixed with ferrocyanide ($5 \cdot 10^{-4}$ M) in 10^{-4} M glycine-NaOH buffer to give a final pH of 9.6. The progress of reduction was monitored on an oscilloscope.

point redox potentials calculated at the end of the fast phase and at the end of the slow phase are shown in Fig. 5A.

These results demonstrate that at pH values greater than 8.5, *Rm. vannielii* cytochrome c_2 undergoes the same type of ionisation coupled to a slow conformational equilibrium (with an apparent $pK = pK_{O2}$) that has been proposed for horse cytochrome *c* [32] and *Rps. sphaeroides* cytochrome c_2 [12]. However, the kinetic results of Fig. 5 and the results of the NMR spectroscopy show that at pH values below 8.5, the pH-dependent changes in redox potential do not involve a slow conformation change of the protein.

Group B – structural basis for pH dependence of redox potential

NMR studies of Rps. viridis cytochrome c_2. The pH* dependence of *Rps. viridis* ferri- and ferrocytochrome c_2 in ^2H_2O at 27°C was studied in the pH* range 4.4–9.2. None of the assigned aromatic resonances, resolved haem resonances or methionine ligand resonances were shifted in either redox state. In the ferricytochrome c_2 spectrum, a singlet resonance from the C-4 proton of the sole unliganded histidine (His-39) shifted with a pK_a of

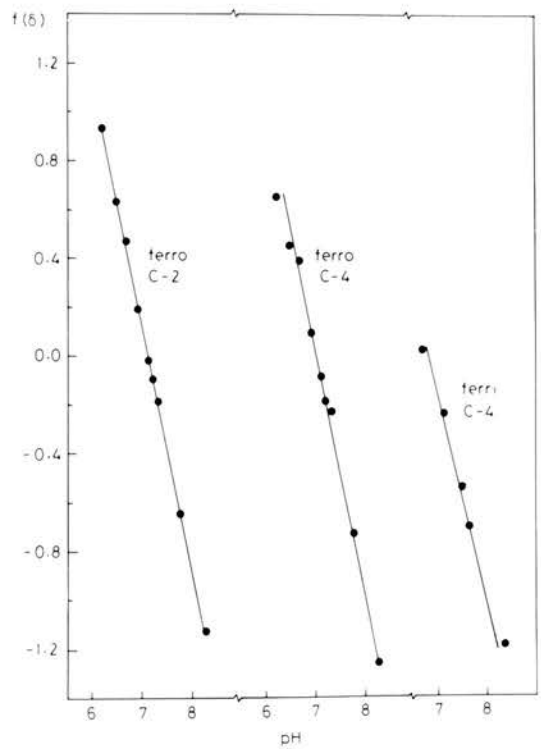

Fig. 6. Hill plot of the pH* dependence of resonances of His-39 of *Rps. viridis* cytochrome c_2 at 27°C. ($f(\delta)$ is $\log\{(\delta - \delta_A)/(\delta_{HA} - \delta)\}$, where δ is the chemical shift at a given pH*, δ_{HA} the chemical shift of the fully protonated species and δ_A the chemical shift of the fully deprotonated species. The solid lines are best fits through the experimental data (●) and yield for the ferrocytochrome, C-2 $pK_a = 7.10$ ($n = 1$) and C-4 $pK_a = 7.05$ ($n = 1$), and for the ferricytochrome, C-4 $pK_a = 6.8$ ($n = 0.9$).

approx. 6.8 (Fig. 6). In the ferrocytochrome c_2 spectrum, both the C-2 and C-4 proton resonances of His-39 were identified and found to titrate with a pK_a of 7.1 (Fig. 6). The NMR data show that the haem propionates do not ionise over the pH* range studied.

Modification of His-39 of Rps. viridis cytochrome c_2 Diethylpyrocarbonate (final concentration, 225 μM) was gradually added to *Rps. viridis* cytochrome c_2 (45 μM). The change in absorbance at 238 nm indicated that 1 mol of histidine per mol of cytochrome had been modified [23]. After removal of excess reagent and breakdown products, the redox potential of the modified cytochrome was determined between pH 5 and pH 9. It was found to be essentially independent of pH, in contrast to the pattern observed for the unmodified protein (Fig. 7). The modification does not result in major structural changes in the cytochrome, since both the redox potential at alkaline pH and the absorbance at 695 nm were almost unchanged.

pH dependence of redox potential of C. oncopelti cytochrome c-557 and S. cerevisiae iso-1 cytochrome c. Among the mitochondrial cytochrome *c* bacterial cytochrome c_2 family, only *Rps. globiformis* cytochrome c_2 and the cytochromes *c* from *C. oncopelti, S. cerevisiae* and *Candida krusei* are like *Rps. viridis* cytochrome c_2 in having a histidine at position 39. The pH dependence of redox potential of *C. oncopelti* cytochrome *c*-557 and *S. cerevisiae* cytochrome *c* is shown in Fig. 8 and compared with that for horse cytochrome *c*.

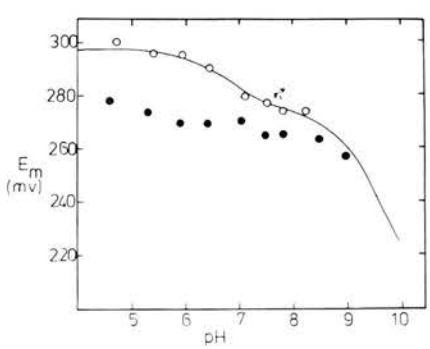

Fig. 7. The effect of histidine modification on the pH dependence of redox potential of *Rps. viridis* cytochrome c_2. ○, single-point determinations of midpoint potential of native cytochrome in the presence of 0.5 mM ferrocyanide and 0.017 mM ferricyanide. Buffers were 2 mM in acetate, phosphate, Tris or borate. The solid line is a theoretical curve described by Eqn. 1 with the parameters $pK_{O1} = 6.7$, $pK_r = 7.1$ and $pK_{O2} = 9.2$, which gave the best fit to the published experimental results for *Rps. viridis* cytochrome c_2. $\tilde{E}$ was here taken as 297 mV (309 mV gave the best fit to the original results). ●, single point determinations of midpoint potential of cytochrome proposed to be modified at His-39. Conditions were as above.

The data for horse cytochrome *c* can be accurately fitted by a theoretical curve with a single pK_o of 8.75 in the oxidised form as described by Eqn. 2. We propose that the data for *C. oncopelti* cytochrome *c*-557 and *S. cerevisiae* cytochrome *c* deviate significantly from the curve described by this simple equation (broken line of Fig. 8b and 8c) and are fitted best by Eqn. 1 with $pK_{O1} = 6.6$ and $pK_r = 7.0$ in the case of the *Crithidia* cytochrome *c*, and $pK_{O1} = 6.9$ and $pK_r = 7.3$ for the *Saccharomyces* cytochrome. pK_{O2} values are given in the figure caption.

We were unable to determine the pH dependence of redox potential for *Rps. globiformis* cytochrome c_2 because of the very slow equilibration of this cytochrome with the ferri-ferrocyanide couple. Measurements at pH 7 suggest that the midpoint potential may be more positive than 450 mV.

Group C – the pH independence of redox potential of Rps. capsulata cytochrome c_2 *and horse cytochrome c*

NMR studies of Rps. capsulata cytochrome c_2. The ^1H NMR spectrum of *Rps. capsulata* ferricytochrome c_2 was studied at different pH* values in ^2H_2O at 27°C. Although some of the haem methyl resonances shifted in the pH* range 5.0–9.0, the effects were very much smaller than those observed for the haem methyls of *Rm. vannielii* ferricytochrome c_2 (Fig. 2 and 3). Also, the single proton resonances, P1–P3, some (or all) of which came from haem propionic acids, did not shift with pH*. Thus, the haem propionate groups of *Rps. capsulata* cytochrome c_2 do not ionise in the pH* range 5.0–9.0.

The pH dependence of redox potential of horse cytochrome c cleaved at Arg-38. In view of the emphasis we place on the role of Arg-38 in modulating the ionisation of haem propionate-7 (see Discussion) we studied two of the two-fragment complexes of horse cytochrome *c* in which the

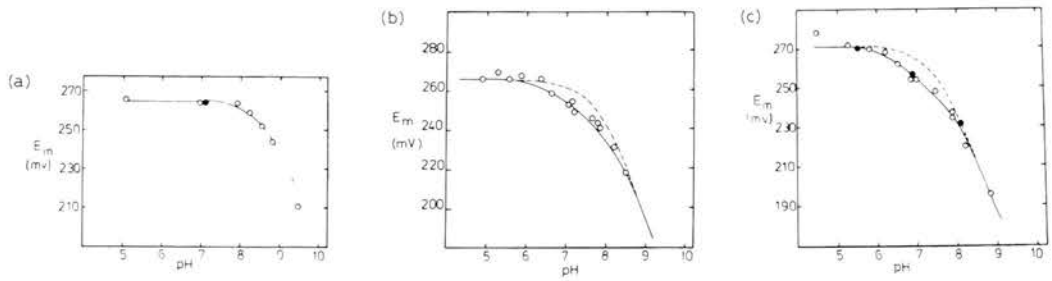

Fig. 8. The pH dependence of redox potential of (a) horse cytochrome *c*; (b) *S. cerevisiae* cytochrome *c*; (c) *C. oncopelti* cytochrome *c*-557. ○, single-point determinations of midpoint potential. In all cases, ferrocyanide was 0.5 mM. In (a) ferricyanide was 0.004 mM, and in (b) and (c) it was 0.0083 mM. Cytochromes were $2 \cdot 10^{-6}$ M and buffers were 2 mM acetate, phosphate, Tris or borate. ●, full oxidative titrations in the presence of 0.5 mM ferrocyanide and varying concentrations of ferricyanide. The cytochromes were reduced with 50 mM ascorbate and excess reductant removed by gel filtration. Thus the titrations started with fully reduced cytochrome. The solid line in (a) is a theoretical curve described by Eqn. 2 with $pK_{O2} = 8.75$ and $\tilde{E} = 265$ mV. The solid line in (b) is a theoretical curve described by Eqn. 1 with $pK_{O1} = 6.9$, $pK_r = 7.3$, $pK_{O2} = 8.3$ and $\tilde{E} = 266$ mV. The broken line in (b) is for a single ionisation with $pK_{O2} = 7.85$. The solid line in (c) is a theoretical curve described by Eqn. 1 with $pK_{O1} = 6.6$, $pK_r = 7.0$, $pK_{O2} = 8.0$ and $\tilde{E} = 271$ mV. The broken line in (c) is for a single ionisation with $pK_{O2} = 7.55$.

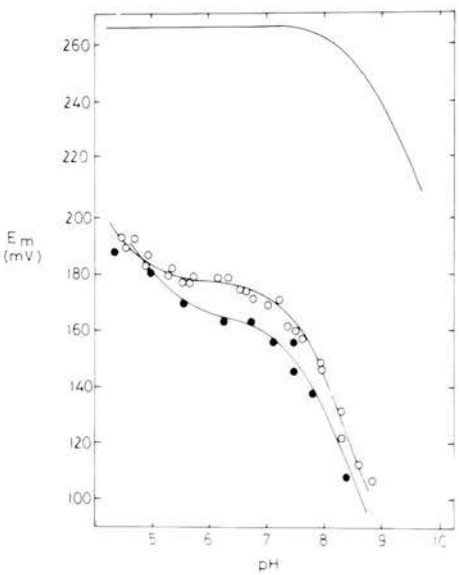

Fig. 9. The effect of removal of Arg-38 on the pH dependence of redox potential of horse cytochrome *c*. The experimental points (○ and ●) were obtained from three-point titration data, using 0.5 mM ferric ammonium sulphate in 10 mM EDTA as the mediator and 0.1 M ferrous ammonium sulphate as the titrant in the presence of a Pt-Ag|AgCl electrode in an argon-flushed cuvette. Buffers were 0.1 M in acetate, Tris or glycine and 0.05 M in phosphate. Cytochromes were 10^{-5} M. ○, horse cytochrome *c* (1–38·39–104). The line is a theoretical curve according to Eqn. 3 with $pK_r = 4.3$ and $pK_o = 7.6$. ●, horse cytochrome *c* (1–37·39–104). The line is a theoretical curve according to Eqn. 3 with $pK_r = 4.9$ and $pK_o = 7.6$. The top curve is taken from Fig. 8a for unmodified horse cytochrome *c*.

Arg-38–Lys-39 bond is selectively cleaved; the parent complex (1–38 · 39–104) and the complex in which the exposed C-terminal Arg-38 had been removed by carboxypeptidase B (1–37 · 39–104). Both of these systems were autoxidisable and redox titrations were performed anaerobically in the presence of a Pt-Ag|AgCl combination electrode and the Fe-EDTA couple. The results are shown in Fig. 9 and were analysed according to the equation:

$$E_m = \tilde{E} + \frac{RT}{nF} \ln\left(\frac{[H^+]^2 + K_r[H^+]}{[H^+] + K_o}\right) \quad (3)$$

which defines the theoretical curves. A similar pattern of pH dependence was obtained in both cases, with $pK_r = 4.3$ and $pK_o = 7.6$ for (1–38 · 39–104) and $pK_r = 4.9$ and $pK_o = 7.6$ for (1–37 · 39–104).

pH titration of the ferricytochromes was performed and followed spectroscopically between 500 and 750 nm. The 695 nm bands, indicative of methionine coordination to the iron [29,33,34], were present and were lost with a pK of approx 7.8 in (1–38 · 39–104) and approx. 7.9 in (1–37 · 39–104). The ionisations with pK_r may be the haem propionate-7 ionisations.

Discussion

The ionisation of a haem propionic acid in cytochrome c_2

The redox potential of *Rm. vannielii* cytochrome c_2 was influenced by an ionisation in the oxidised protein, with $pK_{O1} = 6.3$, and in the reduced protein, with $pK_r = 7.4$ (Fig. 1). These pK values are in addition to the pK_{O2} of 9.4 in the oxidised protein [10], which involves loss of the methionine-iron coordination and is found in all cytochromes c_2, although at different pH values [11]. A simple interpretation of pK_{O1} and pK_r is that they represent the ionisation of the same group but with the proton dissociation being influenced by the redox state of the haem [10]. NMR spectroscopy of the ferricytochrome has allowed direct identification of a haem propionate as the ionising group with pK_a of 6.3. In the spectrum of the ferrocytochrome c_2, the haem propionate resonances were not resolved but resonances of Trp-59 shifted with a pK_a of 7.4. Because the corresponding tryptophan is hydrogen-bonded to the inner haem propionate (propionate-7) in *R. rubrum* cytochrome c_2 [2] and tuna cytochrome *c* [3], we conclude that its resonances reflect the propionate ionising with a pK_a of 7.4 in *Rm. vannielii* ferrocytochrome c_2. Thus, we propose that the $pK_{O1} = 6.3$ and $pK_r = 7.4$ deduced [10] from the pH dependence of redox potential are due to the ionisation of the inner haem propionic acid with the proton being lost more readily from the ferricytochrome c_2 due to the electrostatic influence of the ferric haem. In the pH range in which these ionisations occur, the methionine-iron bond remains intact. This pattern of pK_{o1} and pK_r is similar to that found for the *Pseudomonas* cytochromes *c*-551 [26,30].

The propionic acid NMR resonances of *Rps. viridis* and *Rps. capsulata* cytochromes c_2 do not shift with pH* in the range 5.0–9.0 and in this respect they resemble those of horse cytochrome *c* [29,35]. On the basis of the X-ray crystallographic structure of tuna cytochrome *c* [3], Arg-38 lies close enough to the inner haem propionate to form a hydrogen bond or salt link. Only *R. rubrum* and *Rm. vannielii* cytochromes c_2 of the mitochondrial cytochrome *c*-bacterial cytochrome c_2 family lack this residue; they have an asparagine or glutamine instead. Therefore, we propose that the function of Arg-38 is to interact with the haem propionate in such a way that the propionate does not ionise in the physiological pH range. This could be achieved in two ways: (i) the inner haem propionate is maintained in the unionised state by the hydrophobic interior of the protein and the extensive set of interactions in which it is involved; (ii) the positively charged Arg-38 stabilises the ionised form and thereby lowers the pK_a. According to this view, Gln-38 of *Rm. vannielii* cytochrome c_2 could not act in the same way and, as a consequence, the propionate pK_a values are in the range 6–8. Thus, the second possibility seems most likely.

Cleavage of the Arg-38–Lys-39 bond in horse cytochrome *c* and subsequent removal of Arg-38 yields a protein with the methionine-iron bond intact at pH 7 but with a midpoint potential 90 mV more negative than that of the unmodified cytochrome (Fig. 9). We propose that this effect is due to an increase in the relative stabilisation of the oxidised form of the modified protein by the unneutralised negative charge of propionate-7. It is interesting that simple cleavage of the arginyl-lysyl peptide bond without removal of the arginine yields a protein with a very similar pattern of pH dependence of redox potential to the system with the arginine removed. Possibly, the appearance of a new α-carboxylate close to the guanidino group interferes with the ability of the latter to interact with the haem, propionate, thus giving rise to similar effects on the redox potential as the removal of the arginine itself. Consistent with this view is the conspicuous absence of acidic amino acids on the surface of cytochromes *c* and cytochromes c_2 close to Arg-38. In the loop of residues 30–42 in the 67 mitochondrial cytochrome sequences given in the compilation of Dickerson and Timkovich [36], and in the 14 cytochrome c_2 sequences given by Ambler et al. [1], acidic amino side-chains are found only three times and all three cases occur in *R. rubrum* and *Rm. vannielii* cytochromes c_2.

The effect of histidine ionisation on the redox potential of cytochromes c

In the case of *Rps. viridis* cytochrome c_2, the haem propionates have been shown not to ionise in the pH* range 5.0–9.0 and yet the redox poten-

tial is influenced by a group with a $pK_a = 6.7$ in the oxidised form and a $pK_a = 7.1$ in the reduced form (Fig. 1). NMR spectroscopy identified this group as His-39 (Fig. 6). After modification of this histidine by diethylpyrocarbonate, the redox potential becomes independent of pH and has a value close to that of the unmodified protein at pH 8 (Fig. 7). The more positive value of the midpoint potential at acid pH for the native protein is consistent with an electrostatic effect resulting in destabilisation of the ferric cytochrome relative to the ferrous cytochrome due to the protonated histidine, a destabilisation not possible in the modified protein until very low pH values because the pK_a of *N*-ethoxyformylhistidine is 3.4 [37].

Our study of *Rps. viridis* cytochrome c_2 led us to predict that the few members of the cytochrome c_2-mitochondrial cytochrome *c* family that contained His-39 would show a similar pH dependence of redox potential. This was demonstrated for *C. oncopelti* cytochrome *c*-557 and *S. cerevisiae* cytochrome *c* (Fig. 8) and it is consistent with previous NMR studies showing that His-39 of *S. cerevisiae* cytochrome *c* ionises with a pK_a of 6.8 in the ferric protein and a pK_a of 7.2 in the ferrous protein [38]. It seems likely that similar histidine effects occur in the pH dependence of redox potential of *Rps. palustris* and *Rps. sphaeroides* cytochrome c_2 where the separation of pK_o and pK_r is 0.5 and 0.3 pH units, respectively [10,11]. However, in these cytochromes histidine does not occur at position 39 but at positions 53 and 63, and at position 92, respectively [1].

There are three possible explanations for the histidine effects which we cannot yet distinguish. Firstly, the ionisation of a histidine may be directly influenced by the redox state of the iron and may in turn perturb the redox potential by the same mechanism of electrostatic interaction that we found for the haem propionate. Secondly, a protonated histidine may contribute to the shielding of the propionate charge and deprotonation would therefore result in a less positive redox potential. Thirdly, the small conformational change which occurs at the rear of the cytochrome molecule [3,39] (and which may be triggered by changes in the electrostatic relay $Fe(III)–CO_2^- –Arg\text{-}38^+$ on reduction) may result in a difference in the environment of histidines in this region of the protein in the two redox states.

Energies of interaction between the haem iron and ionisable groups

Using Coulomb's law:

$$E = \frac{1347\, q_1 \cdot q_2}{\epsilon \cdot D} \qquad (4)$$

where q_1 and q_2 are the charges on two groups, D is the distance between them, ϵ is the effective dielectric constant and E is the energy of interaction, it is possible to assess the effect that an ionising propionic acid would have on the redox potential [40]. The actual fall in redox-potential associated with this ionisation in *Rm. vannielii* cytochrome c_2 is 65 mV, which is equivalent to -6.27 kJ · mol^{-1} (Table IA). Energies of interaction of this size can be obtained from Eqn. 4 if the product $q_1 \cdot q_2$ is taken as -1 (i.e., $+1$ charge on the iron and -1 on the propionate), D taken as 10 Å and ϵ taken as 20 (Table IB). Since $q_1 \cdot q_2$ and ϵ are unknown quantities which may be impossible to determine accurately, this calculation does not provide a definitive answer, but it does serve to

TABLE IA

ENERGIES OF INTERACTION BETWEEN THE HAEM IRON AND IONISABLE GROUPS

Cytochrome	ΔpK	ΔE_M (mV)	ΔG (kJ · mol^{-1})	Ionisable group
Rm. vanielli cytochrome c_2	1.1	65	−6.27	haem propionate-7
Rps. viridis cytochrome c_2	0.4	23	−2.22	His-39

TABLE IB

ENERGY OF INTERACTION CALCULATED FROM EQN. 4

$q_1 \cdot q_2$	ϵ	D (Å)	E (kJ · mol^{-1})
−1	20	10	−6.73

demonstrate that energies of the appropriate size can be produced by the type of interaction proposed. The energies associated with histidine ionisation are smaller (Table IA) and in view of our uncertainty as to the detailed mechanism operating in these cases, it is difficult to decide on the cause of this smaller effect. However, it is probable that the effective dielectric constant between the iron and a surface histidine will be larger than that between the iron and an internal propionate (judging from the position of Lys-39 of tuna cytochrome *c*, His-39 is approx. 18 Å from the iron which with $\epsilon = 20$, gives an E of $-3.75\ \mathrm{kJ \cdot mol^{-1}}$). It is interesting to note that the fall in redox potential (90 mV) observed on removal of Arg-38 from horse cytochrome *c* (Fig. 9) is comparable to the fall observed on propionic acid ionisation in *R. vannielii* cytochrome c_2 (65 mV) (Fig. 1). This is consistent with the suggested role for Arg-38 in neutralising the negative charge of the propionate in the interior of the unmodified cytochrome.

Biological aspects of haem-linked ionisations

The pH dependence of the redox potential of purified *Rps. sphaeroides* cytochrome c_2 at alkaline pH (pK_{O2}) [10] was not observed for the cytochrome attached to the chromatophore membrane [41]. Nor was pH-dependent behaviour observed if the redox potential was estimated after a rapid phase of reduction of the cytochrome [12]. Brandt et al. [32] have shown for horse cytochrome *c* that the apparent pK of 9 could be viewed as due to an ionisation with a pK of 11 coupled to a conformation change with a pK of 2, and in applying this analysis to *Rps. sphaeroides* cytochrome *c*, Prince and Bashford [21] have argued that the conformation change in this cytochrome is suppressed upon attachment of the cytochrome to the chromatophore membrane and that the redox potential is consequently independent of pH between 7–11. These authors thus concluded that pH-dependent effects of redox potential of purified cytochromes c_2 were not relevant to the physiological situation. We accept their elegant analysis of the nature of the apparent pK_o near 9, which is observed in all cytochromes and involves loss of methionine coordination. However, we have shown by NMR spectroscopy and by kinetics of reduction that pK_{O1} and pK_r of *Rm. vannielii* cytochrome c_2 do not involve a slow conformational change and are thus different in nature from pK_{O2}. The question as to whether pK_{o1} and pK_r operate in situ thus remains open.

There is much interest at present in how electron transport may drive vectorial proton translocation across a bioenergetic membrane [42–45]. Both mitochondrial cytochrome oxidase and cytochrome *c* reductase have been proposed to be proton pumps in which electron transfer at the redox centre is coupled via the intervening polypeptide chain to deprotonation events in an analogous way to the Bohr effects in haemoglobin. Although we do not suggest that the soluble periplasmic cytochromes considered here could act in such a transmembrane role, they may serve as useful scalar models for how the more complex systems work. We propose that simple electrostatic considerations will result in an imposed redox-state-dependent separation of pK values of a group close to the redox centre and that this will give rise to proton-coupled electron transfer in the intervening pH range. Such a mechanism avoids the kinetic problems associated with schemes requiring slow conformation changes, and for systems in which the effective dielectric constant is low, which is probably the case for intrinsic membrane proteins, it provides substantial interaction energies over a large distance. The question of how the proton gate operates remains open [44,45]. It is difficult to envisage a mechanism whereby proton translocation against a proton gradient is controlled entirely by electrostatic terms and a small conformational change, which may involve no more than the orientation of a few amino-acid side-chains or a helix, may be required.

Acknowledgements

We are indebted to Prof. M.D. Kamen and Drs. R.G. Bartsch and T.E. Meyer for providing the facilities and expertise for the growth of *Rm. vannieli, Rps. viridis* and *Rps. capsulata* S.L. G.W.P. thanks the Wellcome Trust and the SERC for financial support and G.R.M. thanks the Science and Engineering Research Council for an Advanced Fellowship. F.A.L. acknowledges an SERC studentship.

References

1 Ambler, R.P., Daniel, M., Hermoso, J., Meyer, T.E., Bartsch, R.G. and Kamen, M.D. (1979) Nature 278, 659–660
2 Salemme, F.R., Kraut, J. and Kamen, M.D. (1973) J. Biol. Chem. 248, 7701–7716
3 Takano, T. and Dickerson, R.E. (1981) J. Mol. Biol. 153, 79–115
4 Smith, G.M. and Kamen, M.D. (1974) Proc. Natl. Acad. Sci. U.S.A. 71, 4303–4307
5 Cookson, D.J., Moore, G.R., Pitt, R.C., Williams, R.J.P., Campbell, I.D., Ambler, R.P., Bruschi, M. and Le Gall, J. (1978) Eur. J. Biochem. 83, 261–275
6 Keilin, D. (1966) The History of Cell Respiration and Cytochrome, Cambridge University Press, London
7 La Monica, R.F. and Marrs, B.L. (1976) Biochim. Biophys. Acta 423, 431–439
8 Dutton, P.L. and Prince, R.C. (1978) in The Photosynthetic Bacteria (Clayton, R.K. and Sistrom, W.R., eds.), pp. 525–610, Plenum Press, New York
9 Margalit, R. and Schejter, A. (1973) Eur. J. Biochem. 32, 492–499
10 Pettigrew, G.W., Meyer, T.E., Barsch, R.G. and Kamen, M.D. (1975) Biochim. Biophys. Acta 430, 197–208
11 Pettigrew, G.W., Bartsch, R.G., Meyer, T.E. and Kamen, M.D. (1978) Biochim. Biophys. Acta 503, 509–523
12 Prince, R.C. and Bashford, C.L. (1979) Biochim. Biophys. Acta 547, 447–454
13 De Klerk, H., Bartsch, R.G. and Kamen, M.D. (1965) Biochim. Biophys. Acta 97, 275–280
14 Bartsch, R.G. (1978) in The Photosynthetic Bacteria (Clayton, R.K. and Sistrom, W.R., eds.), pp. 249–279, Plenum Press, New York
15 Meyer, T.E. (1970) Ph.D. Thesis, University of California at San Diego
16 Pettigrew, G.W., Leaver, J.L., Meyer, T.E. and Ryle, A.P. (1975) Biochem. J. 147, 291–302
17 Harris, D.E. and Offord, R.E. (1977) Biochem. J. 161, 21–25
18 Harris, D.E. (1978) in Semisynthetic Peptides and Proteins (Offord, R.E. and DiBello, C., eds.), pp. 127–138, Academic Press, London
19 Hanania, G.I.H., Irvine, D.H., Eaton, W.A. and George, P. (1967) J. Phys. Chem. 71, 2022–2030
20 Bates, R.G. (1954) Electrometric pH Determinations, p. 208, Wiley, New York
21 Kolthoff, I.M. and Auerbach, C. (1952) J. Am. Chem. Soc. 74, 1452–1456
22 Wilson, G.S. (1978) Methods Enzymol. 54, 396–410
23 Miles, E.W. (1977) Methods Enzymol. 47, 431–442
24 Clark, W.M. (1960) Oxidation Reduction Potential of Organic Systems, Williams and Wilkins, Baltimore, MD
25 Keller, R.M. and Wüthrich, K. (1978) Biochim. Biophys. Acta 533, 195–206
26 Leitch, F.A., Moore, G.R. and Pettigrew, G.W. (1984) Biochemisitry, in the press
27 La Mar, G.N., Frye, J.S. and Satterlee, J.D. (1979) Biochim. Biophys. Acta 428, 78–90
28 McDonald, C.C. and Phillips, W.D. (1973) Biochemistry 12, 3170–3186
29 Ångstrom, J., Moore, G.R. and Williams, R.J.P. (1982) Biochim. Biophys. Acta 703, 87–94
30 Moore, G.R., Pettigrew, G.W., Pitt, R.C. and Williams, R.J.P. (1980) Biochim. Biophys. Acta 590, 261–271
31 Chacko, V.P. and La Mar, G.N. (1982) J. Am. Chem. Soc. 104, 7002–7007
32 Brandt, K.G., Parks, P.C., Czerlinski, G.H. and Hess, G.P. (1966) J. Biol. Chem., 241, 4180–4185
33 Harbury, H.A., Cronin, J.R., Fanger, M.W., Hettinger, T.P., Murphy, A.J., Myer, Y.P. and Vinogradov, S.N. (1965) Proc. Natl. Acad. Sci. U.S.A. 54, 1658–1664
34 Schecter, E. and Saludjian, P. (1967) Biopolymers 5, 788–790
35 Gupta, R.K. and Koenig, R.H. (1971) Biochem. Biophys. Res. Commun. 45, 1134–1143
36 Dickerson, R.E. and Timkovich, R. (1975) in The Enzymes (Boyer, P., ed.), 3rd Edn., Vol. 11, pp. 397–547, Academic Press, New York
37 Melchior, W.B. and Fahrney, D. (1970) Biochemistry 9, 251–258
38 Robinson, M.N., Boswell, A.P., Huang, Z.H., Eley, C.G.S. and Moore, G.R. (1983) Biochem. J. 213, 687–700
39 Moore, G.R., Williams, R.J.P., Chien, J.C.W. and Dickinson, L.C. (1980) J. Inorg. Biochem. 12, 1–15
40 Moore, G.R. (1983) FEBS Lett. 161, 171–175
41 Prince, R.C. and Dutton, P.L. (1976) Biochim. Biophys. Acta 459, 573–577
42 Wikström, M.F.K. and Krab, K. (1979) Biochem. Soc. Trans. 7, 880–887
43 Von Jagow, G. and Engel, W.D. (1980) FEBS Lett. 111, 1–5
44 Wikström, M.F.K., Krab, K. and Saraste, M. (1981) Annu. Rev. Biochem. 50, 623–655
45 Williams, R.J.P. (1983) in The Enzymes of Biological Membranes (Martonosi, A., ed.), Plenum Press, New York, in the press